Modeling the effects of hard structures on dune erosion and overwash

Hindcasting the impact of Hurricane Sandy on New Jersey with XBeach

C.M.(Kees) Nederhoff

Master of Science Thesis

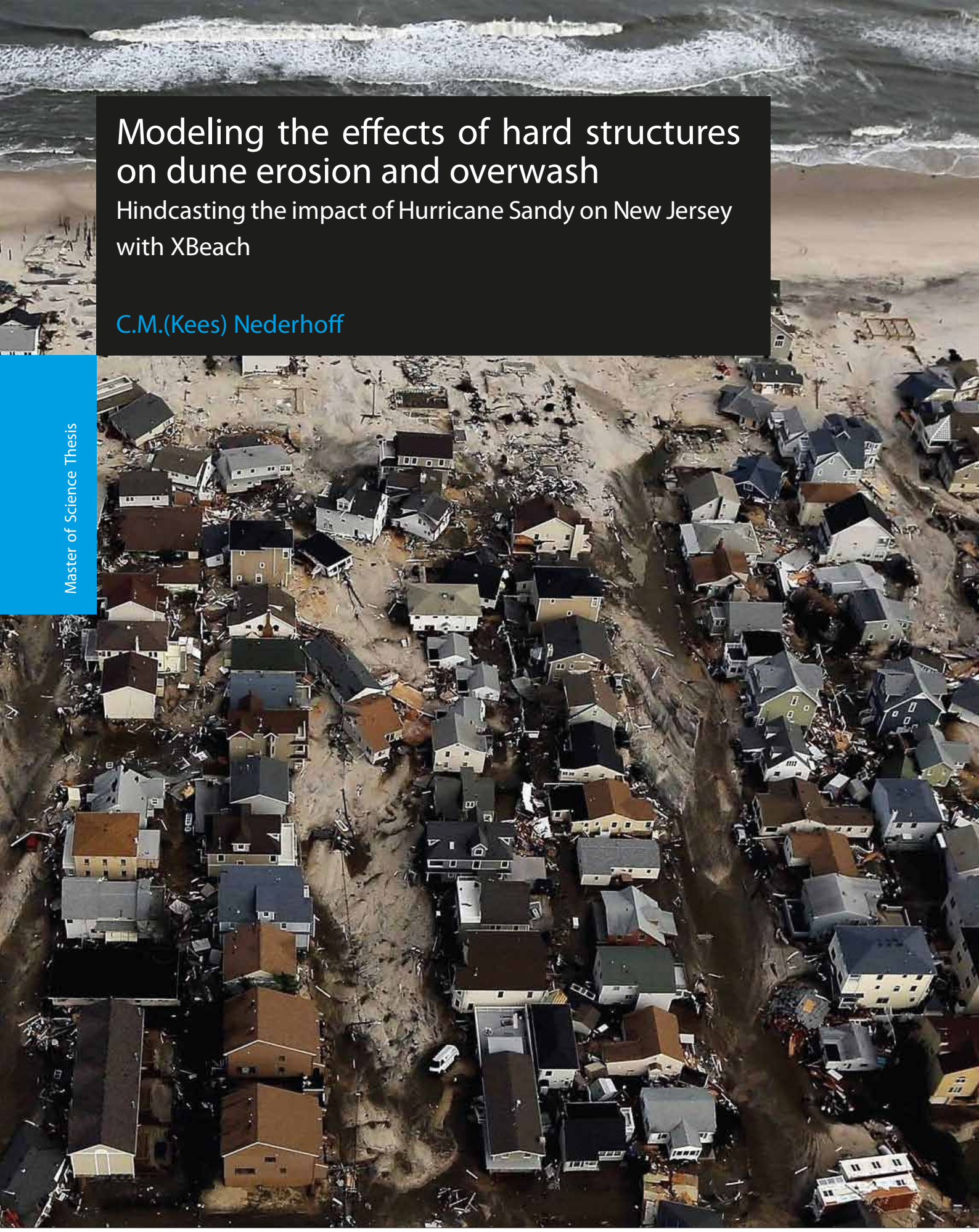

TU Delft Delft University of Technology

Rijkswaterstaat
Ministerie van Infrastructuur en Milieu

Deltares
Enabling Delta Life

Challenge the future

Front cover: During Hurricane Sandy, a combination of storm waves and surge cut across the barrier island at Mantoloking, NJ, eroding a wide beach, destroying houses and roads, depositing sand up the barrier island and into the back bay. [Source: NJ.com]

Modeling the effects of hard structures on dune erosion and overwash

Hindcasting the impact of Hurricane Sandy on New Jersey with XBeach

by

C.M. (Kees) Nederhoff

in partial fulfillment of the requirements for the degree of

Master of Science
in Civil Engineering

at the Delft University of Technology,
to be presented in public on Monday the 14^{th} of November 2014 at 15:00h.

Thesis committee	Prof. Dr. Ir. M.J.F. Stive	Delft University of Technology
	Drs. Q.J. Lodder	Rijkswaterstaat
	Dr. Ir. M. Boers	Deltares
	Ir. J.P. den Bieman	Deltares
	Dr. Ir. A.P. van Dongeren	Deltares
	Dr. Ir. M. Zijlema	Delft University of Technology

An electronic version of this thesis is available at http://repository.tudelft.nl/.

Preface

This thesis concludes the Master of Science program in Civil Engineering at Delft University of Technology, the Netherlands. This thesis has been carried out at Deltares, Rijkswaterstaat and Stevens Institute of Technology.

I would like to thank all my supervisors for the opportunity to work with them on this interesting project. I very much enjoyed working with Quirijn Lodder who gave me the freedom to find my own path within this research. I would also like to thank Joost den Bieman for his detailed feedback and XBeach help, Marien Boers and Ap van Dongeren for the academic support from Deltares and Marcel Stive and Marcel Zijlema for the constructive meetings.

Apart from my supervisors I would like to thank John Miller, Omar Lopez-Feliciano and the other staff of Stevens for my pleasant stay at Stevens Institute of Technology in Hoboken, NJ. I am also grateful to my friends for making the last years enjoyable and my graduation colleagues at Deltares for the nice lunches and coffee breaks. Last, but certainty not least, special thanks to my parents for their encouragements and unconditional support.

C.M. (Kees) Nederhoff
Delft, October 2014

Summary

Introduction and problem description Many of the most densely populated areas are located near the coast. Climate change and population growth put more and more pressure on these coastal areas. As free space is becoming sparse, coastal disaster risk reduction plans need to be spatially efficient. In this thesis the sandy coast with hard structures, such as buildings or dune revetments, is addressed. These structures can either provide additional protection, enhance local erosion by developing a scour hole in cross-shore direction or result in extra retreat of the barrier in longshore direction. Field measurements and experimental data featuring these phenomena are scarce, but the measurements of the devastating impact of Hurricane Sandy (October 2012) on the New Jersey shore provides new model validation possibilities.

XBeach (Roelvink et al., 2009) is used in this thesis as a tool to describe the morphodynamic behavior and to investigate the importance of each individual process. The main objective of this thesis is to obtain a better understanding of the effects of hard elements on the erosion process during storm surges. This will be done by validating and evaluating existing theory, calculation rules and models both in a conceptual study and against three new field cases in New Jersey, USA, during Hurricane Sandy. The secondary objective is to determine how to calibrate XBeach in order to accurately reproduce overwash conditions, since the model currently shows substantial overestimation of the erosion rates.

Conceptual study and DnA calculation rules In a conceptual model the cross-shore and longshore effects of hard structures are reproduced. In cross-shore direction a structure cuts off the sediment supply to the beach. A positive effect is the prevention of erosion causing lower erosion volumes in hard cross-sections. One downside of a hard element is that less sediment can be deposited in the nearshore and therefore the efficiency of dissipating wave energy is lower (WL | Delft Hydraulics, 1987). This results in higher energetic conditions in front of the hard element, which can result in the development of a scour hole. Structures also have an impact in longshore direction. First of all, an alongshore exchange of sediment, driven by set-up differences, will result in less accretion. Second, locally higher short waves will result in more erosion. The impact of the hard element is that at the sides the barrier will retreat more (increased set-back). This increase in retreat is effective over certain length (influence length). Erosive processes are in XBeach for the collision regime responsible for 2/3 of the longshore effect.

In order to describe the longshore effect of hard structures, the DnA calculation rules are developed. In addition,Deltares and Arcadis (2013) suggested that the increased set-back is linearly related to the normal set-back at the side of a hard element. Next, the influence length linearly relates with the increased set-back. The DnA calculation rules are developed as conservative addition factor for DUROS+ (Van Gent et al., 2008). A comparison between the longshore effect calculated by DnA and simulated by XBeach confirms this conservatism. The average ratio between the two is a factor 2. Change in coastal or storm-induced parameters do not affect the predictability. In this thesis the

DnA calculation rules have been modified in order to describe the longshore effect of hard structures for overwash cases. This is achieved by formulating the output parameter *additional erosion in adjacent locations* (A_2) instead of the formulation of *increased set-back* (d_2). The conceptual study for the overwash regime confirms this modification.

Case study: calibrating XBeach and the impacts of hard structures For the case study, XBeach is calibrated by applying a two-step calibration approach. The first step is to increase the parameterized wave asymmetry sediment transport component ($facua$). A higher value will result in less net offshore sediment transport and is suitable for calibrating the collision regime. The second step is to increase roughness of the barrier. A higher roughness will result in less sediment transport on top of the barrier, and is applied to calibrate the overwash regime. With the suggested calibration approach a Brier Skill Score (BSS) of 0.83 and a bias of -0.21 m are achieved in hindcasting the impact of Sandy on Bay Head, NJ. This BSS score can be seen as *excellent* according to the classification of Van Rijn (2003).

In cross-shore direction a structure can result in the development of scour at the toe. However, in the post-Sandy bathymetry at the (buried) seawall, no scour holes were found. XBeach simulations have reproduced these profiles and suggest this is the result of infilling of scour after the peak of Sandy. In addition, it is concluded that the seawall was an effective protection method during Hurricane Sandy in reducing the amount of erosion and preventing overwash. For example: without the seawall the erosion volumes would have been 55% larger and a comparable level of protection could be achieved with an 18 m wide sandy dune.

In longshore direction a hard element can result in the extra erosion at the sides of the structure. XBeach simulations have shown that during Sandy the presence of a condo at Camp Osborne, NJ, resulted in 32% additional erosion in adjacent locations. Eventually, in the simulations, the weakened cross-section erodes even more due to backwash. This motion is driven by the second flood event from the bay, which results in a water level gradient from the bay to the sea. The effect is a further increase of erosion with 163%. The additional erosion occurred, however, mainly at the left side of the condo as a result of oblique wave attack. The influence length of the condo during Sandy was 266 m. Without this second flood event the modified DnA calculation rules would have predicted 87% of the additional erosion due to the presence of the condo.

Practical meaning: integrated coastal zone management (ICZM) The main effect of a structure is the impact on the sand balance (both cross-shore and longshore), by cutting of (part) of the sediment supply. This can result in an effective and spatial-efficient protection method, but also shown also downsides. Structures can for example result in the development of a scour hole in cross-shore direction and will have an impact in longshore direction via additional erosion in adjacent locations. These effects have been reproduced in the case study of Hurricane Sandy. However, this is no reason to state that multifunctional use of the barrier is *not* possible. Its applicability needs to be addressed case-by-case. Process-based models, like XBeach, can accurately reproduce the cross-shore and longshore effects noticed in the field. The DnA calculation rules do not reflect the true complexity, but can give a rough first indication of the longshore effect.

Acronyms

BSS	Brier Skill Score (Sutherland et al., 2004)
CRM	Coastal Relief Model (NGDC, 2014)
DnA	Calculation rules for a NWO derived by Deltares and Arcadis (2013)
DUCKS	Dynamic Underwater and Coastal Kinematic (Miller et al., 2009)
$facua$	Importance of the onshore directed asymmetric flow, keyword in XBeach
ICZM	Integrated Coastal Zone Management
$jetfac$	Option to mimic turbulence production near revetments, keyword in XBeach
LiDAR	Light Detection And Ranging
morfac	Morphological accretion factor
MSL	Mean Sea Level
NAP	Amsterdam Ordnance Datum 'Normaal Amsterdams Peil (NAP)', approximately equal to Mean Sea Level (MSL).
NAD83	North American Horizontal Datum of 1988
NAVD88	North American Vertical Datum of 1988. An American reference level comparable with the Dutch NAP and also approximately equal to MSL
NOAA	National Oceanic and Atmospheric Administration
NWO	Structure without a function in the flood defense. Acronyms from Dutch: Niet-Waterkerend Object (NWO). See Deltares and Arcadis (2013) for more information
sECOM	The Stevens Estuarine and Coastal Ocean Model (Orton et al., 2012)
SSL	Storm Surge Level
$swrunup$	Parametric relation to include short wave run-up, keyword in XBeach
RMSE	Root Mean Square Error
USACE	United States Army Corps of Engineers
USGS	United States Geological Services
UTM	Universal Transverse Mercator. A coordinate system that uses a 2-dimensional Cartesian coordinate system
UTC	Coordinated Universal Time is the primary time standard by which the world regulates clocks and time. The difference is -4 for Eastern Standard Time (EST) and +2 for Central European Time (CET)

Nomenclature

α_1	Constant used by WL | Delft Hydraulics (1993) to describe ΔA_B	[–]
α_2	Constant used by Deltares and Arcadis (2013) to describe increased set-back (d_2)	[–]
α_3	Constant which describes the ratio between erosion volume and retreat distance	$[m]$
β	Constant used for determining the increased erosion due to structures	[–]
Δ	Difference operator	[–]
γ_{ua}	Importance of the nonlinear velocity for sediment transport ($facua$)	[–]
λ	Constant used in DnA rules for influence length (l_2)	[–]
ρ	Density of water	$[kg.m^{-3}]$
ρ_s	Density of sediment	$[kg.m^{-3}]$
σ	Intrinsic wave frequency	$[s^{-1}]$
τ_b	Bed shear stress	$[kg.m^{-1}.s^{-2}]$
τ_s	Wind shear stress	$[kg.m^{-1}.s^{-2}]$
θ	Angle of incidence with respect to x	$[rad]$
A	Surface	$[m^2]$
A	Wave action density	$[J.m^{-2}.s^{-1}]$
A_0	Difference in cross-sectional area of the soft (A_A) and hard cross-section (A_B)	$[m^2]$
A_0	Normal erosion *not* in the erosion zone of a structure	$[m^3.m^{-1}]$
A_1	Normal erosion *in* the erosion zone of a structure	$[m^3.m^{-1}]$
A_2	Additional erosion in adjacent locations due to the presence of a structure	$[m^3.m^{-1}]$
A_{ero}	Erosion volume	$[m^3.m^{-1}]$
A_{sb}	Coefficient bed load sediment transport formulation van Rijn (2007)	[–]
A_{sb}	Coefficient suspended sediment transport formulation van Rijn (2007)	[–]

A_s	Wave asymmetry parameter	$[m.s^{-}1]$
C	Chezy parameter	$[m^{0.5}.s^{-1}]$
C	Depth-averaged sediment concentration	$[m^3.m^{-3}]$
c	Wave propagation velocity	$[m^{0.5}.s^{-1}]$
c_f	Dimensionless bed roughness coefficient	$[-]$
c_g	Wave group propagation velocity	$[m^{0.5}.s^{-1}]$
C_{eq}	Depth-averaged equilibrium sediment concentration	$[m^3 m^{-3}]$
D	Dune height	$[m]$
D	Sediment particle size	$[m]$
d_0	Normal dune set-back before a structure is present in cross-shore direction	$[m]$
d_1	Normal dune set-back at the side of a structure in cross-shore direction	$[m]$
d_2	Increased set-back due to the presence of a structure in the dunes	$[m]$
D_h	Horizontal sediment diffusion coefficient	$[m^2.s^{-1}]$
$d_{2,red}$	Reduced increased set-back, formulated in this thesis	$[m]$
D_{50}	Medium sediment particle size	$[m]$
D_{max}	Dune top level	$[m]$
D_{roller}	Dissipation term for roller energy	$[W.m^{-3}]$
D_{SSL}	Relative dune height above SSL	$[m]$
D_s	Sediment diffusion component	$[m^2.s^{-1}]$
D_{waves}	Dissipation term for waves	$[W.m^{-3}]$
dz_{max}	Maximum dune face erosion rate	$[m^3.ms^{-1}]$
E_{roller}	Roller energy density	$[J.m^{-2}.s^{-2}]$
E_{waves}	Wave energy density	$[J.m^{-2}.s^{-2}]$
F	Wave force	$[N.m^{-2}]$
f	Coriolis coefficient	$[s^{-1}]$
f_{mor}	Morphological acceleration factor ($morfac$)	$[m.s^{-}1]$
g	Gravitational acceleration constant	$[m.s^{-2}]$
h	Wave depth	$[m]$

h_0	Difference between the closure depth and the depth of the structure	$[m]$
h_A	Depth of closure	$[m]$
h_i	Depth of the structure	$[m]$
H_{m0}	Spectral wave height = $\sqrt{2}.H_{rms}$	$[m]$
H_{rms}	Root mean square wave height	$[m]$
h_{switch}	Water depth at the interface $m_{cr,wet}$ and $m_{cr,dry}$	$[m]$
k_s	Sand roughness of Nikuradse	$[m]$
k_b	Turbulence energy near the bed	$[m^2.s^{-2}]$
L	Length	$[m]$
l_2	Influence length due to presence of a structure in the dunes	$[m]$
L_0	Deep water wave length	$[m]$
m_{cr}	Critical slope for avalanching	$[-]$
n	Manning roughness coefficient	$[-]$
n	Porosity	$[-]$
P	Retreat point	$[m]$
R	Hydraulic radius	$[m]$
R	Retreat line	$[m]$
R	Run-up	$[m]$
S	Radiation stress	$[N.m^{-1}]$
S	Sediment transport	$[m^2.s^{-1}]$
S	Storm Surge Level (SSL)	$[m]$
s	Directional spreading	$[-]$
S_k	Wave skewness parameter	$[-]$
T	Wave period	$[s]$
t	Time	$[s]$
T_p	Peak wave period	$[s]$
$T_{m-1.0}$	Spectral mean wave period	$[s]$
T_s	Adaptation time in the advection diffusion equation	$[s]$

u	Flow velocity in cross-shore direction	$[m.s^{-1}]$
u^E	Eulerian velocity in cross-shore direction	$[m.s^{-1}]$
u^L	Lagrangian velocity in cross-shore direction	$[m.s^{-1}]$
u^s	Stokes drift in cross-shore direction	$[m.s^{-1}]$
u_A	Mean flow component due to nonlinear waves	$[m.s^{-1}]$
u_{cr}	Critical flow velocity above which sediment is enforced	$[m.s^{-1}]$
u_{rms}	Orbital velocity	$[m.s^{-1}]$
V	Volume	$[m^3]$
v	Flow velocity in longshore direction	$[m.s^{-1}]$
v^E	Eulerian velocity in longshore direction	$[m.s^{-1}]$
v^L	Lagrangian velocity in longshore direction	$[m.s^{-1}]$
v^s	Stokes drift in longshore direction	$[m.s^{-1}]$
W	Width of the structure	$[m]$
w_s	Sediment fall velocity	$[m.s^{-1}]$
x	Cross-shore axis coordinate	$[m]$
y	Longshore axis coordinate	$[m]$
z	Vertical axis coordinate, upward is positive	$[m]$
z_b	Bed level	$[m]$
z_s	Water level	$[m]$

List of Figures

1.1 Pre- and post-storm oblique photographs of Camp Osborne 1
1.2 Visualization of the (global) structure of this thesis 4

2.1 Definition of nearshore areas, adapted from USACE (2008). 5
2.2 Principle sketch of dominant wave frequency nearshore 7
2.3 Definition sketch of different storm regimes 9
2.4 Response in cross-shore as a result of overwash 10
2.5 Three types of depositional features of overwash 10
2.6 Sketch of the processes involved in the effects of hard structures 12
2.7 DUROS morphological response parameters 14
2.8 Overview of the DnA approach used for NWO's 15

3.1 Used reference profile in the conceptual study for the collision regime 17
3.2 Used configurations in the conceptual study for the collision regime 18
3.3 Development of the bed level for 1D conceptual collision 19
3.4 Development of a single cross-section over time for 1D conceptual collision 19
3.5 Development of short and long waves for 1D conceptual collision 20
3.6 Analysis of the effects of SSL for 1D conceptual collision 21
3.7 Spatial bed level plot for different configuration for 2DH conceptual collision 23
3.8 Three dimensional plot of the bed and sea levels for 2DH conceptual collision 23
3.9 Cross-section of the bed level for 2DH conceptual collision 24
3.10 Development of R and A_{ero} for 2DH conceptual collision 24
3.11 Alongshore retreat line for 2DH conceptual collision 25
3.12 Causes for impact variation between hard and soft for 2DH conceptual collision 26
3.13 Decomposed sediment (B1 vs. A) for 2DH conceptual collision 28
3.14 Decomposed sediment (C1 vs. A) for 2DH conceptual collision 28
3.15 Relation between A_{ero} and R for 2DH conceptual collision 28
3.16 Alongshore erosion patterns for 2DH conceptual collision 29
3.17 The effects of a hard structure for 2DH conceptual collision 31
3.18 Alongshore retreat for various wave angles for 2DH conceptual collision 31
3.19 Factorial deviation for A_{ero} and d_2 for 2DH conceptual collision 32
3.20 DnA values in terms of d_2 and l_2 for 2DH conceptual collision 33
3.21 Retreat line for the sensitivity analysis of 2DH conceptual collision 34
3.22 Used reference profile in the conceptual study for the overwash regime 36
3.23 Used configurations in the conceptual study for the overwash regime 37
3.24 Development of the bed level for 1D conceptual overwash 38
3.25 Development of the retreat and erosion for 1D conceptual overwash 38
3.26 Alongshore erosion patterns for 2DH conceptual overwash 40

4.1 Track of Hurricane Sandy 42

4.2 Map of the area of consideration for the case study 44
4.3 Two examples of damage after Hurricane Sandy 46
4.4 Two examples of depositional features in the field 46
4.5 Locations of the information sources for water and wave data 48
4.6 Nesting of XBeach in Delft3D and eSCOM 49
4.7 Boundary conditions imposed in XBeach 49
4.8 Images of the impact of Sandy at the seawall 50
4.9 Measurements and simulations for the bed level of Profile 7 at the seawall 51
4.10 Bed level development over time at the seawall 51
4.11 Bed level difference for measurements and XBeach at the seawall 52
4.12 Development of the erosion and scour at the seawall 52
4.13 Simulations and measurements for the bed level of Profile 5 at the seawall 53
4.14 Development of the morphological skill over time for Profile 7 at the seawall 54
4.15 Post bed level for various values for $facua$ at the seawall 54
4.16 Post bed level for multiple what-if simulations at the seawall 55
4.17 Satellite images of the impact of Sandy at Bay Head 58
4.18 LiDAR data both pre- and post-Sandy at Bay Head 59
4.19 Several cross-sections for the bed levels at Bay Head 59
4.20 Spatial post bed level plot and sedero at Bay Head 60
4.21 Alongshore distribution of the maximum crest height at Bay Head 61
4.22 Barrier volume above SSL at Bay Head 61
4.23 Morphological performance indicators for the simulation at Bay Head 62
4.24 Post bed levels for various cross-sections for various values of Chezy at Bay Head . . . 63
4.25 Water marks both measured and modeled in XBeach at Bay Head 66
4.26 Cross-sections for the post bed level for the avalanching analysis at Bay Head 67
4.27 Satellite images of the impact of Sandy at Camp Osborne 69
4.28 LiDAR data both pre- and post-Sandy at Camp Osborne 70
4.29 Several cross-sections for the bed levels at Camp Osborne 70
4.30 Cross-sections of the bed level over time at Camp Osborne 71
4.31 Morphological evolution after 40 hours at Camp Osborne 72
4.32 Morphological evolution between 40-48 hours at Camp Osborne 72
4.33 Morphological evolution between 48-50 hours at Camp Osborne 73
4.34 Morphological evolution between 52-72 hours at Camp Osborne 73
4.35 Three dimensional plot pre- and post-Sandy at Camp Osborne 74
4.36 Spatial post bed level at Camp Osborne 75
4.37 Cross-sections of the bed level at Camp Osborne 76
4.38 Alongshore distribution of the maximum crest height at Camp Osborne 76
4.39 Development of the alongshore erosion volumes at Camp Osborne 77
4.40 Barrier volume above SSL at Camp Osborne 77
4.41 Morphological performance indicators at Camp Osborne 78
4.42 Alongshore erosion volumes at Camp Osborne 80

A.1 Time and spatial scales of hydrodynamics 99
A.2 The coordinate system used in XBeach (Roelvink et al., 2010) 100
A.3 Different modules in XBeach, arrows indicate connectivity (Daly, 2009) 100
A.4 Definition sketch of wave asymmetry (left) and skewness (right). 106
A.5 Meaning of various Chezy and Manning values in terms of k_s 107

C.1 Development of the Eulerian velocity for 1D conceptual collision 113

C.2 Development of the sediment concentration for 1D conceptual collision 114
C.3 Development of the sediment transport for 1D conceptual collision 115
C.4 Wave heights and Eulerian velocities for 2DH conceptual collision 118
C.5 Sediment concentration and transport for 2DH conceptual collision 118
C.6 Morphological response for configuration C for 2DH conceptual collision 120
C.7 Comparison for the z_b and $H_{RMS,LF}$ for oblique 2DH conceptual collision 121
C.8 Comparison for the v_E and C for oblique 2DH conceptual collision 121
C.9 Decomposed eroded sediment for oblique 2DH conceptual collision 122
C.10 Factorial deviation for retreat for 2DH conceptual collision 124
C.11 Retreat line alongshore for variation of the front position of the structure 126
C.12 Retreat line alongshore for variation of the width of the structure 126
C.13 Retreat line alongshore for variation of the length of the structure 126
C.14 Increased set-back for variation of the front position of the structure 127
C.15 Increased set-back for variation of the width of the structure 127
C.16 Increased set-back for variation of the length of the structure 127
C.17 Sedero patterns for the sensitivity analysis of 2DH conceptual collision 129
C.18 Development of the retreat line over time for 2DH conceptual collision 130
C.19 Sediment components for 1D conceptual overwash 132
C.20 Scour and erosion analysis for 1D conceptual overwash 133
C.21 Spatial bed level plot for 2DH conceptual overwash 133
C.22 Accretion and erosion plot for Profile 1 for 2DH conceptual overwash 134

D.1 General photo's of the impact of Sandy 135
D.2 Oblique photo at Bay Head 136
D.3 Overview and detail images of Bay Head 136
D.4 Oblique photo at Camp Osborne 137
D.5 Overview and detail images of Bay Head 137

E.1 LiDAR-data of Mantoloking by the USGS 139
E.2 LiDAR-data of Bay Head by the USGS 139
E.3 Profiles of the barrier island near Camp Osborne, New Jersey 139
E.4 Nearshore profiles of the barrier island at Camp Osborne, NJ 140
E.5 Fit between bathymetric sources 141
E.6 Pre-Sandy model bathymetry for Bay Head 141
E.7 Model grid coverage for Bay Head 142

F.1 Water and wave levels during Sandy as modeled by Delft3D 144
F.2 Development of Sandy as modeled by Delft3D 144
F.3 Water levels plotted for four stations and models Delft3D plus eSCOM 146
F.4 Wave heights plotted for two measurement stations and Delft3D 147
F.5 Multiple measurement points in the bay 148

G.1 Post storm bed level for various values for $facua$ at a soft cross-section 150
G.2 Post storm bed level for variations in boundary conditions at the seawall 151
G.3 Scour and erosion analysis for SSL variation at the seawall 152
G.4 Post storm bed level in a sensitivity analysis at the seawall 153
G.5 Three dimensional plot of z_s and z_b pre- and post-Sandy at Bay Head 155
G.6 Three dimensional plot for a Chezy analysis at Camp Osborne 156
G.7 Spatial post bed level for multiple values for D_{50} at Bay Head 157
G.8 Alongshore water marks modeled by XBeach at Bay Head 158

G.9 Spatial plot of the short waves for two roughness options at Bay Head 159
G.10 Spatial plot of the long waves for two roughness options at Bay Head 159
G.11 Spatial plot of the Eulerian velocity for two roughness options at Bay Head 159
G.12 Spatial bed level plot for the morfac options at Bay Head 166
G.13 Spatial bed level comparison for the morfac options at Bay Head 167
G.14 Alongshore maximum crest height for the morfac analysis at Bay Head 167
G.15 Difference in the alongshore erosion volumes for the morfac at Bay Head 167
G.16 Spatial bed level plot for morfac options at Camp Osborne 168
G.17 Spatial bed level comparison for morfac options at Camp Osborne 169
G.18 Alongshore maximum crest height for the morfac analysis at Camp Osborne 169
G.19 Difference of the alongshore erosion volumes for morfac at Camp Osborne 169

List of Tables

3.1 Parameters used in the conceptual study for the collision regime 17
3.2 Configurations used in the conceptual study for the collision regime 18
3.3 Morphological response in DUROS output parameters for conceptual collision 22
3.4 DnA morphological response parameters for 2DH conceptual collision 25
3.5 Sediment exchange rates for 2DH conceptual collision 27
3.6 Parameters in the conceptual study for the overwash regime 36
3.7 Configurations used in the conceptual study for the overwash regime. 37
3.8 Various simulations with different profiles in 2DH conceptual overwash 40

4.1 Simulation results for various cross-sections at the seawall 53
4.2 Comparison between measurement data and XBeach at Bay Head 62
4.3 Individual contribution of each calibration step at Bay Head 64
4.4 Comparison between measurement data and XBeach at Camp Osborne 78
4.5 Influence in terms of erosion of the condo at Camp Osborne 80

A.1 XBeach settings related to the avalanching algorithm 108

C.1 All the conceptual study simulations applied in this thesis 111
C.2 Multiple results with various wave angles for 2DH conceptual collision 122
C.3 Multiple sensitivity values for 2DH conceptual collision 124

E.1 Overview of the available bathymetry data sources 138

F.1 Overview of the available hydrodynamic data sources 143
F.2 Difference in bias and RMSE between the Delft3D and the eSCOM model 145

G.1 Results for various values for $facua$ at Profile 7 at the seawall 149
G.2 Results for various values for $facua$ at a soft cross-section 150
G.3 Results of variations in boundary conditions at the seawall 151
G.4 Result for variations in XBeach parameters for the seawall 153
G.5 Model performance of several values of barrier roughness at Bay Head 154
G.6 Morphological results for various values of D_{50} at Bay Head 157
G.7 Hydrodynamic results for various values of roughness at Bay Head 158
G.8 Model performance of several values of avalanching at Bay Head 160
G.9 Sensitivity in response for calibration steps at Camp Osborne 162
G.10 Influence of bay variation on the results at Camp Osborne 163
G.11 Sensitivity in response for variations in boundary conditions at Camp Osborne 164
G.12 Sensitivity in response for individual contributions in XBeach at Camp Osborne . . .164
G.13 Model performance indicators for the morfac analysis at Bay Head 166
G.14 Model performance indicators for the morfac analysis at Camp Osborne 168

Table of Contents

Preface i

Summary ii

List of Acronyms iv

Nomenclature viii

List of Figures ix

List of Tables xiii

Table of Contents xvi

1 Introduction 1
- 1.1 Background . . . 1
- 1.2 Problem description . . . 2
- 1.3 Objective . . . 2
- 1.4 Research questions . . . 3
- 1.5 Approach and outline . . . 3

2 Literature study 5
- 2.1 Coastal terminology . . . 5
- 2.2 Infragravity waves: causes and effect . . . 6
- 2.3 Morphological processes . . . 7
  - 2.3.1 General aspects of sediment transport . . . 7
  - 2.3.2 Storm regimes of Sallenger (2000) . . . 8
  - 2.3.3 Effects of hard structures on erosion . . . 11
- 2.4 Dune erosion models . . . 13
  - 2.4.1 DUROS . . . 13
  - 2.4.2 XBeach . . . 13
  - 2.4.3 DnA calculation rules . . . 15

3 Conceptual study 16
- 3.1 Introduction . . . 16
- 3.2 Model set-up . . . 16
  - 3.2.1 Dune profile: schematic reference profile . . . 16
  - 3.2.2 Applied boundary conditions . . . 17
  - 3.2.3 Baseline configuration . . . 17
- 3.3 Results 1D: cross-shore effect . . . 18
  - 3.3.1 Reproduction theory: impact structures . . . 18

3.3.2 Parameters affecting the impact of structures . . . 19
3.3.3 Effects of water level variations . . . 21
3.3.4 Conclusion . . . 22
3.4 Results 2DH: cross-shore and longshore effects . . . 22
3.4.1 Reproduction theory: impact structures . . . 22
3.4.2 Parameters affecting the impact of structures . . . 26
3.4.3 Sand volume balance: accretion versus erosion . . . 27
3.4.4 Wave obliquity: cause and impact . . . 29
3.4.5 Sensitivity analysis . . . 31
3.4.6 Conclusion . . . 35
3.5 Conceptual overwash . . . 36
3.5.1 Model-set-up . . . 36
3.5.2 1D results: cross-shore effect . . . 37
3.5.3 2DH Results: cross-shore and longshore effects . . . 39
3.5.4 Conclusion: cause and impact of storm regime variation . . . 41

4 Case study **42**
4.1 Introduction . . . 42
4.2 New Jersey into perspective . . . 44
4.3 Description of available data . . . 45
4.3.1 Morphodynamics . . . 45
4.3.2 Hydrodynamics . . . 47
4.4 Buried seawall: cross-shore effect . . . 50
4.4.1 Introduction . . . 50
4.4.2 Data analysis: using DUCKS . . . 50
4.4.3 Base simulation results . . . 51
4.4.4 Morphological calibration and skill: facua . . . 53
4.4.5 Absence of a hard element: beach or dune extension? . . . 55
4.4.6 Model sensitivity . . . 55
4.4.7 Conclusion . . . 57
4.5 Bay Head: modeling overwash with XBeach . . . 58
4.5.1 Introduction . . . 58
4.5.2 Data analysis: LiDAR provided by USACE . . . 58
4.5.3 Base simulation results . . . 60
4.5.4 Morphological calibration and skill: Chezy . . . 62
4.5.5 Hydrodynamic conditions: evaluate and reproduce . . . 65
4.5.6 Model sensitivity: avalanching algorithm . . . 67
4.5.7 Conclusion . . . 67
4.6 Camp Osborne: effects of a condo . . . 69
4.6.1 Introduction . . . 69
4.6.2 Data analysis: LiDAR provided by USGS . . . 69
4.6.3 Base simulation results . . . 71
4.6.4 Morphological skill . . . 78
4.6.5 The effects of the hard structure . . . 79
4.6.6 Model sensitivity . . . 81
4.6.7 Conclusion . . . 83

5 Discussion **85**
5.1 General . . . 85

5.2 Case study specific 86

6 Conclusion **87**
6.1 Conclusion towards the thesis objective 87
6.2 Conclusion towards the research questions 88
6.2.1 First objective: effects of a hard structure 88
6.2.2 Second objective: calibration method XBeach 90

7 Recommendations **92**

Bibliography **94**

Appendix A Description of XBeach **99**

Appendix B Evaluation method **110**

Appendix C Supportive material for conceptual study simulations **111**

Appendix D Aerial and satellite photographs of the impact of Sandy **135**

Appendix E Bathymetric data sets used **138**

Appendix F Hydrodynamic conditions used **143**

Appendix G Supportive material for the case study simulations **149**

Chapter 1

Introduction

1.1 Background

Worldwide, many of the most densely populated areas are located near the coast. Climate change and population growth put more and more pressure on these coastal areas. As free space is becoming sparse, coastal disaster risk reduction plans need to be spatially efficient. For example, for the Netherlands, Deltares (2011b) explored the possibilities of applying several functions to the coastal area and stated that multifunctional use of the barrier could be possible, but for this functionality more fundamental knowledge is needed about the behavior of hard structures in these coastal areas. Figure 1.1 shows the devastating impact of a Hurricane Sandy (October 2012) on the morphology around a condo at Camp Osborne, Brick, NJ. One hypothesis is that hard structures, such as this condo, result in extra erosion.

XBeach (Roelvink et al., 2009) is used in this thesis as a tool to describe the morphodynamic behavior and to investigate the importance of each individual process. XBeach is a nearshore numerical model to assess the natural coastal response during storm and hurricane conditions including dune erosion, overwash and breaching. XBeach is depth-averaged and solves 2DH equations for long wave propagation, short wave energy, flow, sediment transport and bottom changes. The XBeach version applied in this thesis is 1.21.3657 with the code name 'Groundhog Day'.

Figure 1.1 *Pre- and post-storm oblique aerial photographs of the impact of Hurricane Sandy (2012). Pictured is a dominant placed condo in the barrier of Camp Osborne, Brick, NJ. The hypothesis is that additional erosion in the overwash fan left of the condo was a result of the condo itself. Pictures are taken on 21/05/2009 and 05/11/2012. Taken from the U.S. Geological Survey (USGS) website.*

1.2 Problem description

The processes related to the response of the sandy coast during storm conditions are relatively well understood. For example, in the Netherlands, the DUROS+ model (Van Gent et al., 2008) is the prescribed model for the safety assessment of the dunes. In situations where the safety assessment with the DUROS-model is not adequate, coastal zone managers can decide to use more generic models. Several comparisons between process-based models such as XBeach or DUROSTA (Steetzel, 1993) have been carried out (Van Thiel de Vries, 2009b; Den Heijer, 2013)

This level of knowledge is not present for the impact of a hard element or the impact of a hard-soft transition on the amount of erosion during storm surges. The effects which have been described in theory and in experiments are divided in:

1. **Cross-shore direction**. Experiments (WL | Delft Hydraulics, 1987) have reproduced the development of scour holes during storm surges, both in front and behind hard elements. This effect has been reproduced in a process-based model (Van Thiel de Vries, 2009a). Structures can however also provide additional protection, since it cuts (part) of the sediment supply to the beach.
2. **Longshore direction**. Flume experiments (Boers et al., 2011) have shown that structures can result in an increased set-back of the dune. This effect has been reproduced in a process-based model (Van Geer et al., 2012). In order to describe this effect calculation rules are derived to determine the increase in dune retreat (Deltares and Arcadis, 2013).

Field measurements and experimental data featuring these phenomena are scarce, but the measurements of the devastating impact of Hurricane Sandy on the New Jersey shore provides new model validation possibilities. The downside of this case study is the storm regime (overwash), since most of the theory is developed for the collision regime. In order to hindcast the impact of hard elements and to investigate the influence of individual processes a process-based model such as XBeach can be used.

XBeach has been designed to describe all the regimes of Sallenger (2000), but in various studies overwash modeling with XBeach resulted in overestimation of the morphodynamic changes (McCall, 2008; McCall et al., 2010b; Den Bieman, 2012). When the Shields number in sediment stirring equations was limited to one, better scores were obtained. However, this limiting has unexpected side effects (Terlouw, 2013; De Vet, 2014).

1.3 Objective

The first objective of this thesis is to obtain a better understanding of the effects of hard elements on the erosion process during storm surges both for the collision and overwash regime. This will be done by validating existing knowledge, calculations rules and models both in a conceptual study, as well as against new field cases in New Jersey, USA, during Hurricane Sandy. The second objective is to determine how to calibrate XBeach in order to accurately reproduce overwash conditions.

1.4 Research questions

In order to fulfill the first objective described, six research questions (Rq.) are formulated. These research questions are intended for the conceptual study and the case study.

1. Which (forcing) mechanisms are responsible for scour holes (cross-shore effect) and increased set-back (longshore effect) and what is the impact of the effects mentioned?
2. Does XBeach simulate all these (forcing) mechanisms and does the simulations result in the expected impact? If not, how and with which contributions can the cross-shore and longshore effects be reproduced?
3. In what way does wave obliquity has an influence on the effects of hard elements?
4. What is the sensitivity of the morphological behavior of the barrier and especially for the effects of hard elements for variations in coastal and storm-induced parameters?
5. What is the influence of variation in structural properties on the effects of hard elements?
6. What is the potential of describing the longshore effect of hard structures by the DnA calculation rules (Deltares and Arcadis, 2013)?

For the second objective the following two research questions (Rq.) are formulated. These questions are only related to the case study:

7. How can XBeach be calibrated in order to describe overwash conditions, without the use of artificial limiters, and what are the sensitive contributions for this approach?
8. What is the predictive skill of XBeach in reproducing the moprhodynamics for overwash conditions in field cases with the approach applied and what are the limitations of this approach?

1.5 Approach and outline

The research questions (Rq.) are addressed throughout several chapters, eventually leading to fulfilling the thesis objectives and answering the problem definition. In Figure 1.2 a visualization of this process is given. The total outline will contain three phases, knowing the literature study (phase 1), the conceptual study (phase 2) and the case study (phase 3).

First phase In the first phase a literature review will be carried out. This will focus on the hydrodynamic and morphological processes which play a role in the effects of hard structures during storm conditions. Both the description of these processes as well as models predicting the morphological behavior during storm surges are reviewed. The literature review can be found in Chapter 2.

Second phase The second phase will be used to present the conceptual model. In a conceptual study the complex spatial variability of the bed level is not taken into account. Therefore, it is possible to reproduce theory and analyze the contributions of individual parameters. The first parts of the second phase (Chapters 3.2 - 3.4) will focus on the collision regime and the last part will focus on the possibility of applying the derived knowledge for the overwash regime (Chapter 3.5). This last

step is needed to link our knowledge from the collision regime with the case study (overwash regime) and vice versa.

In the conceptual model for the collision regime the first target will be to model the development of scour holes (cross-shore effect) in an 1D XBeach model. The focus is to address the differences in hydrodynamic and morphological development between soft and hard cross-sections. Second, the more complex 2DH interaction of a hard structure is described. This includes both the development of scour as well as increased set-back (longshore effect) due to the presence of the structure. For the collision regime Dutch representative storm conditions, as described by Vellinga (1986) and Deltares and Arcadis (2013), are applied.

After identifying the causes and impacts of hard structures, more complex phenomena can be analyzed. First, the effects of wave obliquity on the cross-shore and longshore effects of hard elements are analyzed. This will be carried out by varying the main wave angle between normal incident waves and wave angles of +30 degrees with respect to shore normal. Second, the sensitivity for variation in coastal and storm-induced parameters is analyzed. This will be carried out by varying wave height, wave period, dune height above storm surge level (SSL) and by changing the sediment diameter. On top of that, the impact of structural properties is modeled in XBeach. This will be carried out by varying the width, length and position in cross-shore direction. The last part of the conceptual study for the collision regime will contain a sensitivity analysis of XBeach settings.

The last subsection of this chapter will be to derive the conceptual study for the overwash regime and to determine if and in what way the theory of the effects of hard structures (both cross-shore as well as longshore) are applicable for overwash conditions. The conditions applied are based on the case study of Hurricane Sandy in Chapter 4.

Third phase In the third phase the case study will be carried out. This will be done by analyzing the effects of hard structures (first objective) and done for calibrating XBeach for overwash conditions (secondary objective). The case study will contain three field cases during Hurricane Sandy. First, the focus will be on the 1D cross-shore effect of a buried seawall and calibration of the collision regime (Chapter 4.4). The second part will be used for the calibration of the overwash regime and to evaluate the predictability of XBeach in such conditions (Chapter 4.5). The last part will be used to analyze the longshore effect of a condo at Camp Osborne, NJ (Chapter 4.6). Validation of the morphological response is carried out based on the Brier Skill Score (BSS) and bias.

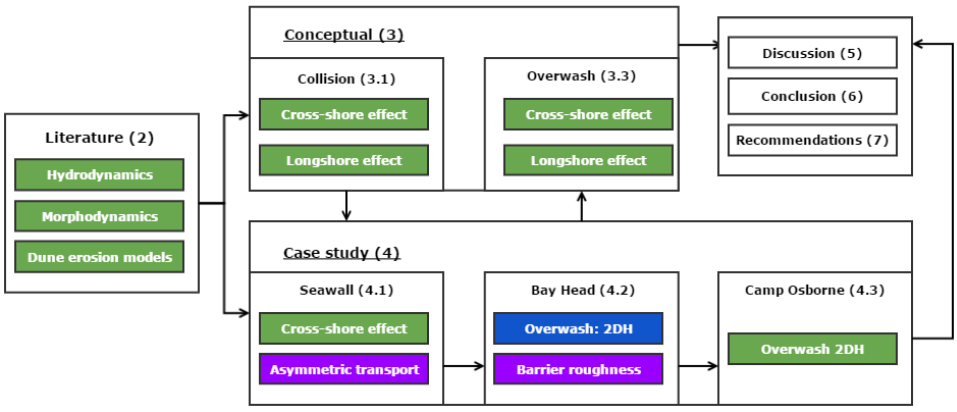

Figure 1.2 *Visualization of the structure of this thesis. Numbers between the brackets refer to the corresponding chapters. Blue blocks relate to the sandy barrier, green is used for the effects of hard structures and purple is defined as the calibration step.*

Chapter 2

Literature study

2.1 Coastal terminology

In this thesis references are made to a number of definitions describing areas in the coastal zone. The terminology from the Coastal Engineering Manual (USACE, 2008) is used. The most relevant aspects are explained below and visually presented in Figure 2.1.

The nearshore extends from the foreshore down to a water depth of 20 meters. More seawards the offshore starts. In the nearshore, waves start to break in the breaker zone, propagate up to the beach in the surf zone and eventually run-up and run-down can take place in the swash zone.

The beach is a combination of the foreshore and backshore where swash occurs.

The dunes are an important aspect to protect land from the sea. The foredune, or dune face, is the most seawards positioned dune. The dune top, or dune crest, is the top of the dune. For situations with **barrier islands** the area behind the dunes is called back barrier with eventually a back barrier bay. For situations without a bay, this is called hinterland.

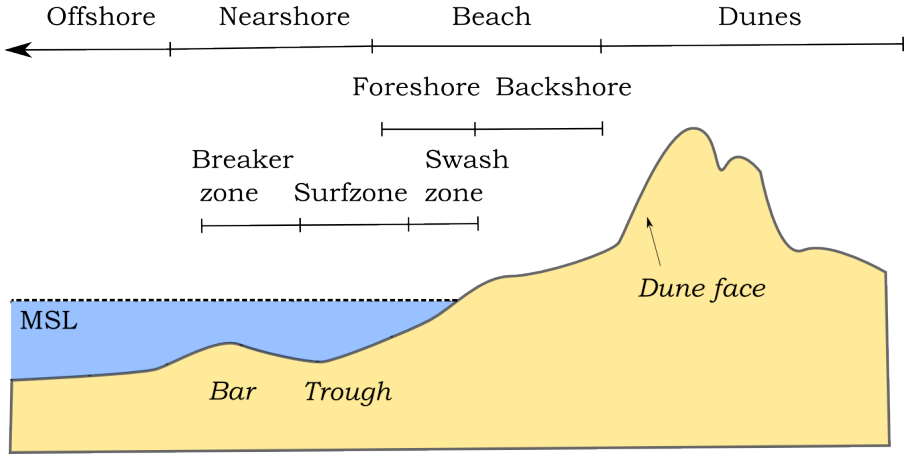

Figure 2.1 *Definition of nearshore areas, adapted from USACE (2008).*

2.2 Infragravity waves: causes and effect

General Waves in the surf zone often contain large amounts of energy at frequencies lower than the incident swell and wind waves (Bosboom and Stive, 2013). The wave period related to these low frequency waves are around 20 seconds up to several minutes and are called infragravity waves or long waves.

The mechanism of the generation of infragravity waves has been studied for the last fifty years. Long waves were first described by Munk (1949) and called 'surf beat', because he believed waves were generated in the surf zone by groups or beats. Longuet-Higgins and Stewart (1964) were the first to describe the release of the bound long wave.

Generation in deep water The theory of Longuet-Higgins and Stewart (1964) is based on the concept of wave radiation stress. When wave groups travels towards the shore an amplitude variation of short waves will result in a variation of radiation stress, since in regions with high wave energy the radiation stress is greater than in regions with low wave energy. This gradient in radiation stress can be seen as a force in the water which is opposed by a water surface gradient. The effect is that in regions with high short waves there will be a dip in the water level and in regions with lower short waves there will be a rise. This water level variation is called a long or infragravity wave.

The short and long wave have a phase difference of 180 degrees, because the short waves are responsible for the forcing behind the water level variation described as the long wave. Longuet-Higgins and Stewart (1964) speculated that long waves are bound to the wave groups and are 'released' when the short waves start to break. The term 'bound' is only used when the long and short wave travel at the same speed, which is the case in deep water.

Entering more shallow water All waves shoal when they enter more shallow water. The shoaling process for long waves is however different compared to short waves. This is due to the fact that long waves are less steep and wave energy is transferred from the short to the long wave. This is possible since short wave lead the long wave with the phase difference discussed in the previous paragraph.

In a recent study Van Dongeren et al. (2007) concluded that the growth rate of the incoming long wave during shoaling varies between the limit of Longuet-Higgins and Stewart (1964) ($\widehat{\eta_{lf}} \sim h^{-2.5}$) and Green's Law ($\widehat{\eta_{lf}} \sim h^{-1/4}$) and depends on dimensionless and normalized bed slope β. The β parameter is analogous to the surf similarity parameter or Iribarren parameter (Battjes, 1974). For steep slopes the growth rate is small. The converse is observed for small values of β.

The boundness of the long wave is related to the wave group scale. When the short waves start to break the forcing behind the bound long wave disappears and the long wave will be 'released'. Free long waves are released infragravity waves.

Reflection and dissipation Infragravity waves will partly dissipate and partly reflect in the surfzone. Little is known about the long wave dissipation process, but Van Dongeren et al. (2007) stated that the β value also controls the ratio reflection and long wave breaking, since long waves that are not dissipated will be reflected at the shore.

For normal incident waves it is most likely that long waves reflect away from the coast and escape to the nearshore. These waves are called leaky waves. It is also possible for waves to become trapped.

These waves are called edge waves (USACE, 2008).

Nearshore importance As short waves approach the shore, they start to break and eventually disappear in very shallow water. On the other hand, long waves have much longer wave lengths and are less steep than the incident short wave. Therefore, infragravity waves are less likely to break on the foreshore. In addition, as stated in previous paragraph, energy is transferred from the short to the long waves.

The combination of these two effects will result in long waves dominating the velocity and surface level amplitude in very shallow water. This dominance of energy is important for processes such as run-up and dune erosion as stated by Van Thiel de Vries (2009b) and visual presented in Figure 2.2.

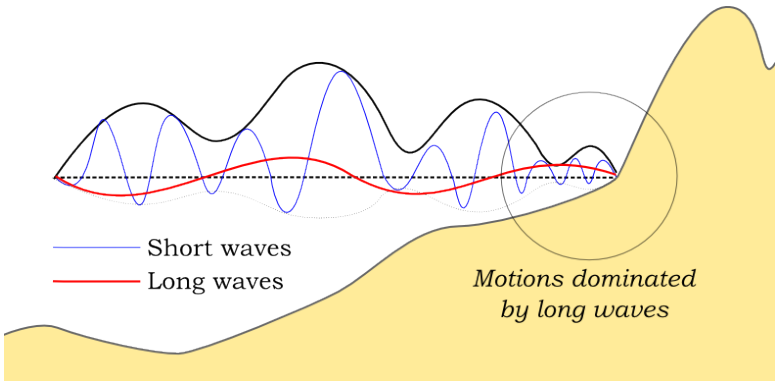

Figure 2.2 *Principle sketch of the dominant wave frequency nearshore, adapted from Deltares (2012).*

2.3 Morphological processes

The morphological processes can be divided into three subsections. First, sediment transport is discussed in 2.3.1. Second, the normal response of a coastal system is treated in 2.3.2. With normal response the effect of the storm forced parameters on a complete sandy dune or barrier is intended. In the last subsection the effects of hard structures on the dune erosion is described in 2.3.3.

2.3.1 General aspects of sediment transport

General Changes in coastal morphology are the result of gradients in net sediment transport (S). A net positive gradient means erosion and a negative gradient in sediment transport means deposition or accretion. In general sediment particles will start moving when a critical velocity (U_{cr}) or shear stress is exceeded. The interaction of hydrodynamics and sediment transport is very complex, but can be described with a basic continuity relation (also known as Exners' Law):

$$\frac{\partial z_b}{\partial t} + \frac{1}{1-n}\left(\frac{\partial S_x}{\partial x} + \frac{\partial S_y}{\partial y}\right) = 0 \tag{2.1}$$

In this formulation $\partial z_b/\partial t$ is used for the bed level change in the time, n is the porosity of the bed and $\partial q_x/\partial x$ is used for the gradient of the sediment transport in x-direction.

Sediment transport can be divided into bed transport, suspended transport and sheetflow. The difference between bed load and suspended load is that during bed load the sediment particles flow in a thin layer close to the bed and during suspended transport particles loose any contact with the bed. At higher shear stresses particles moves in multiple layers over the bed, which is known as sheet flow transport (Kobayashi et al., 1996).

Cross-shore transport Sediment transport in the cross-shore direction is a mix of multiple transport modes and is mainly caused by the vertical velocity profile generated by waves. Roelvink and Stive (1989) listed the most relevant cross-shore processes for morphological change by decomposing the third odd velocity moment:

1. **Short wave skewness**: nonlinear effects in wave propagation result in an increase of onshore velocity. Sediment transport is proportional to an exponent of the water velocity and therefore a wave-averaged net onshore transport under skewed waves is present.
2. **Undertow**: the presence of waves creates an onshore mass flux which is compensated by undertow. Sediment concentrations are higher near the bed and therefore the undertow causes a sediment transport offshore.
3. **Long waves**: long and short waves travel in anti-phase. When the short waves start to break two important processes occur. First wave breaking will result in turbulence and thus sediment is stirred up. This results in higher sediment concentrations. The second important process is the releasing of the bound long wave. The effect of the first process is sediment transportation in offshore direction, since during the period of short wave breaking (and thus higher sediment concentrations) the horizontal component of the orbital velocity of the long wave is offshore directed. The importance of the second process is that the offshore transport only occurs when the long and short waves travel in anti-phase. The released long wave will result in onshore sediment transport.

Practical applications In practical applications sediment transport is calculated as a total load by combining the quasi-steady bed load transport plus the current-related suspended sediment transport. The formulas used are empirical. It is common for these sediment predictions to vary in magnitude (Bosboom and Stive, 2013). Therefore, calibration of sediment transport formulas is important.

2.3.2 Storm regimes of Sallenger (2000)

General According to Sallenger (2000) the impact of storms on a barrier island does not only depend on the magnitude of the storm forced parameters, such as storm surge, waves and run-up, but is also dependent upon the geometry of the coastal dune. The hydrodynamic forcing is described by a maximum run-up R_{high}, maximum wave run-down R_{low}, a dune base D_{low} and a dune crest D_{high}, as demonstrated in Figure 2.3. Sallenger introduces four so-called impact levels or regimes.

1. **Swash**: run-up is confined to the foreshore.
2. **Collision**: wave run-up exceeds the threshold of the base of the dune.
3. **Overwash**: wave run-up occasionally exceeds the dune crest.
4. **Inundation**: storm surge completely and continuously submerges the dune crest.

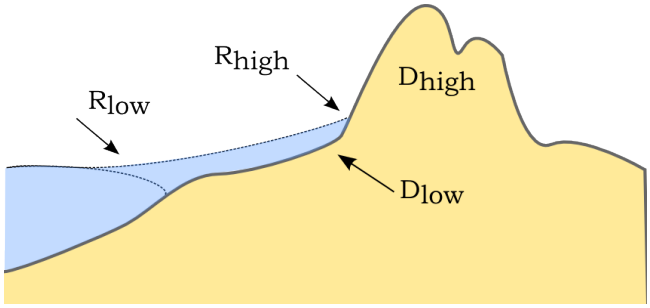

Figure 2.3 *Definition sketch describing variables used in scaling the impact of storms on the coastal dune system, adapted from Sallenger (2000). NB: the system is in the collision regime.*

Note: not all these regimes will occur during every storm. Smaller storms may only reach the collision regime. In the Netherlands, usually, only the swash and collision regime occurs, but for example during Hurricane Sandy all regimes occurred.

Swash regime The swash regime represents relativity low energy storm conditions. As stated in Sallenger (2000) such conditions lead to sediment transport from the foredune and the beach offshore. Generally, this sediment returns over a period of weeks up to months when forcing conditions return to less energetic levels.

Collision regime The collision regime is mostly associated with dune erosion. During a storm the MSL rises, set-up increases and waves are able to reach the dune face. The waves are much higher than usual and have a large impact on the dune. Episodically lumps of sediment slide on to the beach and are being transported seawards. Slumping down of sediment is called avalanching. Both short and long waves are important for the morphodynamic process in front of the dunes. Long waves are especially effective in triggering the avalanching of the dune face (Van Thiel de Vries, 2009b).

During a storm there is a large wave-induced mass flux towards the shore. The onshore mass flux is compensated by a strong undertow. The combination of this undertow with the high concentrations of sediment will result in a net transport offshore (Van Thiel de Vries, 2009b). Offshore the water depth increases and the undertow decreases, which will eventually result in settling of sediment.

A new coastal profile is formed during the storm. As the storm progresses the bottom in the surf zone rises. This new profile is more efficient in dissipating energy of the incoming waves and the break point moves more seaward. This results in two effects. First, less waves reach the dune face. Second, the waves that do reach the dune have less energy. As the storm progresses the long waves become relatively more important than short waves, because the dissipating effect of the rising nearshore has mainly an effect on the short waves. This is related to the steepness of the long waves and longer wave length of infragravity waves which result in limited dissipation in the nearshore. On top of that, energy is transferred from short to the long waves, as seen in Section 2.2.

After the storm the beach has become wider. The post-surge dune profile is not in equilibrium with *normal* forcing conditions. Therefore, the dune profile will start to reshape the bathymetry back towards to the original pre-surge dune profile. If the storm duration is long enough the post-surge profile is independent of the initial profile (Van Thiel de Vries, 2009b).

Overwash and inundation Sallenger (2000) associates overwash and inundation regimes with large depositions of sediment from the beach and dunes on the back barrier. Transport of sediment can take place over large distances. Although the forcing conditions differ between overwash and inundation, the morphological response has a less clear distinction.

Donnelly (2007) analyzed 50 pre- and post-storm cross-shore profiles and came to the conclusion that barrier islands have seven types of morphological response to overwash / inundation, as can be seen in Figure 2.4.

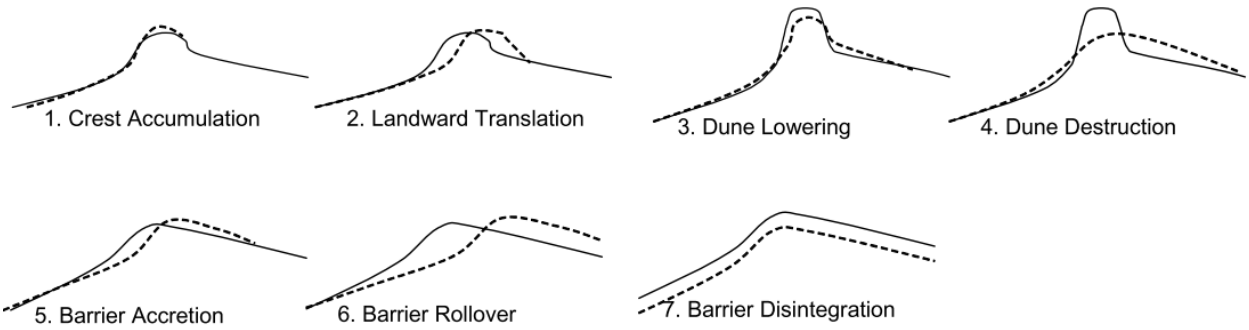

Figure 2.4 *Response of the cross-shore profile of different overwash types. Dotted line stands for the profile after an event (Donnelly, 2007).*

On coastlines with varying dune heights, overwash generally exploits existing gaps in the foredune. At a single overwash location water is funneled through the gap in the foredune. At this point the throat of the overwash fan is located. Sediment transport in the overwash event, the so-called washover, is deposited on the back barrier. The shape of this deposition also depends on the shape of the back barrier. In case of inundation, water flow is not constricted to these channels and weak spots. In that case the water flow covers the entire back barrier (Donnelly, 2007). In Figure 2.5 three depositional features are presented.

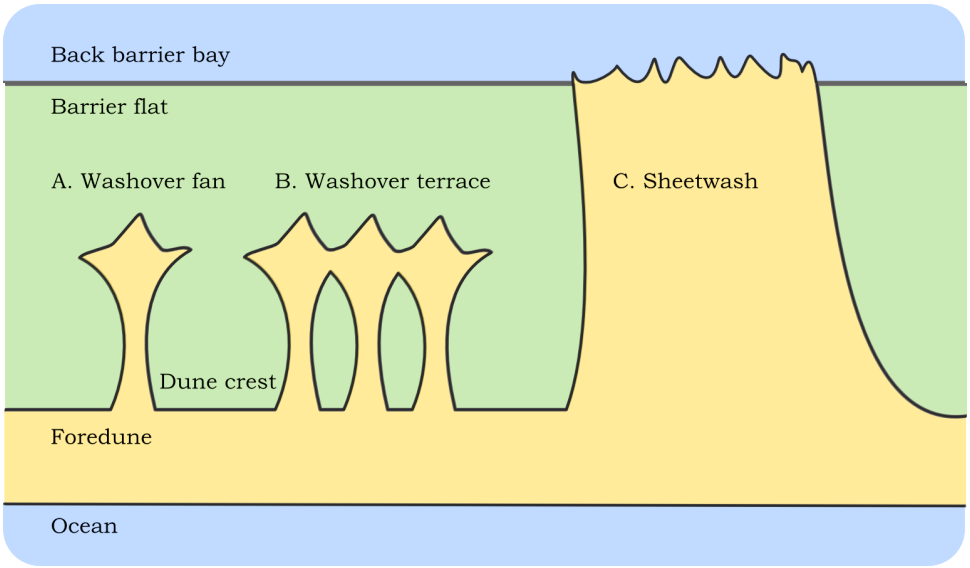

Figure 2.5 *Three types of depositional features: washover fan, washover terrace and sheetwash. Adapted from Donnelly et al. (2006).*

2.3.3 Effects of hard structures on erosion

General At several locations along the Dutch coast, the dune system contains hard elements such as dune foot revetments, seawalls, groins, breakwaters, dikes and buildings. During a storm surge the water level rises and the beach is flooded. The storm profiles develops and gets more dissipative via sediment, which is avalanching from higher areas and deposited further in seaward direction in the nearshore. In the presence of a structure the process of dune erosion is strongly affected both in cross-shore and in longshore direction, as visualized in Figure 2.6. Constructive elements, objects as well as hard structures in general can according to Deltares and Arcadis (2013) be distinguished in:

1. Structures **with a function in the flood defense**, such as for example dike-dune structures or seawalls.
2. Structures **without a function in the flood defense** (in Dutch: Niet-Waterkerend Object, known as acronym NWO), such as for example houses and hotels.

Cross-shore effect: scour at the toe In the cross-shore direction the dune face can be intersected with a hard element. The effect of such a structure is that sediment supply from the dune is (partly) blocked/replaced whereas the initial offshore transport capacity in front of the object remains. The lack of sediment prevents the coastal profile to adjust to the storm conditions.

In normal conditions sediment is transported from the coast and deposited in the nearshore. The effect is that the cross-section is more capable in dissipating wave energy. In front of the hard element this process can only partly occur and therefore the waves attacking the seawall remain high throughout the storm. The result is that sediment near the toe of the hard structure is brought into suspension and sediment is transported seawards. As a result a scour hole develops (WL | Delft Hydraulics, 1988).

The amount of scour at the toe of the revetment can vary considerably and depends on: where the waves break, if they reflect, overtop or break at the structure and on the sediment characteristics (Sumer and Fredsoe, 2002).

Longshore effect: increased set-back Besides the effect of hard structures in the cross-shore direction, also an alongshore interaction is expected. The hypothesis is that hard structures can locally increase the erosive processes which results in the order of 10 up to 20 meters increased set-back (d_2) (WL | Delft Hydraulics, 1993).

The general concept is that two profiles can be distinguished. An A-profile which is applicable for an undisturbed soft profile and a B-profile which is applicable for the situation with structures in it. At the transition location there is a large discontinuity in cross-sections and during the process of dune erosion this discontinuity will result in a longshore transport. In principle this will be done by subtracting material from the A-profile which is transported towards the B-profile. The relations describing this interaction are presented in Equation 2.2.

$$\begin{aligned} &\Delta A_B = \alpha_1 \left(A_A - A_B\right) = \alpha \cdot \Delta A_0 \\ &\text{in which } \alpha_1 = 1 - \frac{h_0 d_2}{\Delta A_0} \\ &\Delta V_B = \beta_B \cdot L_B \cdot \Delta A_0 \end{aligned} \tag{2.2}$$

In the derivation of WL | Delft Hydraulics a volume balance in combination with proportionality coefficient, α_1 and β, are used. WL | Delft Hydraulics (1993) is not clear which physical processes contribute to the processes observed. L_B stands for the influence zone of the B profile. A_A is an erosion volume per meter and V_A is a total erosion volume. h_0 is the difference between the closure depth and the height of the structure.

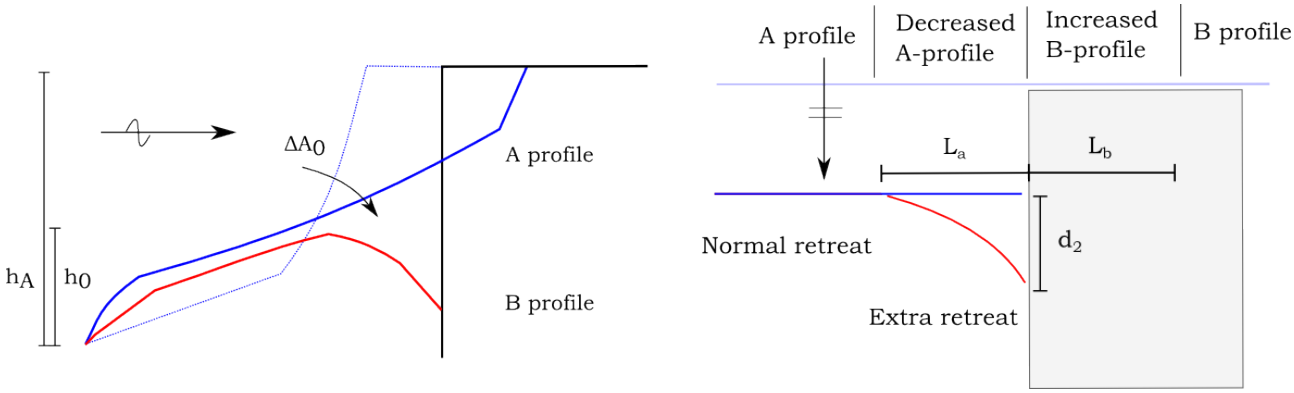

Figure 2.6 *Principle sketch of the processes involved in the effect of hard structures. Left the cross-shore effect (scour, side-view) and right the longshore effect (increased set-back, top-view). Adapted from WL | Delft Hydraulics (1993)*

In the paper of Van Geer et al. (2012) a list of 6 process-steps, responsible for the increase in erosion, is presented. The basis of this summary are laboratory experiments and numerical simulations in XBeach:

1. **Difference in bathymetry**: the B-profile has less supply of sediment than the A-profile. Therefore, the depth in the B-profile is larger than in the A-profile.
2. **Difference in wave breaking**: due to differences in depth waves break earlier at the dune. Therefore, the assumption that long waves dominate the dune erosion process is not completely valid with respect to the interaction between hard structures and the sandy dune (Deltares, 2012).
3. **Difference in water level set-up**: differences in wave breaking causes a difference in water level set-up. This results in a water level gradient from the dune towards the hard structure.
4. **Lateral sediment transport**: the alongshore current transports sediment from A towards the B-profile.
5. **Decrease in sedimentation nearshore**: sediment that was normally deposited in the nearshore of the A-profile is now deposited in the B-profile as a result of the alongshore current.
6. **Additional erosion of the dune front**: a consequence is that the bathymetry of the dune right next to the hard structure has a less dissipating nearshore. The effect is an increase in wave load and therefore erosion of the dune. On top of that, Boers et al. (2011) and Van Geer et al. (2012) pointed out phase differences will occur due to the fact waves are later on the dune than on the structure. This phase difference can cause an increase in erosion generated by an oscillating motion. It is however questionable if this results in a *net* sediment transport.

2.4 Dune erosion models

Over the last three decades several dune erosion models have been developed. Larson et al. (2004) stated that there are essentially two types of numerical dune erosion models: equilibrium profile theory models and wave impact approach models. In this section both the Dutch standard for assessment of dune erosion: DUROS, which is an empirical model, is described in Section 2.4.1. Additionally, the process-based model XBeach is presented. This part can be found in Section 2.4.2. In a process-based model the most important physical processes which drive dune erosion are modeled and coupled. This is a fundamental difference approach compared to empirical models and should be kept in mind, since an empirical model does not calculate the actual processes which take place. In addition the DnA calculation rules, that describe the longshore effect of hard structures on dune erosion, are presented in Section 2.4.3.

2.4.1 DUROS

General Vellinga (1986) carried out series of tests in order to develop an empirical dune erosion prediction model based on the equilibrium profile approach applicable for the Dutch coast. This model, DUROS, is based on the observation that a typical erosion profile develops during storm surges. According to Vellinga the profile can be represented as a function of the Storm Surge Level (SSL), wave height (H_s) and the settling velocity of the eroded sand (w_s).

Approach DUROS-models are based on two major assumptions. First of all, the post-storm dune profile is assumed to be parabolically shaped. Vellinga carried out series of tests and confirmed the equilibrium profile of Bruun (1954) in the process of dune erosion. Second, it is assumed that sediment which is eroded settles on the beach and the foredune. The DUROS model simply fits a parabolic shape in the post-storm dune profile such that the eroded volume equals the settled volume, as can be seen in Figure 2.7. Vellinga stated that the profile is closed at a depth of $y = 0.75H_s$. This depth is called the closure depth. It is possible to include the longshore effect of hard elements by adding an extra margin in the calculations. The DUROS+ model is based on DUROS, but introduces an additional term to account for the wave period (Van Gent et al., 2008).

Dutch standard for assessment of dune erosion The DUROS model has been the prescribed model up to the year 2006 and after that the DUROS+ model became the standard model for the assessment of dune erosion in the Netherlands (ENW, 2007). Dune erosion can be expressed with numerous parameters each having their own advantages. DUROS parameters used for the collision regime are the retreat line R (or set-back), which can be divided into a normal setback without a structure (d_0), set-back at the side of a structure (interaction size: d_1) and an increased set-back (d_2). The retreat distance can thus be decomposed in: $\Delta R = d_0 + d_1 + d_2$. In addition, total erosion volume and above MSL are used plus the definition of the accretion volume is common to use (all in $m^3 \cdot m^{-1}$). Last output parameter of interest is the erosion point (P).

2.4.2 XBeach

General XBeach (Roelvink et al., 2009) is the most recent process-based model designed to describe the different storm regimes, as described by Sallenger (2000) and is used in this thesis as a tool. XBeach is developed after the hurricane season of 2004 and 2005 after initiative by the USACE.

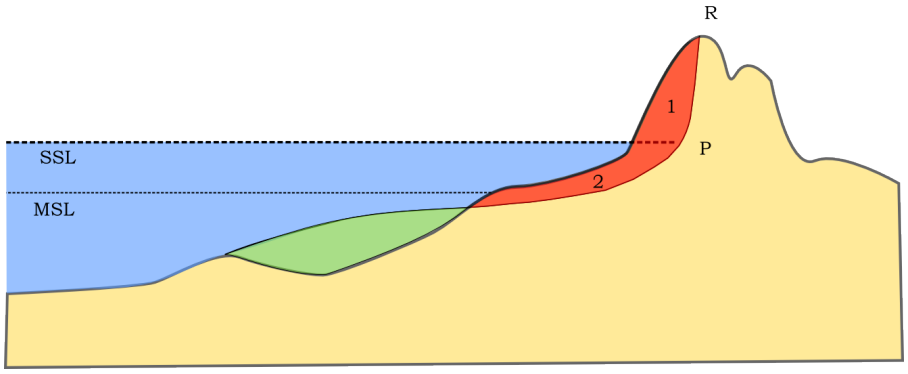

Figure 2.7 *Standard morphological response parameters called also DUROS-variables. In red erosion volumes and in green accretion. Symbol P is used for the retreat point and R for the retreat line. Adapted from ENW (2007).*

XBeach is open-source and developed for eXtreme Beach behavior. XBeach is therefore on first hand a morphological model which is capable of modeling all the different regimes: swash, collision, overwash and inundation. This subsection only briefly discusses the main features of the XBeach model. A comprehensive description of the model, including all equations, can be found in Appendix A or in Roelvink et al. (2010).

Approach XBeach has been created to resolve the equations of wave propagation, flow, sediment transport and bathymetry development for time-varying wave and current boundary conditions. The model resolves the so-called 'surf-beat', also known as the long wave motions created by wave groups. These infragravity waves are responsible for most of the swash waves which actually attack the dunes, such as described in Section 2.2. XBeach is capable of describing the propagation of these long waves, in contrast to process-based models such as Delft3D, as can be found in Section A.4.

XBeach can accurately reproduce dune erosion (collision) via the implementation of a robust avalanching algorithm. Material is triggered by the long wave and is avalanching downwards. The avalanching algorithm uses a dry and wet critical slope. When this slope is exceeded sediment is exchanged between the cells. The avalanching algorithm is of importance for the supply of sediment to the foredune (Van Thiel de Vries, 2009b).

XBeach uses a 2DH-approach, which means processes are resolved in the horizontal and averaged over the vertical. On top of that, the momentum-conserving staggered scheme of Stelling and Duinmeijer (2003) is used to describe to propagation of *shock* waves on the beach. The settings used in this thesis can be found in Appendix A.5.

Incorporation of hard elements In recent studies the capabilities of XBeach of modeling both the cross-shore as well as longshore effects of hard elements on dune erosion have been successful (Van Thiel de Vries, 2009a; Van Geer et al., 2012). Most of the physics are reproduced correctly in XBeach, but some of the challenges in modeling remain due to the fact that part of the physics responsible for the impact are taken into account parameterized (turbulence via $jetfac$) and some effects are absent. For example, the variations of individual short waves as a result of the phase-resolving approach. Van Geer et al. (2012) assumed that also short wave run-up is of importance in describing the behavior around hard elements. This effect is parametrically taken into account with the keyword $swrunup$

and is also applied in this thesis. Van Geer et al. assumed short wave run-up is of importance for avalanching material on top of the revetment.

Problems related to the description of the overwash regime XBeach is initially developed for the four regimes as described by Sallenger (2000), but is mainly calibrated and validated for collision cases. For overwash and inundation the default settings of XBeach overestimate erosion. This is related to the sediment transport formulation. The formulation implemented in XBeach (Soulsby-Van Rijn) is not strictly valid for sheet flow conditions. In order to achieve a realistic behavior the equilibrium sediment concentration is limited during sheetflow (parametric solution). Limiting is carried out with the use of an upper-bound Shield parameter for the start of sheet flow (keyword s_{max}). This results in sediment transport during overwash becomes linear dependent of the flow velocity. This approach is in line with Kobayashi et al. (1996) and successfully demonstrated in a field case by McCall et al. (2010b). However, De Vet (2014) suggest that these limitations may not be realistic, because observed side-effects and the lack of proof of validity.

2.4.3 DnA calculation rules

Deltares and Arcadis (2013) continued the work done by WL | Delft Hydraulics (1993); Van Geer et al. (2012) and made use of 2 tracks to describe the impact of hard structures on the dune erosion process. Overview of the different tracks can be found in Figure 2.8. In both relations the extra dune set-back d_2 is a function of the normal dune set-back d_1 and in this thesis the calculation rules derived by Deltares and Arcadis (2013) for the increased set-back are named by the acronym DnA.

Track 1 is valid for the situation when the object in the barrier fails. This means that the coastal system has a large gap in the system which will result in an increased set-back. Track 2 is valid for the transition between objects and the rest of the sandy dune . The values Deltares and Arcadis (2013) found in an regression analysis are an α_2-value of 0.30 and a λ-value of 30. The additional dune set-back can be described with equation 2.3. In this thesis only track 2 will be used, because the field case of Sandy only gives possible validation of this track.

$$\begin{aligned} d_2 &= \alpha_2 \cdot d_1 \\ l_2 &= \lambda \cdot d_2 \end{aligned} \tag{2.3}$$

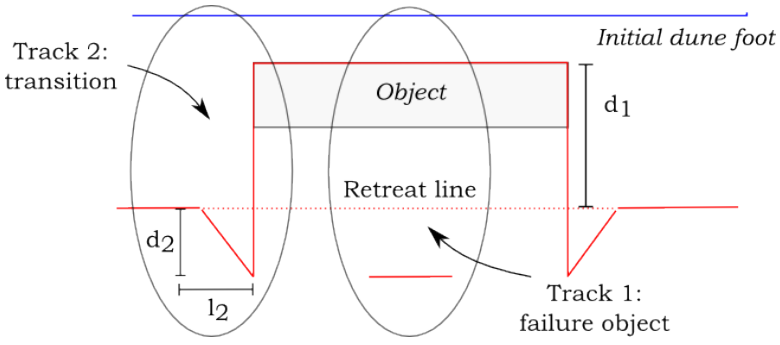

Figure 2.8 *Overview of the two tracks in calculating the effect of NWO with the DnA-rules. Adapted from Deltares and Arcadis (2013).*

Chapter 3

Conceptual study

3.1 Introduction

This chapter describes the analysis of the morphological behavior of a barrier which is intersected with a hard element. It is important to have a sound understanding of all the processes involved, before modeling more realistic case studies. A useful tool which can function as a guide line is a conceptual model. In such a model it is possible to exclude the more realistic but complex conditions such as varying bathymetry or changes in water level. The settings used in this conceptual study are presented in Appendix A.5.

The main part of this conceptual study will focus on the Dutch situation where a design storm will attack a representative dune profile. In Section 3.2 the model set-up for this part is presented. This section describes the profile and boundary conditions used. First, the cross-shore effect of hard structures is analyzed in 1D in Section 3.3. Second, the more complex combination of effects, both in cross-shore as well as in longshore direction, in 2DH are presented in Section 3.4. All these calculations will be in the so-called collision regime.

To also incorporate the difference in regimes, several calculations have been made to analyze the effects of hard structures for the overwash regime. The bathymetry and hydrodynamic conditions used are comparable for the situation of Hurricane Sandy at the coast of New Jersey and described in Chapter 4. This subsection can be found in Section 3.5.

3.2 Model set-up

3.2.1 Dune profile: schematic reference profile

The dune profile is an important parameter in the determination of the amount of dune erosion during storm surges (Den Heijer, 2013). However, in this conceptual study, a schematized reference profile is used to exclude the influence of the dune profile on the results, which are considered to be representative for the Dutch coast and is presented in Figure 3.1.

The dune face is 1:3 and ends at 3 m +NAP in the dune foot. From thereon the slope is 1:20 to a level of NAP. From NAP to -3 m +NAP the slope is 1:70. From that point on seaward the slope is 1:180. The normal Dutch reference profile, as specified by Vellinga (1986) has a height of 15 m +NAP. In this thesis the profile as specified by Deltares and Arcadis (2013) is applied. In this profile the mean dune top height is reduced to 10 m + NAP in order to enhance the influence of the NWO.

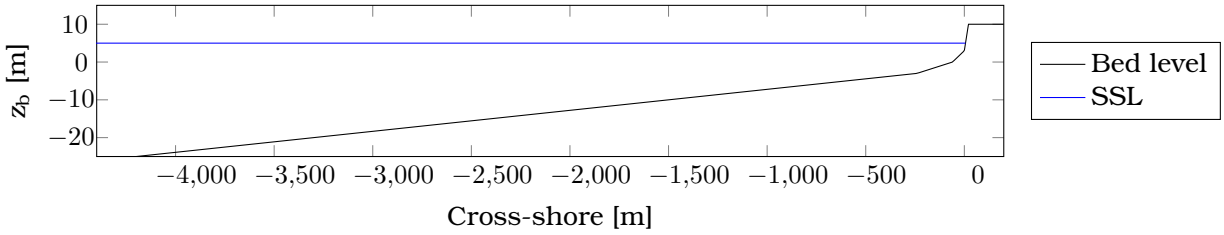

Figure 3.1 *The reference profile used in the conceptual study in the collision regime.*

3.2.2 Applied boundary conditions

The standard conditions are again schematisations which are considered to be valid for a representative storm along the Dutch coast. These conditions are applied for five hours and are constant over time. The result in terms of dune erosion is approximately the same as for a complete storm cycle with ebb and flood phases. This analysis has been carried out for the Dutch design storm of 1953 based on profiles measured at Delfland (Vellinga, 1986). The conditions are deep water conditions and valid at water depths up to 25 meters. The conditions used are the same as applied by Deltares and Arcadis (2013).

Table 3.1 *The parameters used in the conceptual study in the collision regime.*

Parameters	Symbol	Unit	Value
Storm Surge Level	SSL	m	5
Spectral wave height	H_{m0}	m	9.0
Peak wave period	T_p	s	16
Sediment diameter	D_{50}	μm	225
	D_{90}	μm	338

3.2.3 Baseline configuration

The baseline computation is carried out for five different situations. The first simulation, the 'A' configuration, is the 'soft' base situation. Additionally, four different hard structures are implemented. The reason for this approach is to include the effect of the position and width of the structure in an early stage of this research. The front and back position of the element is based on the landwards position of the dune top.

The major difference between the 'B' configuration and the 'C' configuration is the combination of length and position. The B-configuration is placed from the middle of the domain up to the boundary. Therefore, only one hard-soft transition is present. This structure can thus be seen as *semi-infinite*. The C-configuration is placed in the center of the domain with a fixed width. Therefore, two hard-soft transitions are present in the domain. The baseline configuration is presented in Table 3.2 and Figure 3.2. The approach applied in this thesis is influenced by the approach of Deltares and Arcadis (2013). In this study also semi-infinite and fixed NWO's are modeled in XBeach.

Table 3.2 *Configurations used in the conceptual study for the collision regime.*

Name	Description	Front [m]	Back [m]	Length [m]
A	Sandy	-	-	-
B1	Semi-infinite	20	80	1000
B2	Semi-infinite	30	80	1000
C1	Fixed width	20	80	100
C2	Fixed width	20	80	50

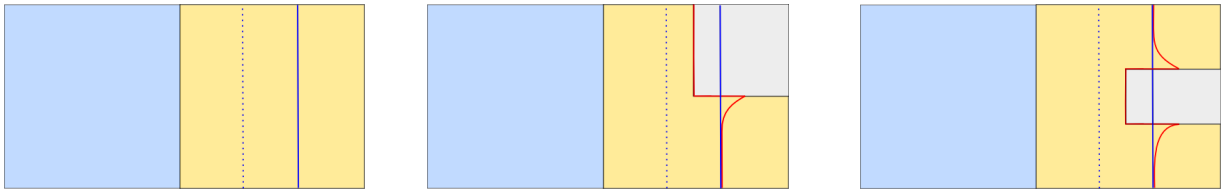

(a) *Complete sandy profile* **(b)** *Semi infinite NWO* **(c)** *NWO with fixed dimensions*

Figure 3.2 *Overview of the different profiles as used in the conceptual study for the collision regime.*

3.3 Results 1D: cross-shore effect

3.3.1 Reproduction theory: impact structures

General In this subsection the morphological response of both the soft and the hard barrier is investigated. In Figure 3.3 the bottom elevation (impact) at the start, half-way and at the end of the simulation for both the soft as well as the hard barrier is presented. In addition, in Figure 3.4 the development of the bed level over time for a given cross-section can be found.

Soft cross-section For the soft situation the beach becomes wider and the dune foot moves in landward direction. In the first hour the dune front changes rapidly. As the storm progresses the time interval between each episodic collapse of the dune front increases and the erosion gradient decreases in time. This effect can be seen in Figure 3.3 where the bed level is plotted for three time periods (pre-, half-way, post-storm). On top of that the difference between the erosion volume above SSL and the total erosion volume increases. This difference is a result of the change in dune face, which becomes less steep. The mean total soft erosion volume is 196.6 $m^3 \cdot m^{-1}$.

Hard cross-section For the situation with a hard element a scour hole develops. The scour depth increases quickly in the first hours and as the storm progresses the growth rate decreases rapidly. The erosion above SSL of the hard structure is about half of the soft barrier which is a result of the cut off of sediment due to the presence of the hard element. After 0.5 hours only sediment below SSL is transported and the retreat line does not change anymore. This is also the time needed for 80% of the scour hole depth to develop. The maximum depth modeled is 4.1 m. The definition of the scour is the maximum difference between the bed level of the soft barrier and that of the hard barrier which is measured at the toe of the structure. The hard cross-section suffered from 10% less erosion than the soft cross-section (-19.7 $m^3 \cdot m^{-1}$).

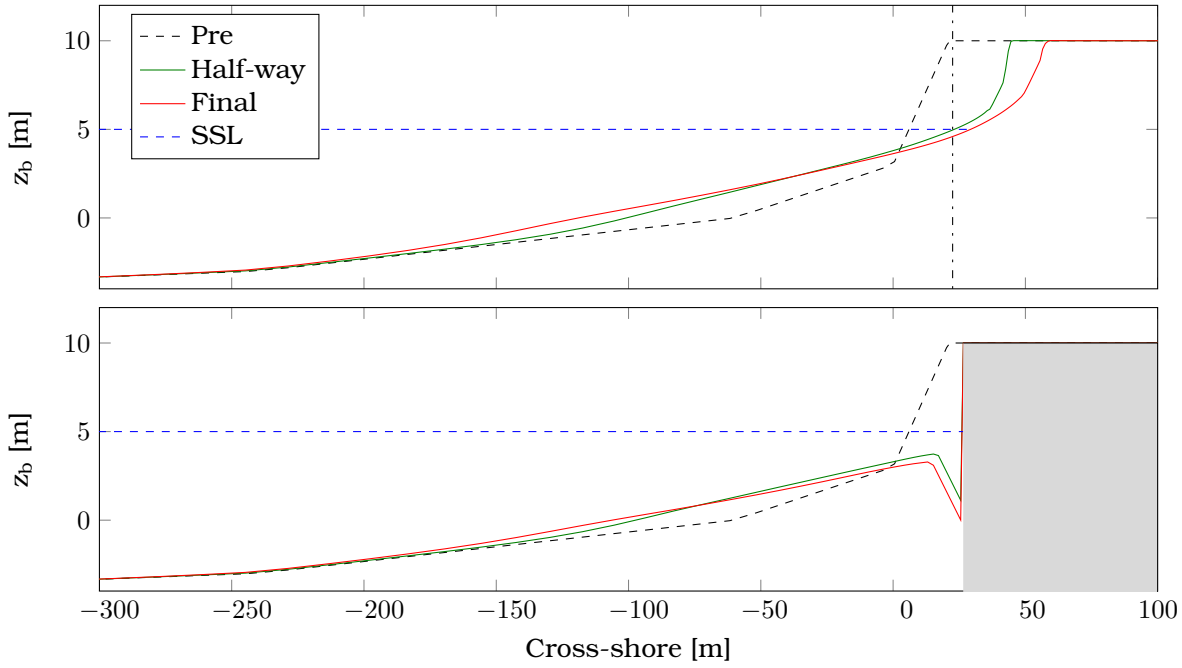

Figure 3.3 *Development of the bed level for both the soft (upper panel) and the hard barrier (lower panel). Development of a particular cross-section (dash-dot) given is plotted in Figure 3.4.*

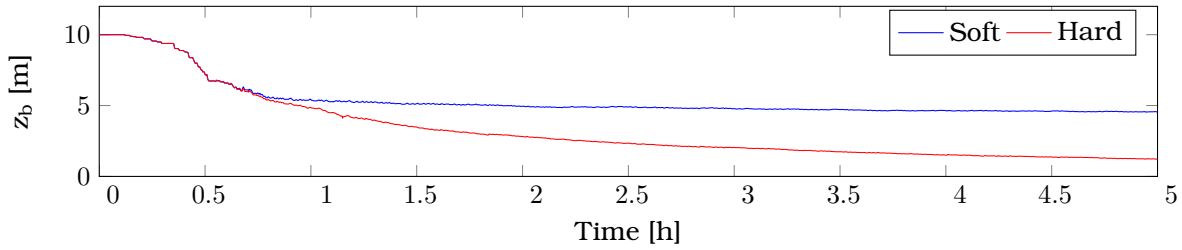

Figure 3.4 *Development of the bed level over time for a single cross-section such as given (dashed-dot) in Figure 3.3 both for the soft as well as the hard barrier.*

3.3.2 Parameters affecting the impact of structures

General XBeach has been developed in order to describe all the regimes of Sallenger (2000) and has proven skill in reproducing the morphological response during the collision regime with the default parameters (Deltares, 2013). Also the impact of hard elements can be modeled with accuracy by mimicking turbulence at the toe of hard elements via the parametric formulation called $jetfac$ (Deltares, 2013). This is needed since XBeach does not describe wave reflection and wave run-down.

In the previous subsection the morphological impact is presented. In this subsection the causes for this impact are analyzed. The complete analysis of the causes can be found in Section C.2.2. This includes a comparison in changes in waves, flow, sediment concentration or sediment transport between the soft and hard barrier. In Figure 3.5 the development of the long and short waves for both the hard and soft barrier are presented. Change in energetic conditions is the most important driver for the differences between two barrier types.

Soft cross-section During a storm dunes erode and provide sediment to the beach profile. The nearshore rises and the short wave height and wave forces decrease in front of the barrier. This is the case since the new profile is more effective in dissipating wave energy. The barrier adapts to the storm conditions and tries to get in equilibrium with the new forcing (Van Thiel de Vries, 2009b). This results in a decrease in offshore sediment transport as a result of both lower sediment concentrations (-29%) as well as a weaker return current (-50%). Both are related to a decrease in short wave energy. The importance of the long wave increases as can be seen in Figure 3.5.

Hard cross-section In front of a hard element the rise of the nearshore during storm conditions only partly occurs. The cross-section provides less sediment which can be deposited in the nearshore and therefore the efficiency of dissipating wave energy is less. This results in higher energetic conditions in front of the structure (H_{RMS}: +0.26 m, +17%). In reality, the combination of wave reflection and wave run-down result in high turbulence intensities at the toe of the structure. These effects are not described by XBeach and taken into account parametric via the keyword $jetfac$. This results, despite the lack of sediment supply and lower sediment concentrations (-31%), in stirring up of sediment which erode away due to a (weaker) return current (-12%). The storm-averaged total sediment transport in the entire hard cross-section is 36% lower than for the soft cross-section, but an erosion hole at the toe of the structure can develop.

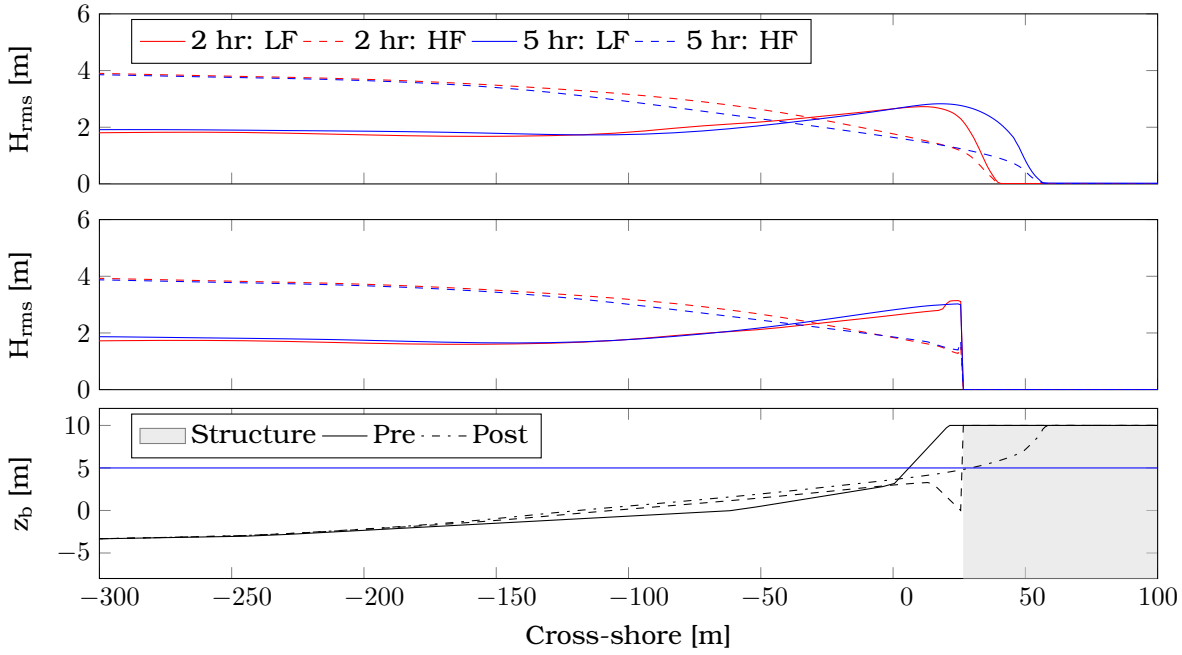

Figure 3.5 *Development of the short and long root-mean-square wave height for both the soft (top panel) and the hard barrier (middle panel). LF stands for low frequency waves and HF stands for high frequency waves.*

3.3.3 Effects of water level variations

General In the conceptual approach suggested by Deltares and Arcadis (2013) a constant storm of 5 hours is modeled. This is based on the approach of Vellinga (1986) which assumed that a storm of prototype scale with a constant SSL and a constant H_s of 5 hours is comparable with a storm

3.3.3 Effects of water level variations

General In the conceptual approach suggested by Deltares and Arcadis (2013) a constant storm of 5 hours is modeled. This is based on the approach of Vellinga (1986) which assumed that a storm of prototype scale with a constant SSL and a constant H_s of 5 hours is comparable with a storm including ebb and flood phases. This approach is based on the Dutch design storm of 1953. In this subsection varying water levels and varying wave heights are applied, comparable with the tidal record of the design storm of 1953. In Figure 3.6 the development of scour hole and total erosion volume for both a simulation with a constant SSL as well as with a variable SSL are presented.

Quantitative effects The following effects can be noticed. First of all, the erosion volume for a varying Storm Surge Level (SSL) increases with 15% (+28.9 $m^3 \cdot m^{-1}$) compared to a constant SSL. This is related to an over-forcing of the barrier due to the schematic input of wave heights and water levels. On the other hand, scour as a result of the hard element already decreases with 17% (-0.75 m), which is a direct result of the hydrodynamic variation over time.

Qualitative effects The patterns for the development of the erosion volumes and the scour are for a constant SSL parabolically shaped. However, for a varying SSL the erosion volume mainly increasing during rising water levels. On the other hand, the scour hole gets filled up during falling water levels and only develops for *rising* water levels. These findings should be taken into account for future more realistic applications.

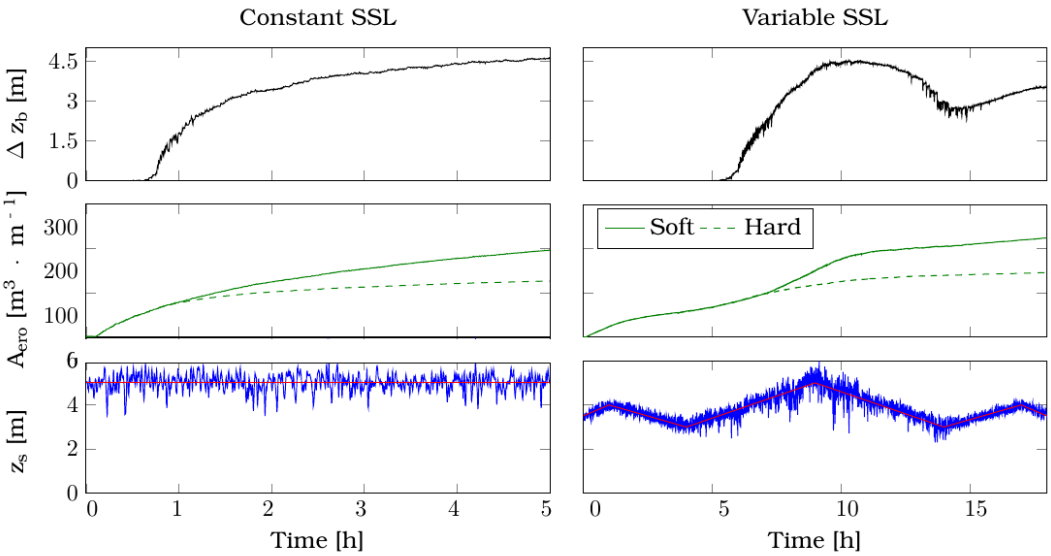

Figure 3.6 *Analysis of the effect of variation in SSL (ebb and flood). This is done both for the scour hole development (upper panel) and the erosion volume (middle panel). Erosion volume is presented both for the soft (solid) as well as the hard cross-sections (dashed). In the lower panel the water level (lower panel) are given both for a constant SSL (left panels) and variable tidal record from 1953 (left panels).*

3.3.4 Conclusion

In the previous subsections the effect of hard structures in cross-shore direction have been analyzed. Regarding this analysis the following conclusions can be made:

1. The cross-shore effect of hard structures is reproduced in XBeach. At the toe of the structure there is by default a limited amount of turbulence. This can be explained by the physics included in the model. XBeach does not take into account processes such as wave reflection and wave run-down. These effects can be mimicked with the keyword $jetfac$ (Deltares, 2013). In the conceptual study for the collision regime the hard structure resulted in a decrease of the erosion volume with 10% and the development of a scour hole of 4.1 m.
2. The main cause for these impacts is related to the sediment supply. The presence of a structure will limit the natural response of the system and thus less sediment is deposited in the nearshore. Therefore, higher energetic conditions occur in front of the structure, which will result in stirring up of sediment and the formation of a scour hole.
3. Variation in hydrodynamic forcing can result in infilling of scour. This mainly occurs during falling water levels. During rising water levels scour is formed and most of the erosion was noticed in XBeach simulations.

3.4 Results 2DH: cross-shore and longshore effects

3.4.1 Reproduction theory: impact structures

General The simulation is analyzed in terms of morphological response. This is carried out based on the output variables described by ENW (2007) and Deltares and Arcadis (2013). In this thesis the retreat line R, retreat distance ΔR, retreat point distance ΔP, erosion, accretion are called DUROS-variables and the increased set-back d_2 and influence length l_2 goes by the name DnA-variables. It is important to note that there are two erosion volumes. The first erosion volume (A_{ero}) is the erosion used in literature and measured above SSL. The second erosion volume is the total erosion and is used in this thesis, since it gives more insight in the morphological response of the system. The difference between the two is about 10% and both are presented in Table 3.3. The different output variables have been calculated for the different configurations and more detailed information about these output variables can be found in Figure 2.6 and Figure 2.7. The spatial bed level plot is presented in Figure 3.8.

Table 3.3 *Morphological response in DUROS output parameters for the baseline configuration.*

Type	Name	Retreat distance ΔR $[m]$	Retreat point ΔP $[m]$	A_{ero} $[m^3 \cdot m^{-1}]$ above SSL	Total
A: Sandy	XBeach	39.5 (100%)	22.8 (100%)	186 (100%)	207 (100%)
	DUROS+	56.6 (143%)	66.2 (290%)	388 (208%)	388 (188%)
Configuration	B1	46.3 (117%)	29.9 (131%)	216 (116%)	241 (117%)
	B2	43.6 (110%)	29.9 (131%)	206 (110%)	229 (111%)
	C1	45.7 (116%)	30.1 (132%)	215 (115%)	241 (117%)
	C2	45.1 (114%)	28.7 (126%)	211 (113%)	235 (114%)

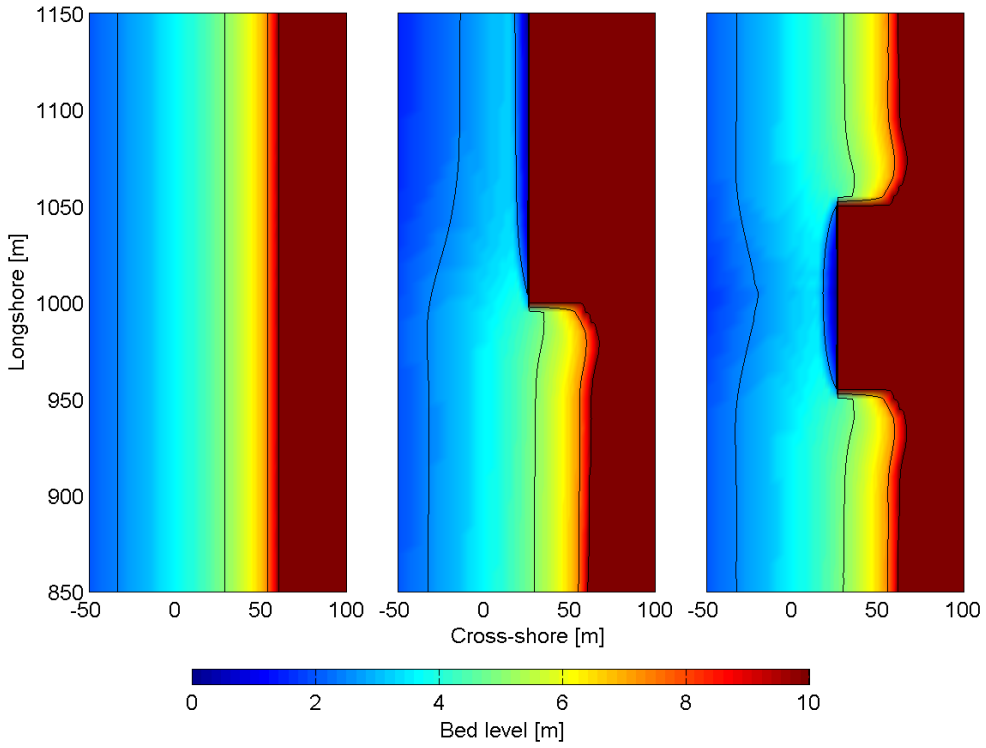

Figure 3.7 *Spatial bed level plot for different configuration after 5 hours of simulation in which the bed level is in m. The black depth contours are given at 0, +2.5, +5 and +10 m +NAP.*

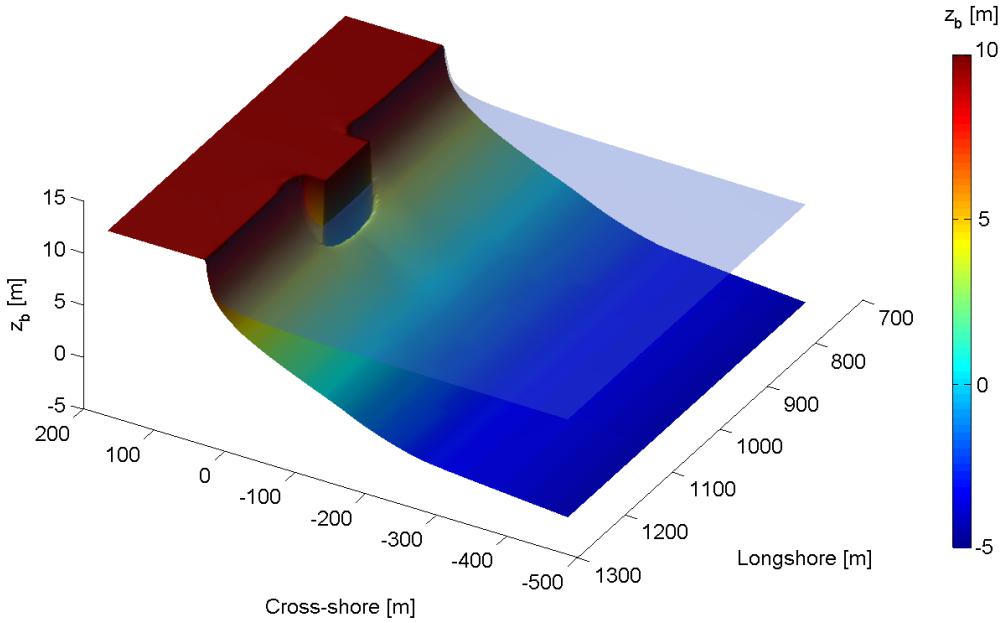

Figure 3.8 *Three dimensional bed level and water level plot for C1 after 5 hours of simulation. The structure can be found in the middle of the modeling domain.*

Morphological response: DUROS output parameters The DUROS+ model is an empirical model and thus not qualified for modeling storm impact in complex cases. This is in contrast to the XBeach model which contains description of the most important physical processes. DUROS simply fits a parabolic profile. The main difference occurs at the dune face, which is modeled in DUROS+ with a slope of 1:1, in contrast to XBeach, as can be seen at the value for ΔP as in Figure 3.9.

A coastal system with a hard element will result in a combination of cross-shore and longshore effects. The scour hole reproduced in Section 3.3 is also noticed in 2DH. On top of that, the barrier has a stronger morphological response at the sides of the structure. The increase in retreat distance is in the order of 10-17% (+4.1 up to 6.8 m). The values for maximum erosion increases with 11-17% (+22 up to 34 $m^3 \cdot m^{-1}$), as can be seen in Table 3.3. These values change with the different configurations and therefore it is already clear that the morphological response depends on the position and width of the hard element.

In time, the retreat line and -point obtain a parabolic shape. The barrier adapts to the higher energetic conditions and tries to get in equilibrium (Van Thiel de Vries, 2009b). When comparing the change of the retreat line and retreat point over time one can see that the decrease of the retreat gradient is smaller for the situation with a hard element in it, as can be seen in Figure 3.10. The discontinuity in the development of the retreat line is the result of the episodic collapse of the dune front.

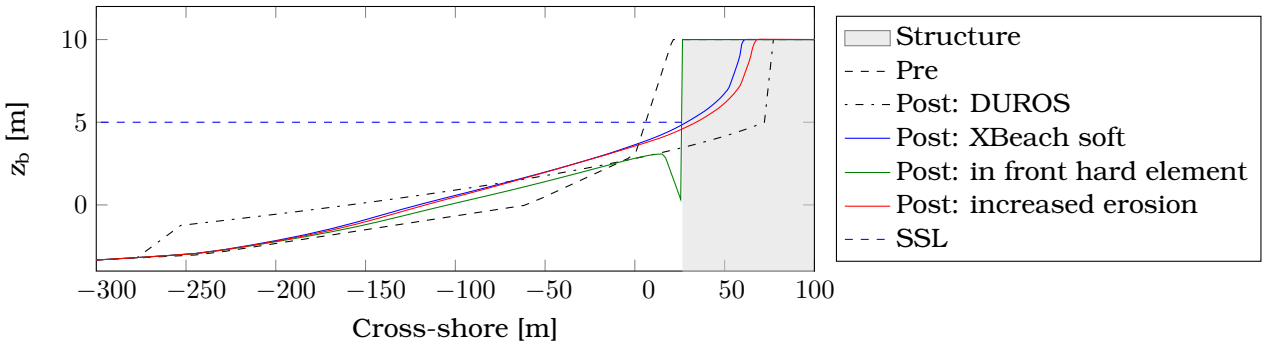

Figure 3.9 *Cross-section of the bed level for comparing both the soft as well as the hard cross-section for XBeach plus DUROS+.*

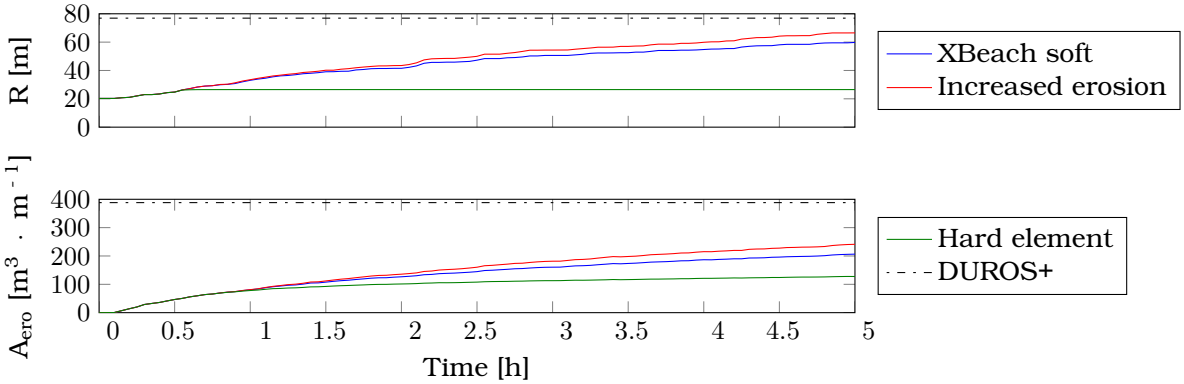

Figure 3.10 *Development of the retreat line and the erosion volume over time for the soft cross-section, hard cross-section and increased erosion due to the presence of the structure, as calculated by both XBeach and DUROS+.*

Morphological response: DnA output parameters The DnA calculation rules are a method to describe the longshore effect of hard structures. The calculation rule are linearly related to normal set-back (d_1), increased set-back (d_2) and influence length (l_2). These relations are described in Equation 2.3.

The position of the hard element in the barrier is an important parameter. An object which is placed 10 m towards the coastline means a decrease in d_2 with 35% (-2.6 m). In addition, the relation between the width of the NWO and the increased set-back can be seen by comparing C1 and C2. The effect is however moderate, because a decrease of 50 m in width means a reduction of 1.1 m in terms of d_2 and 25 m in terms of l_2.

When comparing the longshore effect calculated by DnA and by XBeach, the values calculated by DnA seem conservative. The mean ratio for the increased set-back and influence length varies between 27-68% (XBeach compared to DnA). The overestimation was expected, since the DnA calculation rules are developed as a conservative addition factor for DUROS+. The overestimation of d_2 and l_2 increases when the d_2 decreases. The results show that the increased set-back is closely related to the position of the NWO in cross-shore direction. The influence length has a strong relation with both the increased set-back and the width of the NWO. A more elaborated study regarding the effects of the object size can be found in Section C.2.6. In Figure 3.4 the results for XBeach both with and without a hard structure are presented.

Table 3.4 *Morphological response in DnA-parameters + XBeach without a structure (DnA) versus XBeach in which the barrier is intersected with a hard element (XBeach).*

	d_2 [m]		l_2 [m]	
Name	DnA	XBeach	DnA	XBeach
B1	10.0	6.8 (68%)	300	110 (37%)
B2	7.0	4.2 (60%)	210	70 (34%)
C1	10.0	6.2 (62%)	300	145 (49%)
C2	10.0	5.7 (57%)	300	80 (27%)

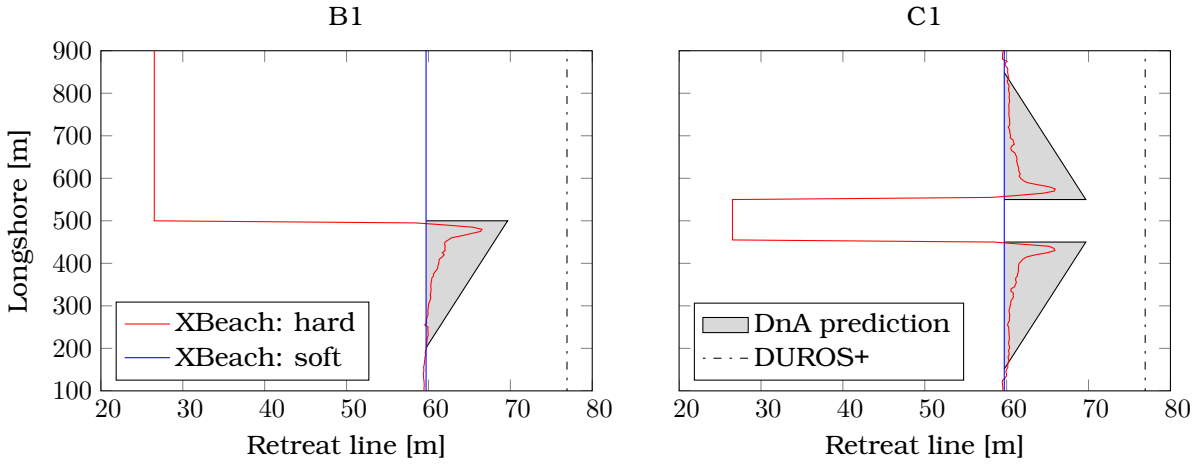

Figure 3.11 *Retreat line for the B1 configuration (left panel) and C1-configuration (right panel) with the DnA prediction and the actual result in XBeach and DUROS+.*

3.4.2 Parameters affecting the impact of structures

General In the previous subsection the morphological impact was presented. In this subsection the causes for these changes are analyzed. The complete analysis of the causes can be found in Section C.2.3. This includes a comparison in changes in waves, flow, sediment concentration or sediment transport between the soft and hard barrier. In Figure 3.12 the three most important causes are presented. The combined effect results in an increase of sediment transport in cross-shore (2/3) and longshore direction (1/3). The cross-shore component is related to an increase in mass flux by locally higher short waves. The longshore component is mainly related to the water level gradient by set-up differences.

1) Higher energetic conditions Hard elements in the coastal barrier have a large impact on the profile development during storm conditions. The nearshore in front of a hard structure is due to limited sediment supply not capable of adapting to the higher energetic conditions. The effect is that higher energetic conditions (+10% in wave energy) in front of the structure occur throughout the storm. This effect is visible in the left panel of Figure 3.12. In cross-shore direction higher turbulence intensities at the toe of the structure make it possible for a scour hole to develop. This is a typical cross-shore effect of hard structures.

2) Water level gradient In longshore direction there is a mean water level gradient of 0.10-0.20 m. The difference in wave breaking between hard and soft cross-sections cause this difference in water level set-up. This creates a water level gradient from the dune towards the structure. This effect is visible in the middle panel of Figure 3.12. The morphological effect is less accretion at the soft side of the transition. This material is deposited in front of the structure.

3) Local higher waves At the soft side of the transition locally higher short waves arrive. There are two sources for these higher waves. First, waves get dissipated less because part the accretion is deposited in front of the hard structure. This effect was also noticed by Van Geer et al. (2012). Second, higher waves will diffract around the structure. The combined effect is visible at the energy peak in the left panel of Figure 3.12. In total the mean increase of the short wave heights is +0.22 m (+19%).

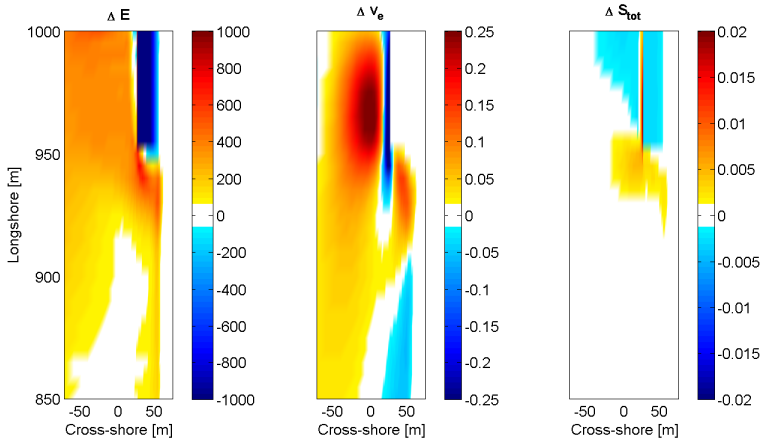

Figure 3.12 *Comparison between the A configuration and the C1 configuration in the wave energy (left panel), alongshore velocities (middle panel) and total sediment transport rates (right panel).*

3.4.3 Sand volume balance: accretion versus erosion

General In the initial idea of WL | Delft Hydraulics (1993) a sand volume balance was introduced. The concept was that two profiles could be distinguished: a sandy profile, A_A, and a hard profile, A_B. In the paragraphs of this subsection the alongshore distribution of sediment is derived. Also a relation between erosion and retreat is found, which is applied to describe the longshore effect in another output parameter. This is possible with the description of additional erosion in adjacent locations (A_2), which opens the way to describe the longshore effect also for practical overwash situations and to derive the modified DnA calculation rules.

Volumes sand exchanged The exchange of sediment for the B1 and C1 configuration can be divided in change in erosion and accretion (both in $m^3 \cdot m^{-1}$). This makes it possible to calculate the origin in alongshore distribution. The results can be found in Table 3.5 where the maximum erosion and accretion per cross-section are presented. On top of that, the total exchanged sediment in m^3 is calculated. A visual impression of the alongshore distribution can be found in Figure 3.13 and 3.14.

Table 3.5 *Sediment exchange rates per cross-section type and in total.*

Name	Type	Unit	B1	C1
Soft side	Erosion	$m^3 \cdot m^{-1}$	34.7	34.6
	Accretion	$m^3 \cdot m^{-1}$	19.2	13.4
	Total net	$m^3 \cdot m^{-1}$	49.6	44.7
Hard side	Erosion	$m^3 \cdot m^{-1}$	32.2	30.1
	Accretion	$m^3 \cdot m^{-1}$	62.9	69.1
	Total net	$m^3 \cdot m^{-1}$	95.1	99.2
Total	Net exchanged	m^3	5070	7409

Four important aspects can be distinguished:

1. The alongshore distribution of sediment is a result of erosion and accretion. The ratio between these processes differ for the hard and soft side of the transition and for different configurations.
2. The distribution of sediment is mainly (63-75%) the result of increased erosion and is less dependent on a decrease in accretion (37-25%) at the soft side. Increased erosion at the soft side is related to locally higher short waves . The decrease in accretion is driven by an alongshore water level gradient and becomes less important when the width of the structure decreases.
3. The maximum net effect per meter is at the hard side of the transition two times the value of the soft side. This means that deposition at the hard side occurs in a smaller area then where the material comes from and therefore this signal is more peaked. It is also possible for the influence area to overlap when a structure with fixed dimensions is modeled.
4. The volumes exchanged between the hard and soft side for the C1 configuration are larger than for the B1 configuration. An increase in transition with 100% (2 versus 1) results in 25% more sand deposition in front of the hard element. This underlines the fact that the process is only partly supply-driven.

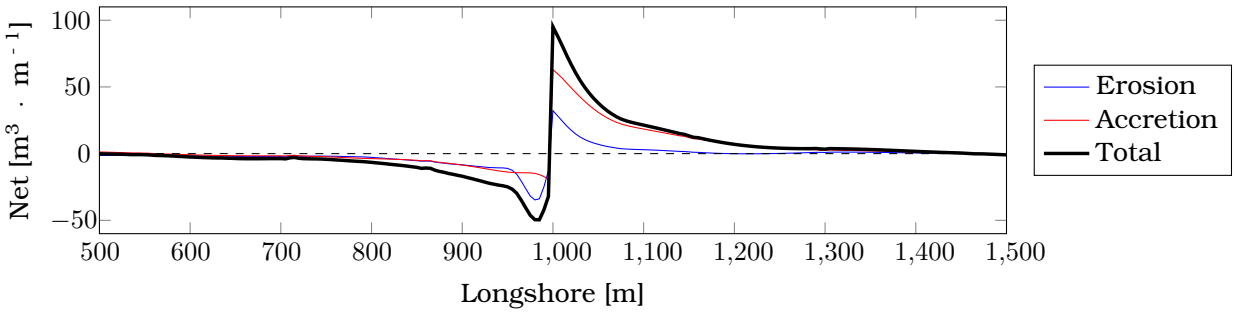

Figure 3.13 *Decomposed exchanged sediment compared to the reference profile in terms of erosion and accretion [$m3.m^{-1}$] for B1 with A.*

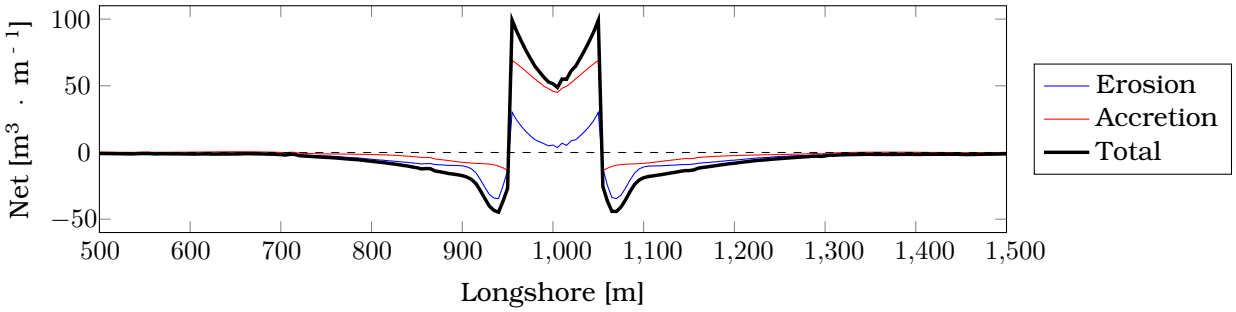

Figure 3.14 *Decomposed exchanged sediment compared to the reference profile in terms of erosion and accretion [$m3.m^{-1}$] for C1 with A.*

Relation between erosion volume and retreat After calculating the development of the total erosion volume and the alongshore retreat line over time, a relation can be derived. The relation found is that for every 5 $m^3 \cdot m^{-1}$ erosion the dune face will retreat with 1 meter. This simple linear relation with an α_3 of 5 m also holds for the increased set-back d_2 and has an $R2$ of 0.9635. The relation is presented in Figure 3.16. The α_3 of 5 m happens to be similar to the dune height above SSL.

$$A_{ero} = \alpha_3 \cdot \Delta R \tag{3.1}$$

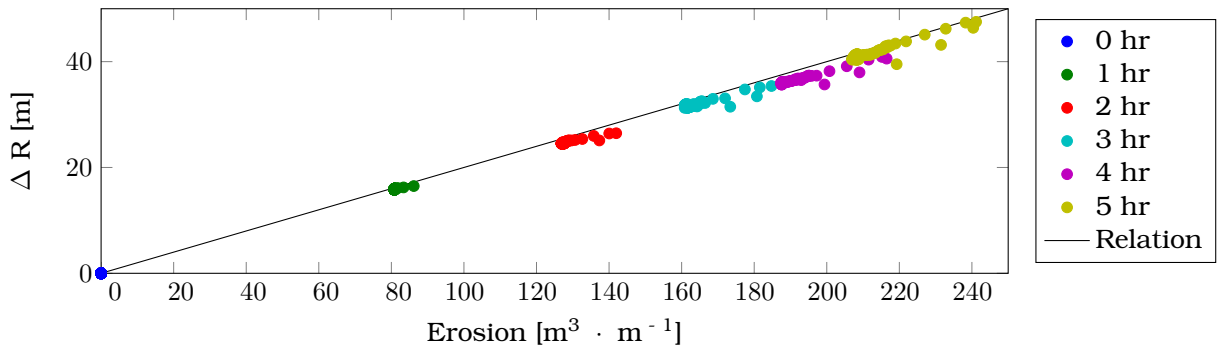

Figure 3.15 *Relation between the erosion volume and the retreat line*

Initially the calculation rule focused on the increased set-back d_2. Setback d or difference in retreat line ΔR is divided into d_0, d_1 and d_2. It is also possible to divide the erosion volume A_{ero} into these terms. The relations derived will be called the modified DnA calculation rules, since these relations have a broader area of application and can for example be used for overwash cases where ΔR cannot be used accurately. The term A_2 will be used to describe additional erosion in adjacent locations. On top of that, A_1 is used for the erosion in the erosion zone of a structure and A_0 for the opposite (*not* in the erosion zone). The relation between the retreat distance and erosion volume will be used to calculate the influence length (l_2). In Figure 3.16 an example can be found.

$$\begin{aligned} A_{ero} &= A_0 + A_1 + A_2 \\ A_1 &= A_{ero,soft} - \alpha_3 \cdot d_0 \\ A_2 &= \alpha_2 \cdot A_1 \\ l_2 &= \frac{\alpha_2 \cdot A_2}{\alpha_3} \end{aligned} \tag{3.2}$$

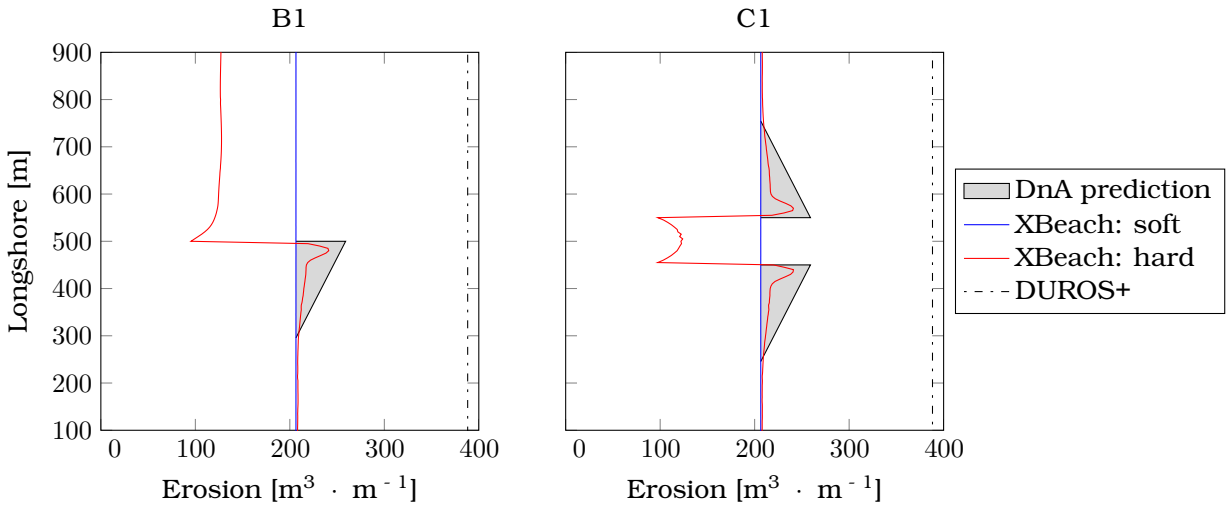

Figure 3.16 *Relation between the erosion volume in $m3.m^{-1}$ for the soft barrier and the increased erosion volume for configuration B1 and C1 with the modified DnA calculation rules as calculated by XBeach.*

3.4.4 Wave obliquity: cause and impact

The majority of dune erosion experiments and numerical models only include cross-shore dimensions. However, in a conceptual XBeach model the effect of wave obliquity on dune erosion has been demonstrated (Den Heijer, 2013). In this subsection the effect of hard structures under oblique wave attack is analyzed. The parameter which has been varied is the wave angle. Variations between normal incident waves and 30 degrees with respect to shore normal are applied. Supporting analysis, tables and figures can be found in Appendix C.2.4.

The most important conclusions of this analysis are:

1. In XBeach simulations the increase in retreat distance and relative increase of the erosion volume due to wave obliquity, as proposed by Den Heijer (2013), is reproduced. A wave angle of

15 degrees will result in an increase of the mean erosion volume by +9.4%, which is smaller than the proposed value of +25% (17 versus 45 $m^3 \cdot m^{-1}$).

2. For the effects of hard structures on the erosion process during storm surges two of the three causes identified in Section 3.4.3, become of less importance. In addition, one new cause is important for oblique wave attack. An impression of the effects is presented in Figure 3.17.
   (a) The importance of exchange of sediment in longshore direction (less accretion in soft cross-sections) decreases since the gradient of the alongshore water levels decreases.
   (b) The decrease of dissipation in the soft cross-section will (partly) not occur, as a result of the alongshore distribution of sediment decreases (listed in a).
   (c) The increase in short wave height due to diffraction around the structure is also present for simulations with oblique wave attack. However, these higher short waves will, due to obliqueness, be distributed in a broader area downstream.
   (d) Longshore transport becomes important. This transport component can be responsible for locally large impact in terms of set-back, as demonstrated by De Vries (2011). This impact, however, does not occur for NWO's with fixed dimensions. This is related to a draining effect of really high longshore velocities (order 7 $m.s^{-1}$) which will only develop since the presence of the semi-infinite structure. The impact which does occur for NWO's with fixed dimensions is updrift and downdrift, as can be seen in Figure 3.17.
3. In upstream direction sediment will pile up against the structure resulting in a decrease in setback generated by updrift. The effect for wave angles larger than 20 degrees is already sufficient for accretion to counteract the erosive processes.
4. In downstream direction the impact in terms of increased set-back (d_2) or additional erosion (A_2) does not increases for large wave angles, in contrast to the study of De Vries (2011). The *total* additional erosion volume ($\sum A_2$) however does increase as a result of downdrift. This is the result of an increase in influence length and thus not driven due to an increase in maximum additional erosion per m. The combined total additional erosion (both upstream as well as downstream) first decreases with 28% for wave angles of +10 degrees with respect to shore normal and eventually increases 16% for wave angles of +25 degrees. The reason for this pattern is the complex combined effect of updrift, downdrift and distribution of locally higher short waves.
   (a) For shore normal wave attack the ratio between increased set-back and influence length was 8.2. This ratio increases up to 90.9 for wave attack with an angle of 30 degrees. The proposed value by the DnA calculation rules is 30. This means that the influence length increased from 40 up to 235 m.
   (b) The ratio between the normal set-back and the increased set-back decreases from 0.21 to 0.08 for wave angles of 30 degrees. The proposed value by the DnA calculation rules is 0.30. This means that the increased set-back decreased from 4.9 down to 2.2 m.

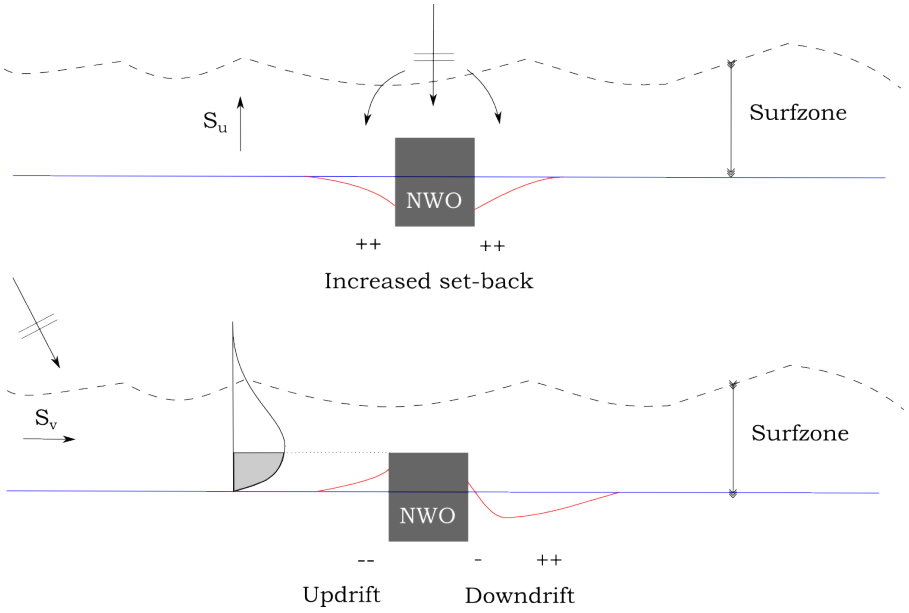

Figure 3.17 *The effect of a hard structure due to cross-shore (upper panel) and longshore transport (lower panel). In blue the soft response and in red the impact due to the presence of the structure.*

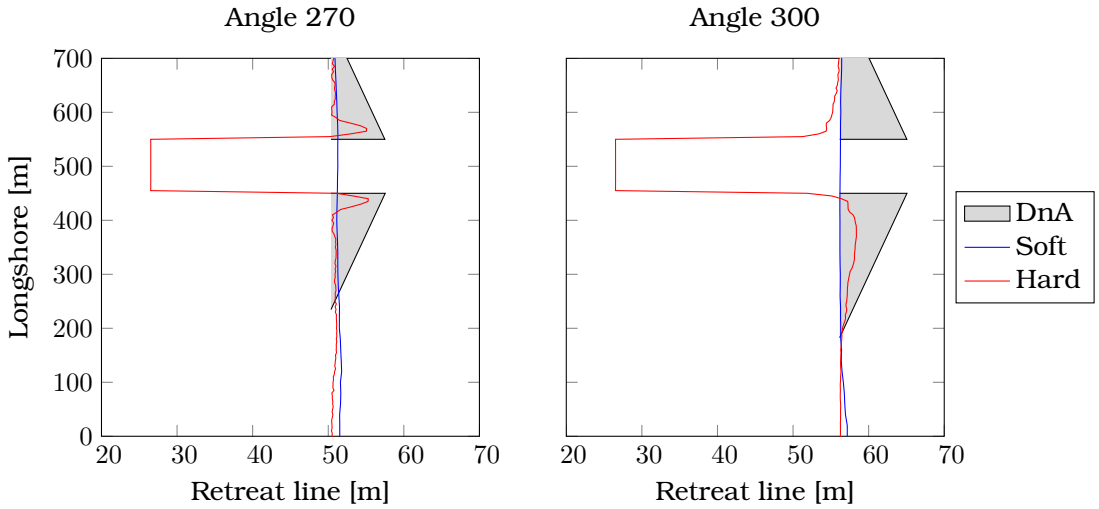

Figure 3.18 *Retreat line for shore normal (left panel) and oblique wave attack with an angle of 30 degrees (right panel). Shore normal attack is from left to right. Oblique attack is from upper-left to bottom-right. The upstream side can be found for increasing values for the longshore distance and can be found on the right side of the structure.*

3.4.5 Sensitivity analysis

In this subsection the sensitivity of the baseline is analyzed. This analysis includes variation in hydrodynamic forcing, change of the object size and investigation of the effect of several XBeach parameters (both physics related and non-physics). The conclusions of each analysis is presented in a paragraph. The complete analysis can be found in Appendix C.

Change in hydrodynamic forcing The morphological response of the coastal system depends on the parameters of the storm, the coastal system and the object itself. In this paragraph the sensitivity of the morphological response for the storm-induced parameters and coastal system are analyzed. The parameters which have been varied are: root-mean square height wave H_{rms}, spectral-mean wave period $T_{m-1.0}$, sediment diameter D_{50} and relative dune height D_{SSL}. Relative dune height is the difference between the dune top and SSL in m. Supporting analysis and figures can be found in Appendix C.2.5. In Figure 3.19 the factorial analysis for the erosion volume and increased set-back can be found.

The response of the system on variation of coastal and storm-induced parameters varies for each individual parameter. The values used are linearly related to the factorial change in input parameter and the result in output parameter. For example: a value of +1.5, means that if the input parameter is increased with 10% the output parameter increases with 15%. The most important conclusions are:

1. Dune height above SSL (D_{SSL}) is the dominant variable for the morphological response in all the different output parameters. It is important to note that for the erosion volume a lower relation value was found (-1.39), compared to the other output parameters. One can conclude that in the XBeach simulations the response of several output parameters is not just the result of change in forcing but often a small change in forcing can already have a large impact on certain output parameters.
2. In XBeach the sensitivity for changes in $T_{m-1.0}$ and sediment diameters show discrepancy with Delta Flume experiments and the older process-based model DUROSTA. In the Delta Flume a relation between factorial change in the spectral-mean wave period and factorial erosion volume had a linear relation of +1.15. This is in contrast to the found value in XBeach of +1.38. On top of that, variation in sediment diameter will only result in a change of -0.19, compared to a two times higher relation in DURSOTA. The reason for this discrepancy remains unclear.
3. An increase in wave height (H_{rms}) will only have a limited effect on the post bathymetry, since a higher wave height will get dissipated before reaching the shore. Therefore, the relation between H_{rms} is only in the order of +0.49. This was expected based on the theory of Van Thiel de Vries (2009b).

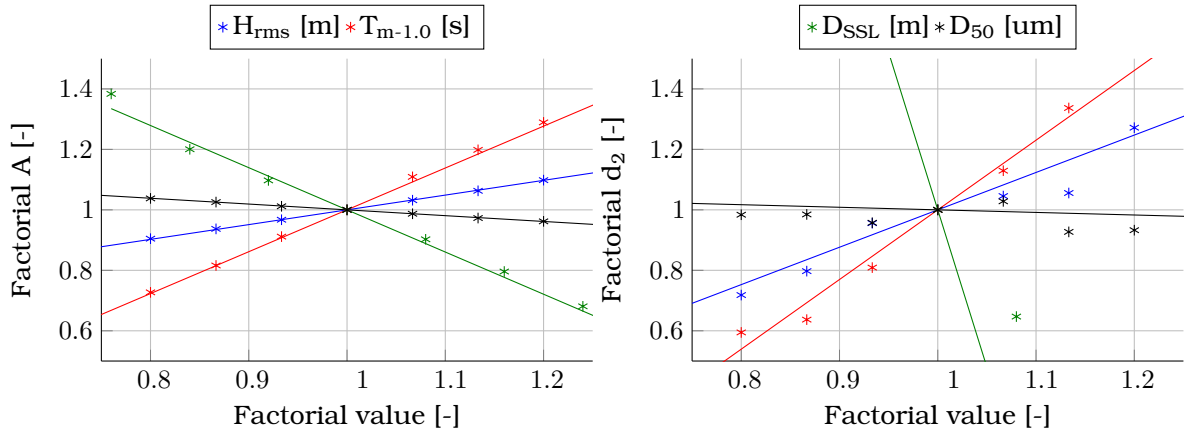

Figure 3.19 *Factorial deviation model for mean erosion volume and the increased set-back d_2 retreat for configuration C1. Individual points are measurement data from XBeach and the solid line is the linear relation found, based on this data.*

Influence of the object size The effect of a structure on the coastal system is closely related to the size of the structure. In the DnA calculation rules the front position of the structure is already implicitly taken into account with the use of the interaction parameter d_1. However, the effect of the width of the object and the back position are not taken into account. In this paragraph the sensitivity of morphological response related to the position, width and length of the structure is analyzed. Supporting analysis and figures can be found in Appendix C.2.6. All the simulated values combined can be found in Figure 3.20.

Changes in front position, width and length behaved as expected based on the DnA calculation rules. The following conclusions are made:

1. The DnA calculation rules are designed to be conservative. However, the difference between the simulated values in XBeach and calculated values via DnA is remarkably high. The mean ratio of the increased set-back is 56% and the mean ratio of the influence length is 35% (when comparing XBeach / DnA, 50% means XBeach is half the DnA value). The maximum value simulated for α_2 is 0.235, with a mean value of 0.168. The maximum value simulated for λ is 24.5, with a mean value of 17.8. The value of the ratio for the influence length is based on the calculated values for the increased set-back and not the simulated values, otherwise the ratio would have been better (59%).
2. With the use of the interaction parameter d_1 the development of the increased set-back d_2 can already be predicted reasonably well for varying front positions of the structure. When the structure is placed 20 m or more to the sea the relation no longer holds.
3. For structures with a width smaller than 100 meter or a length smaller than 10 meter a reduction for the increased set-back, as calculated by the DnA calculation rules, can be applied. A reduction in the form of: if the width of the NWO < 100 m, than $d_{2,red} = \frac{W^{0.25}}{100^{0.25}} \cdot d_2$, seems a reasonable option based on the data in which W is used for the width of the structure.

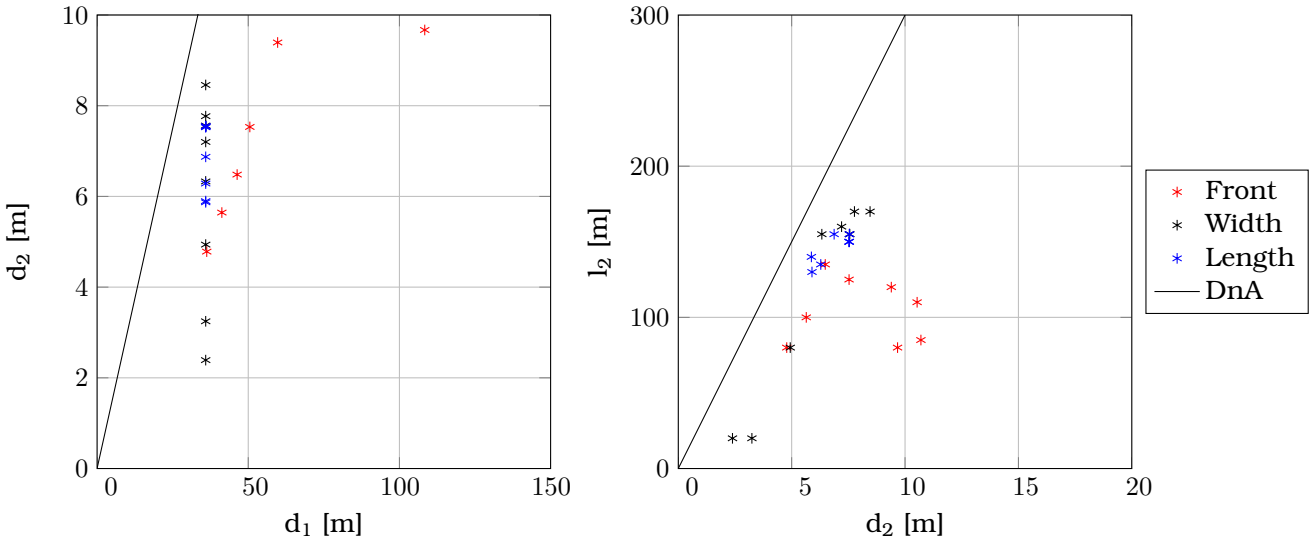

Figure 3.20 *Simulated values for the DnA output variables d_1, d_2 and l_2, as calculated by XBeach and with the DnA calculation rules.*

XBeach settings The physical and non-physical settings used in process-based models have a significant influence on the causes and impact of the outcome of the model. In this paragraph, variation in the use of physical parameters such as parametric relations (for example $swrunup$ and $jetfac$), direction spreading (s), long wave importance and time are analyzed. On top of that, the non-physical settings such as the CFL condition and the MPI method are investigated. Supporting analysis and images can be found in Appendix C.2.7.

Related to the variations mentioned, the following conclusions can be made. As a support for these conclusions Figure 3.21 is provided.

1. The introduction of short wave run-up via the parametric relation $swrunup$ is not of importance in describing the cross-shore or longshore effects of hard structures. The same retreat line pattern can be derived with or without introducing the $swrunup$. This is in contrast to the suggestion of Van Geer et al. (2012).
2. XBeach can mimic turbulence at the toe of a revetment via the parametric relation $jetfac$. This is of importance in order to describe the cross-shore effect of hard structures (scour). However, in a sensitivity analysis with and without $jetfac$ a similar longshore effect was retrieved.
3. The development of the influence length is sensitive for variation in directional spreading. Using higher values for the spreading the influence length will increase. The model set-up with s = 10.000 of Deltares and Arcadis (2013) will result in two times larger influence lengths than with an XBeach default value of s = 20. In addition, the mean erosion volume will be 10% larger.
4. Long waves are not of a major importance in order to describe effects of hard structures on the erosion process. Alongshore sediment exchange is for 28% long wave driven. For example, the lack of long waves would result in a reduction in erosion of 24%. This is comparable with Van Thiel de Vries (2009b) who suggested 30%.
5. In the conceptual collision simulations of 5 hours are applied. When the simulation time is extended to 15 hours the patterns retrieved for the first 5 hours continue.
6. Influence of non-physical parameters in XBeach such as CFL and MPI are analyzed. These settings do not have large influences on the causes and impact of hard structures in XBeach.

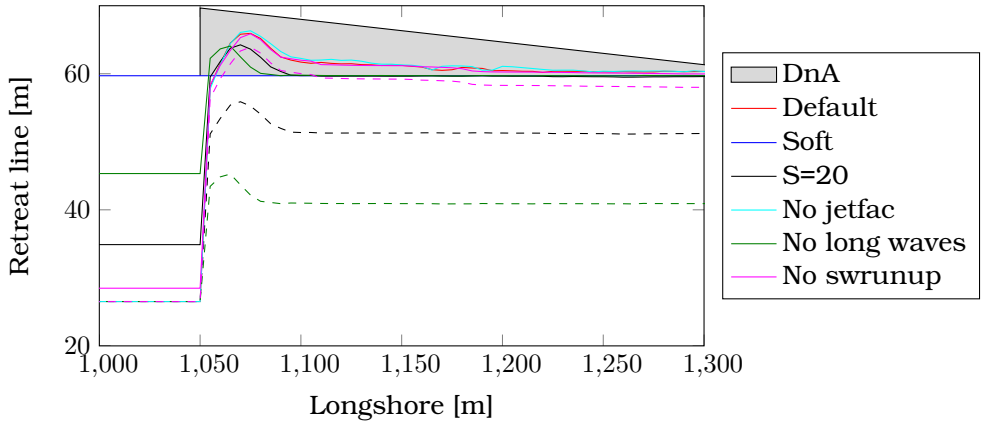

Figure 3.21 *Morphological response of the barrier in retreat line $R*$ alongshore for several XBeach parameters. In the grey area the DnA calculation rules are presented. Dashed lines are non-corrected.*

3.4.6 Conclusion

In the previous subsections the effects of hard structures in longshore and cross-shore direction have been analyzed. Regarding this analysis the following conclusions can be made:

1. The longshore effect of hard structures is reproduced in XBeach. In the conceptual study for the collision regime the hard structure resulted in an increased set-back (d_2) of 4.2 - 6.8 m over an influence length (l_2) of 70-145 m. Additionally, erosion increased with 11-17%. The DnA calculations results in a similar pattern, but overestimates with a factor 2 (27-68 % compared to XBeach).
2. The causes for the effect are an increase of sediment transport in cross-shore (63-75%), but also in longshore direction (37-25%) . The longshore component is related to the water level gradient due to set-up differences and will drive the alongshore exchange of sediment (less accretion). The cross-shore component is related to the increase in mass flux generated by locally higher short waves. This has two components: higher waves as a result of less dissipation in the soft cross-section (previous cause) and higher waves due to diffraction around the hard element.
3. A linear relation between the erosion volume (A_{ero}) and the retreat line (ΔR) is found. The proposed coefficient is an α_3 value of 5. This relation leads to the possibility to formulate the modified DnA calculation rules in which the output parameter of interest is the additional erosion in adjacent locations (A_2).
4. Oblique wave attack has a large influence on the causes and impacts of the longshore effect of the hard structure. For oblique wave attack the alongshore distribution of sediment, and thus less dissipative soft cross-sections, will become of less importance. Locally higher waves, as a result of diffraction and longshore sediment transport, are of importance. The total downstream additional erosion in adjacent locations increases for large wave angles. This is mainly the result of an increase in influence length, due to the distribution of higher waves in a broader area downstream. In addition, updrift and downdrift becomes of importance.
5. Dune height above SSL (D_{SSL}) is the most important input parameter. This is closely related to the impact of a change of erosion volume on the other output parameters. Variation in spectral mean wave period ($T_{m-1.0}$) and sediment diameter (D_{50}) show a discrepancy in impact with Delta Flume experiments. An increase in wave height (H_{rms}) will have only limited effect on the post bathymetry, because water motions in very shallow water are dominated by long waves.
6. Variation in object size is of major importance in describing the morphological effect. Overall: the wider the structure, the more erosion. Over a width of 100 m the structure can be seen as semi-infinite and a reduction can be applied. By placing the structure more in seaward direction, also more erosion is observed.
7. In XBeach the parametric relations $jetfac$ and $swrunup$ are not of importance in describing the longshore effect of hard structures on the barrier. This is in contrast to the suggestion of Van Geer et al. (2012). Additionally, there is a strong relation between directional spreading (s) and influence length. Applying a value of s = 10.000 will fixate the wave energy to come from one direction which causes 10% more erosion and a two-times larger influence length.

3.5 Conceptual overwash

3.5.1 Model-set-up

Barrier profile The barrier island in the considered area of New Jersey during the case study does not have an uniform shape. There are mainly spatial differences in width and height of the foredune. The dune top has a mean of NAVD88 +6.8 m and varies between NAVD88 +4 and +8 m. In this conceptual study two real cross-sections will be chosen with a dune top level of NAVD88 +7.3 and +6.6 m. The reason that there are multiple cross-sections chosen is related to the importance of the relative dune height above SSL, such as shown in Appendix C.2.5. The profiles chosen are presented in Figure 3.22 and applied uniform over an alongshore distance of 9000 m. The method how these profiles are made is shortly described in Chapter 4 and a more elaborated approach can be found in Appendix E.

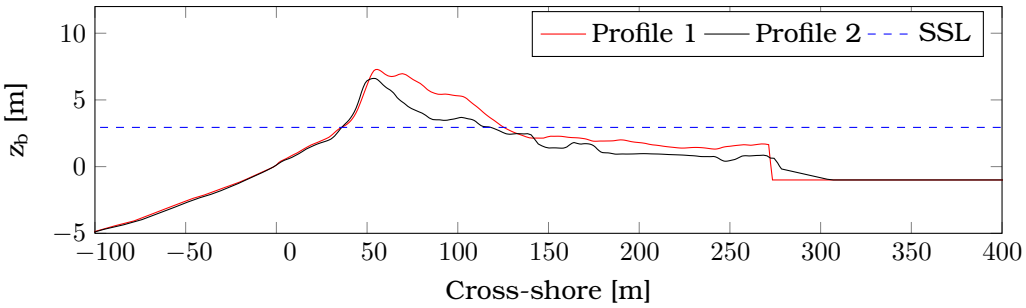

Figure 3.22 *The 2 reference profiles used in the conceptual study in the overwash regime.*

Boundary conditions The hydrodynamic conditions applied are similar to those which occurred during Hurricane Sandy. The reason for this approach is the fact that Sandy can be seen as a design storm for the local authorities. The complete simulation of the storm is three days. This period is needed in order to accurately model the morphological behavior. Validation of the conditions applied can be found in Appendix F.3 and a visualization of the conditions can be found in Figure 4.7. In order to give the reader an impression of the values applied, the maximum and minimum values can be consulted in Table 3.6. The conditions are deep water conditions and valid at water depths up to 25 meters.

Table 3.6 *Parameters and boundary conditions used in the conceptual study for the overwash regime.*

Parameters	Symbol	Unit	Value
Storm Surge Level	SSL	m	-0.5 -2.0
Spectral wave height	H_{m0}	m	0.5-7.0
Peak wave period	T_p	s	2-8
Sediment diameter	D_{50}	μm	300
	D_{90}	μm	400

Baseline computation The baseline computation is carried out for two configurations and two profiles. The first simulation, the 'A' configuration, is the soft base situation. On top of that, a structure with fixed dimensions, 'C', is placed in the coastal barrier. The values applied and a visualization of these values can be seen in Table 3.7 and Figure 3.23.

Table 3.7 *Configurations used in the conceptual study for the overwash regime.*

Name	Description	Front [m]	Back [m]	Length [m]
A	Sandy	-	-	-
C	Fixed width	0	60	100

(a) *Complete sandy profile* **(b)** *NWO with fixed dimensions*

Figure 3.23 *Overview of the different profiles as used in the conceptual study for the overwash regime. Waves travel from left to right. Dark blue represents the sea and light blue the back barrier bay.*

3.5.2 1D results: cross-shore effect

Description: morphological development The bed level development during the simulated storm varies between Profile 1 and Profile 2. The combination of dune volume above SSL and dune height is of major importance. The first profile is the most robust one with the highest dune and most volume above SSL (318 $m^3 \cdot m^{-1}$). The second profile is somewhat lower and has 2/3 of the volume of the first profile.

During the start of the peak of Sandy both profiles are in the collision regime. This means that waves hit the dune face and material is avalanching downwards. Run-up does not exceed the dune top in the first 40 hours of simulation. Sediment is transported to the nearshore by the short wave driven undertow. Eventually the second profile will get in the overwash regime and sediment is (partly) deposited on the back barrier instead of the nearshore. The mean total soft erosion volume varies between 131.1 up to 143.6 $m^3 \cdot m^{-1}$ (Profile 2 and 1). For both profiles most erosion (51%) occurs between the 5 hours before and 5 afters landfall of Sandy.

The behavior of two hard cross-sections is similar. Sediment is taken away in front of the structure and no clear scour hole can be found in the post simulation bathymetry. This is remarkable since in the previous section scour was found in the post bathymetry. This is most likely related to the variation of water levels at sea, since infilling of the scour in the order of 0.5 m occurred during decreasing water levels after the peak of the storm. The different profiles can be be found in Figure 3.24. In terms of erosion one can conclude that the presence of a hard element will reduce the amount of erosion volume with 22-25 % (-29 down to -35 $m^3 \cdot m^{-1}$)

Inapplicable: retreat line. Applicable: erosion volume From Figure 3.25 one can conclude that the DUROS output parameter ΔR is not useful in situations where overwash occurs. This is related to the difference in morphological response between collision and overwash. In addition the output parameter erosion volume (A_{ero}) is more insightful, because it varies over time instead of the discontinuous pattern of the retreat line. The post bathymetry of Profile 1 reveals a classic parabolic shape known from the collision regime. Profile 2 suffers from a combination of both dune lowering as well a some barrier rollover.

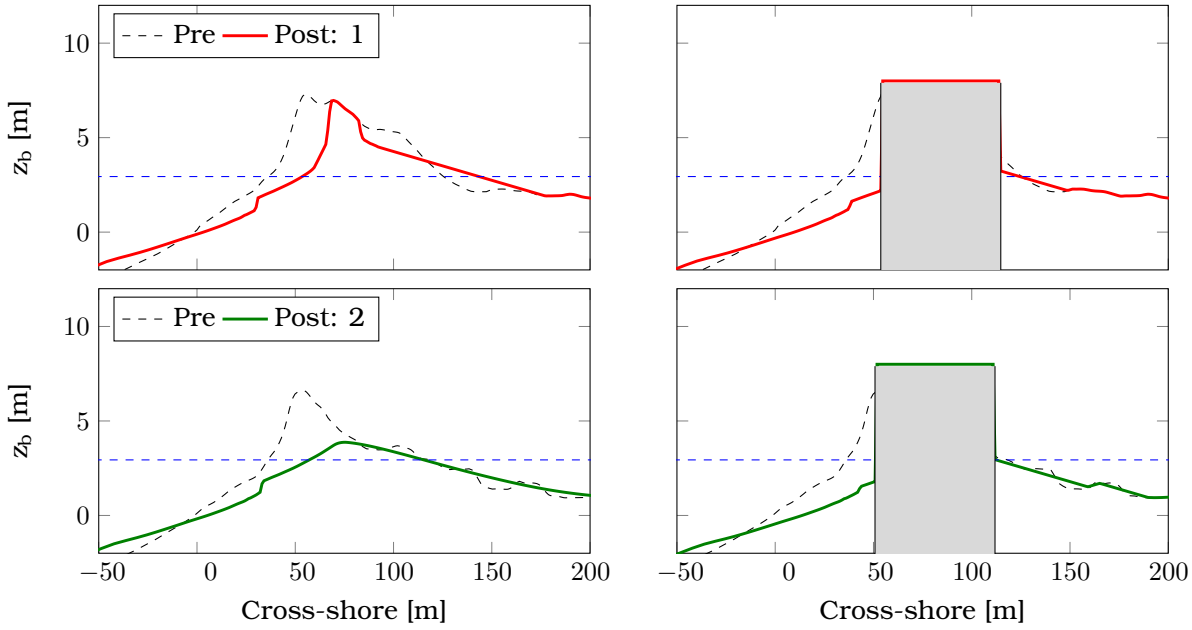

Figure 3.24 *Development of the bed level for both the soft (left panels) and the hard barrier (right panels). The red line is used for Profile 1 and the green line for Profile 2.*

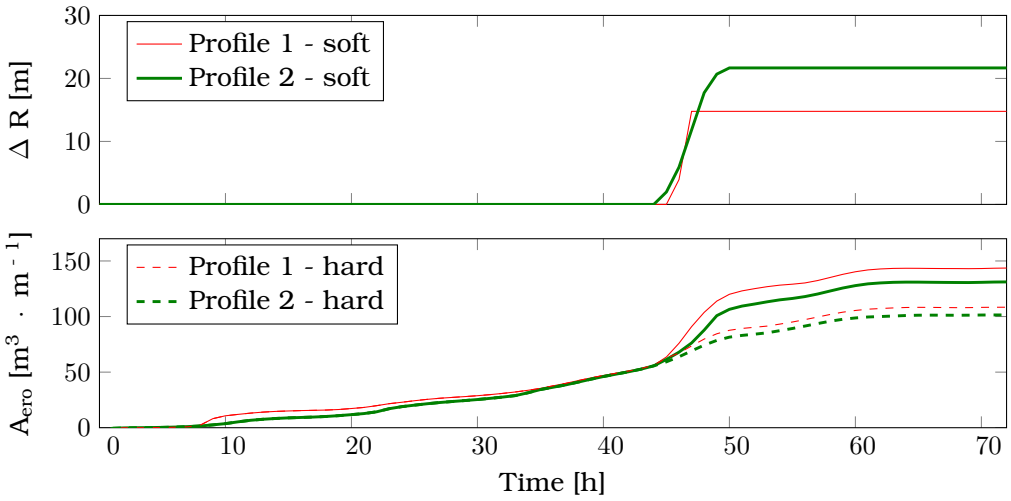

Figure 3.25 *Development of the retreat line and erosion volumes for profiles both the soft and the hard barrier. The red line is used for Profile 1 and the green line for Profile 2.*

Causes for the impact In the previous paragraphs the morphological impact in cross-shore direction has been reproduced. In this paragraph the cause of this impact is analyzed. The complete analysis can be found in Appendix C.3.2. For the hard cross-sections similar patterns, compared to Section 3.4.2 are reproduced, but for the soft profiles some variations are found. These differences in causes are related to the variation in storm regime (overwash instead of collision).

During overwash, water motions and sediment transport on top of the barrier island are found. This means that during the peak of the storm, transport occurs both in offshore direction in the nearshore (driven by the undertow) as well as in onshore direction on top of the barrier (driven by the

long wave). This is related to the fundamental difference in the water motions between Profile 1 and Profile 2 (overwash versus collision). Sediment transport on the barrier has a higher concentration than transport in the nearshore.

Scour development Surprisingly, the post bathymetry with a hard structure did not result in the development of a scour hole. This is related to the variation in hydrodynamic forcing, as was shown in Section 3.3.1. During falling water levels from sea the scour hole is filled up again. A reference simulation with a constant SSL confirms this observation. An XBeach simulation with a constant SSL will result in +8.6% more erosion (+9.5 $m^3 \cdot m^{-1}$). A constant SSL is also responsible for the development of a scour hole of 1.2 m. The analysis can be found in Figure C.20.

3.5.3 2DH Results: cross-shore and longshore effects

Importance of the directional spreading (s) and wave obliquity It is first important to stress that there are two major differences in the settings applied between the conceptual study in the collision and in the overwash regime: directional spreading and wave obliquity. The settings are different because the information for the boundaries is related to the case study. More information about the boundary conditions can be found in Figure 4.7.

First, the directional spreading (s): in the previous section one could notice that lower values for s do not result in differences in increased set-back. However, the simulated influence length in XBeach decreased with 50% when applying a s of 20 instead of 10.000 [-]. More information can be found in Section 3.4.4. The mean directional spreading applied is 33.

Second, the wave obliquity: in the previous section one could notice that for oblique wave attack the causes and impact will start to differ. The most important differences found are related to the lack of alongshore sediment exchange and up- plus downdrift. For the upstream side less additional erosion is expected. For the downstream side the total additional erosion increases, but this is the result of an increase in influence length and not of an increase in maximum additional erosion per m. The mean wave angle applied is 83.7 degrees.

Modified DnA output parameters: additional erosion and influence length The morphological analysis in terms of the DnA output parameters will be done for the influence length (l_2) and the additional erosion in adjacent locations (A_2). This is done since increased set-back can only be accurately determined in the collision regime. The modified DnA calculation rules are derived in Equation 3.2. The results are presented in Table 3.8 and Figure 3.26.

Additional erosion mainly occurs at one side due to oblique wave attack. Left of the structure only 24 up to 28% of the calculated additional erosion is simulated by XBeach. For the right side this percentage increases up to 48-58%. This ratio is somewhat lower than for the collision regime. For example, waves with an angle of 10 degrees resulted in 25% and 61% for the collision regime. One *cannot* make the conclusion that the relation between normal 'soft' erosion and additional erosion is lower for the collision regime than for the overwash regime, because it is not known if the relation found is coincidence or just random and based on differences in set-up.

The ratio between the measured and calculated influence length is for both sides also smaller (38-42% and 51-60%). This is however most likely related to directional spreading (s). For a comparable collision simulation values between 25-64% were found. Therefore, one *can* make the conclusion that the ratios between the mean erosion, additional erosion and influence length are comparable for different regimes (collision and overwash).

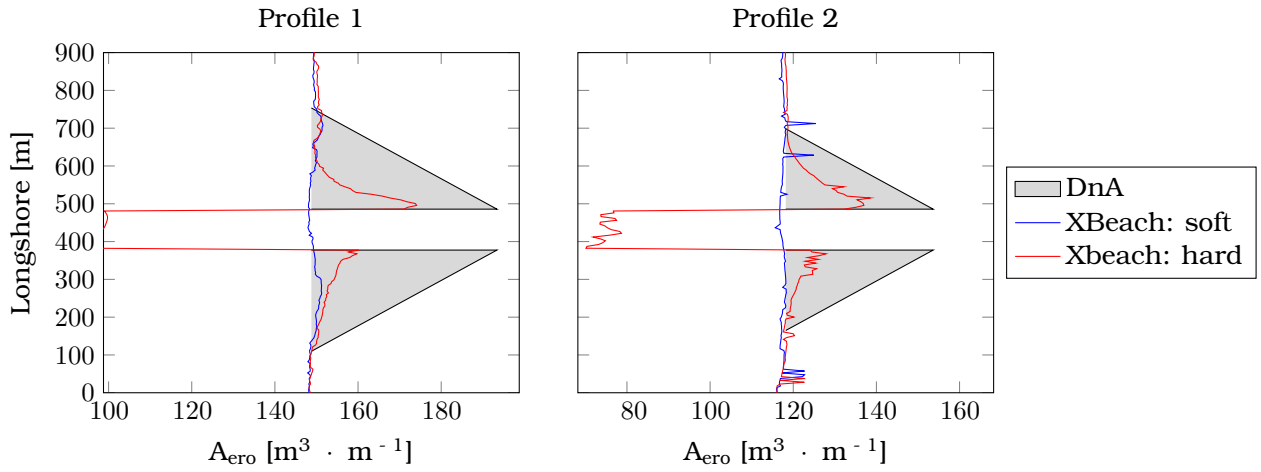

Figure 3.26 *Relation between the erosion volume in $m^3 \cdot m^{-1}$ for the soft barrier and the increased erosion volume with the modified DnA calculation rules as calculated by XBeach. Oblique attack is from bottom-left to upper-right. In the left panel Profile 1 and right panel Profile 2.*

Table 3.8 *Results calculated with DnA + XBeach without a structure (DnA) and simulated with XBeach with a structure (XB.). Erosion volumes are given in $m^3 \cdot m^{-1}$. Simulated values are presented on the left (L.) and right (R.) side of the structure.*

		A_2			l_2 $[m]$		
Runs	$\overline{A_{ero}}$	DnA	XB. -L.	XB - R.	DnA	XB. -L.	XB. -R.
Profile 1	149	44.8	10.8 (24%)	26.0 (58%)	269	103 (38%)	138 (51%)
Profile 2	118	35.3	10.0 (28%)	21.7 (48%)	212	113 (42%)	162 (60%)

Causes for the impact In the conceptual study for the collision regime already an analysis was made for the causes of the longshore effect of hard structures on dune erosion. The main conclusion of Section 3.4.2 was that there were three major reasons which are responsible for the increased setback. First there is an alongshore sediment exchange (less accretion) due to a water level gradient driven by set-up differences. This exchange is responsible for less dissipation and thus higher short waves which results in more erosion in the soft cross-section. On top of that, more erosion occurs as a result of diffraction of higher short waves around the hard element. About 2/3 of the increased set-back was erosion-related. Also for the conceptual study for the overwash regime an analysis is carried out. This full analysis can be found in Appendix C.22.

In the analysis of the conceptual study for the overwash it is found that the alongshore water level gradient, which caused 1/3 of the increased set-back in the collision regime, is less present for overwash simulations than for the collision simulations. This is related to two factors. First, the tidal movement on sea, which varies. This is in contrast to a fixed SSL such as used in the collision regime. Second, there are differences in water motions due to the overwash regime. During overwash conditions set-up flows over the barrier instead of contributing to the actual set-up. Therefore, alongshore water level gradients (partly) cannot take place. For Profile 1, 72-83% of the alongshore exchanged sediment is erosion-related. For Profile 2 this increases to 79-84%. For the conceptual collision situation this ratio was a low as 66%. It is therefore assumed that for overwash situations the alongshore water level gradients has a decreasing importance and the additional erosion is more erosion-driven.

3.5.4 Conclusion: cause and impact of storm regime variation

In the previous subsection the effects of hard structures in cross-shore and longshore direction have been analyzed. Regarding this analysis the following conclusions can be made:

In cross-shore direction

1. The cross-shore effect of hard structures are also reproduced for the overwash regime in XBeach. In the conceptual study for overwash the hard structures did not result in the developmont of a scour hole at the end of the simulating. This is related with infilling of scour during falling water levels. A reference simulation with a constant SSL resulted in 9% more erosion and a scour hole of 1.2 m. The hard structures did result in a decrease of the erosion volume with 22-25% compared to the soft cross-section.
2. The avalanching algorithm becomes more important, since cross-sections need to avalanche first in order to get into the overwash regime. Profiles in the overwash regime cannot be described with the output parameter retreat distance, but can be described with erosion volumes. Additional advantage of this relation is that it is more insightful.
3. Water motions on top of the barrier are peaked (low mean value but a relative high maximum value). The water movement on the barrier is long-wave driven. This is related to the dominance of the infragravity wave in very shallow water (Van Thiel de Vries, 2009b). In XBeach sediment transport on the barrier during overwash occurs with lower velocities and higher concentrations than a similar magnitude of transport in the nearshore.

In longshore direction

5. The longshore effect of hard structures are also reproduced for the overwash regime in XBeach. In the conceptual study for overwash the hard structure resulted in 10.0-26.0 $m^3 \cdot m^{-1}$ (8.4 up to 18.4%) additional erosion in adjacent locations over an influence length (l_2) of 103-162 m. The modified DnA calculations results in a similar pattern for the overwash regime as was expected and reasonably predict the patterns (24 up to 60% compared to XBeach).
6. In the overwash regime the causes for the longshore effect become more erosive-driven (collision: 63-75% and overwash: 79-84%). This is related to the decrease in importance of the water level gradients in longshore direction. The importance of the erosive processes increases when the system suffers from more overwash.

Chapter 4

Case study

The XBeach model has been used in a conceptual model in order to reproduce the cross-shore and longshore effects of hard structures for both the collision and the overwash regime. In this chapter three field cases will be validated. The case study has been partly made at Stevens Institute of Technology in Hoboken, NJ, United States, which is hereby gratefully acknowledged for their support.

4.1 Introduction

Hurricane Sandy originated from the Western North Atlantic Ocean in October 2012. The storm caused flooding, wind and wave damage. It first swept in the Caribbean and continued across the entire East Coast of the United States, as can be seen in Figure 4.1. During Hurricane Sandy the state of New York and New Jersey were most severely hit (National Hurricane Center, 2012). Sandy made landfall on October 29, 2012 at 12:00 PM UTC during spring tide near Atlantic City, NJ. Hurricane Sandy caused wide-spread erosion of the coastal system as well as barrier island breaching at several spots. Sandy was the second costliest hurricane in the United States history with a total of 68 billion dollar in property damage (National Hurricane Center, 2012).

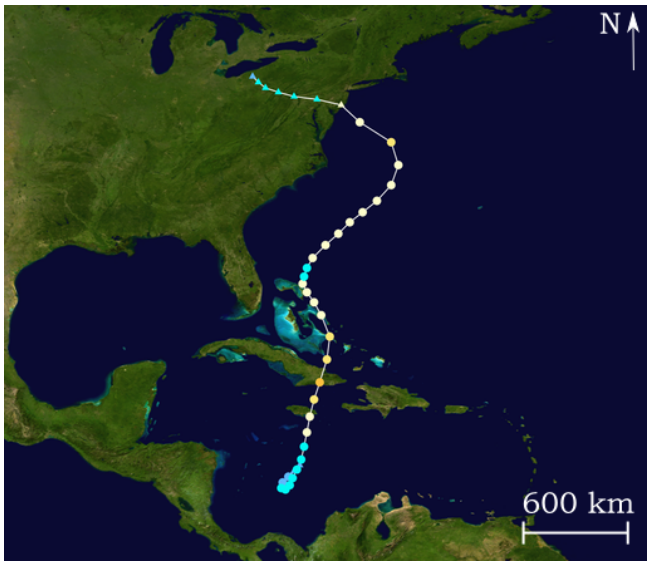

Figure 4.1 *Track of Hurricane Sandy. Traveling from South to North Sandy interacted with a non-tropical weather system transforming from hurricane to a post-tropical cyclone. Colors from blue to red represents hurricane intensity. [Sources: National Hurricane Center (2012) and Wikipedia].*

After the storm measurements were performed by Stevens Institute of Technology. Teams assessed structural damage and measured elevations throughout the different towns (Lopez-Feliciano, 2014; Walling et al., 2014). On top of that, the USACE and USGS performed large-scale LiDAR measurements both pre- (USACE, 2010) and post-Sandy (USACE, 2012; USGS, 2012a). It is therefore possible to compute the erosion patterns, but also to model the system accurately with the use of the nearshore information collected by Stevens. Therefore, the measurements of the devastating impact of Sandy on the New Jersey shore provide new model validation possibilities.

Area of interest The geographical location of the case study is the northern part of the New Jersey shore near the cities of Seaside Heights, Lavalette, Mantoloking and Bay Head. The area of interest is the part of the barrier island which was hit most severe by Hurricane Sandy (Irish et al., 2013) and involves all the land between Seaside Height in the South and Bay Head in the North. These lands were first settled in the late 1800's on a small narrow barrier spit and a have grown in affluent vacation communities (Wicker, 1950). An overview of the area can be found in Figure 4.2.

The case study will consist of three parts. The first part will be to model a (buried) seawall near Bay Head in 1D. This part will focus on the cross-shore effect of hard structures. The second part will be to model the effects around Bay Head in 2DH, but here the focus is to reproduce the overwash regime in XBeach. The last part of the case study will be to make a 2DH-model of the area around a condo in Camp Osborne, Brick, NJ. This part will focus on the combination of both cross-shore and longshore effects of a hard structure.

1. **Bay Head: cross-shore effect of a (buried) seawall**. The seawall near Bay Head has been covered with sand for decades. The stone seawall was constructed in 1882 and has a length of 1260 meter (NJDEP, 2012). During Sandy the sand in front and on top of the seawall was eroded away. A recent study showed that the seawall had a large effect in reducing the impact of Sandy. With a Boussinesq-type wave model Irish et al. (2013) showed that without the seawall the wave-averaged forces on the ocean front structures of Bay Head would have been twice as large. This subsection can be found in Section 4.4. In Appendix D.2 both oblique and satellite images of the area are presented.
2. **Bay Head: overwash in XBeach 2DH.** South of the seawall of Bay Head large areas suffered from overwash conditions during Hurricane Sandy. Within the region of Bay Head and Mantoloking three weak spots were presented which (partly) breached during Sandy. This subsection will focus the accurate reproduction of the morphological response during overwash. This part is necessary since by default XBeach overestimates the erosion during overwash conditions on 'soft' barrier islands without the use of artificial limiters (McCall et al., 2010a). This part can be found in Section 4.5.
3. **Camp Osborne: impact of a hard structure during Sandy**. Camp Osborne is one of the well-developed beaches of Brick, NJ. However, in October 2012 nearly all 118 bungalows were either swept away by the storm surge of Sandy or ravaged by a fire which officials suspect was caused by a gas leak in the rubble. Only seven bungalows, a large condo and a parking lot were salvageable (Spoto, 2013). This subsection can be found in Section 4.6. In Appendix D.3 both oblique and satellite images of the area are presented.

Calibration approach (secondary thesis objective) XBeach is calibrated by applying a two-step calibration approach. The first step is to increase the wave asymmetry sediment transport component called $facua$. A higher value will result in less net offshore sediment transport and makes it possible

to calibrate the collision regime. This will be done in Section 4.4. The second step is to increase roughness of the barrier. A higher roughness will result in less sediment transport on the barrier and makes it possible to calibrate to overwash regime. This will be done in Section 4.5.

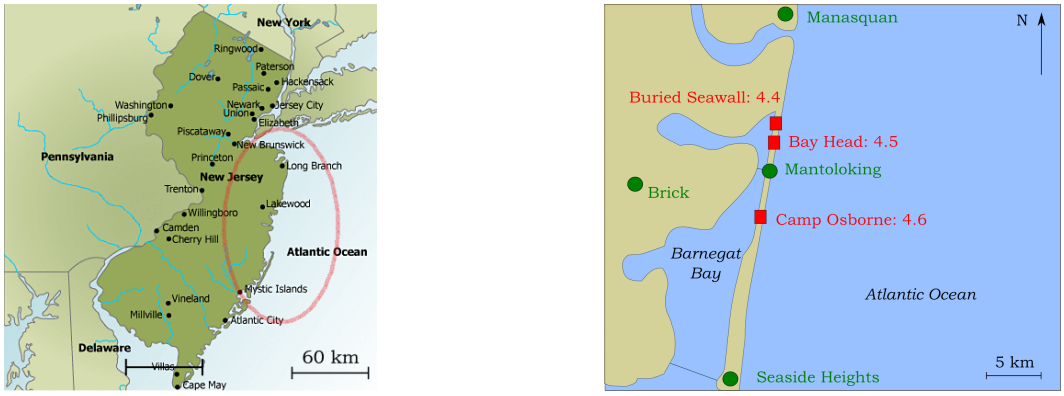

(a) *Overview map of New Jersey state* **(b)** *Detailed map of the Jersey shore*

Figure 4.2 *Maps of the area of interest. Camp Osborne is located near Lakewood (in a) and Lavalette (in b) (NJDEP, 2014). The area of consideration is 80 km South of New York City.*

4.2 New Jersey into perspective

General The New Jersey coast is probably the most important recreational asset of the United States. This is due to the nearby densely populated metropolitan areas of New York City and Philadelphia in combination with the hot and humid summer months. The development of this shoreline as recreational resource began two hundred years ago at Cape May (Wicker, 1950). The total coastline is 200 kilometers and offers both sandy beaches for tourism as well as a place to live for residents. The total industry related to the shoreline of New Jersey is estimated to be worth over 16 billion dollars annually (NJDEP, 2014).

Jersey's Shore Protection Program In order to provide protection, preserve coastal resources and to maintain waterways, the Jersey's Shore Protection Program was created by the state of New Jersey. The program is carried out by the Bureau of Coastal Engineering and it is responsible for administering beach nourishments, shoreline protection and coastal dredging projects throughout New Jersey (NJDEP, 2014).

Protection methods Protection has involved many different structural solutions beginning with timber bulkheads and piles. During the 20th century large rocks were added to stop the erosional shorelines. Concrete came into play to create seawalls and eventually other structural solutions were used. In the last decades however the State prefers 'soft' beach nourishment to compensate for erosion instead of hard structural solutions. Between 1990 and 2005 over half a billion dollars was spent for 50 % of the developed shoreline between Sandy Hook and Cape May (The Richard Stockton College, 2007).

Financial construction Finance for coastal zone management is carried out by a cost-share combination of Federal (65%), State (25%) and local (10%) finances. The municipality must however

play an active role by requesting funding for a nourishment project at the State bureau. Also the Federal budget needs to be granted by Congress each time for each project. Often one important requirement for receiving Federal budget is adopting the standard beach 'template' of the USACE. This combination that each individual nourishment project need to be granted via Federal and State authorities, plus the need to adopt a standard beach 'template' of the USACE results in large differences in protection (level) for local beaches.

Current practice Currently the USACE prefers a combination of hard and soft solutions in storm damage reduction design. For example a rock or steel sheet pile seawall buried within a dune was constructed in Virginia Beach to protect the naval infrastructure (Basco, 1998). These approaches have recently been adopted by the USACE since they provide both a cost-efficient and environment friendly alternative (compared to only nourish or only hard protection), at least according to the USACE they do. In the fall of 2014 such a combination of hard and soft will be used near the cities of Mantoloking and Bay Head for their protection against storm conditions such as Hurricane Sandy (NJDEP, 2014).

4.3 Description of available data

4.3.1 Morphodynamics

Introduction In this subsection first the morphological impact of Hurricane Sandy is described. This is done with the use of photographic information and by analyzing pre- and post-Sandy beach profiles. Also the individual bathymetric data sets are presented. This is done to give the reader insight in the method of making the bathymetry and computational grid. For more distinct elaboration and several visual impressions, see Appendix E.

Impact of Sandy in general Like stated in Section 4.1, the area of consideration is the most severely hit part of the East Coast of the United States during Hurricane Sandy. The entire 20 km of barrier island is developed and is partly protected by hard structures. The damage people endured was a combination of wave forces which ruined houses plus high water levels which resulted in flood damage. Wave energy from sea resulted in the damage via scouring of the foundation and at the back of the barrier houses suffered from flood damage as a result of water level elevations from the bay (Walling et al., 2014). Also large amounts of sand were deposited on the back barrier. Photographic support is presented in Figure 4.3 and in Appendix D.

Within the 20 kilometer coastline two breaches occurred. One major breach in the center of Mantoloking and one minor breach between Mantoloking and Bay Head. During these overwash conditions water exploits existing weak spots and water level gradients between the sea and the bay are an important driver for erosion during overwash and inundation (Donnelly, 2007; McCall, 2008). At both breaches a road was constructed all the way from the dune top up to the back barrier bay creating a weak spot. In addition, both sites had limited barrier width resulting in large water level gradients over the barrier.

Other depositional features such as washover fans can also be distinguished from satellite images. Multiple washovers were recognized, mainly by humps of sediment in the bay, and the location of these washover fans is (often) closely related to weak spots in the coastal barrier. Weak spots in developed areas like New Jersey are often related to human impact due to for example the structure of beach access points or roads. Examples can be found in Figure 4.4.

(a) *Water damage: flood from the bay*

(b) *Wave damage: houses break in the middle*

Figure 4.3 *Two characteristic examples of damage which occurred during Sandy (Lopez-Feliciano, 2014). Both pictures are taken on November 3th 2012.*

(a) *Breach between Mantoloking and Bay Head*

(b) *Washover fan at Mantoloking*

Figure 4.4 *Two examples of depositional features, such as described by Donnelly (2007). Satellite information is from September 21th 2010 (pre-Sandy) and November 3th 2012 (post-Sandy). [Source: Google Earth].*

Making the model grid In order to make the bathymetry for XBeach, three data sources are used. The different data sources are used layer by layer and are used in the order presented. The horizontal datum used is NAD83, vertical datum used is NAVD88 and time is recorded in UTC. All distances are in m and the protection method used is UTM. The used data are:

1. **LiDAR** information both pre- and post-Sandy was available via the USACE and USGS. The information used is from 28-08-2010 (USACE, 2010) and 16-11-2012 (USACE, 2012; USGS, 2012a). The information from the USACE is of higher quality than the information retrieved from the USGS. This is related to a difference in response type (first versus last response) and filtering differences.
2. Also the **DUCKS** system from Stevens is used. DUCKS stands for Dynamic Underwater and Coastal Kinematic (Miller et al., 2009). Survey data from Lopez-Feliciano (2014) is used to qualify the nearshore profile up to a depth of NAVD88 - 10 m. In addition via Stevens also post Sandy bathymetry of the seawall at Bay Head is retrieved.

3. For the remaining parts the **Coastal Relief Model** (CRM) (NGDC, 2014) will be used. This information is of the lowest quality.

LiDAR is the most important information to model the barrier. After this step a uniform nearshore profile, based on DUCKS (Lopez-Feliciano, 2014) and CRM (NGDC, 2014) is made, which starts at NAVD88. This averaged uniform nearshore profile is smoothed and used up to a depth of 25 m. For all the undescribed parts of the model, mainly parts of the bay, the CRM is used. For a more elaborate approach one is referred to Appendix E.

4.3.2 Hydrodynamics

Introduction The hydrodynamic conditions used in XBeach will be derived from two existing hurricane models of Sandy. This means that the model will be nested in other computational models for deriving information needed at the XBeach boundaries. Both a sECOM model (Orton et al., 2012) and a Delft3D-model (Van Ormondt, 2014) will be used and validated at forehand against measurement data. The area of consideration in these models is presented in Figure 4.6. The hydrodynamic measurement data available is both from the NOAA and the USGS. A description of Hurricane Sandy can be found in Appendix F.2.

Data sources which are used are described below. More information of the different data sources can be found in Appendix F.1. A visual representation of the area can be found in Figure 4.5.

1. **Ocean surge** information via the NOAA, with the use of tide gauge 8534720 near Atlantic City, 8531680 near Sandy Hook, 8518750 near Battery. On top of that, the USGS has a tidal gauge near Manasquan River (01408050) (NOAA, 2012; USGS, 2012b).
2. For the **wave forcing** (wave heights and periods) buoy 44065 and 44025 offshore of Sandy Hook of the 'National Data Buoy Center from the NOAA is used (NDBC, 2012)
3. **Bay surge** information via the 'Hurricane Sandy Storm Tide Mapper' from the USGS is consulted, with in total four different stations in Barnegat Bay (USGS, 2012b).

In this subsection the validation will only briefly be discussed. For a more elaborate approach one is referred to Section 4.5

Ocean surge level The National Oceanic and Atmospheric Administration (NOAA) has four tidal gauge stations near Camp Osborne. The tidal gauge closest to the area of consideration is the one near Sandy Hook. This tidal gauge however stopped recording during the peak of Hurricane Sandy. All the other tidal gauges continued working throughout the storm.

Validation with sECOM and Delft3D-FLOW show that the RMSE of both models are in the range of 0.14 and 0.5 m. On average the water level peak is overestimated by Delft3D and underestimated by sECOM , but overall the sECOM shows a somewhat lower RMSE and will thus be used in XBeach to impose the water levels. The complete validation can be found in Appendix F.3

Waves: heights and periods No nearshore or shallow water in-situ measurements exist for the study area. The nearest measurement station for waves can be found offshore near Sandy Hook at the entrance of the New York City harbor. There is also a station 300 kilometers to the South-East (Station 44025).

Information of these stations is validated with Delft3D-WAVE (SWAN). Delft3D predicts the wave heights reasonably well with a RMSE of 0.92 m. The error of sECOM for the wave heights is an order

Figure 4.5 *Location of information sources used for determining the accuracy of two other models to apply at the boundaries of XBeach (nesting). Red are tidal gauges, green are wave buoys and blue is the project location. [Source: Google Earth].*

higher than Delft3D and will not be further validated. The reason for this error is that the model is based on the Great Lakes model. The wave periods are somewhat harder to predict than the wave heights. During the peak of Sandy the error of the simulated values decreases significant. It is assumed that Delft3D-WAVE can be accurately used. The output spectra calculated by Delft3D-WAVE is directly incorporated in XBeach.

Bay surge level In the considered area there are several gauges in the bay available. When comparing the different gauges the maximum difference in the peak is 0.3 m over a distance of 5 km. The moment of the peak is more or less similar across the entire bay. Neither Delft3D nor sECOM provides information of the water levels in the back barrier bay, and therefore the closest record is directly used in XBeach. This approach is an oversimplification, since no alongshore variability at the back of the XBeach is present.

Boundary conditions Given the number of uncertainties in the offshore forcing it is difficult to specify with 100% certainty the hydraulic boundary conditions to model the entire system. Therefore, the simulation will be carried out with a so-called base simulation. The sensitivity of uncertainties in the boundaries will be analyzed per field case.

In the base simulation the sECOM water levels and Delft3D-WAVE spectra are used as input. The simulations start at October 28, 2012 00:00 and will end on of October 31, 2012 00:00. The conditions imposed can be found in Figure 4.7. The maximum significant wave height is 6.5 m and occurs around 22:00 on October 29th UTC. The peak in water level has a value of 2.83 m and occurs 2 hours later. The lag in the bay is 4.5 hours.

From Figure 4.7 and Walling et al. (2014) one can conclude that the area of interest endured *two separate* flood events. The first event occurred right before landfall of Sandy and resulted in high water levels from sea in combination with high wave heights. This first flood event effected the beaches, dunes and possibly the back barrier. The second flood event is responsible for inundation of large parts of the back barrier.

The mean directional spreading of the Delft3D-WAVE input is 33 with a mean wave angle during the peak of Sandy of 83.7 degrees. A nautical reference frame is used, which means that the peak of the storm came from North-East.

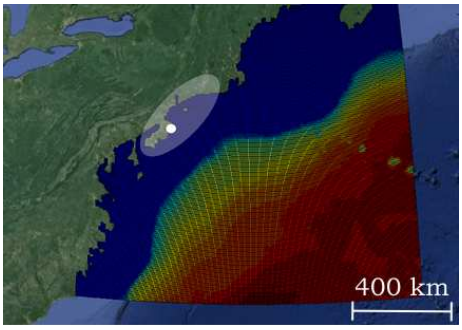

(a) *Delft3D: US Atlantic East model*

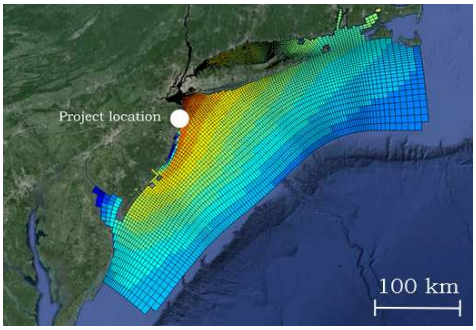

(b) *esCOM: detailed level*

Figure 4.6 *Satellite image of the area of interest in which Delft3D (left) and eSCOM (right) are plotted. In the left image the bathymetry and in the right image water levels during the peak of Sandy are plotted. White circles indicate the project location and the white transparent ellipse represents the eSCOM model.*

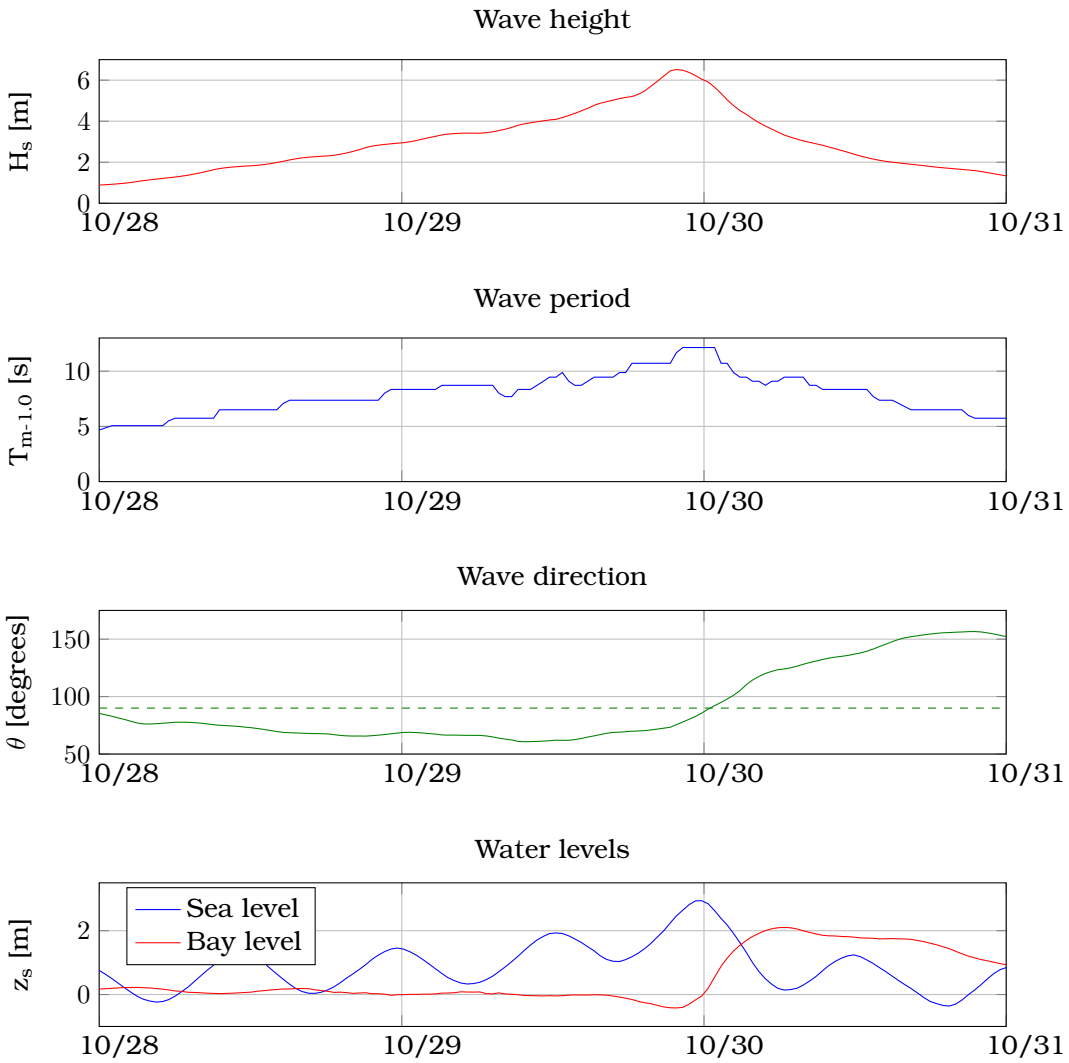

Figure 4.7 *Boundary conditions imposed in XBeach.*

4.4 Buried seawall: cross-shore effect

4.4.1 Introduction

The area of interest in this subsection is the buried seawall at Bay Head. Eight cross-sections will be modeled using XBeach in 1D. This is equivalent to each 150 meters. The computational grid has a variable cross-shore direction with a minimal distance of 1 meter near the water level. The area behind the seawall is schematized with a bed level of NAVD88 +3 m. The focus in this section is bipartite. First of all the impact of hard elements in the cross-shore will be examined. This is done both in Section 4.4.2 and 4.4.3. Also a calibration step will be made which is also needed in the following subsections where an XBeach model for Bay Head and Camp Osborne is applied in 2DH. Discussions related to the morphological skill and calibration will be done in Section 4.4.4 Photographic material of the seawall is presented in Figure 4.8 and Appendix D.2.

(a) *Oblique photograph* **(b)** *Impact on the ground*

Figure 4.8 *Images of the impact of Sandy on Bay Head. Left image is taken by USGS on 05/11/12. Right image is taken by Lopez-Feliciano (2014) on 16/11/12.*

4.4.2 Data analysis: using DUCKS

Stevens Institute of Technology made use of a Dynamic Underwater and Coastal Kinematic Surveying (DUCKS) system (Miller et al., 2009) to gather elevation profiles of a groin field on September 22, 2011 at the city of Bay Head, NJ in front of the (buried) seawall. The information after Sandy is retrieved on November 20, 2012.

When comparing the pre- and post-DUCKS the following remarks can be made:

1. Hurricane Sandy resulted in a mean bottom level change of 1 m with a maximum change of 3 m. The total erosion volume measured in the area is 93910 m^3 (Lopez-Feliciano, 2014).
2. No clear scour holes are present in the data. This is remarkable, because in the conceptual study for the collision regime scour holes at the toe of hard structures did occur. The likely reason is the fact that during the first 2 weeks after Sandy the erosion holes are filled up by the tidal movement (as seen in the previous chapter). Another possibility is human impact.

4.4.3 Base simulation results

Pre- and post-Sandy XBeach is capable of reproducing the morphological response of the system in front of the (buried) seawall during Sandy in an accurate way with a Brier Skill Score (BSS) of 0.93 and a bias of +0.08 m. Sediment is taken away between 0 and 80 m in front of the seawall and deposited in the nearshore. The system tries to get in equilibrium with the storm conditions, but the cut off of sediment due to the structure will hinder the development of the nearshore. Like stated in Section 4.4.1, eight cross-section are modeled. In this paragraph Profile 7 (the best fit) and Profile 5 (least best fit) are presented. The results for Profile 7 are presented in Figure 4.9.

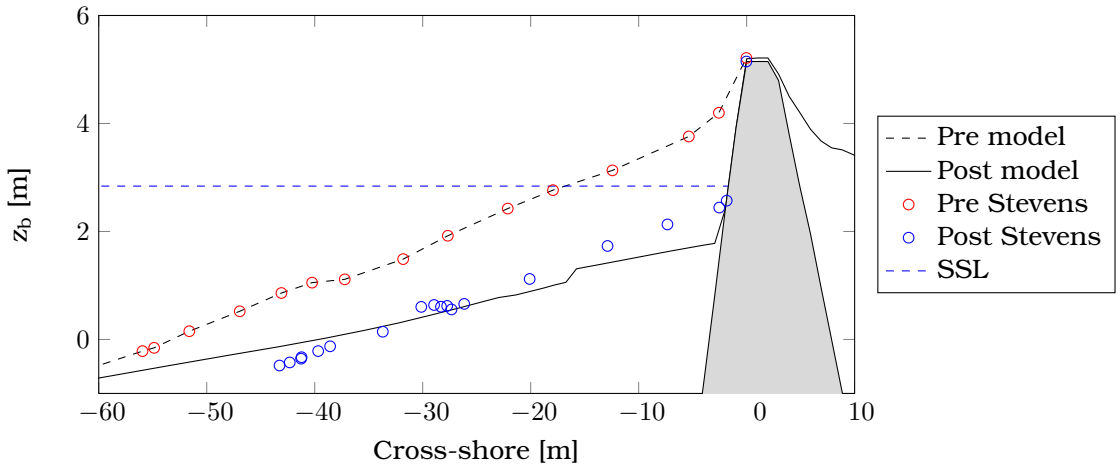

Figure 4.9 *Model set-up, post measurement data and the post profile as calculated by XBeach for Profile 7.*

After 36 hours of simulation the beach starts to erode when the significant wave height exceeds 3 m. During the peak of the storm a scour hole in front of the structure develops. However, the next 12 hours this bed level difference is partly compensated and the scour is filled up again as a result of the combination of ebb and decreasing significant wave heights, as can be seen in Figure 4.10.

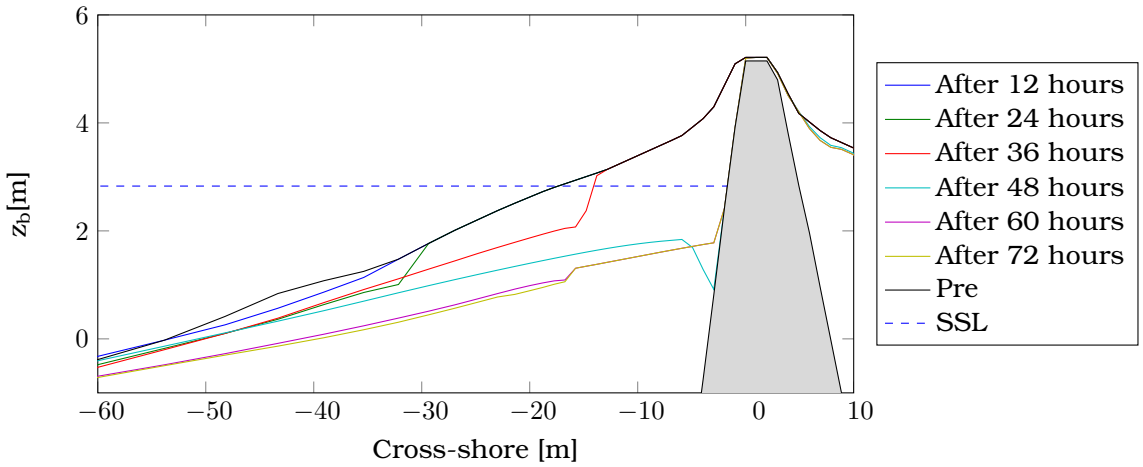

Figure 4.10 *Development of the bed level plotted each 12 hours as calculated by XBeach.*

Erosion The erosion patterns as calculated by XBeach agrees well with the measurement data. For measurement points with a cross-shore distance of 25 m or larger an almost complete fit can be found. Discrepancy between the data occurs for points more close to the toe of the structure, as can be seen in Figure 4.11. This was expected based on the data analysis of Section 4.4.2 where the lack of scour hole development was noticed. A possible reason is infilling of the scour hole during ebb and flood, which also (partly) occurred during the XBeach simulation of three days. Another possibility is the impact of humans on the system, since measurement data is retrieved two weeks after Sandy and photographic material already shows human activity in 3 days after Sandy.

The morphological response is the result of the combination of wave energy and water levels. The peak of Sandy occurred at 00:00 UTC on 10/30 and during the simulation of this period water hits the seawall constantly for a period of 18 hours (9 hours before and 9 hours after landfall). Most of the erosion occurs in the second half of 10/29 during the highest waves, as can be seen in Figure 4.12. Right before landfall of Sandy, during the combination of high waves and high water levels, a scour hole is developed. This hole is filled up again between 00:00 and 02:00 UTC of 10/30. Overall the erosion volume is about 80 $m^3 \cdot m^{-1}$.

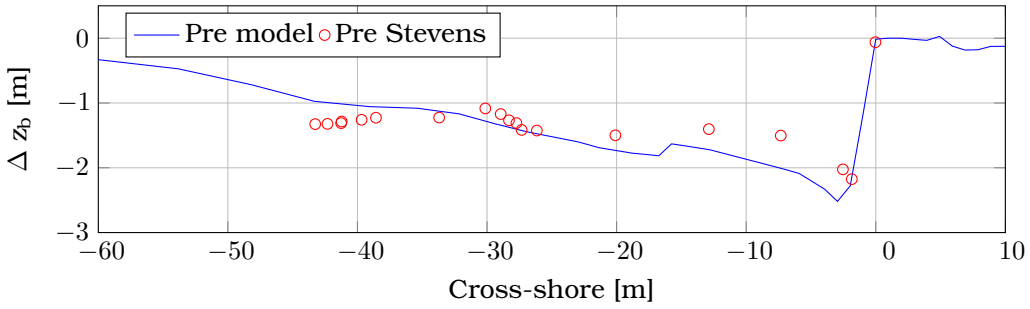

Figure 4.11 *Bed level difference (pre- minus post-storm) for measurement data and as calculated by XBeach.*

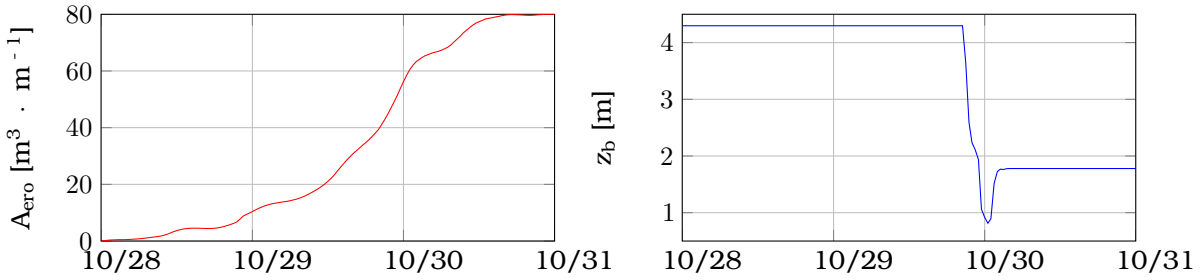

Figure 4.12 *Development of the erosion volume [$m^3 \cdot m^{-1}$] and score hole in front of the structure [m].*

Different profiles Up to now the results of only one profile, Profile 7, were presented. The other profiles behave more or less similar as the result of Profile 7. The total erosion modeled is 99288 m^3. The calculation is based on the average erosion volume per m and the total length of the structure. The total erosion measured from the DUCKS survey (Lopez-Feliciano, 2014) is 93910 m^3. XBeach overestimates this erosion volume with 5 %, but this is most likely related to the differences right in front of the seawall where some accretion is not reproduced by XBeach which possibly occurred the weeks after Sandy due to sediment transport driven by tidal movement. The results of all the

different profiles are presented in Table 4.1.

When comparing the results for Profile 5, the profile with the lowest score (BSS of 0.89) plus the highest positive bias (+0.37 m), the following stands out. First of all, there is still sediment on top of the structure. In reality the entire barrier was exposed after Sandy. This difference could be related to short wave run-up which is taken into account via a parametric relation. Second, the beach slope is somewhat too steep compared to measurement data. This could be related to the forcing via the incorporation of too much spectrum energy. There are two other possibilities for these differences. First, an 1D approach is applied in a complex area with a beach within groin. A discrepancy between the LiDAR and DUCKS which resulted in too much sediment in the pre-simulation set-up. Profile 5 can be found in Figure 4.13.

Table 4.1 *Various simulation results for different cross-sections. In which $\Delta z_{b,toe,min}$ is the maximum bed level change at the toe of the structure, which is calculated in a window of 10 grid cells.*

Profile	A_{ero} $[m^3 \cdot m^{-1}]$	$\Delta z_{b,toe,max}[m]$	BSS [-]	Bias $[m]$
1	79.73	-3.2	0.95	0.07
2	77.49	-1.9	0.95	-0.09
3	84.75	-3.0	0.93	0.39
4	78.19	-2.7	0.96	-0.04
5	72.80	-2.7	0.89	0.37
6	76.62	-2.3	0.91	-0.16
7	79.99	-2.5	0.97	-0.02
8	80.73	-2.6	0.92	0.08
Mean	78.79	-2.6	0.93	0.08

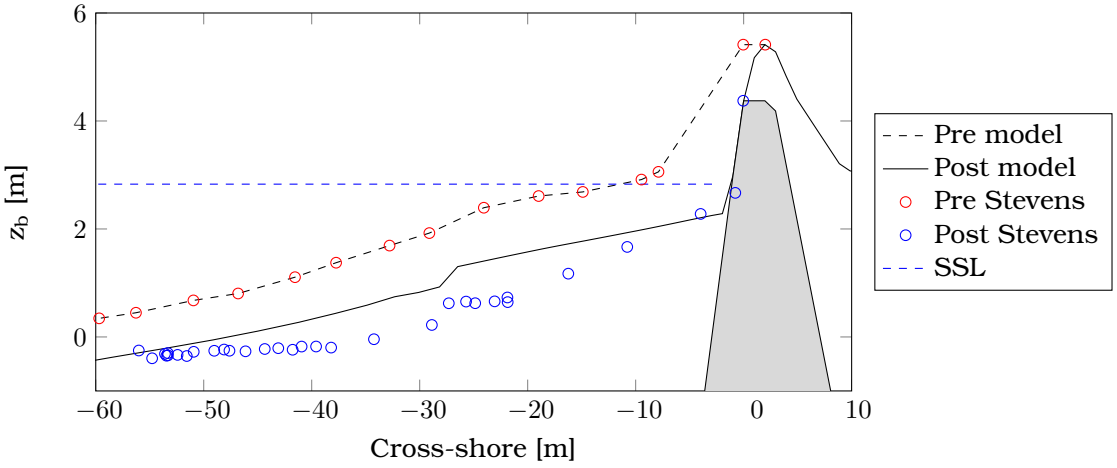

Figure 4.13 *Model set-up, post measurement data and the post profile as calculated by XBeach for Profile 5.*

4.4.4 Morphological calibration and skill: facua

Skill The skill of reproducing the morphological response of all the profiles simulated are *excellent* according to the classification of Van Rijn (2003). Skill and bias change rapidly during the peak of the storm right before landfall. Overall the erosion at the toe is overestimated, but the overall bias has a positive value.

Most differences in terms of BSS and bias occur in the 12 hours before landfall. This is a direct result of the hydrodynamic forcing, since in this part of the storm the highest significant wave heights and water levels occurred. The first and last 12 hours of the simulation are of limited importance for the morphological response of the system, as can be seen in Figure 4.14.

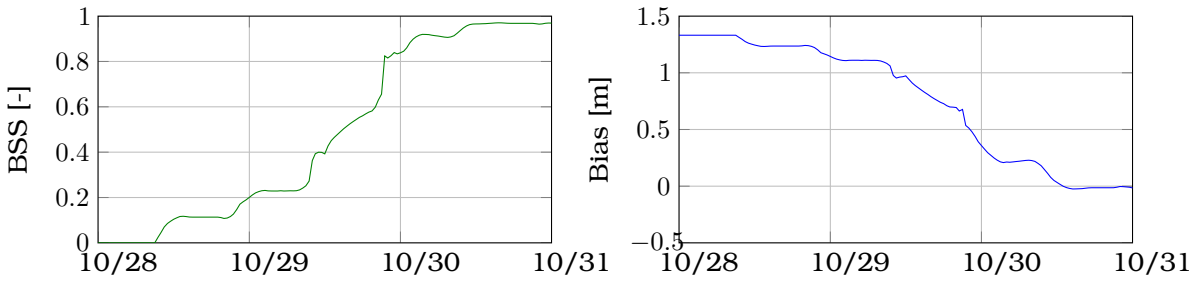

Figure 4.14 *Development of the BSS [-] and bias [m] of Profile 7 over time.*

Calibration All the XBeach simulations are carried out with 'default' settings and only the $facua$ parameter has been changed. This parameter is related to wave asymmetry and skewness. By increasing the $facua$ the erosion will be (partly) counteracted with an asymmetric onshore sediment transport. The default value for $facua$ is 0.1 and in theory values of 0.3 can been applied (Van Rooijen, 2011). More information about the $facua$ can be found in Appendix A.5.3. In this paragraph the conclusions are presented, but the complete table can be found in Appendix G.1.1.

The range of XBeach predictions with a high $facua$ and without this component are enormous. The range between the highest and the lowest prediction is an erosion volume difference of 120 $m^3 \cdot m^{-1}$ and a bed level difference of 2 m, as can be seen in Figure 4.15.

For a default value XBeach predicts 60 % too much erosion and has a skill of 0.56 which can be seen as *moderate* according to the classification of Van Rijn (2003). By counteracting offshore sediment transport with a $facua$ of 0.25 the erosion volumes, BSS and bias are in line with the measurements. This is reflected with a BSS of 0.97 which can be seen as *excellent*. An evaluation of this value for a soft cross-section resulted in a BSS of 0.84.

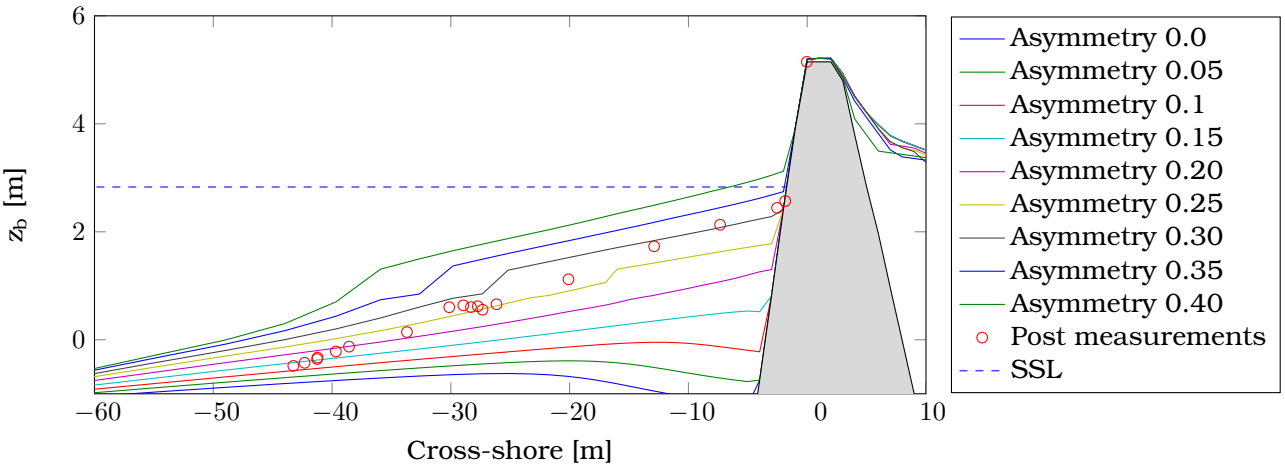

Figure 4.15 *Post bed levels for a single hard cross-section for various values of $facua$.*

4.4.5 Absence of a hard element: beach or dune extension?

Introduction The existence of the buried seawall came as a surprise for the residents of Bay Head. The seawall was buried for about hundred years and a reference simulation in XBeach has shown that without the seawall already at 22:30 UTC overwash would have occurred. This is 1.5 hour before the peak of the storm. In this subsection what-if questions will be assessed in order to analyze and evaluate several protection methods.

Dune extension When the entire area behind the top of the structure was sand, the dune retreat would be in the order of 16 meters. This means that the same protection as the seawall could have been created with a completely natural dune of NAVD88 + 5 m of about +/- 18 m long. This is however not a feasible option, since already 10 m after the seawall human activity is present.

Beach extension Another possibility to protect the hinterland is by extending the beach. This is the approach currently adopted by the USACE in New Jersey. They use a standard template in which soft protection is combined with a hard structure such as for example a seawall. The area of Bay Head however did not benefit from a nourishment program of the USACE and therefore the pre-Sandy beach width was limited to 20 meters. However, when the beach is extended with an extra 30 m the barrier would have still *not* be able to withstand Sandy and still overwash would have occurred, as can be seen in Figure 4.16. A beach extension without seawall will limit the erosion by 16 $m^3 \cdot m^{-1}$.

Do nothing: no additional protection In terms of erosion volume the situation without a protection at all (without seawall) erodes most. Waves will overwash the barrier and about 44 $m^3 \cdot m^{-1}$ of extra sediment is eroded (+55 %). In addition, the wave-averaged forces on the ocean front structures of Bay Head would have been twice as large (Irish et al., 2013).

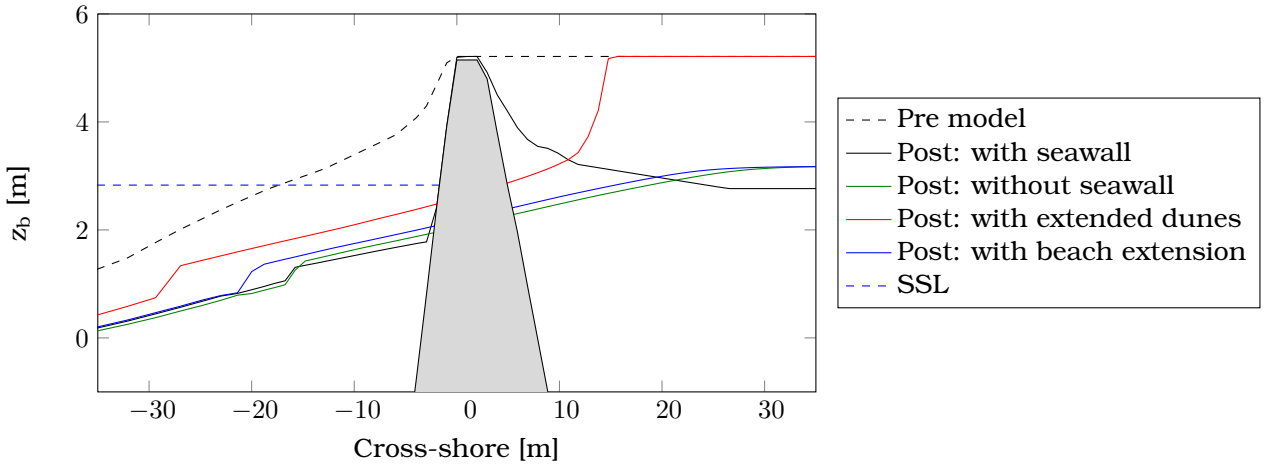

Figure 4.16 *Post bed levels for multiple what-if simulations such as a dune extension.*

4.4.6 Model sensitivity

Introduction The flexibility of XBeach makes it possible to check the relative influence of several factors which are applied in the model set-up. In this subsection first the uncertainty in the boundary

conditions is treated. Second, the scour development is analyzed. In the last part the impact of several XBeach parameters / settings is analyzed. This subsection only treats the conclusions per paragraph. The complete analysis can be found in Appendix G.2.

Uncertainty in boundary conditions The uncertainty in the boundary conditions is analyzed by first of all varying the spectrum energy and also by varying the water levels. Variation in spectrum energy is applied by enhancing and reducing the energy with 25%. For the water levels both a general base variation of 0.1 m and a peak variation of 0.5 m is applied. This is related to the bias of the sECOM between measurement data and Delft3D as can be found in Appendix F.3. In this paragraph the conclusions of this analysis are described. For the full analysis one is referred to Appendix G.2.1.

The following conclusions can be made related to the effects of the uncertainty in boundary conditions:

1. The linear relation proposed by Fisher et al. (1986) is reproduced. This means a variation of 25% in spectrum energy will result in a variation of 25% in erosion volume. A decrease in spectrum energy with 25% will result in a 3 m higher minimum bed level at the toe of the structure.
2. Variation of the water levels will have an impact on the minimum bed level at the toe and less on the erosion volume. A base water level variation of 0.1 m will only result in a 2% variation in erosion volume, but means a 0.6 m deeper scour hole.

Scour hole development In the conceptual study for the collision and overwash regime it was found that infilling of scour can occur during decreasing values for the hydrodynamic forcing. For the field case of the (buried) seawall a reference simulation is carried out in which the SSL is kept constant. The results are compared to the baseline with a varying SSL. The result is a reproduction of what was found in the conceptual study. Infilling of scour is mainly related to falling water levels, but also variation in spectrum energy can trigger infilling of a scour hole. The full analysis can be found in Appendix G.2.2.

Importance several XBeach parameters In XBeach several physical descriptions are represented in the source code in order to reproduce the morphological behavior in the most accurate way. These contributions can be deactivated in order to analyze the impact of each factor. In this paragraph the contribution of $swnrunup$, $jetfac$, long waves and avalanching are analyzed. First two relations are implemented in XBeach since the version of December 2013 and applied based on the recommendations described by Van Geer et al. (2012). For the full analysis one is referred to Appendix G.2.3.

The following conclusions can be made related to the effects of XBeach parameters

1. The parametric relation $jetfac$ is not of importance in the description of the erosion volume nor for the scour depth. A similar conclusion is made for the $swrunup$. It is not clear if this is the result of a bug or the result of a specific process, but is remarkable since both relations are included in order to better reproduce erosion near hard structures. For the $jetfac$ small differences for the turbulence generation are found, but this had limited effect. The parametric relation $swrunup$ did not result in avalanching of all the material on top of the seawall.
2. Without long waves the model would have eroded 29% less than with long waves. This percentage is comparable with the value found in the conceptual study.

3. The avalanching algorithm is responsible for 5% of the erosion, compared to an XBeach simulation without avalanching. This is a remarkable low percentage compared to other studies. The algorithm is however important in getting the seawall exposed.

4.4.7 Conclusion

In this section the impact of Hurricane Sandy on the (buried) seawall is modeled. It is possible to model the system with an 1D XBeach model in a morphological accurate way with the default settings and calibration of only one parameter, despite the difficult surroundings of a nearby groin field. The following conclusions can be made:

1. In the post Sandy measurements no scour holes at the toe of the structure were visible. This post bathymetry is however also reproduced by XBeach. Modeling the exact elevation in front of the structure, however, remains difficult. This is related to the influence of varying water levels (ebb and flood). Simulations suggest that during Sandy the scour at the toe of the seawall was filled during falling water levels. The total erosion measured via DUCKS in front of the seawall was 93910 m^3. The XBeach simulated value is 99288 m^3 (+5%).
2. In XBeach $facua$ is a powerful tool in order to calibrate the model. In this case study a value of 0.25 will be applied compared to 0.10 as default. The result is a BSS which can be seen as *excellent* for both the soft (BSS of 0.84) as well as the hard cross-sections (BSS of 0.93). Without the variation of $facua$ the model will suffer from 60% too much erosion.
3. A similar protection as the buried seawall provides, can be achieved with an 18 m wide sandy dune. This is however not a feasible option, since after 10 m already human activity is presented. The hard element was a useful method in order to reduce the impact of Hurricane Sandy. Without the seawall the erosion volumes would have been 55% larger and the wave-averaged forces on the ocean front structures of Bay Head would have been twice as large (Irish et al., 2013).
4. Fisher et al. (1986) proposed a relation between the wave impact force and the erosion volume. This relation has been reproduced with a variation in spectrum energy. Change in water levels (both a base and a peak variation) will mainly influence the scour depth and have minor impact on the erosion volumes.
5. Several parametric relations ($jetfac$, $swrunup$) developed in XBeach in order to model the effects of hard elements in a more accurate way, have a negligible impact on the simulated post-storm bed level and erosion volume. The reason for this limited impact is currently not known. This can be related to a bug or to a specific process (counter force).

4.5 Bay Head: modeling overwash with XBeach

4.5.1 Introduction

The area of interest in this subsection is the site between the cities of Bay Head and Mantoloking. The area of interest is roughly one kilometer wide. The complete XBeach model used has a domain of 9 by 7 km in order to reproduce the hydrodynamics accurately in the area of interest. A grid size varying from 50x10 m (offshore) down to 2x5 m (on the barrier) is used. The focus of this section is to accurately model overwash in XBeach. This second calibration step is needed since XBeach has some difficulties in describing overwash conditions without the use of artificial limiters (McCall et al., 2010b). The satellite image, presented in Figure 4.17, shows evidence of both overwash fans and a fixed breach which occurred at the location of a road which connected the bay with the sea.

(a) *Pre-Sandy* **(b)** *Post-Sandy*

Figure 4.17 *Detailed satellite images of the area of interest at Bay Head from Google Earth. Pre-information is from 09/21/2010 and post-Sandy information is from 04/11/2012.*

4.5.2 Data analysis: LiDAR provided by USACE

Figure 4.18 presents the available LiDAR data of the area. The latest information prior Sandy was collected on Augustus, 28, 2010 (USACE, 2010). The data set after Sandy was collected on November 16, 2012 (USACE, 2012). It is important to note that the difference between the impact of Sandy and the measurement data is 15 days. This will result in the fact that already some human impact on the sedimentation and accretion patterns could have occurred.

Based on the LiDAR data sets and the theory of Chapter 2 a more detailed analysis can be made of the morphological response of the area. The following remarks can be made based on Figure 4.17 and 4.18.

1. The mean erosion as measured by subtracting the pre- and post-Sandy LiDAR is 179.8 $m^3 \cdot m^{-1}$.
2. Erosion has led to a severe decrease in dune top level. The mean dune top level ($\overline{D_{\max}}$) decreased from 6.50 to 3.96 m. The maximum dune slope has a value of 0.22 [-].
3. Deposition on the back barrier bay is (partly) absent in the LiDAR. This is most likely due to human interference right after Sandy. For example the two alongshore roads have been cleaned which is clearly visible in the post LiDAR.

4. A minor breach occurred at y = 4700 m, but this is not visible in the LiDAR as a result of filling the breach by the USACE right after Sandy. The LiDAR is retrieved several days after the hurricane event.
5. Possibly some dune recovery after Sandy (human impact) has taken place at y = 4700 - 4400 m and at y = 4100 m.

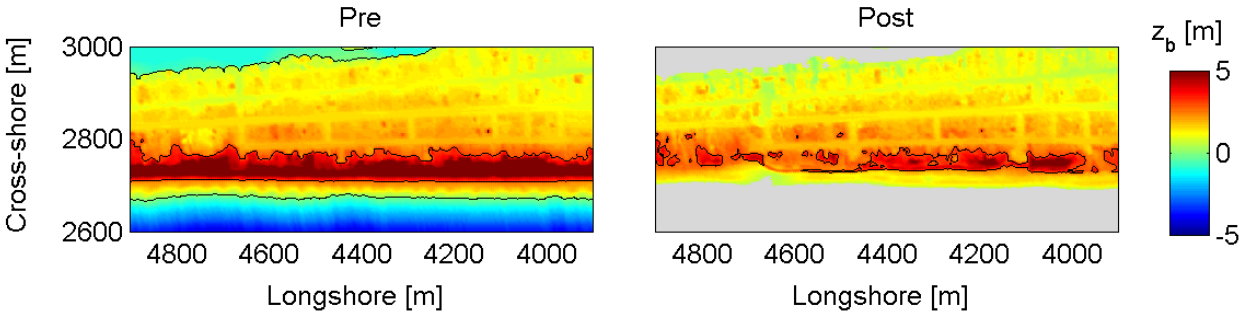

Figure 4.18 *Pre- and post-Sandy LiDAR data presented for the area of interest at Bay Head. Spots without data are marked grey. The black depth contours are provided at an elevation of 0 and 3 m relative to NADV88.*

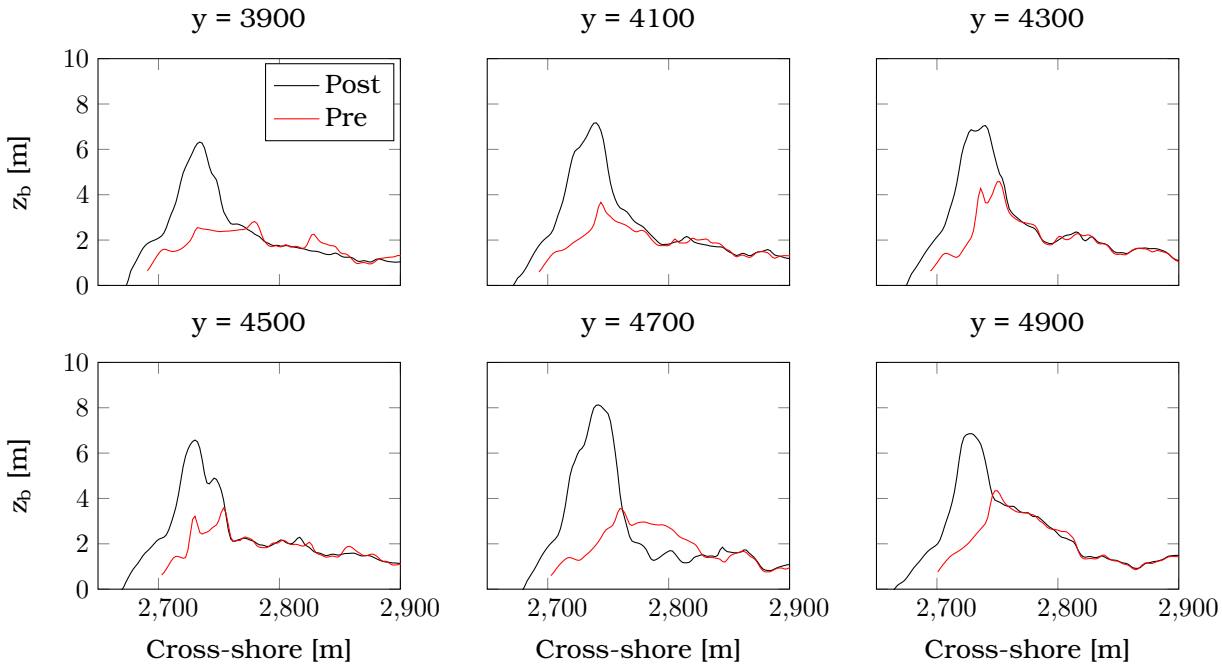

Figure 4.19 *Several cross-sections for the bed level both pre- and post-Sandy of Bay Head.*

4.5.3 Base simulation results

Pre- and post-Sandy XBeach is capable of reproducing the morphological response of the system during Sandy in an accurate way with a BSS of 0.84 and a bias of +0.10 m. Material is taken from the coastal dunes and deposited both in the nearshore as well as on the back barrier. Only during the peak of Sandy overwash takes place. There is good similarity between the patterns in both the post profile and for the erosion/accretion, as can be seen in Figure 4.20. Note that the breach at y = 4700 m is *not* reproduced in the data *and* simulation. On top of that, deposition calculated by XBeach is not incorporated in the LiDAR, as a result of human recovery in the days after Sandy.

When comparing the development over time the first 40 hours of the simulation the entire barrier stays in the collision regime. Sediment is taken away from the dune face and deposited in the nearshore. In the next 8 hours waves start to increase until significant waves heights of about 6 m. The effect is severe dune erosion and eventually waves will overtop the coastal barrier. Most erosion occurs during this overwash period. In the last 12 hours of the simulation hardly any morphological activity can be noticed.

The erosion rates alongshore are in the order of 178 $m^3 \cdot m^{-1}$. This is 98% of the measured erosion. Remarkable is that about 26% of the simulated erosion occurs between in the 48 to 54 hour of simulation. This is after landfall when already the largest surge and waves have occurred. Erosion is thus not only hydrodynamic-driven, but depends also on the system itself. During the overwash regime less sediment is deposited in the nearshore and therefore the inhibitory effect of erosion can only partly take place. This underlines the importance of feedback loops in morphological systems. During the 10 hour storm peak about 47% of the erosion occurs.

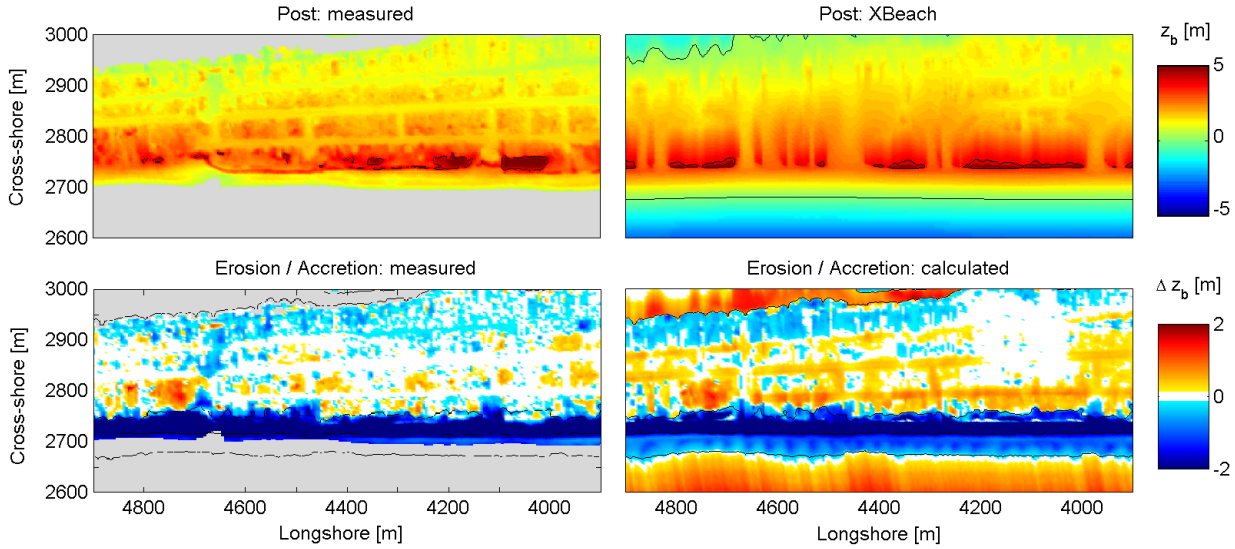

Figure 4.20 *Spatial post bed levels and erosion/accretion plots after the storm event presented for the area of interest at Bay Head. Spots without data are marked grey. The black depth contours are provided at an elevation of 0 and 3 m relative to NADV88.*

Different cross-sections When comparing the different profiles with the pre- and post-Sandy measurements it is clear that the morphological end result is strongly related to the avalanching parameters of the maximum wet slope ($m_{cr,wet}$) and dry slope ($m_{cr,dry}$). The peaks in the profile seems somewhat unrealistic and too steep. Figure 4.21 shows that overall the calculated maximum dune

top high is reasonable simulated. Some local peaks like for example at y = 4300 m, are too high and some overwash fans are too low (have eroded too much) compared to the LiDAR. The mean dune top decreases in the XBeach simulation from NAVD88 +6.5 to +4.4 m, which is an underestimation of 0.50 m compared to measurement data. A possibility for this overestimation is that the critical slope is exceeded since excessive rain fall could have triggered avalanching. During Sandy 122 mm of rain fell in the area in a short period of time (National Hurricane Center, 2012), so the hypothesis seems at least possible.

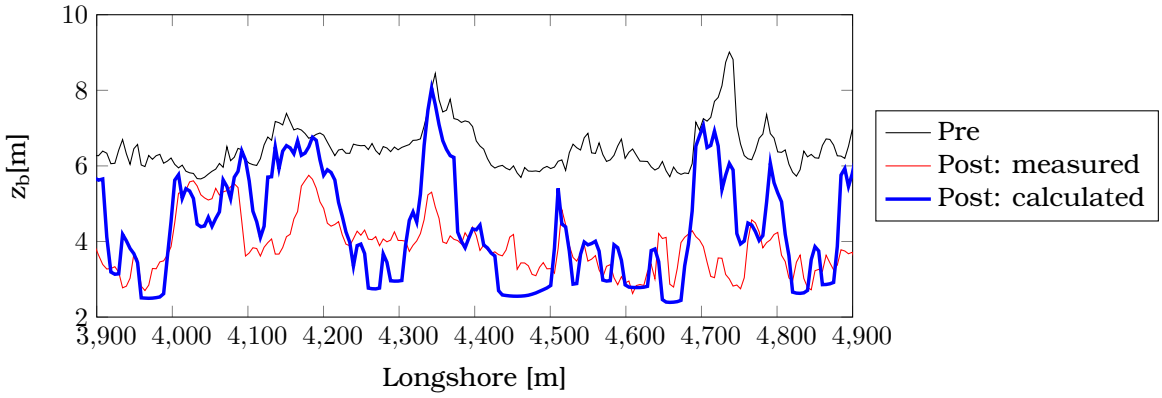

Figure 4.21 *Maximum crest height in longshore direction is calculated with pre-Sandy, post-Sandy and post-calculated by XBeach.*

Identifying weak spots Potential weak spots can be identified by calculating the amount of sediment above SSL. For the area of interest this calculation routine has been carried out. From Figure 4.22 one can already recognize the breach at y = 4700 m, shown in the red circle, which occurred during Sandy. Second a large breach at y = 4350 m is distinguished.

The background behind this relation is first of all that the relative dune height above SSL was the most important parameter in the sensitivity analysis of Appendix C.2.5 for determining the morphological response of the system. In addition, for overwash cases, the dune top height is of minor importance and the dune volume above SSL has a larger impact on the behavior of the system. The threshold is set on 135 $m^3 \cdot m^{-1}$, which is related to the minimum amount of erosion measured. This simple calculation routine can be used by the local authorities in order to identify weak spots in the coastal barrier.

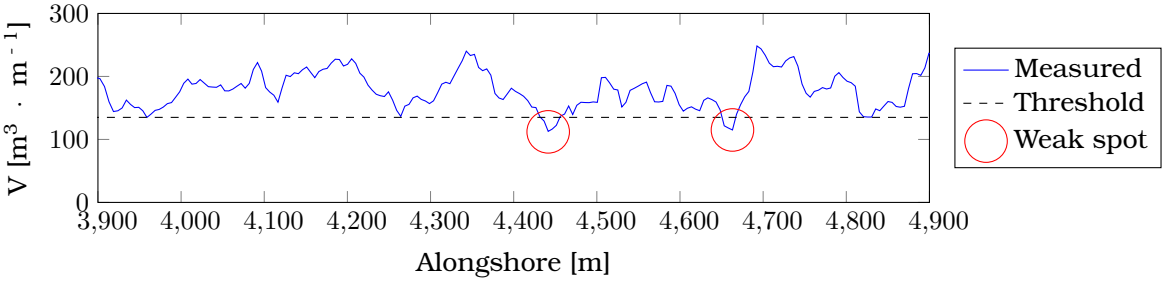

Figure 4.22 *Barrier volume in $m^3 \cdot m^{-1}$ above SSL which is a tool to indicate potential weak spots during storm events. This analysis is made for the area of interest at Bay Head. In the red circles the breach location at y = 4700 m and the major overwash fan at y = 4350 m.*

4.5.4 Morphological calibration and skill: Chezy

Brier Skill Score (BSS) and bias The BSS and the bias have a large spatial variation and are plotted with a so-called moving window of 6x6 grid cells. This gives the reader a clear insight of the different skill score per region instead of focusing too much on a mean score. From Figure 4.23 one can conclude that the BSS in the area with dunes is *excellent* according to the classification of Van Rijn (2003). The model does not have a skill on the back barrier. This is related that both deposits are removed the weeks after Sandy and that the bed level differences are small (0.1 m).

The moving window for the bias results in a similar image. First of all the patterns of the roads are clearly visible with a positive bias. This is the result of sedimentation which occurred in the simulation, but is not present in the LiDAR, because the roads were cleaned the first days after Sandy. The area where limited down to no deposition occurs, between x = 2900 and 3000 m, the skill scores increases and becomes positive. In Figure 4.21, one could notice that the dune tops are modeled too high in XBeach, which results from a positive bias around the dune top. The areas of two large overwash fans at y = 4700, 4500 and 4350 m result in negative bias values.

Overall the morphological skill of the XBeach model is *excellent*, despite that locally the breach is not reproduced. The mean value of the BSS and bias are 0.84 and 0.10 m. When only the erosion of the dune is taken into account the score is somewhat better (BSS of 0.91), but the bias increases up to +0.46 m. Important to note that the mean BSS of multiple cells is *not* similar to the BSS computed directly. This is related to the quadratic character of Equation B.3 and therefore there is no direct relation between the BSS in Table 4.2 and Figure 4.23.

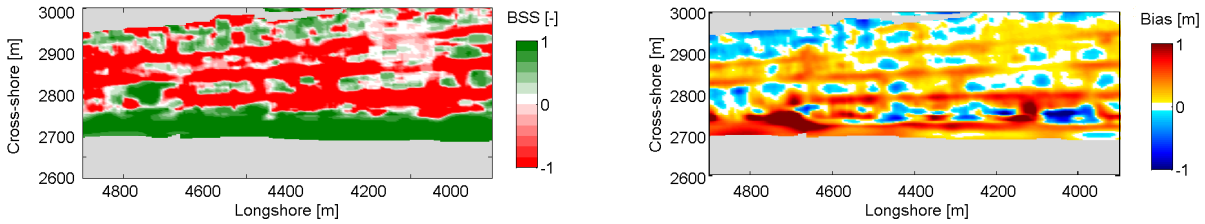

(a) *BSS* **(b)** *Bias*

Figure 4.23 *Morphological performance indicators in both the BSS (left panel) and the bias (right panel) presented in a moving windows of 6x6 cells for the area of interest at Bay Head.*

Table 4.2 *Comparison between measurement data and the XBeach simulation.*

	BSS [-]		Bias [m]		Other	
Runs	All	Erosive	All	Erosive	A_{ero} [$m^3 \cdot m^{-1}$]	$\overline{D_{max}}$ [m]
Measurement	-	-	-	-	179.8	3.96
XBeach	0.844	0.909	0.104	0.464	177.6	4.5

Calibration of the roughness: Chezy value In the previous section calibration of the collision regime has been carried out with the $facua$ parameter. In this subsection calibration of the overwash regime is carried out by varying the roughness on the barrier. In practice this means that a lower Chezy coefficient is applied at the barrier. This will result in more friction and thus less erosion. The default value in XBeach for Chezy is 55 $m^{0.5}.s^{-1}$ and in theory values of 10 $m^{0.5}.s^{-1}$ can be applied (Van Velzen et al., 2003). A calculation for the expected roughness based on the Nikuradase sand

roughness (k_s) of 0.5 m in a water depth of 1.0 m results in a Chezy value of 25 $m^{0.5}.s^{-1}$. More information about the roughness can be found in Appendix G.3.

The range of XBeach predictions with and without extra roughness are enormous. The range between the highest and the lowest prediction is an erosion volume difference of 705 $m^3 \cdot m^{-1}$. For a default value XBeach predicts 397% too much erosion and has a skill of -2.8 which can be seen as *bad* according to the classification of Van Rijn (2003). At every overwash spot large amounts of sediments are taken away and potential breaches. A lower Chezy value can be seen as friction generated by the combined effort of both vegetation and structures. The Chezy coefficient of 30 $m^{0.5}.s^{-1}$ will result in the highest BSS, lowest bias and more ore less similar amount of erosion. This is reflected with a BSS of 0.84, which can be seen as *excellent*. It is important to note that the mean reproduction is good, but locally differences can occur. The complete table can be found in Appendix G.3. The results are visually presented in Figure 4.24.

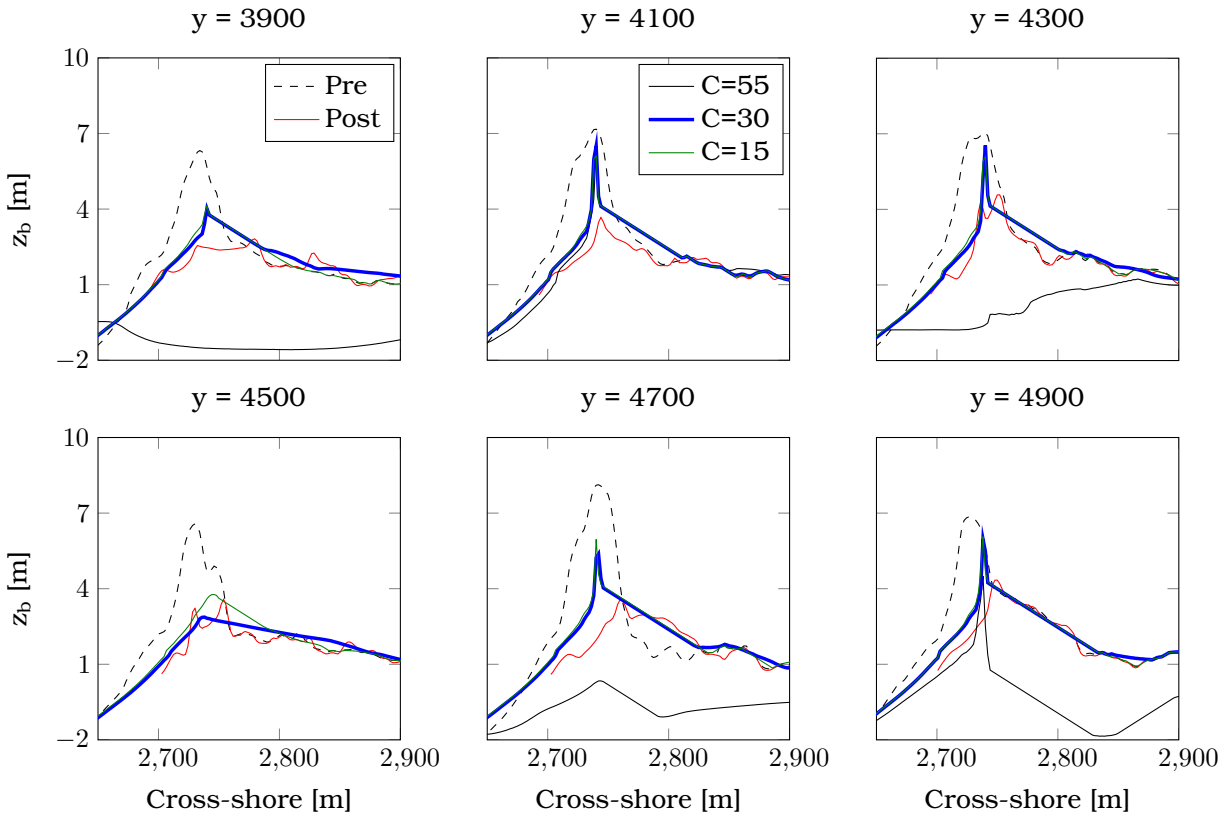

Figure 4.24 *Post bed levels for various cross-sections: pre-Sandy, post-Sandy and calculated for multiple Chezy values. The legend present is valid for all individual subfigures.*

Evaluation: individual contributions Calibration has been carried out based on both a higher asymmetric transport parameter and by applying a lower Chezy value on the barrier island. When each individual parameter or calibration step is applied separate, the impact *per* adjustment can be elaborated. In Table 4.3 the results of this analysis are presented. Simulations without any calibration, with only the increased $facua$, with only the increased roughness, with both calibration steps applied and a simulation with the artificial limiter based on the Shields number (s_{max}) are presented in this table.

Running an XBeach model without a higher value for the $facua$ and no increased roughness on the barrier will result in too much erosion, both in the earlier collision regime and during the peak of the storm when the barrier is overwashed. The BSS and bias are in the same order as comparable simulations for case studies Santa Rosa and Fire Island (McCall et al., 2010b; De Vet, 2014). The combination of $facua$ and roughness makes it possible to describe the field case in a morphological accurate matter with a BSS of 0.84.

When only the $facua$ is applied the collision regime (dune erosion) is modeled accurately, with less offshore sediment transport when compared to the default XBeach run. However, when at a spot overwash occurs too much sediment is eroded. Roughness is needed to reduce erosion during overwash conditions. The simulation with only an increased barrier roughness will reduce the erosion per moment overwash. However, the barrier will avalanche more and thus at more places for longer periods of time overwash will occur.

Also a reference simulation with s_{max} is applied. Artificial limiters based on the Shields number (s_{max}) have been applied successfully in order to reduce the overestimation of the morphological changes (McCall et al., 2010b; Den Bieman, 2012). When this limiter is deactivated in XBeach the morphological predictions increases compared to the 'blank' option. The mean erosion volume calculated is however 25% lower than measured. Also the mean dune top level is not reproduced correctly. The option of both a higher asymmetric sediment transport component and a higher friction on the barrier will result in better skill scores, better reproduction of the mean erosion volume and a mean dune top level more comparable with measurement data. However, a simulation with s_{max} makes it possible to model overwash during hurricane events in XBeach without any calibration. This can be an attractive approach when only limited time is available.

Table 4.3 *Individual contributions of the $facua$ and barrier roughness for Bay Head. Note: erosive means that only points which erode are taken into account in the calculation of the skill and bias.*

Runs	BSS [-] All	Erosive	Bias [m] All	Erosive	Other A_{ero} [$m^3 \cdot m^{-1}$]	$\overline{D_{max}}$ [m]
Blank	-3.931	-0.539	-1.777	-2.930	1124.8	0.3
$facua$ on	-2.690	-0.245	-1.282	-2.281	880.0	1.9
Roughness on	-0.430	0.460	-0.521	-1.364	500.1	2.0
Both on	0.844	0.909	0.104	0.464	177.6	4.5
s_{max} on	0.541	0.602	0.192	1.183	138.5	6.3

Impact of uncertainty in sediment diameter The sediment diameter applied in the XBeach model of the case study has a D_{50} of 300 um, but in reality a distribution of this diameter in the area modeled is expected (Lopez-Feliciano, 2014). The recent nourishments will enhance this spatial distributional of sediment diameters, since coarse sediment (order 500 um) is applied in contrast to the *default* diameter of 200-300 um. In a reference simulation the sediment diameter is reduced and enlarged in order to investigate the effects.

For the collision simulation the impact of variation in D_{50} had a limited impact, as described in Appendix C.2.5. For the case study, however, a much larger impact of the sediment diameter is found. This is related to the difference in storm regime (overwash versus collision). XBeach is mainly sensitive for a reduction in the diameter. A reduction of 50% will result in 4 breaches in the area of interest. A decrease of only 25% will result in 30% more erosion. An increase of 100% (from 300 to 600 um) will result in a decrease in erosion volume of 24 %. This is a somewhat stronger response (+26%) than found for the conceptual collision study. The compete table and spatial bed levels of all

options can be found in Appendix G.3.2.

Morphological acceleration factor Appendix G.6.1 analyses the errors by using a morphological acceleration factor (morfac) for the Bay Head field case. The morfac is used to achieve workable calculation times (1.5 days instead of 15 days). The general idea is that a morfac of 10 can be applied without over-accelerating the system.

The conclusion is that the advantages of morfac = 10 are larger than the downsides of the acceleration. There are two major downsides. First of all the dune erosion is overestimated with 7.5%. This downside is however taken into account with calibration based on the $facua$. Second, the development of the overwash fans will result in too much erosion and thus the fans are modeled too wide and too deep *with* a morphological acceleration. The advantage is a model which has a computational time of 36 hours instead of 360 hours.

4.5.5 Hydrodynamic conditions: evaluate and reproduce

Water marks: water depth and levels evaluation Besides a validation based on the morphological behavior also water marks are compared. After Sandy measurements were performed by Stevens Institute of Technology. Teams assessed structural damaged and measured water marks throughout the different towns (Walling et al., 2014). In total 189 points in the area of Bay Head were gathered which are used in this paragraph. In this paragraph the focus is to reproduce the water marks measured by Stevens.

First of all, in XBeach an alongshore uniform nearshore profile and uniform roughness is applied. This results in the simulation of a *mean* hydrodynamic and morphological behavior. Locally differences will occur. This was the case for the morphodynamic predictions and will (thus) also be the case for the hydrodynamics. Second, in the area of interest all the cross-sections needed avalanching during the first flood event of Sandy to get in the overwash regime. When a cross-section gets in the overwash regime an overwash fan/terrace will develop. At these locations higher watermarks are expected. After this first, rough, flood event a second flood from the bay occurs. During this second, more calm flood event large parts of Bay Head were submerged. In the XBeach hindcast 77-83% of Bay Head was flooded during the second flood event (bay-side driven). The rest of the area suffered from flood damage during the first event. In XBeach the highest water marks are measured at the ocean front side, especially in the situation where the profile stayed in the collision regime. In this situation the highest set-up is achieved. A spatial plot of the water levels can be found in Figure G.8.

The mean water level measured is NAVD88 +2.169 m. The mean water level modeled is NAVD88 +2.191 m. The difference is a small bias of +0.022 m, but the mean prediction is thus comparable. When looking in more detail at the individual measurements, about 58% of the points lie within a band around the mean of 0.1 m. These measurements are related to the second flood event. The peaks in the measurement data of NAVD88 +8.41 or +5.63 m are not reproduced by XBeach. These values are most likely the result of splashing of individual short waves during the first flood event. These motions are however not resolved by XBeach due to phase-averaging. The maximum value modeled by XBeach is NAVD88 +4.75 m. Overall the RMSE is 0.52 m and the R2 has a value of 0.71. In Figure 4.25 the results are presented.

XBeach is as a result of several reasons not capable in reproducing the complete spatial varying water levels as measured by Walling et al. (2014). This is only partly related to an inaccurate morphological response in XBeach, since the results in the 1 km area of interest (red stars) also showed a tendency

to reproduce the imposed bay water level of NAVD88 +2.1 m (second flood event). The reproduction gets somewhat better in the area of interest, which is related to the better morphodynamic prediction. The most likely reason for these differences found is the lack of spatial variation in both roughness and bed level. Another possible source for errors is individual short waves which are not resolved in XBeach.

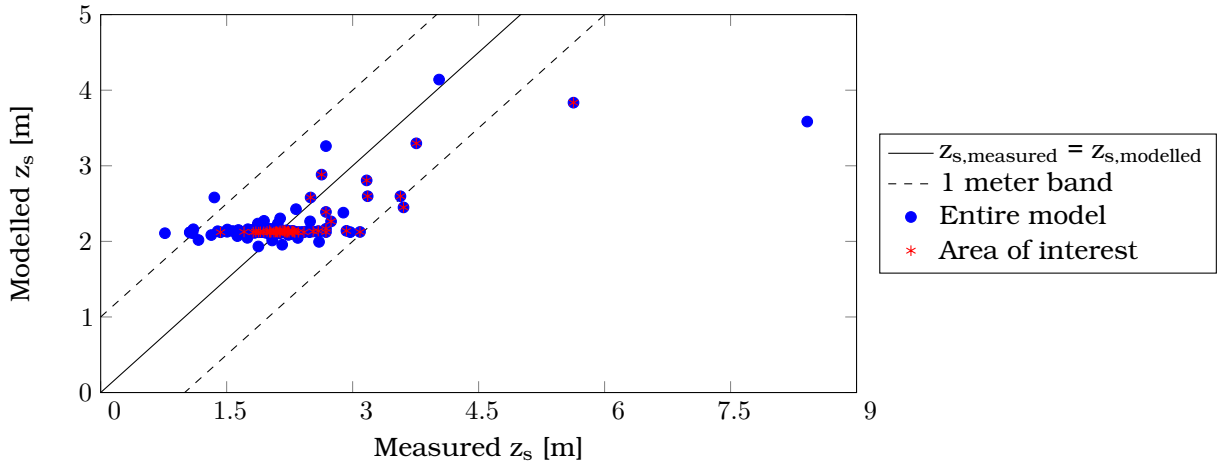

Figure 4.25 *Comparison between both the water marks measured and simulated in XBeach.*

Patterns in wave heights and wave heights: evaluate Roughness on the barrier island is needed in order to protect the material on the barrier from overwash conditions. Without extra roughness (in the form of a lower Chezy value) every location where some overwash occurs is breached. The impact of a Chezy variation has however both impact on the sediment transport formulations via the calculation of the equilibrium sediment concentration (Equation A.12) and on the shallow water equations via the bed shear stress (Equation A.8). In this paragraph the focus is to derive the patterns in hydrodynamic parameters such as velocity and wave heights. The complete information can be found in Table G.7.

The wave heights on top of the barrier behave more or less as expected. At overwash fans the long wave height will increase for higher Chezy values. The same is the case for the short wave height, but in a somewhat lesser extend since in shallow water the long waves will dominate. There is no measurement data available for the wave heights, but the patterns show a consistent distribution over the different roughness values.

On the other hand, the patterns in Eulerian velocity are more remarkable. For this output parameter large differences in value (both for the maximum and for the mean) are found as a result of small variations in Chezy. A Chezy decrease with 5 $m^{0.5}.s^{-1}$ already results in a completely different velocity pattern. For example for a Chezy value of 30 $m^{0.5}.s^{-1}$ the maximum Eulerian velocity on the barrier is 0.1 $m.s^{-1}$, but for a value of 35 the maximum Eulerian velocity is 3.27 $m.s^{-1}$. This is a factor 32! These large differences are most likely the result of an impact of a higher bed shear stress which results in a large decrease in velocity via the shallow water equations. Also for the velocities no measurement data is available, but the patterns show a questionable distribution as a result of variation in Chezy.

4.5.6 Model sensitivity: avalanching algorithm

The critical slopes in XBeach are of major importance in the morphological end result, as presented in Figure 4.24. The dominance of the parameters related to the avalanching algorithm are analyzed in this subsection. The default run has a $m_{cr,wet}$ of 0.2, which is lower than default in XBeach. This lower value is found in a data analysis (value of 0.22 found). The other parameters in the algorithm are applied with default values. These are respectively: $m_{cr,dry}$, the water depth at the interface wet and dry (h_{switch}) and maximum dune face erosion per time period (dz_{max}). In this subsection only the results will be presented, for the full analysis one is refereed to Section G.4.

Regarding the avalanching algorithm the following conclusions are made:

1. The avalanching algorithm is needed to weaken individual cross-sections in order to get in the overwash regime. Without this algorithm XBeach will not have any skill (BSS of 0) in the Bay Head field case.
2. XBeach is not sensitive for changes in $m_{cr,dry}$, h_{switch} or dz_{max}. Variation of these parameter will only have limited impact (max 3.5% in erosion volume). The default setting for dz_{max} should, according to Van Thiel de Vries (2009b), be lower than currently applied in XBeach. The effect is that the model will avalanche too fast. The reason why there is a variation between the two is not known by the author.
3. The model is sensitive for change in a critical wet slope. The value of 0.2 was found in a data analysis, in contrast to the default value of 0.3. Lower values means more erosion (10 up to 16% per 0.1 change) and a lower mean dune top level (0.8 up to 1.2 m per 0.1 change). Overall the morphological skill will increase for lower values of the critical slope. The highest skill is found for 0.1 (BSS of 0.867 versus 0.844). Also the dune top level is (much) better represented with a lower wet critical slope. The effect of the critical wet slope can be found in Figure 4.26.

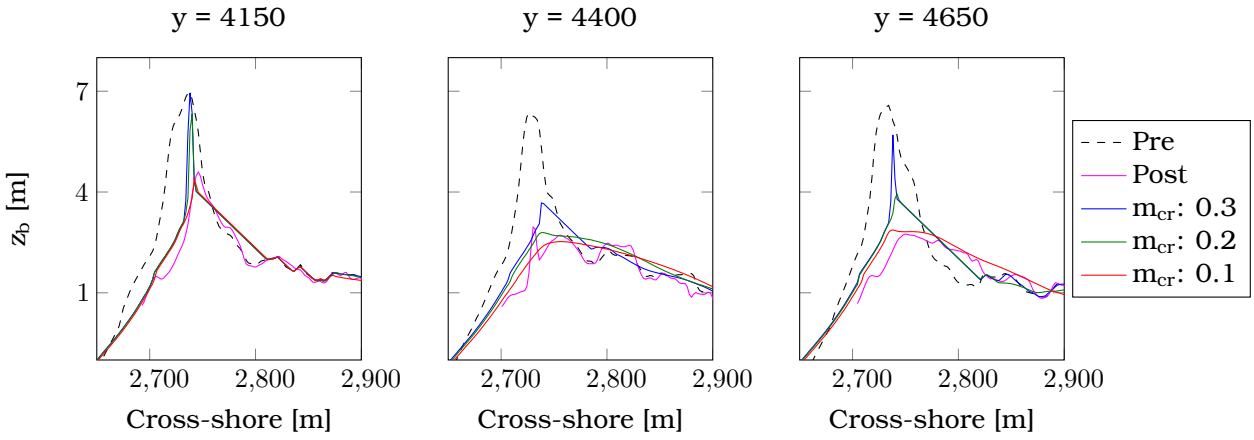

Figure 4.26 *Comparison between multiple cross-sections as measured and as modeled with several values for the critical wet slope in the avalanching algorithm in XBeach.*

4.5.7 Conclusion

In this section the impact of Hurricane Sandy on the city of Bay Head, NJ is modeled. It is possible to model the system with a 2DH XBeach model in a morphological accurate way with the default settings,

higher $facua$ and by calibration of an alongshore uniform roughness. The following conclusions can be made:

1. The LiDAR data only represents the morphological response of the system to a limited extend. Human impact on the deposition and breaches are clearly visible. This makes morphological reproduction in an environment with human activity (somewhat) challenging.
2. By analyzing all the model results, it is concluded that the major morphological changes during Sandy occurred during the 10 hour storm peak (47% of the erosion volume). During this period potential weak spots are created. After the storm surge peak there is a period of 20 hours with a negative water level gradient (backwash) from the bay to the sea (second flood event). Small initial breaches will, in combination with this water level gradient, erode even more and can result in island breaching.
3. No artificial limiters such as McCall et al. (2010b) are needed to accurately model the overwash regime in XBeach when applying a two-step approach suggested in this thesis. This includes both a higher wave asymmetry factor ($facua$) and the introduction of extra roughness on the barrier (lower Chezy value). In total the mean erosion volume measured via the use of LiDAR data at Bay Head was 180 $m^3 \cdot m^{-1}$. The mean simulated XBeach value is 178 $m^3 \cdot m^{-1}$ (-1%). The model has a BSS of 0.84 and a bias of x m.
4. Applying one alongshore uniform roughness profile is an oversimplification. The overall mean morphological result was good with a Chezy value of 30 $m^{0.5}.s^{-1}$ and a $facua$ of 0.25, but for example in the area of interest the breach at y = 4700 m was not reproduced. This is major downside of applying one alongshore uniform roughness, because this approach is not capable in reproducing the spatial variability.
5. The individual contributions of $facua$ and Chezy are needed to model the system in an accurate way. Without the $facua$ calibration step still a negative skill score is found and too much erosion occurs (+181%). Without the additional friction all the locations were (some) overwash occurred are breached. This is a result of too much erosion (+395%). The artificial limiter s_{max} is a quick-and-dirty approach to model the impact of a hurricane.
6. The dune top level is not represented correctly by the model. This is possibly due to the impact of individual avalanching parameters, since the critical slopes dominate the development of the profile. The highest BSS is found by lowering the default value for the critical wet slope from 0.30 to 0.10. This value is not represented in a data analysis were a value of 0.22 is found. Variation of other parameters in the avalanching algorithm have only limited impact on the profile.
7. Weak spots in the coastal system can be easily identified by calculating the cross-sectional area above SSL. This can be a quick-and-easy tool for the local authorities to investigate weak spots in the system. A threshold of 135 $m^3 \cdot m^{-1}$ can be seen as a good estimate for a design storm such as Sandy at New Jersey.
8. The model has limited skill in reproducing the hydrodynamics. XBeach tends to reproduce a mean water level (bay-related) instead of reproducing the values of individual water marks found after Sandy (Walling et al., 2014). This is most likely related to the approach in which one alongshore uniform nearshore and roughness is applied (lack of spatial variability). Additionally, the patterns in Eulerian velocity on top of the barrier show a remarkable pattern for increasing values of roughness. It is at least questionable if the roughness applied will result in realistic processes or result in just in good morphological predictions.

4.6 Camp Osborne: effects of a condo

4.6.1 Introduction

The area of interest in this subsection is the study site called Camp Osborne in the town of Brick, NJ. Camp Osborne is one of the developed beaches in which a prominent condo is placed. The complete XBeach model used has a domain of 9 by 7 km in order to reproduce the hydrodynamics accurately in the area of interest. A grid size varying from 50x10 m (offshore) down to 2x5 m (on the barrier) is used. The satellite image, as presented in Figure 4.27, shows evidence of a large overwash fan at the left side of the condo.

(a) *Pre-Sandy* **(b)** *Post-Sandy*

Figure 4.27 *Detailed satellite images of the area of interest at Camp Osborne from Google Earth. Pre-Sandy information is from 09/21/2010 and post-Sandy information is from 04/11/2012.*

4.6.2 Data analysis: LiDAR provided by USGS

Figure 4.28 presents the available LiDAR data of the area. The latest information prior to Sandy was collected on Augustus, 28, 2010 (USACE, 2010). The data set after Sandy was collected on November 16, 2012 (USGS, 2012a). Two important remarks: also this data set has a difference of 15 days between the impact of Sandy and the measurement data for the area of Camp Osborne, but even more important the LiDAR type describing Camp Osborne is unfiltered and is of first response. The result is noise in the data and on top of that all the houses are still present. It is therefore difficult to interpret the erosion and accretion plots as will become clear in the coming paragraphs.

Based on the LiDAR data sets and the theory of Chapter 2, a more detailed analysis can be made of the morphological response of the area. The following remarks can be made based on Figure 4.27 and 4.28:

1. The mean erosion as calculated by subtracting the pre- and post-Sandy LiDAR is 132.8 $m^3 \cdot m^{-1}$. The maximum erosion calculated in a cross-section is 204.1 $m^3 \cdot m^{-1}$. The mean erosion is 26% lower than for Bay Head, this could be related to the difference in LiDAR source.
2. The coastal dunes suffered from severe erosion and total dune destruction. Total dune destruction could not be be recognized at Bay Head. The mean dune top level ($\overline{D_{max}}$) decreased from 6.47 to 3.71 m. The minimum dune top decreased from 4.28 to 2.31 m.
3. An example of an overwash fan occurred at y = 4500 m. This is also represented in the profile plots where an elevation of about NAVD88 +2.5 m can be distinguished.

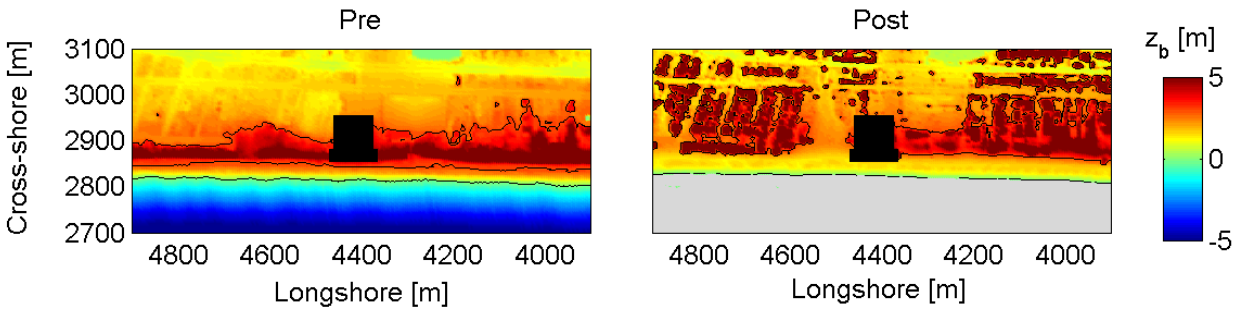

Figure 4.28 *Pre- and post-Sandy LiDAR data presented for the area of interest at Camp Osborne. Spots without data are marked grey. The black depth contours are provided at an elevation of 0 and 3 m relative to NADV88. Note: post LiDAR is unfiltered and of first response.*

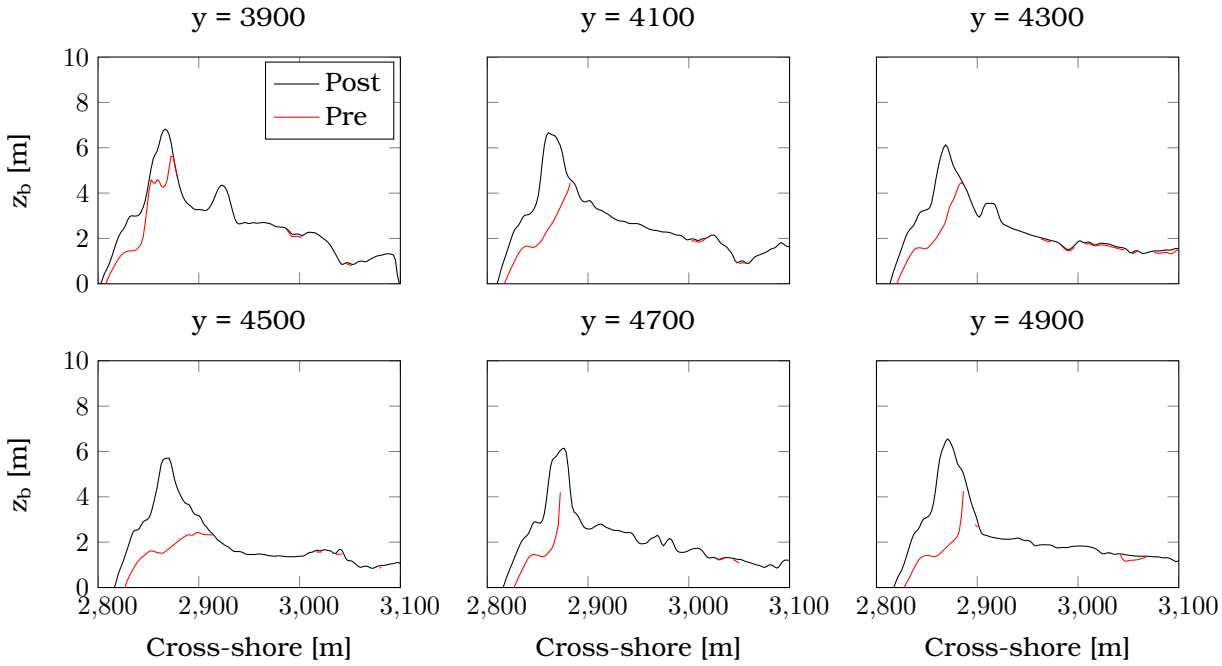

Figure 4.29 *Several cross-sections for the bed level both pre- and post-Sandy. Note: only erosive points of the LiDAR are presented.*

4.6.3 Base simulation results

Process over time: 4 snap shots Figure 4.31 provides an overview of the area of interest together with the water levels. The bed level is presented at two moments in time. The accretion and erosion patterns are presented both total and incremental. In the longshore limited variation in morphological response can be noticed. The profile developed after 40 hours is more effective in dissipating wave energy. At the back of the barrier some avalanching occurred due to the fact that the initial profiles exceeds the critical wet slope.

In the next 8 hours, in 40-48 of the simulation time, water levels and wave heights increase in height and the first overwash occurs. Sediment is taken from the foreshore plus dune top and deposited (partly) on the back barrier. During the peak of Sandy avalanching is effective in lowering the dune top.

In the period of 48-52 hours of the simulation most overwash occurs. This is related to dune lowering, which took place in the 8 hours before landfall. From y = 4350 m and further upstream (for smaller values for y) overwash fans continue to develop and also some material is deposited in the nearshore. From y = 4500 m and further downstream (for larger values for y) sheetwash results in dune destruction and large amounts of deposition on the back barrier.

After the peak of Sandy the water levels at sea and the wave heights will decrease. As a result of the spiral movement of Hurricane Sandy water levels in the bay start to increase in height and 4 hours after landfall there is a negative water level gradient. This means that there are higher water marks in the bay than at sea. In the last 20 hours of the simulation there is a constant negative water level gradient (second flood event) and this pressure will eventually result in water motions through existing weak spots, like at y = 4500 m. This motion is called backwash. The result is a severe increase in erosion volume next to the condo, but also for the rest of the barrier some erosion can be noticed. Material which is eroded during backwash is deposited in offshore direction. Right next to the condo the overwash fan is in the process of becoming a breach.

Cross-sections: importance of avalanching In the first 24 hours of the simulation hardly any morphological response could be noticed. Material is avalanching from NAVD88 +2.5 m up to a depth of NAVD88 -2.5 m. Between 24-40 hours the morphological response is similar to the first 24 hours of simulation. Sediment is taken away from the coastal barrier and deposition occurs in the nearshore. After 48 hours dune lowering can be distinguished in Figure 4.30 for profiles at y = 3300 & 3600 m. This is caused by avalanching of the cross-section.

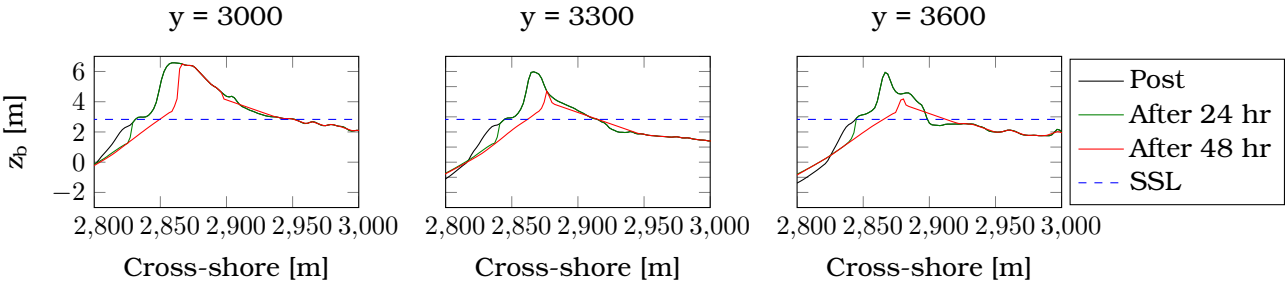

Figure 4.30 *Several cross-sections showing the erosion of the shore and dunes in the first 48 hours of the model. Bottom level with respect to NAVD88.*

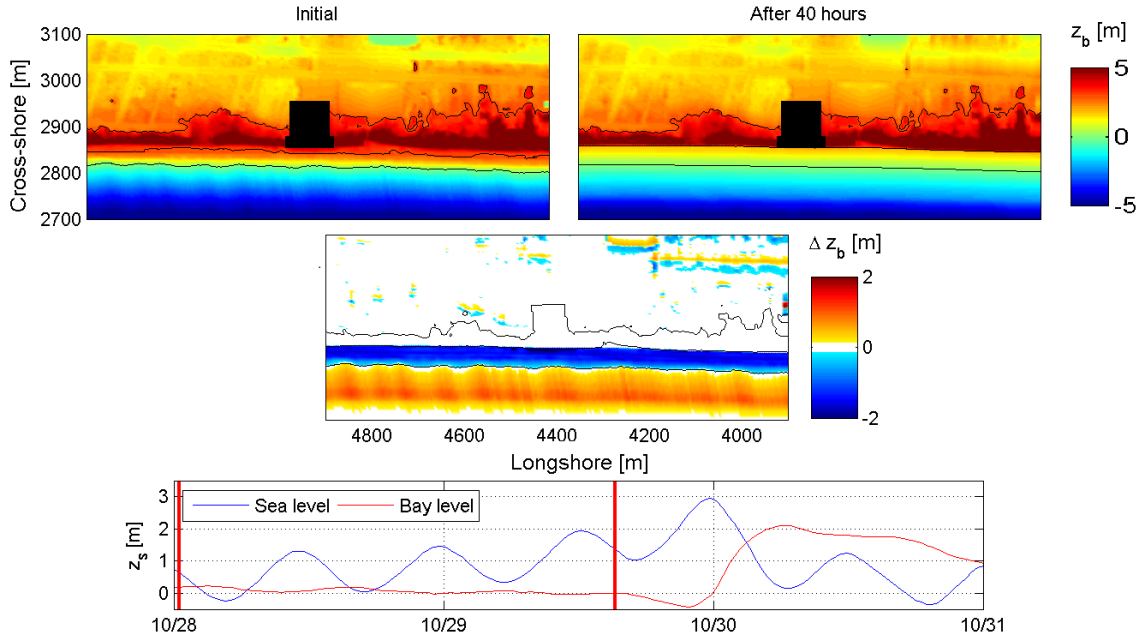

Figure 4.31 *Morphological evolution during the first 40 hours. Plot in the middle is accretion / erosion plot. The black contour plots are provided at an elevation of 0 and 3 m relative to NAVD88.*

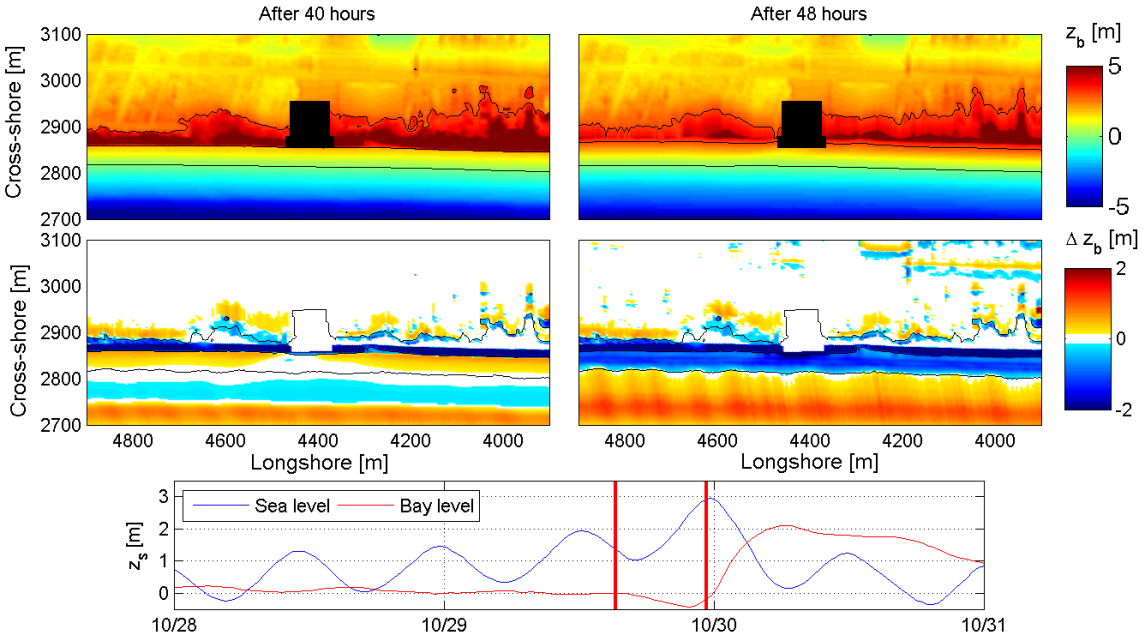

Figure 4.32 *Morphological evolution between 40-48 hours of simulation time. Plots in the middle are accretion / erosion plots, both incremental (middle, left) and total (middle right). The black contour plots are provided at an elevation of 0 and 3 m relative to NAVD88.*

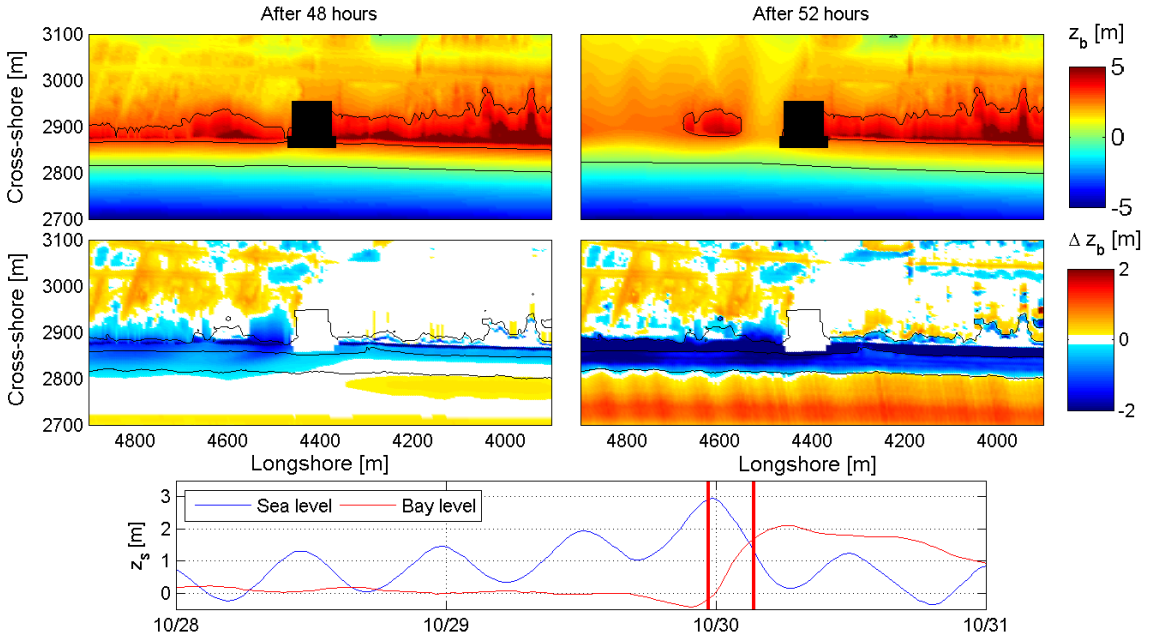

Figure 4.33 *Morphological evolution between 48-52 hours of simulation time. Plots in the middle are accretion / erosion plots, both incremental (middle, left) and total (middle right). The black contour plots are provided at an elevation of 0 and 3 m relative to NAVD88.*

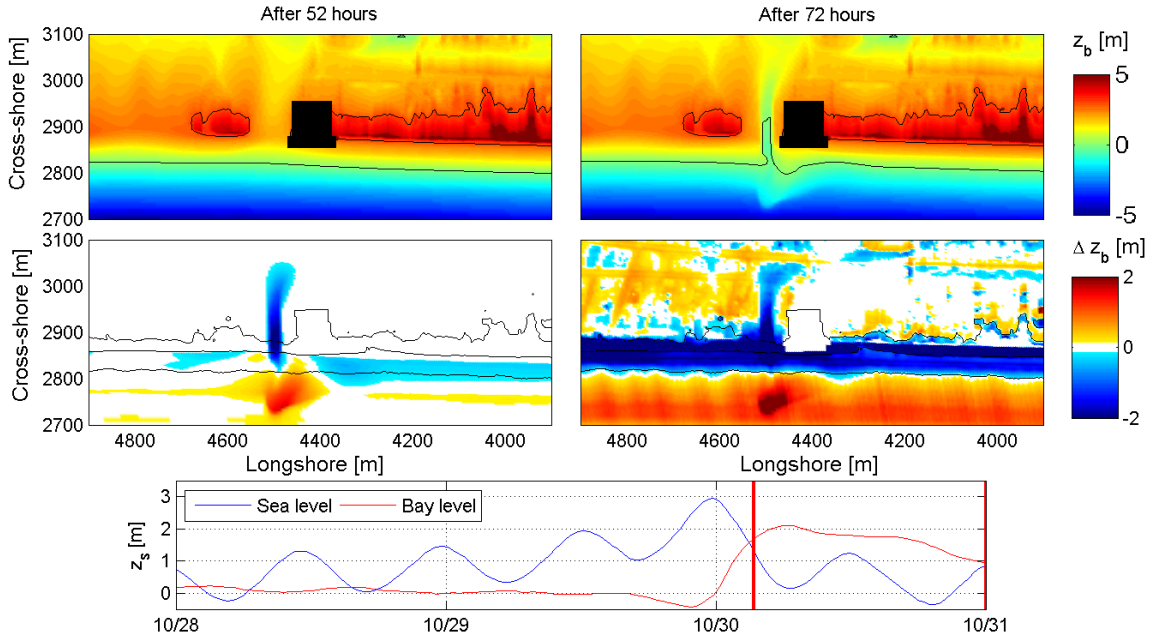

Figure 4.34 *Morphological evolution between 52-72 hours of simulation time. Plots in the middle are accretion / erosion plots, both incremental (middle, left) and total (middle right). The black contour plots are provided at an elevation of 0 and 3 m relative to NAVD88.*

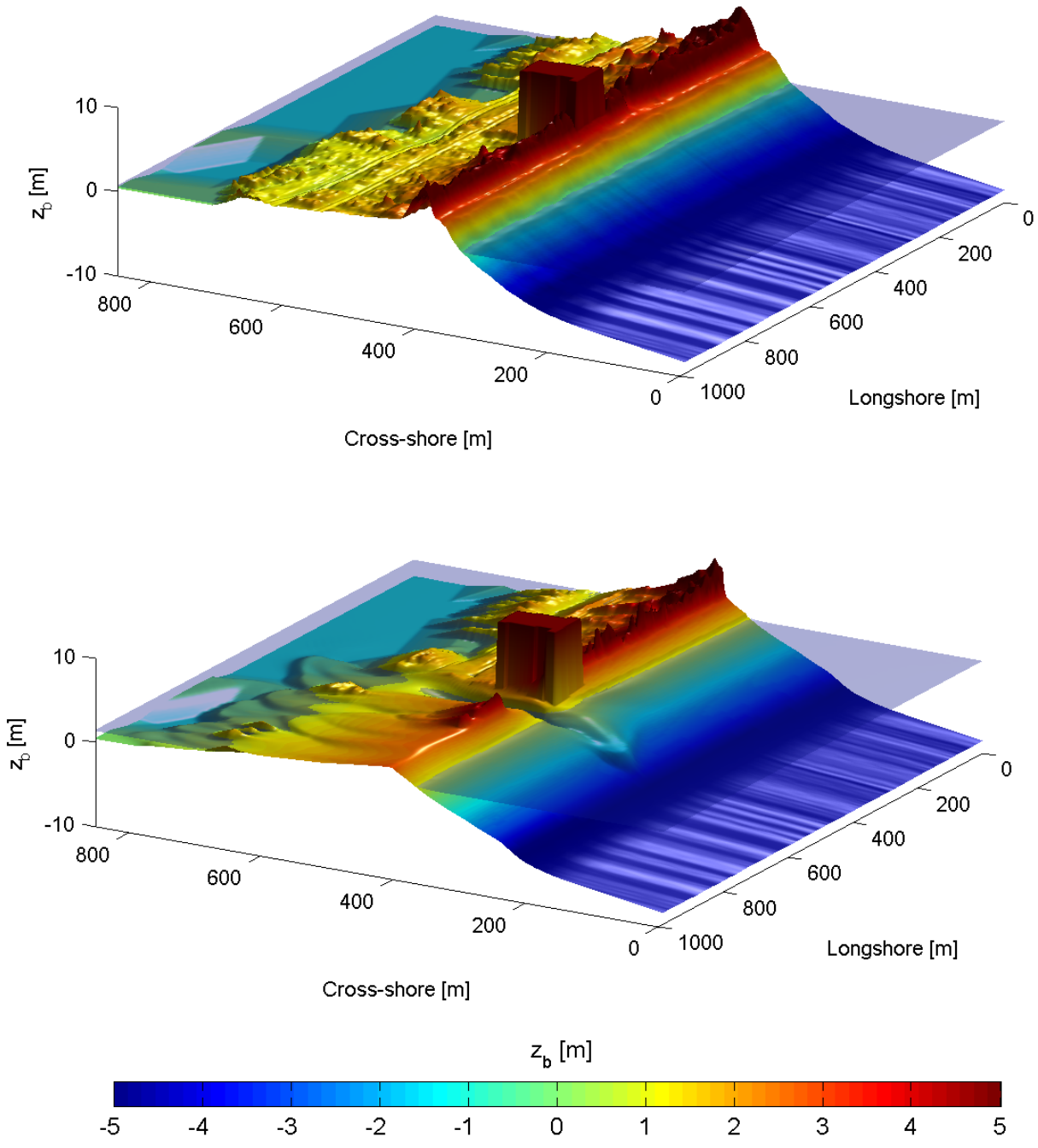

Figure 4.35 *Pre- (top panel) and post-Sandy (lower panel) in a three dimensional plot with both bed and water levels. Note: the erosion hole at the side of the condo is overestimated in XBeach, as will be elaborated.*

Pre- and post-Sandy: comparison with measurements It is also possible to model the interaction between hard-soft in a practical overwash case during Hurricane Sandy in a morphological accurate way with a BSS of 0.89 and a bias of -0.25 m. These results have been achieved after the two-step calibration approach in the previous subsections. Note: for the calculating of this score only the *erosive* points are taken into account, due to the quality plus type of the LiDAR. (for Bay Head the BSS *normal* was 0.84 and BSS *erosive* was 0.91). The behavior of the system can be divided into three parts: overwash fans, side of the structure and sheetwash. The result is presented in Figure 4.36.

The patterns from y = 3900 - 4500 m are reproduced accurately. This part of the system suffered from some overwash as a result of the combination of avalanching of the dune top and offshore sediment transport.

The overwash fan at y = 4500 m right next to the condo is overestimated. The bed level is eroded +/- 1 m too much, as can be seen in at y = 4500 in Figure 4.37. The maximum erosion in the simulation is also overestimated (512 $m^3 \cdot m^{-1}$ (+220%). This large difference is the result of a cross-section which is weakened sufficient to be vulnerable for the large pressure difference during the second flood event. In reality this cross-section eroded somewhat less and did not became vulnerable to backwash.

The part which suffered most from overwash, y = 4500 - 4900 m, resulted in large amounts of sediment deposition in XBeach and severe dune destruction. This deposition cannot be compared to the post LiDAR, but satellite images confirms these initial findings. In the satellite image from Figure 4.27 deposition between the houses can be recognized. The amount of dune destruction seems however somewhat overestimated compared to LiDAR.

The erosion volumes as calculated by XBeach have a mean value of 170 $m^3 \cdot m^{-1}$ which is 8 $m^3 \cdot m^{-1}$ smaller than for the previous subsection, but 9 $m^3 \cdot m^{-1}$ larger than the measurement data of Camp Osborne. This is mainly the result of the overwash fan at y = 4500 m which is eroded somewhat too much in the simulation, but also the discrepancy between LiDAR types could be the cause for this difference.

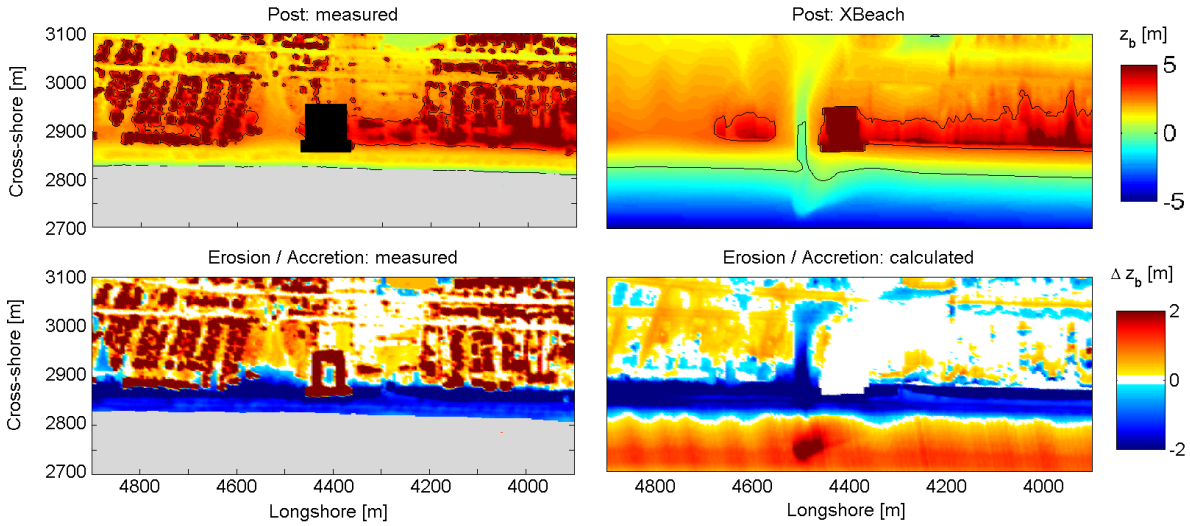

Figure 4.36 *Spatial post bed levels and erosion/accretion plots after the storm event presented for the area of interest at Camp Osborne. Spots without data are marked grey. The black depth contours are provided at an elevation of 0 and 3 m relative to NADV88.*

When comparing the different profiles with the pre- and post-Sandy measurements the area of interest can be divided into the stronger overwash side and the weaker sheetwash side. Profiles from y = 4500 m and further downstream sheetwash and dune destruction, which can be observed in Figure 4.37. For the other profiles only limited overwash occurred. Also the impact of the critical dry slope (1:1) can be distinguished in y = 3900 and 4100 m. The mean dune top lowers in the XBeach simulation from NAVD88 +6.5 to +4.6 m, which is an underestimation of 0.90 m compared to measurement data. This can be seen in Figure 4.38.

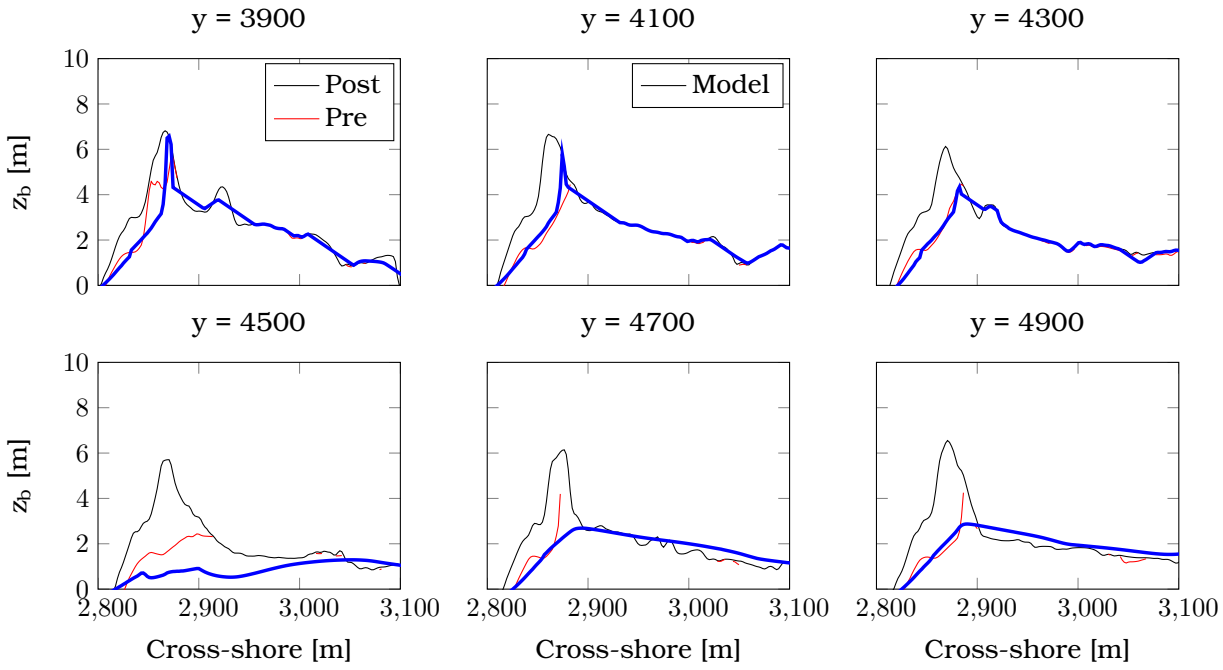

Figure 4.37 *Cross-sections: pre-Sandy, post-Sandy and calculated with the chosen set-up by XBeach as for Camp Osborne. The cross-sections provided at certain coordinates correspond with the other figures.*

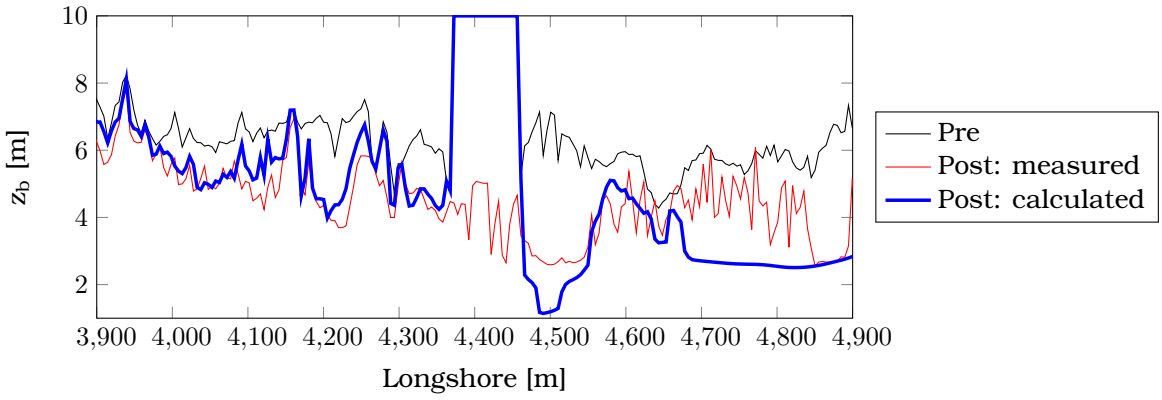

Figure 4.38 *Maximum crest height in longshore direction: pre-Sandy, post-Sandy and as calculated by XBeach. The overwash fan at y = 4500 m is eroded too much in the XBeach simulation.*

Alongshore erosion patterns The alongshore erosion patterns per time step have been plotted in Figure 4.39. In the first 36 hours the alongshore variation is limited and after this period of time a mean erosion volume of 66 $m^3 \cdot m^{-1}$ can be noticed. After this time the impact of the structure becomes noticeable. The effect is more erosion at the sides of the structure and less erosion in front of the condo. This is line with findings in the conceptual study of this thesis.

In the last 24 hours an interesting development can be distinguished. In this time period hardly any extra erosion occurs at the weak spot at the side of the structure. This spot suffers from severe erosion due to a water level gradient from the bay into the sea (backwash).

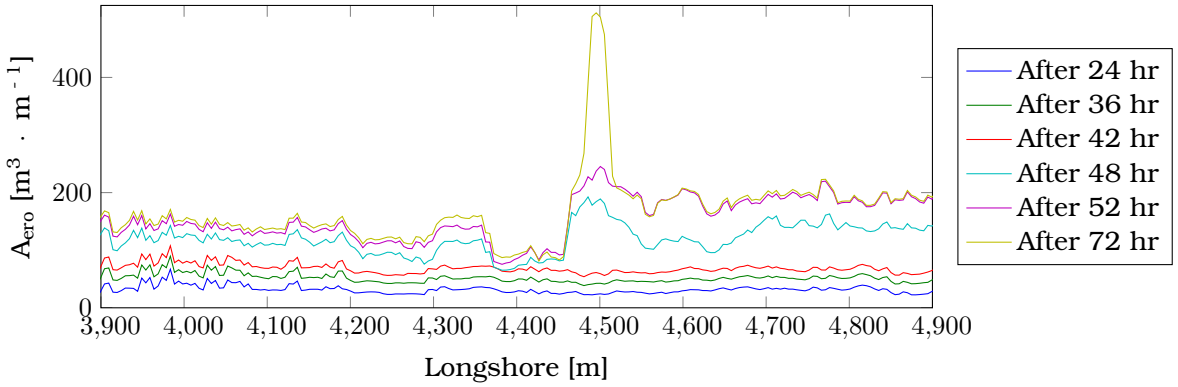

Figure 4.39 *Development of the alongshore erosion volumes in $m^3 \cdot m^{-1}$ over time. Notice the erosion peak in the overwash fan at y = 4500 m.*

Identifying weak spots As seen in previous section potential weak spots can be identified by calculating the amount of sediment above SSL. In Figure 4.40 the same approach and threshold is applied. One can identify in this figure that half of the area of interest (specifically y = 4700 m and further downstream) is potentially weak. This explains the sheetwash observed in XBeach. On top of that, a local minimum is found, but this is not enough to explain an increase of 220 % in erosion volume. The local minimum is presented with the first red circle at y = 4500 m.

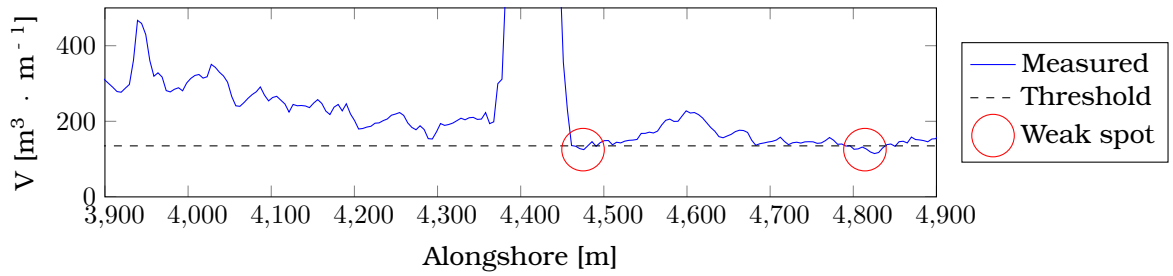

Figure 4.40 *Barrier volume in $m^3 \cdot m^{-1}$ above SSL which is a tool to indicate potential weak spots during storm events for the area of interest at Camp Osborne. The black-dashed line is the lower limit.*

4.6.4 Morphological skill

Spatial BSS and bias For this field case it is complex to validate the morphological skill of the model. Reason for this complexity is the fact that there are 2 providers of the LiDAR data (pre- and post-Sandy) and there is a discrepancy between the data. In Figure 4.41 the morphological indicator BSS and bias are presented with the use of a moving window of 6x6 cells. This is similar as the approach in Section 4.5.4 and presented in Figure 4.41.

Overall erosion patterns for Camp Osborne are calculated with reasonable accuracy with a BSS of 0.89 and bias of -0.25 m. Just like for the previous subsection it is not possible to get good scores on the back barrier. This is due to the combination of small bed level changes, the impact of humans in the first 2 weeks after Sandy and the fact that individual structures are not taken into account.

The erosion in the overwash fan next to the condo (y = 4500 m) is overestimated. This is most likely related to a lack of sufficient friction. Therefore, the overwash fan next to the condo has a BSS of -1. XBeach does have skill in describing overwash fans. For example the overwash fans at the parking lot at y = 4300 m are reproduced and have a positive BSS.

The part of the barrier island with dunes is simulated accurately. Therefore, the results of the moving windows of the BSS are promising. Some discrepancy in terms of bed level occur on the beaches and foredunes. The sheetwash area has a negative BSS score.

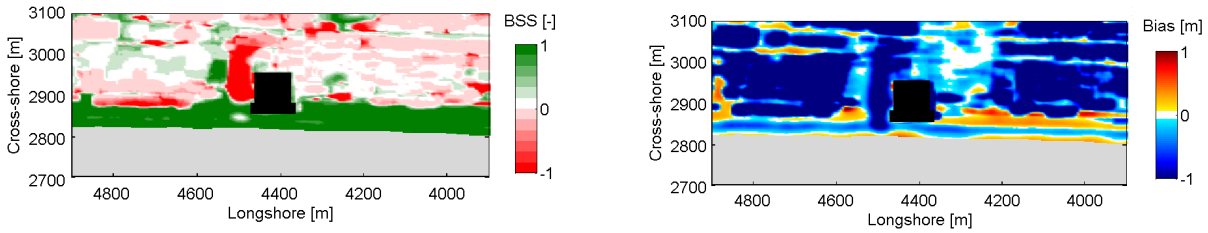

(a) *BSS* **(b)** *Bias*

Figure 4.41 *Morphological performance indicators BSS [-] and bias [m] for the simulation. In black the condo is presented.*

Table 4.4 *Comparison between measurement data and the XBeach simulation.*

Runs	BSS [-] All	Erosive	Bias [m] All	Erosive	A_{ero} Max	Mean	D_{max} [m] Min	Mean
Measurement	-	-	-	-	204.1	132.8	2.31	3.71
Default	0.216	0.893	-1.225	-0.245	512.1	169.7	1.10	4.60

Evaluation: calibration steps applied Calibration has been carried out with both a higher asymmetric transport parameter and by applying a lower Chezy value on the barrier island. When each individual contribution is applied separate and together, the impact can be analyzed. The complete analysis can be found in Section G.5.1.

The following conclusions are made related to the effects of the calibration approach applied:

1. The simulation for Camp Osborne resulted in somewhat too much erosion, mainly at the weak spot (y = 4500 m). When analyzing the impact of the two step calibration approach, one will find:

(a) Without the higher value for $facua$ the barrier suffers from too much erosion. For example the weak spot at the side of the structure is completely breached. A higher BSS is possible when applying a value of 0.30 instead of 0.25 (BSS increases from 0.89 to 0.92).

(b) Without extra roughness at the barrier, the barrier would have been breached at three individual spots in the area of interest. A higher BSS is possible when applying a value of 25 instead of 30 $m^{0.5}.s^{-1}$ (BSS of 0.89 to 0.94).

2. The approach with the s_{max} is also for Camp Osborne a quick-and-dirty method to model the impact of Hurricane Sandy. About 3/4 of the erosion measured is simulated. However the overwash patterns are suppressed too much.

4.6.5 The effects of the hard structure

In this subsection the impact of the condo is investigated. This is done by a comparison between simulations with plus simulations without the condo. In a simulation without the condo the bathymetry and the non-erodible layer, specified in the model set-up, changes. It is not known what kind of barrier was present before the condo was build. Therefore, two profile types (higher left side or lower right side) can be applied to overwrite the condo. In this subsection a default comparison, a comparison based on a width variation and a comparison in the collision regime are applied.

Default: with or without condo Without the presence of the condo the system would have behaved differently, according to several XBeach simulations. The peak in erosion next to the condo would not have occurred. In Figure 4.42 the differences in erosion patterns are presented. In the comparison with and without the condo the erosion increases with +329 $m^3 \cdot m^{-1}$. Remarkable is the fact that this pattern of increase in erosion only occurs at one side (at y = 4450 - 4700 m).

The reason for this large increase in the simulations is the water level gradient from the bay to the sea. After the peak of Sandy backwash exploits existing weak spots in the system by a large pressure difference. This occurs between 52-72 hours in the simulation. A comparison for the erosion between a simulation with and without structure can also be made before the water level gradient from the bay to the sea starts to erode existing weak spots. In Figure 4.42 such a comparison is made. It is clear that the erosion patterns after 52 hours of simulation behave more or less as expected based on the conceptual study and also follows the patterns described by the modified DnA calculation rules. When the simulation continues the simulations erodes too much compared to measurements data due to the previous mentioned backwash.

A complete comparison is presented in Table 4.5. After 52 hours the modified DnA rules predicts the impact of the hard element with accuracy. A mean increase in erosion of 51.5 (107%) versus 48.3 $m^3 \cdot m^{-1}$ calculated with DnA are reproduced. At the end of the complete simulation, however, the DnA calculation rules underestimate the erosion with 281 $m^3 \cdot m^{-1}$ (+579%) as a result of the pressure difference over the barrier driven by the water levels in the bay (backwash). The influence length however is remarkably well calculated by DnA for both moments in time.

There is a range of possible outcomes, since it is not clear which profile was present when the condo would not have been build. It is possible to apply a higher (red) or lower (blue) profile. The higher the bathymetry applied, the larger the impact of the structure is. Note: the peaks in Figure 4.42 are related to pre-Sandy bathymetry (initial) differences in the profile between the different simulations.

Table 4.5 *The influence of hard structures on the situation of Camp Osborne during Sandy as modeled by XBeach. First number presented is valid for the left side, second number is for the right side of the condo. Erosion volumes are given in* $m^3 \cdot m^{-1}$.

Runs	Time	A_{ero} Mean	A_2 [-] DnA	XBeach	l_2 [m] DnA	XBeach
Mean	52 hr	157	48.3	2.8 / 51.5	290	0 / 266
	72 hr	170	48.3	8.9 / 328.9	290	15 / 266
Option 1	52 hr	165	48.3	1.6 / 47.3	290	0 / 197
	72 hr	170	48.3	1.3 / 320.0	290	0 / 192
Option 2	52 hr	156	48.3	10.2 / 60.8	290	84 / 266
	72 hr	161	48.3	19.6 / 337.8	290	84 / 266

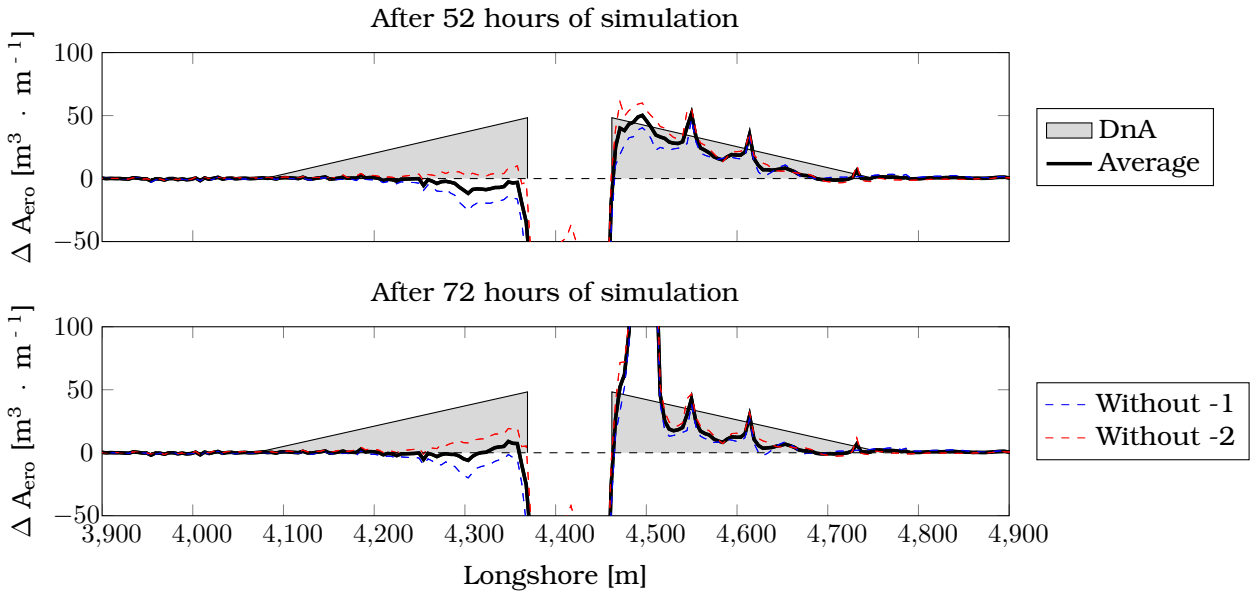

Figure 4.42 *Alongshore erosion volumes both simulated with XBeach and calculated with the DnA calculation rules after 52 hours (top panel) and after 72 hours of simulation (lower panel). The profile replacing the hard element has 3 configuration options: left, right or mean bathymetry.*

Variation in condo width In the previous paragraph the effects of the condo on the erosion patterns during Sandy were reproduced. In the conceptual study of Appendix C.2.6 the width of the structure was a parameter with a strong morphological impact. Structures with a width of 100 m or more could be seen as semi-infinite (just like the condo at Camp Osborne) and for smaller structures a reduction for the DnA calculation could be applied in the order of $d_{2,red} = \frac{W^{0.25}}{100^{0.25}} \cdot d_2$. In this paragraph a comparison is made between the situation with a condo of 100 m, 60 m and without a condo.

The reference simulation confirms the suggested reduction for a comparison after 52 hours. For a condo with about half the width the total additional erosion ($\sum A_2$) of 3104 $m^3.m$ would have decreased, compared to 5188 m^3 for a condo with a width of 100 m. This means a reduction of 40% versus 23% suggested by the reduction rule formulated in this thesis. The reduction is *not* valid for the maximum values of the additional erosion (A_2) at the side of the condo. The extremes are more or less similar for a condo of 100 m and 60 m. The maximum at the right side of the condo only

decreases from 51 down to 47 $m^3 \cdot m^{-1}$ (-3%) which is 97% of the value calculated with the modified DnA rules.

After 72 hours the difference between the two simulations (condo with a width of 100 m and 60 m) increases. The simulated backwash for the default case did not occur for a smaller condo. This can be interpreted that in XBeach the system with a condo of 100 m results in sufficient total additional erosion to get the system in a situation where it is vulnerable for backwash during the second flood event. In the default simulation this resulted in another 6142 m^3 of eroded material. For the smaller condo, however, hardly any additional erosion occurs in the last 20 hours of simulation.

Decrease in the forcing: effects during the collision regime The hydrodynamic forcing applied in the previous paragraphs was a hindcast of Hurricane Sandy. This resulted in a combination of both a high surge (NAVD88 +3.0 m) and high wave heights (+6 m). However, for the Dutch situation, it is interesting to reduce the SSL with 0.5 m to prevent overwash from happening. When the peak is lowered the entire barrier stays in the collision regime where only dune erosion occurs. In this paragraph the impact of the condo is analyzed with this reduced forcing.

For the simulations in the collision regime the impact of the condo decreases. The additional erosion has a value of 28 $m^3 \cdot m^{-1}$ (73%), compared to 38 $m^3 \cdot m^{-1}$ suggested by the DnA calculation rules. This means that the ratio XBeach simulated versus DnA predicted decreases for the collision regime compared to the overwash regime. This was expected since in the overwash regime the feed-back loop of morphological change is not activated. The total additional erosion has a value of 1923 m^3 for the reduced storm conditions (collision regime).

4.6.6 Model sensitivity

Introduction The flexibility of XBeach makes it possible to check the relative influence of several factors which are applied in the model set-up. In this subsection first the effect of the bay (both in bed and water levels) is examined. In the last two parts the uncertainty in the boundary conditions and the impact of several XBeach parameters & settings are analyzed.

Influence of the bay bed levels Water level gradients over the barrier are one of the determining parameters for the morphological behavior of barrier islands under storm conditions such as hurricanes (Donnelly, 2007; McCall, 2008). In this paragraph variations in bay forcing are applied. This includes changes in water level, both in height and in lag, and a variation of bay depth is applied. In this paragraph the conclusions of this analysis are described. For the full analysis one is referred to Section G.5.2.

The following conclusions can be made related to the effects of the bay:

1. The time difference between the individual flood events (lag) is of major importance in describing the morphological response of the system. One could say that every 4 hours of lag results in an increase of 10% in mean erosion. This is related to:
   (a) The water level gradient during an overwash event. The larger the water level gradient the more erosion occurs during overwash.
   (b) The larger the water level gradient over the barrier during the second flood event, the larger the pressure difference and thus the force the barrier island needs to withstand. The bay water levels exploit initial small breaches and can result in island breaching. Larger

gradient during the second flood event will result in a more extreme alongshore distribution of the erosion patterns.

2. The bay bed levels are of minor importance for overwash and dune erosion, but are of importance for breaching. First, for decreasing bay bed levels alongshore variability also increases. This is related to the formation of the flood tidal delta during breaching. Formation of this tidal delta is based on sediment from the bay. The more easily sediment can be taken from the bay (rich in sediment), the more easily the tidal delta develops. Second, deeper bay bed levels will increase the mean erosion, mainly because more avalanching occurs at the bay-side of the back barrier.

Uncertainty in the boundary conditions The uncertainty in the boundary conditions is analyzed by first of all varying the spectrum energy and by varying the water levels. Variation in spectrum energy is applied by enhancing and reducing the energy with 25%. For the water levels both a general base variation of 0.1 m and a peak variation of 0.5 m is applied. This is related to the bias of the sECOM between measurement data and Delft3D, as can be found in Appendix F.3. For the full analysis one is referred to Appendix G.5.3.

The following conclusions can be made related to the effects of the uncertainty in boundary conditions:

1. Variation in wave spectrum is of minor interest. This is related to the fact that the alongshore variation in erosion stays more or less similar. The erosion varies more or less as proposed by Fisher et al. (1986), but has a somewhat weaker relation (25% variation forcing versus 10-20% impact). The alongshore variability does not change and thus the exact reproduction of the erosion volume is more a calibration issue than an uncertainty. For the mean dune top level the effect of 25% more energy is a maximum change of 0.25 m.
2. Variation in the water level is more important, since the mean effects are an order larger than the variation for spectrum energy *and* the alongshore distribution becomes more peaked for higher levels. The mean effect of a base water level variation of 0.1 m is 12-17% in terms of mean erosion. The same variation results in a 50% more extreme alongshore erosion distribution. Variations in the peak water levels have the most impact on the morphological response and resulted in a variation of 1.0 m in mean dune top level.

Importance several XBeach parameters In XBeach several physical descriptions are represented in the source code in order to reproduce the morphological behavior in the most accurate way. These contributions can be deactivated in order to analyze the impact of each factor. In this paragraph the contribution of $swnrunup$, $jetfac$, long waves and avalanching are analyzed. For the full analysis one is referred to Appendix G.5.4

The following conclusions can be made related to the effects of XBeach parameters:

1. Simulations with or without the parametric relation $jetfac$ result in similar bed levels and thus erosion volumes. This can be related to a bug or to a specific process (counter force), but the scour at the condo is similar for both simulations. There are small differences in turbulence generation found.
2. The relation of $swrunup$ unjustifiably triggers the avalanching algorithm on the back barrier. This bug will therefore result in an incorrect reproduction of the bed level and a higher BSS can be achieved when turning this relation of.

3. The importance of long waves and the avalanching algorithm increases compared to a similar comparison for the collision regime. Without the long waves only 60% of the erosion would have occurred.

Morphological acceleration factor Appendix G.6.2 analyses the errors by using a morphological acceleration factor (morfac) for the Camp Osborne field case. The morfac is used to achieve workable calculation times (1.5 days instead of 15 days). The general idea is that a morfac of 10 can be applied without over-accelerating the system.

The conclusion is that the advantages of a morfac = 10 are larger than the downsides of the acceleration. There are three major downsides, of which 2 were already noticed in the analysis of Bay Head. The known downsides are: too much dune erosion and somewhat inaccurate reproduction of overwash fans. The effect noticed in the analysis for Camp Osborne is that backwash during the second flood event is underestimated. Also the location of this backwash is somewhat different by comparing a morfac =10 with morfac =1. Overall there is no reason to assume the non-validity of the morfac approach.

4.6.7 Conclusion

In this section the impact of Hurricane Sandy on the beach of Camp Osborne was modeled. It is possible to model the area of interest with a hard element in a 2DH XBeach model with the two-step calibration approach. The following conclusions can be made:

1. There is a discrepancy between the different sources and types of LiDAR. This makes it difficult to compare the measurement data. At the side of the condo a clearly visible overwash fan developed during Sandy.
2. When only the erosive points are taken into account a BSS of 0.89 and a bias of -0.245 m can be achieved. This can be seen as *excellent* according to the classification of Van Rijn (2003). When comparing these scores with Bay Head the skill is comparable, but between the biases there is a difference of 0.71 m. This is related to the fact that in the Camp Osborne simulation too much erosion occurs. The overestimation of erosion occurs mainly in the weak spot at the side of the condo. In total the mean erosion volume measured via the LiDAR at Camp Osborne was 133 $m^3 \cdot m^{-1}$. The mean simulated XBeach erosion is 170 $m^3 \cdot m^{-1}$ (+28%).
3. Simulations show that the presence of the condo at Camp Osborne increases the erosion volume of the adjacent coast with 52 $m^3 \cdot m^{-1}$ (+32%). Eventually this weakened cross-section is deepened due to the water level gradient from the bay to the sea (backwash). This will result in a further increase of erosion with +277 $m^3 \cdot m^{-1}$ (+163%). Without this gradient the modified DnA calculation rules would have accurately predicted the increase of erosion (+48 versus +55 $m^3 \cdot m^{-1}$ modeled). The increased erosion occurred mainly at one side of the condo as a result of oblique wave attack. For a smaller width the condo would have resulted in a similar amount of additional erosion, but an increase in the total additional erosion is noticed in XBeach. For the collision instead of the overwash regime the ratio between the DnA-calculated and the XBeach-simulated value decreases.
4. The description of the water levels in the bay are of major importance in describing the mean and extreme values in the alongshore erosion pattern. Without the water level gradient from the bay to the sea the erosion pattern would have been more uniform (smooth). Introducing 4 hours more lag will result in 10% more erosion. The bed levels in the bay are of minor importance. The

more shallow the bed level in the bay the more rich in sediment the system is during breaching, which enhances the formation of the flood tidal delta.

5. In a sensitivity analysis of the hydrodynamic forcing from the sea it is found that introducing more/less spectrum energy the alongshore erosion pattern will not vary. On top of that, the relation between the forcing and the impact is somewhat weaker than proposed by Fisher et al. (1986). Water level variations have the largest impact on the alongshore erosion patterns (both for the mean as the maximum value). For example a simulation with 0.1 m lower base water levels, will result in a reduction of 13% in terms of the erosion volume simulated. Variations in the peak water levels have the most impact on the morphological response and result in a variation of 1.0 m in the mean dune top level.

6. In XBeach simulations the parametric relations $jetfac$ and $swrunup$ were activated. These relations are, however, not needed to describe the morphological response of the system. The $jetfac$ did not have any effect at all. The $swrunup$ resulted in large changes of the slopes on the back barrier. This is related to a bug in the source code. In addition, it was found that long waves have a larger contribution to the erosion volume during the field cases of Bay Head and Camp Osborne than was found in the conceptual study of the collision regime.

Chapter 5

Discussion

5.1 General

Dutch reference profile In the conceptual model a representative profile for the Dutch design storm was simulated in XBeach. The validity of such an approach has been discussed by Vellinga (1986). However, for more complex situations like coastal curvature, wave obliquity and hard-soft interactions it is at least questionable if these assumptions hold. For example, in this thesis it is found that the development of scour is time and forcing-dependent. In order to accurately reproduce scour in XBeach the complete hydrodynamic signal (ebb and flood) should be taken into account.

Oblique wave attack The morphological effect of the barrier (both for the causes and impact) under oblique wave attack is a *relative* new research domain[1]. In XBeach oblique attack will result in more erosion. XBeach is however mainly validated in the Delta Flume under shore normal wave attack. The reasoning in general, and in this thesis, is that the physical relations describing the cross-shore and alongshore dimensions in XBeach are implemented correctly. The capability of modeling processes in longshore direction is however never *explicitly* validated with measurement data. Therefore, one should be cautious when making hard conclusions based on an invalidated part of a process-based model.

Modified DnA calculation rules The formulation of the modified DnA rules were based on the relation between the erosion volume and retreat distance. It was shown that for the reference profile there was a consistent relation between the two in the collision regime. It is however questionable if this is valid in general. If this is *not* the case, the DnA calculated values for the influence length will start to vary. On top of that, it is not clear how to divide the erosion volume in the modified DnA calculation rules for more complex cross-sections. Therefore, in this thesis, all the erosion is taken into account for the calculation of the additional erosion, which possibly can result in overestimation of the additional erosion.

Stability of structures The DnA calculation rules originally identified two different tracks. The first track is valid for a structure which fails in the barrier. The second track is valid for the situation when a structure does not fail and will have a longshore effect in terms of increased set-back over a certain influence length. Track 1 was outside the scope of this thesis, because of the lack of

[1]There is one research undertaken in which oblique wave attack during storm surges was a topic of interest (Tilmans, 1981). The main reason why there were no follow-up experiments carried out, were challenges related to pumping the longshore transport from one side to the other.

validation possibilities during Hurricane Sandy. In reality, however, potential failing of a structure in the barrier is of importance. In this thesis, it is assumed that foundations never fail, despite the scour in front of the structure. Structures with large volumes which do fail, can have large morphological impacts on for example the patterns in the retreat line.

Infilling of scour holes In the field case at the (buried) seawall no clear scour holes were present. One hypothesis in this thesis to support these findings was the concept of infilling of scour during falling water levels. This concept has been proved with XBeach simulations, however there is no measurement data to *undeniably* support these findings. It is therefore questionable if infilling of scour is indeed a process with a significant contribution. This uncertainty becomes even larger when one keeps into mind that XBeach does not solve all the physics needed to reproduce scour and an parametric relation ($jetfac$) is needed to mimic turbulence near structures.

5.2 Case study specific

Field cases in general: uncertainty The problem with a case studies in general is the combination of the large amount of data required and the inaccuracy of this data. The result is that there is a large spreading of potential morphological responses. For example in this thesis the morphological impact of a small variation in the water levels applied, was already substantial. It is therefore important to keep in mind that hindcasting attempts in XBeach are not *the truth*, even if a certain model has a good predictive skill. Models are a useful tool to understand the system and to assess what-if questions.

Calibration based on pre- and post-storm bed levels Currently the need for calibrating models is inevitable, despite efforts to improve process-based models such as XBeach with more accurate physical relations. It is common practice to validate calibration with the morphodynamic information available (often pre- and post-storm bed levels). A result is that (usually) this information is represented correctly. It is however not known what the skill over time is, or how well the hydrodynamic conditions are described. In this thesis for example a higher bed roughness resulted in a better morphodynamic reproduction, but this calibration step had a major impact on the velocity patterns on top of the barrier. One should always be critical with calibration and its (unexpected) downsides.

Local versus mean reproduction: spatial variability In reality there is a spatial distribution in terms of vegetation, structures, sediment characteristics or hydrodynamic conditions. However, in this thesis is was assumed that the bed level roughness is uniform in time and space. This results in a *mean reproduction* of the morphology, but locally difference will occur, as showed in the field case of Camp Osborne. More research is needed to analyze the advantage of taking into account more spatial-orientated information and the added value of each information type. The problem which will arise with this spatial variability in data is that often there is a lack of available site specific information.

Chapter 6

Conclusion

In this thesis insight is obtained in the processes related to the effects of hard structures during storm surges (first objective). This is done in the literature study (phase 1), with the conceptual study (phase 2) and by modeling the case study of Hurricane Sandy (phase 3). Challenge in this research was the difference in the storm regime between known effects in literature (collision regime) and the observed effects during Sandy on the coast of New Jersey (overwash regime). With the help of the conceptual study it was possible to link both the theory with the case study as well as the other way around. This was specifically possible with the use of the description of the output parameter *additional erosion in adjacent locations* (A_2) in contrast to the formulation *increased set-back* (d_2). Also the DnA calculation rules were modified to describe this output parameter.

With the method summarized, conclusions are stated separate towards the thesis objective of Section 1.3 (general conclusions) and the research questions (Rq.) of Section 1.4 (specific conclusions). The reason for this approach is that there is a difference between the practical meaning of a thesis and the results of the research itself.

6.1 Conclusion towards the thesis objective

In this section the *general* conclusions per objective number are presented. The first objective in this thesis is to obtain a better understanding of the effects of hard elements on the erosion process during the collision and overwash regime. The second objective is to determine how XBeach could be calibrated to describe overwash conditions. The following *general* conclusions are made:

1. Cross-sections with hard elements provide less sediment which can be deposited in the nearshore and therefore the efficiency of dissipating wave energy is lower when a hard element is present (WL | Delft Hydraulics, 1987). This results in higher energetic conditions in front of structures.

   (a) In cross-shore direction higher turbulence intensities at the toe of the structure make it possible for an erosion hole to develop. For the Dutch reference simulation scour at the toe did indeed develop in XBeach. For the field case there was no scour noticeable in the post-Sandy bathymetry at the (buried) seawall. XBeach simulations suggest this is related to infilling of scour during falling water levels. This means that scour did occur and cannot be neglected for the structural integrity of the structure, but one should take into account that the development of scour is time- and forcing-dependent. On the other hand, hard structures are an effective and spatial-efficient protection method.

   (b) In longshore direction the process of increased set-back is for the Dutch reference simulation primarily (2/3) the result of additional erosion and secondarily (1/3) of a decrease in accretion. The decrease in accretion is driven by a water level gradient from the

soft towards the hard cross-section as a result of set-up differences (Van Geer et al., 2012). The increase in erosion occurs due to locally higher short waves originating from a less dissipative soft cross-section and by diffraction around the hard element. The field case of Camp Osborne (Hurricane Sandy, 2012) resulted in the first validation on prototype scale were a hard element had an effect in longshore direction. XBeach simulations suggest that in this field case there is an increase of 32% in terms of additional erosion in adjacent locations due to the presence of the condo.

(c) For coastal zone managers it is important to realize that the barrier volume is the most important factor in determining the morphological response of the barrier. The main effect of a structure is the impact on the sand balance (both cross-shore and longshore), by cutting of (part) of the sediment supply. This can result in an effective and spatial-efficient protection method, but will also have an negative impact in cross-shore and longshore direction. These effects have been reproduced in the case study of Hurricane Sandy. However, this is no reason to state that multifunctional use of the barrier is *not* possible. Its applicability needs to be addressed case-by-case. Process-based models, like XBeach, can accurately reproduce the cross-shore and longshore effects noticed in the field. The DnA calculation rules do not reflect the true complexity, but can give a rough first indication of the longshore effect.

2. XBeach can be calibrated by applying a two-step calibration approach. The first step is to increase the parameterized wave asymmetry sediment transport component ($facua$). A higher value will result in less net offshore sediment transport and is suitable for calibrating the collision regime (dune erosion). The second step is to increase roughness of the barrier. A higher roughness will result in less sediment transport on top of the barrier and is applied to calibrate the overwash regime. Good results have been found by applying this approach in the case study of Hurricane Sandy which resulted in overwash and breaching across the entire state of New Jersey.

6.2 Conclusion towards the research questions

6.2.1 First objective: effects of a hard structure

The first objective is to obtain a better understanding of the effects of hard elements. Research questions (Rq.) related to this objective are first of all focusing on the causes and impacts due to the presence of a hard element (Rq. 1). Second, the capability of modeling these effects in XBeach is determined (Rq. 2). Also wave obliquity (Rq. 3), sensitivity for coastal and storm-induced parameters (Rq. 4) and variation in object size (Rq. 5) are addressed. Last, the potential of calculation rules such as DnA are analyzed. The following *specific* conclusions are made:

1. The effects of a hard structure (both cross-shore and longshore) are reproduced for both the conceptual simulations and for simulations of the case study of Sandy. The main effect of a hard element is related to sediment supply.

   (a) Higher energetic conditions for the Dutch reference simulation in XBeach resulted in a scour hole of 4.1 m (cross-shore effect). In addition, the erosion volume was 10% lower (-20 $m^3 \cdot m^{-1}$) for the hard cross-section. The field case simulations show that the presence of the seawall resulted in 50% lower wave forces on the ocean front houses of Brick, NJ (Irish et al., 2013), 35% less erosion (-44 $m^3 \cdot m^{-1}$) and a similar protection could be achieved with

an 18 meter wide sandy dune. Scour did occur, but was not measured in the post-Sandy bathymetry since infilling after the peak of Sandy took place.

(b) Less accretion and more erosion in the soft cross-section for the Dutch reference simulation in XBeach resulted in an increased set-back of 4.2-6.8 m over an influence length of 70-145 m (longshore effect). The field case simulations show that the presence of the condo at Camp Osborne resulted in 32% additional erosion in adjacent locations (+52 $m^3 \cdot m^{-1}$). Eventually this weakened cross-section is deepened even more as a result of the water level gradient from the bay to the sea (second flood event, backwash). This will result in a further increase of erosion with +163% (+277 $m^3 \cdot m^{-1}$). The influence length of the condo during Sandy was 266 m. For overwash conditions the longshore effect will be more related to an increase in erosion and less with an alongshore exchange of sediment. For the collision regime the longshore effect was 63-75% erosion-related and for the overwash regime this percentage increases up to 79-84%.

2. XBeach is capable of reproducing the morphological response near hard structures, both in cross-shore (scour) and in longshore direction (increased set-back or additional erosion), as described in literature. By default XBeach underestimates the development of erosion holes. The limited amount of turbulence created, is related to not resolving processes such as wave reflection and wave run-down, but can be mimicked with a parametric relation called $jetfac$ (Deltares, 2013). On top of that, short wave run-up ($swrunup$) is stated to be of importance (Van Geer et al., 2012). The introduction of the parametric relations $swrunup$ and $jetfac$ are, however, not of importance in describing the impact of hard elements for the case study of Hurricane Sandy. There were no differences found for the post-storm bathymetry for simulations with/without $jetfac$. It is not clear if the lack of effect of $jetfac$ is related to a specific process (counter force) or that the keyword is not (completely) triggered to introduce more turbulence. There is also a bug found in XBeach for the combination of overwash with $swrunup$. The effect is that the avalanching algorithm is unjustifiably triggered. This results in avalanching of the entire back barrier to the critical wet slope (1:0.3). For the conceptual study for the collision regime $jetfac$ *did* enhance in the development of a scour hole.

3. In the conceptual study the amount of increased set-back near structures only slightly depended on the angle of wave incidence with respect to the shoreline. Dunes situated downstream of the transition 'hard-soft' *can* experience a small increase in set-back, but overall a decreasing tendency was found. Reason is that the locally higher short waves are distributed over a broader area downstream driven by obliqueness. Near the upstream transition sediment will pile up against the structure resulting in an increase in retreat (updrift). In XBeach simulations the total additional downstream erosion volume ($\sum A_2$) does increase when the wave angle increases due to downdrift. This is mainly related to an increase in influence length. Also in the field case additional erosion in adjacent locations, due to the presence of the condo at Camp Osborne, Brick, NJ, occurred mainly at one side due to oblique wave attack.

4. Dune height above SSL (D_{SSL}) is the dominant variable for the morphological response of the barrier. For example, for the field case of Sandy a variation of the base water levels with 0.1 m had already a result of 18% more erosion. The impact of a variation in sediment diameter in XBeach is for the collision regime of minor interest, but for the case study (overwash regime) smaller sediment diameters do have a large impact on the morphological response. A variation in wave height (H_{RMS}) will only have limited impact, since in very shallow water long waves will dominate (Van Thiel de Vries, 2009b). In addition, the linear relation of Fisher et al. (1986) between wave forcing and impact is successfully reproduced for several field cases of Hurricane Sandy.

5. In the conceptual study variations in structural dimensions (width, length and position) had a large morphological impact. Structures placed in seaward direction will result in more erosion at the sides of the hard element. From a position of 20 m seaward erosive and accretive processes cancel each other out. Structures with increasing width will also result in more erosion. Structures with a width of > 100 m do not result in an increase of additional erosion. These structures can be seen as semi-infinite. For the field case a reduction in width of the condo did not result in a reduction of the maximum additional erosion (A_2), but the total additional erosion in adjacent locations ($\sum A_2$) did decrease for a smaller condo.
6. The (modified) DnA calculation rules are reproduced in XBeach for both the conceptual study (collision and overwash) as well as for the field case of Camp Osborne. Important to note that the DnA calculation rules are developed as a conservative addition factor for DUROS+. When comparing the longshore effect calculated by DnA and by XBeach some conservatism is expected. The following conclusion can be made regarding the calculation rules of Deltares and Arcadis (2013):
   (a) When comparing the longshore effect calculated by DnA and simulated by XBeach in the conceptual study for the collision regime, the DnA values are indeed conservative. The mean ratio for the increased set-back is 56% and the mean ratio for the influence length is 35% (when comparing XBeach with DnA). The DnA calculation rules are not capable of describing the longshore effect of hard structures during oblique wave attack.
   (b) Also for the conceptual study for the overwash regime the modified DnA calculation rules are reproduced (ratio DnA and XBeach for A_2: 48-58%). In the field case of Camp Osborne the presence of the condo created a weak spot which eventually eroded even more due to backwash driven by a water level gradient from the bay to the sea (second flood event). Without this gradient the modified DnA calculation rules would have accurately predicted the increase of erosion (+48 $m^3 \cdot m^{-1}$ DnA-calculated versus +55 $m^3 \cdot m^{-1}$ XBeach-simulated). XBeach simulations suggest that the conservatism of the (modified) DnA calculation rules for the overwash regime is lower than than for the collision regime.

6.2.2 Second objective: calibration method XBeach

The second objective is to derive which steps can be taken to calibrate XBeach in order to accurately reproduce overwash conditions. Research questions (Rq.) related to this objective are first of all focusing on the method of calibration (Rq. 7), but also the predictive skill of the calibrated XBeach model in the case study is determined (Rq. 8). The following *specific* conclusions are made:

7. XBeach is calibrated for the overwash regime by applying a two-step calibration approach, as demonstrated by De Vet (2014). The first step is to increase the asymmetric onshore sediment transport component ($facua$). The second step is increasing the roughness of the barrier island.
   (a) A value of $facua$ of 0.25 (0.1 default) results in a good fit with measurement data. Variation of the $facua$ makes it possible to control the amount of erosion which occurs in the collision regime (dune erosion). XBeach is sensitive for a variation of the $facua$. An increase from the default value towards 0.25 means for the buried seawall (1D hard cross-section) a decrease in erosion by 38% (from 129 to 80 $m^3 \cdot m^{-1}$). For Bay Head the influence is a decrease of mean erosion by 65% (from 500 to 178 $m^3 \cdot m^{-1}$). In practice this means that without a higher $facua$ for Bay Head at every location overwash occurs, this is in contrast to reality. There is no *direct* physical meaning of such a value, but in previous studies higher values have been applied (Van Rooijen, 2011; Vousdoukas et al., 2012).

(b) A good fit with the LiDAR is found when a Chezy value of 30 $m^{0.5}.s^{-1}$ is applied on the barrier island and the default value of 55 $m^{0.5}.s^{-1}$ is used in the rest of the model. Introducing a higher friction on the barrier island makes it possible to control the amount of erosion which occurs in the overwash regime. XBeach is sensitive for a variation of the barrier roughness. An increase from the default value towards a Chezy value 30 $m^{0.5}.s^{-1}$ means a decrease in mean erosion for Bay Head by 80% (from 883 to 178 $m^3 \cdot m^{-1}$). In practice this means that without extra roughness on the barrier most of the locations where overwash occurs, will breach in XBeach. The physical meaning of such friction value is a Nikuradase sand roughness (k_s) of 0.5 m in a water depth of 1.0 m.

(c) The avalanching algorithm is of major importance in describing the morphological behavior of barrier islands during overwash conditions. In the case study all the cross-sections needed avalanching to get into the overwash regime. The algorithm is almost insensitive for changes in the critical dry slope ($m_{cr,dry}$), water depth at the interface between critical slopes (h_{switch}) or maximum dune face erosion (dz_{max}). Variation in critical wet slope ($m_{cr,wet}$) is of major importance in describing the behavior during storm conditions. By default XBeach applies a slope of 0.3, in a data analysis a value of 0.22 was found, but the highest BSS was achieved with a lower value of 0.1.

8. When these calibration steps are applied it is possible to model the field case of Bay Head with a BSS of 0.83 and a bias of -0.21 m. Important to note that applying one alongshore barrier roughness profile on the barrier is an oversimplification. One roughness profile will result in good reproduction of the mean morphological behavior, but cannot reproduce all the alongshore variability. The approach applied in this thesis had limited skill in reproducing the hydrodynamics.

Chapter 7

Recommendations

a) Understanding: morphological behavior of the system

1. Experiments of Boers et al. (2011) are the basis of our understanding of the longshore effect of hard structures. However, in these experiments oblique wave attack was not taken into account. In this thesis it is shown that the effect of oblique wave attack is an important contribution in the description of erosion during storm surges (general) as well as for the longshore effect of hard structures (specifically). In order to validate the simulated behavior in XBeach measurements of these processes is needed. However, a physical model which facilitates the longshore dimension of erosion during storm surges will result in scale effects due to the limited dimensions of experimental basins.
2. XBeach has been extensively calibrated and validated with the use of Delta Flume experiments (Vellinga, 1986; Van Thiel de Vries, 2009b). These measurements were however gathered for the collision regime. Measurement data of overwash, inundation and breaching is more scarce. An experimental set-up for overwash and breaching could enhance our understanding of the processes which can help to improve process-based models such as XBeach.

b) Applying: integrated coastal zone management (ICZM)

4. For barrier islands, combinations of hard and soft protection methods seem a practical and realistic solution. In these dense areas, with limited barrier width, there is simply not enough room to create a complete soft solution *and* to provide protection against storm conditions such as Hurricane Sandy. For example without the (buried) seawall the erosion volume at Bay Head, NJ, would have been 55% larger.
5. Weak spots in the coastal system can be easily identified by calculating the cross-sectional area above SSL. This can be a quick-and-easy tool for the local authorities to investigate weak spots in the system. A threshold of 135 $m^3.m^{-1}$ can be seen as a good estimate to ensure resilience of coastal communities of New Jersey for design storms such as Hurricane Sandy.

c) Improving: DnA calculation rules

6. Based on XBeach simulations in the conceptual study the DnA calculation rules can be tightened both in terms of the increased set-back (d_2) as well for the influence length (l_2). A suggestion for α_2 is the range of 0.168-0.235 (DnA: 0.30). A suggestion for λ is the range of 17.8-24.5 (DnA: 30). On top of that a reduction can be included for structures with a width smaller than 100 m, since the calculation rules are currently designed for semi-infinite structures. In this thesis a width reduction is suggested: if the width of the NWO < 100 than $d_{2,red} = \frac{W^{0.25}}{100^{0.25}} \cdot d_2$. The downside of the suggestions is that they are only supported with

numerical simulations in XBeach and noise in the data of experiments (Boers et al., 2011) resulted in these relatively high proportionally coefficients.

7. The DnA calculation rules were modified, since for overwash conditions one could not work with the output parameter retreat distance or set-back. A major advantage of the definition of erosion volume is that it can be more accurately used in complex profiles. An adaptation of the DnA calculation rules towards this, more realistic and insightful, parameter is encouraged. The downside of this adaptation is dividing the erosion volume in separate parts. Specifically, it is troublesome to determine the amount of erosion in the influence area of the structure (A_1).

d) Improving: XBeach model

8. Currently, a simple and robust avalanching algorithm is implemented in XBeach. Improvements of this algorithm are possible by describing simple geotechnical relations in XBeach. This is especially supported since in this thesis cross-sections needed avalanching to get in the overwash regime. The downside of such a relation is that more information is needed prior to modeling.

9. The range of the accepted values for the parameter controlling the asymmetric onshore sediment transport ($facua$) results in remarkable large differences (factor 2 in terms of erosion volume). There are two methods to reduce the unceratainty in the approach applied. First option, a guideline in which applicability when to apply which $facua$ value is described. Second option, a more accurate method to describe/include the asymmetric sediment transport component. A hypothesis is that there is a relation between the steepness of the beach and the $facua$ value needed in XBeach. For example for intermediate-to-reflective beaches Vousdoukas et al. (2012) needed calibration via the $facua$ in order to achieve positive skill scores. In this thesis also calibration via the $facua$ parameter was needed to reproduce the impact of Hurricane Sandy on the steep beaches of New Jersey (slope of 13%).

10. The bottom friction is used both in the flow and in sediment transport module and is currently in XBeach calculated with the use of the Chezy coefficient. First of all, implementing a Manning coefficient, as demonstrated by De Vet (2014), is supported due to the more robust theoretical background and the possibility of applying tables with default coefficients. Second, this opens the way of the possibility of applying roughness indicators based on LiDAR, as demonstrated by Smith et al. (2001). Another possible improvement is varying the bed roughness in z-direction, which makes it possible to model breaching in a more realistic matter. The downside of all these implementations is that more information prior modeling and additional calibration is needed.

Bibliography

Baart, F., Den Bieman, J. P., Van Koningsveld, M., Parteli, E., Plant, N., and Roelvink, J. (2012). An integrated coastal model for aeolian and hydrodynamic sediment transport.

Basco, D. (1998). The Economic Analysis of "Soft" Versus "Hard" Solutions for Shore Protection. *Coastal Engineering*, pages 1449–1460.

Battjes, J. (1974). *Computation of set-up, longshore currents, run-up and overtopping due to wind-generated waves*. PhD thesis, Delft University of Technology.

Boers, M., Van Geer, P., and Van Gent, M. (2011). Dike and dune revetment impact on dune erosion. *Proc. Coastal Sediments*, Miami, FL.

Bosboom, J. and Stive, M. J. F. (2013). *Lecture notes Coastal Dynamics 1*. Delft University of Technology. VSSD. ISBN: 978-90-656-286-0, Delft, 2013 edition.

Brandenburg, P. (2010). Scale dependency of dune erosion models. Technical report, MSc thesis, Delft University of Technology.

Bruun, P. (1954). Coastal erosion and the development of beach profiles. *U.S. Army Corps of Engineers Beach Erosion Board Technical Memo*, 44.

Daly, C. (2009). Low Frequency Waves in the Shoaling and Nearshore Zone A Validation of XBeach. Technical Report June, MSc thesis. Delft University of Technology, Delft.

De Vet, P. (2014). Modelling sediment transport and morphology during overwash and breaching events. Technical report, MSc thesis, Delft University of Technology, Delft.

De Vries, B. (2011). Dune erosion near sea walls - Xbeach validation. Technical report, MSc thesis, Delft University of Technology, Delft.

Deltares (2011a). Delft3D-FLOW: user manual. Technical report, Version 3.15. Revision: 14499.

Deltares (2011b). Multifunctional use the water defences (Dutch: Multifunctioneel medegebruik van de waterkering). Technical report, Code: 1204871-000-VEB-0009.

Deltares (2012). Obects in dunes with a flood defence (Dutch: Niet-Waterkerende Objecten in duinwaterkeringen). Technical report, Code: 1205782-000-HYE-0005.

Deltares (2013). Quality status report XBeach WTI2017. Technical report, Revision: 3322, Delft.

Deltares and Arcadis (2013). Calculation rules objects in dunes (Dutch: Handreiking NWO in duinen). Technical report, Code: 1208163-000-HYE-0018.

Den Bieman, J. P. (2012). Simulating Barrier Island Evolution. Technical report, MSc thesis. Delft University of Technology, Delft.

Den Heijer, C. (2013). *The role of bathymetry, wave obliquity and coastal curvature in dune erosion prediction*. PhD thesis, Delft Unversity of Technology.

Donnelly, C. (2007). Morphologic Change by Overwash : Establishing and Evaluating Predictors. *Journal of Coastal Research*, (50):520–526.

Donnelly, C., Kraus, N., and Larson, M. (2006). State of Knowledge on Measurement and Modeling of Coastal Overwash. *Journal of Coastal Research*, 224(224):965–991.

ENW (2007). Technical report dune erosion (Dutch: Technisch Rapport Duinafslag). Technical report, WL | Delft Hydraulics, Delft.

Fisher, J., Asce, M., Overton, M., and Chrisholm, T. (1986). Field measurements of dune erosion. *19th International Conference on Coastal Engineering, Houston*, pages 1553–1558.

Galappatti, R. (1983). A depth integrated model for suspended transport. *Communications on Hydraulics. Department of Civil Engineering, Delft University of Technology.*

Harnden, T. (2012). The impact of Hurricane Sandy - pictures. *Daily Mail*, pages 12–13.

Holthuijsen, L., Booij, N., and Herbers, T. (1989). A prediction model for stationary, short-crested waves in shallow water with ambient currents. *Coastal Engineering*, 13(1):23–54.

Hoonhout, B. (2009). Dune erosion along curved coastlines. Technical report, MSc thesis, Delft University of Technology, Delft.

Huthoff, F. and Augustijn, D. (2004). Channel roughness in 1D steady uniform flow: Manning or Chezy? *NRC days: Sediment, Hydraulic and Morphology*.

Irish, J. L., Lynett, P. J., Weiss, R., Smallegan, S., and Cheng, W. (2013). Buried relic seawall mitigates Hurricane Sandy's impacts. *Coastal Engineering*, 80:79–82.

Jarrett, R. (1985). Determination of roughness coefficients for streams in Colorado. *United States Geological Survey*.

Kobayashi, N., Tega, Y., and Hancock, M. (1996). Wave reflection and overwash of dunes. *Journal of Waterway, Port, Coastal and Ocean Engeering*, 122(3)(150-153).

Larson, M., Erikson, L., and Hanson, H. (2004). An analytical model to predict dune erosion due to wave impact. *Coastal Engineering*, 51(8-9):675–696.

Lesser, G., Roelvink, J., van Kester, J., and Stelling, G. (2004). Development and validation of a three-dimensional morphological model. *Coastal Engineering*, 51(8-9):883–915.

Longuet-Higgins, M. and Stewart, R. (1964). Radiation stress in water waves: a physical discussion with applications. *Deep-Sea Research*, II:529–562.

Lopez-Feliciano, O. (2014). Implementation of CMS high resolution model to study morphology change in a groin field during Hurricane Sandy. Technical report, MSc thesis, Stevens Institute of Technology, Hoboken, New Jersey.

Marriott, M. J. and Jayaratne, R. (2010). Hydraulic roughness - link between Manning's coeffcient, Nikuradase's equiavalant sand roughness and bed grain size. *University of East London*, pages 27–32.

McCall, R. (2008). The longshore dimension in dune overwash modelling. Technical Report May, MSc thesis, Delft University of Technology, Delft.

McCall, R., Plant, N., and van Thiel de Vries, J. S. M. (2010a). The effect of longshore topographic variation on overwash modelling. *Proceedings 32th International Conference on Coastal Engineering*, pages 1–13.

McCall, R., van Thiel de Vries, J. S. M., Plant, N., Van Dongeren, A., Roelvink, J., Thompson, D., and Reniers, A. (2010b). Two-dimensional time dependent hurricane overwash and erosion modeling at Santa Rosa Island. *Coastal Engineering*, 57(7):668–683.

Miller, J., Mahon, A., and Herrington, T. (2009). Development of the Stevens Dynamic Underwater and Coastal Kinematic Surveying DUCKS system. Technical report, Coastal Protection Technical Assistance Service, Davidson Laboratory TR-2878.

Munk, W. (1949). Surf-beats. *Trans. Amer. Geophys. Union*, 30(6):849–854.

National Hurricane Center (2012). Hurricane Sandy Advisory Archive. Data retrieved from: `http://www.nhc.noaa.gov/data/`.

NDBC (2012). Wave information. Stations 44065 and 44025. National Data Buoy Center of NOAA. Data retrieved from: `http://www.ndbc.noaa.gov/`.

NGDC (2014). Coastal Relief Model (CRM). NOAA: National Geophysical Data Center. Data retrieved from: `www.ngdc.noaa.gov/mgg/coastal`.

NJDEP (2012). New Jersey Shore Protection Master Plan. *Department of Environmental Protection - State of New Jersey*.

NJDEP (2014). Shoreline protection. Information retrieved from `http://www.nj.gov/dep/shoreprotection/`.

NOAA (2012). Tidal gauge information. Stations: 8534720, 8531680 and 8518750. National Oceanic and Atmospheric Administration. Data retrieved from: `http://tidesandcurrents.noaa.gov`.

Orton, P., Georgas, N., Blumberg, A., and Pullen, J. (2012). Detailed modeling of recent severe storm tides in estuaries of the New York City region. *Journal of Geophysical Research: Oceans*, 117(C9).

Phillips, O. (1977). The dynamics of the upper ocean. *Cambridge University Press*, page 366.

Reniers, A. J. H. M. (2004). Morphodynamic modeling of an embayed beach under wave group forcing. *Journal of Geophysical Research*, 109(C1):C01030.

Roelvink, J., Reniers, A., van Dongeren, A., van Thiel de Vries, J. S. M., McCall, R., and Lescinski, J. (2009). Modelling storm impacts on beaches, dunes and barrier islands. *Coastal Engineering*, 56(11-12):1133–1152.

Roelvink, J., Reniers, A. J. H. M., van Dongeren, A., van Thiel de Vries, J. S. M., Lescinski, J., and McCall, R. (2010). XBeach Model Description and Manual. Technical report, Unescio-IHE, Deltares and Delft University of Technology, Delft.

Roelvink, J. and Stive, M. J. F. (1989). Bar-generating cross-shore flow mechanisms on a beach. *Journal of Geophysical Research*, 94:4785–4800.

Ruessink, B., Ramaekers, G., and van Rijn, L. (2012). On the parameterization of the free-stream non-linear wave orbital motion in nearshore morphodynamic models. *Coastal Engineering*, 65:56–63.

Sallenger, A. (2000). Storm impact scale for barrier islands. *Journal of Coastal Research*, 16(3):890–895.

Smith, M., Asal, F., and Priestnall, G. (2001). The use of photogrammetry and LiDAR for landscape roughness estimation in hydrodynamic studies.

Spoto, M. (2013). A new beginning for hurricane-ravaged Camp Osborn in Brick. *True Jersey*.

Steetzel, H. (1993). *Cross-shore transport during storm surges*. PhD thesis, Delft University of Technology.

Stelling, G. and Duinmeijer (2003). A staggered conservative scheme for every Froude number in rapidly varied shallow water flows. *International Journal for Numerical Methods in Fluids*, 43(12):1329–1354.

Sumer, B. and Fredsoe, J. (2002). *The Mechanics of Scour in the Marine Enviroment*. World Scientific in: Advanced Series on Ocean Engineering, 17 edition.

Sutherland, J., a.H. Peet, and Soulsby, R. (2004). Evaluating the performance of morphological models. *Coastal Engineering*, 51(8-9):917–939.

Terlouw, A. (2013). Predicting morphological storm impact on coastal dunes at Ameland. Technical report, MSc thesis, Delft University of Technology.

The Richard Stockton College (2007). NJ Shoreline Protection and Vulnerability. Information retrieved from: `http://intraweb.stockton.edu`.

Tilmans, W. (1981). Study at dune erosion dunring storm in a two dimensional model. (In Dutch: Onderzoek naar duinafslag tijdens superstormvloed). Technical report, WL | Delft Hydraulic - M1653.

USACE (2008). *Coastal Engineering Manual (CEM)*, volume 1100.

USACE (2010). LiDAR: New Jersey. United States Army Corps of Engineers. Data retrieved from: `www.csc.noaa.gov/dataviewer`.

USACE (2012). LiDAR: New Jersey. United States Army Corps of Engineers. Data retrieved from: `www.csc.noaa.gov/dataviewer`.

USGS (2012a). LiDAR: New Jersey. National Water Information System of the U.S. Geological Survey.. Data retrieved from: `www.csc.noaa.gov/dataviewer`.

USGS (2012b). Water level information. Stations: 01408050 and 01408168. National Water Information System of the U.S. Geological Survey.. Data retrieved from: `http://waterdata.usgs.gov/`.

Van Dongeren, A. (2003). Numerical modeling of infragravity wave response during DELILAH. *Journal of Geophysical Research*, 108(C9):3288.

Van Dongeren, A., Battjes, J., Janssen, J., van Noorloos, J., Steenhauer, K., Steenbergen, G., and Reniers, A. J. H. M. (2007). Shoaling and shoreline dissipation of low-frequency waves. *Journal of Geophysical Research*, 112(C2):C02011.

Van Geer, P., De Vries, B., Van Dongeren, A., and Van Thiel de Vries, J. S. M. (2012). Dune erosion near sea walls: model-data comparison. *Coastal Engineering*, pages 1–9.

Van Gent, M., Van Thiel de Vries, J. S. M., Coeveld, E., De Vroeg, J., and Van de Graaff, J. (2008). Large-scale dune erosion tests to study the influence of wave periods. *Coastal Engineering*, 55(12):1041–1051.

Van Ormondt, M. (2014). Delft3D model of waves and surge among the East coast of the USA. Technical report, Deltares, Delft.

Van Rijn, L. (1990). *Princples of fluid flow and surface waves in rivers, estuaries, seas and oceans*. Aqua Publications.

Van Rijn, L. (2003). The predictability of cross-shore bed evolution of sandy beaches at the time scale of storms and seasons using process-based models. *Coastal Engineering*, 47(3):295–327.

Van Rijn, L. (2007). Unified View of Sediment Transport by Currents and Waves . part I, II, III, IV. *Journal of Hydraulic Engineering*, (June):649–667.

Van Rooijen, A. (2011). Modelling Sediment Transport in the Swash Zone. Technical report, MSc thesis. Delft University of Technology.

Van Thiel de Vries, J. S. M. (2009a). Dune erosion above revetments. *ICCE 2012: Proceedings of the 33rd International Conference on Coastal Engineering, Santander, Spain, 1-6 July 2012*, pages 1–13.

Van Thiel de Vries, J. S. M. (2009b). *Dune erosion during storm surges*. PhD thesis, Delft University of Technology, Delft.

Van Thiel de Vries, J. S. M., Van Dongeren, A., McCall, R., and Reniers, A. J. H. M. (2008). The effect of the longshore dimension on dune erosion. *Coastal Engineering*, pages 1–13.

Van Velzen, E., Jesse, P., Cornelissen, P., and Coops, H. (2003). Fluid resistance due to vegetation in floodplains (Dutch: Stromingsweerstand vegetatie in uiterwaarden). *Ministerie van Verkeer en Waterstaat*, (november).

Vellinga, P. (1986). *Beach and dune erosion during storm surges*. PhD thesis, Delft University of Technology, Delft.

Vousdoukas, M. I., Ferreira, O., Almeida, L. P., and Pacheco, A. (2012). Toward reliable storm-hazard forecasts: XBeach calibration and its potential application in an operational early-warning system. *Ocean Dynamics*, 62(7):1001–1015.

Walling, K., Miller, J., and Herrington, T. (2014). Comparison of hurricane sandy impacts in three New Jersey coastal communites. *Coastal Engineering*.

Walstra, D. J. R., Roelvink, J., and Groeneweg, J. (2000). 3D calculation of wave-driven cross-shore currents. In *Proceedings 27th International Conference on Coastal Engineering*, pages 1050–1063.

Wicker, C. (1950). History of New Jersey Coastline. *Memo: US Army Corps of Engineers*.

WL | Delft Hydraulics (1987). Systematic research into the effect of dune base defenses. (Dutch: Systematisch onderzoek naar de werking van duinvoetverdedigingen). Technical report, M2051 - part 2.

WL | Delft Hydraulics (1988). Scour holes. (Dutch: Ontgrondingskuilen). Technical report, H298 - part 4.

WL | Delft Hydraulics (1993). Effect of objects on dune erosion (Dutch: Effect bebouwing duinafslag). Technical report, H1696, Delft.

Appendix A

Description of XBeach

A.1 Introduction

After the hurricane seasons of 2004 and 2005 in the USA, the United States Army Corps of Engineers (USACE) received funding for the MORPHOS-3D project. XBeach (Roelvink et al., 2009) was developed within the MORPHOS-3D framework and is the first 2DH numerical model to assess the natural coastal response during time-varying storm and hurricane conditions. It is designed to reproduce the different storm regimes, as described by Sallenger (2000). XBeach is therefore on first hand a morphological model which focuses on relative small spatial scales and short temporal scales, as can been seen in Figure A.1.

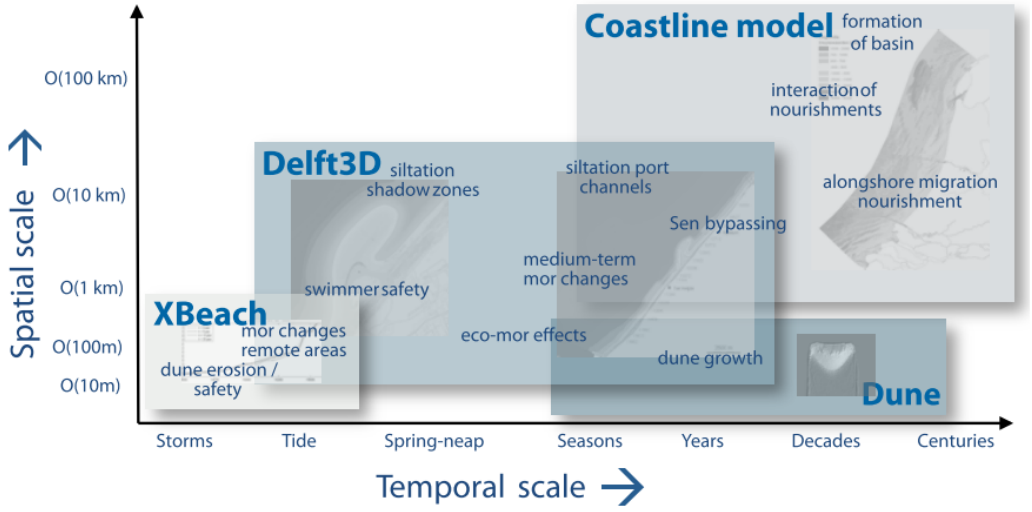

Figure A.1 *Time and spatial scales for hydrodynamic processes and the position of several computational models within this framework (Baart et al., 2012).*

XBeach is open-source and developed by UNESCO-IHE, Delft University of Technology, Deltares and the University of Miami. XBeach is written in Fotran 90/95. This appendix only briefly discusses the main features of the XBeach model. A comprehensive description of the model, including all equations, can be found in the user manual of XBeach (Roelvink et al., 2010).

A.2 Model set-up

XBeach uses a coordinate system in which the x-axis is oriented towards the coast and the y-axis describes the longshore distance. The model uses a staggered grid in which conservative quantities are calculated in the cell centers. Fluxes (such as velocities or sediment transport) are calculated in the cell interfaces. XBeach allows the grid cells to vary in both cross-shore and longshore direction.

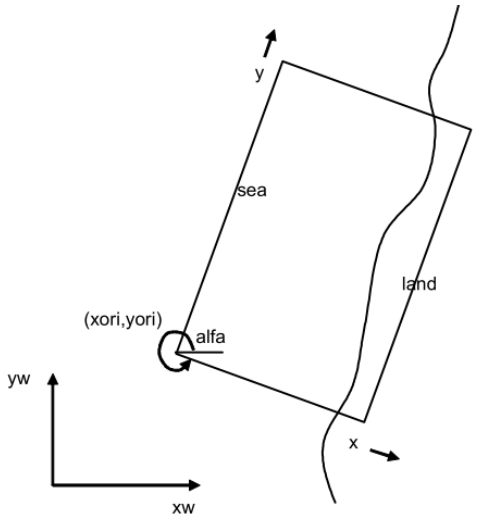

Figure A.2 *The coordinate system used in XBeach (Roelvink et al., 2010).*

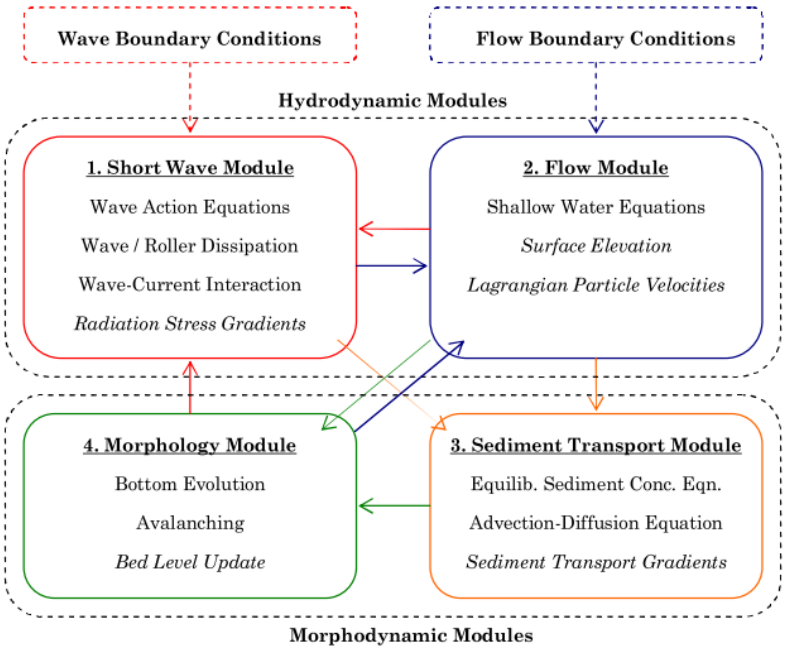

Figure A.3 *Different modules in XBeach, arrows indicate connectivity (Daly, 2009).*

A.3 Governing equations

The functionality of XBeach is divided among a number of modules. In one single numerical step each module is called in a specific sequence. XBeach starts with the wave module. In this module gradients in radiation stress are calculated. The flow module uses the change in radiation stress to calculate surface elevation and velocities. This will lead to sediment transport and eventually towards an update of the bed level, as can be seen in Figure A.3.

A.3.1 Hydrodynamics

Wave action equation Short wave transformation is derived from a time dependent version of the so-called wave action balance equation (Holthuijsen et al., 1989). The wave action(A) depends on the directional distribution of energy (E_w), and the frequency distribution (σ). This frequency distribution is reduced to a single representative peak frequency, as can be seen in Equation A.2.

The wave action balance is given by:

$$\frac{\partial A}{\partial t} + \frac{\partial c_{g,x} A}{\partial x} + \frac{\partial c_{g,y} A}{\partial y} + \frac{\partial c_\theta A}{\partial \theta} = -\frac{D_{waves}}{\sigma} \tag{A.1}$$

Wave action is determined by:

$$A(x, y, t, \theta) = \frac{E_w(x, y, t, \theta)}{\sigma(x, y, t)} \tag{A.2}$$

The wave action propagation speeds in x- and y-direction are given by:

$$\begin{aligned} c_x(x, y, t, \theta) &= c_g \cos\theta + u^L \\ c_y(x, y, t, \theta) &= c_g \sin\theta + v^L \end{aligned} \tag{A.3}$$

In these equations θ represents the angle of incidence with respect to the x-axis. S_w stands for the wave energy density and σ for the intrinsic wave frequency. The propagation speeds in x and y depends on the group velocity (c_g), the angle of incidence and when wave current interaction is included also of the background velocities. For the calculation of the dissipation term (D_{waves}) several calculation methods are implemented in XBeach.

Roller energy equation The roller energy balance is coupled with the wave action balance where dissipation of short wave energy serves as a source for the roller energy balance. Also in the roller energy balance the frequency spectrum is represented with a single frequency.

The roller energy balance is given by:

$$\frac{\partial E_{roller}}{\partial t} + \frac{\partial c_x E_{roller}}{\partial x} + \frac{\partial c_y E_{roller}}{\partial y} + \frac{\partial c_\theta E_{roller}}{\partial \theta} = -D_{roller} + D_{waves} \tag{A.4}$$

In this equation E_{roller} represents the roller energy in each directional bin. For the calculation of the dissipation terms (D_{roller} and D_{waves}) several calculation methods are implemented in XBeach.

Radiation stress gradients Both the wave action balance as well as the roller energy balance result a spatial distribution of wave energy. This distribution can, according to the linear wave theory, be used to calculate the gradients in radiation stress. There are thus two contributions to the radiation stress: roller-induced and wave-induced. These terms are simply added up in XBeach.

$$\begin{aligned} F_x(x,y,t) &= -\left(\frac{\partial S_{xx,waves}+\partial S_{xx,roller}}{\partial x}+\frac{\partial S_{xy,waves}+\partial S_{xy,roller}}{\partial y}\right) \\ F_y(x,y,t) &= -\left(\frac{\partial S_{yy,waves}+\partial S_{yy,roller}}{\partial y}+\frac{\partial S_{xy,waves}+\partial S_{xy,roller}}{\partial x}\right) \end{aligned} \tag{A.5}$$

In this equation F_x and F_y represents the wave forcing in x and y-direction. The radiation stress consists of three parts: wave propagation in x (S_{xx}) in y (S_{yy}) and the shear stress component of the radiation stress (S_{xy}).

Shallow water equations The GLM-formulation (Walstra et al., 2000) makes it possible to take into account the wave induced mass-flux and the return current in shallow water via a depth-averaged formulation. The idea is that the Eulerian shallow water velocities (u^E and v^E for in x and y-direction) are replaced with a Lagrangian equivalent:

$$\begin{aligned} u^L &= u^E + u^s \\ v^L &= v^E + v^s \end{aligned} \tag{A.6}$$

In this equation u^s and v^s represent the Stokes drift in x and y-direction (Phillips, 1977). The Stokes drift is calculated with the use of Equation A.7:

$$\begin{aligned} u^s &= \frac{(E_{waves}+2E_{roller})\cos\theta}{C\rho h} \\ v^s &= \frac{(E_{waves}+2E_{roller})\sin\theta}{C\rho h} \end{aligned} \tag{A.7}$$

The resulting GLM-shallow water equations are given by:

$$\frac{\partial u^L}{\partial t}+u^L\frac{\partial u^L}{\partial x}+v^L\frac{\partial u^L}{\partial y}-fv^L-v_h\left(\frac{\partial^2 u^L}{\partial x^2}+\frac{\partial^2 u^L}{\partial y^2}\right)=\frac{\tau_{sx}}{\rho h}-\frac{\tau^E_{bx}}{\rho h}-g\frac{\partial z_s}{\partial x}+\frac{F_x}{\rho h} \tag{A.8}$$

$$\frac{\partial v^L}{\partial t}+v^L\frac{\partial v^L}{\partial y}+u^L\frac{\partial v^L}{\partial x}-fu^L-v_h\left(\frac{\partial^2 v^L}{\partial x^2}+\frac{\partial^2 v^L}{\partial y^2}\right)=\frac{\tau_{sy}}{\rho h}-\frac{\tau^E_{by}}{\rho h}-g\frac{\partial z_s}{\partial y}+\frac{F_y}{\rho h} \tag{A.9}$$

$$\frac{\partial z_s}{\partial t}=-\frac{\partial u^L h}{\partial x}-\frac{\partial v^L h}{\partial y} \tag{A.10}$$

In these equations u^L and v^L are Lagrangian velocities, u^E and v^E are Eulerian velocities and u^s and v^s are used for the Stokes drift. In the GLM-shallow water equation f is used for Coriolis and v is a viscosity term. At the other side of the equal sign τ_{sx} and τ_{sy} are wind shear stresses, τ_{bx} and τ_{by} are bed shear stresses, z_s is the water level and F_x and F_y are wave forces which are the result of the gradients in radiation stress.

A.3.2 Morphodynamics

Advection-diffusion scheme In XBeach sediment transport is modeled with the use of a depth-averaged advection diffusion equation (Galappatti, 1983).

$$\begin{aligned}&\frac{\partial hC}{\partial t}+\frac{\partial hC(u^E+u_A\sin\theta_m)}{\partial x}+\frac{\partial hC(v^E+u_A\cos\theta_m)}{\partial y}\\&+\frac{\partial}{\partial x}\left(D_s h\frac{\partial C}{\partial x}\right)+\frac{\partial}{\partial y}\left(D_s h\frac{\partial C}{\partial y}\right)=\frac{hC_{eq}-hC}{T_s}\end{aligned} \tag{A.11}$$

In this equation C represents the depth-averaged sediment concentration which varies on the wave group time scale, D_s is the sediment diffusion coefficient. The change of sediment concentration occurs gradually and for this use an adaptation time T_s is applied. This time is a function of the local water depth, h, and the sediment fall velocity w_s.

The entertainment or deposition of sediment is determined by the mismatch between the actual sediment concentration C and the equilibrium concentration C_{eq} . The equilibrium sediment concentration can be calculated with the use of various formulations, but by default the extended transport formulation of Van Rijn (2007) is used.

$$C_{eq}=\frac{A_{sb}}{h}\left(\sqrt{(u^E)^2+0.64u_{rms,2}^2}-u_{cr}\right)^{1.5}+\frac{A_{ss}}{h}\left(\sqrt{(u^E)^2+0.64u_{rms,2}^2}-u_{cr}\right)^{2.4} \tag{A.12}$$

In this equation A_{sb} and A_{ss} stands for the bed load and the suspended load coefficient. Sediment is stirred up by the Eulerian flow velocity and the orbital velocity (u_{rms}). The effect of turbulence due to wave breaking (k_b) is included with the use of an increased orbital velocity formulation (Reniers, 2004):

$$u_{rms,2}=\sqrt{u_{rms}^2+1.45k_b} \tag{A.13}$$

The mean flow as a result of non-linearity (u_A) is both used in the advection-diffusion formulation as well as in the sediment transport formulation. This term is calculated separately in order to include effects of wave asymmetry in which S_k stands for the skewness and A_s for the asymmetry. The reason for this approach is the fact the high frequency wave information on an individual scale is lost as a result of the surf beat approach. The values of S_k and A_s are a function of the Ursell number as formulated by Ruessink et al. (2012). With the γ_{ua} the importance of the asymmetric velocity can be changed. By default the keyword γ_{ua} has a value of 0.1 ($facua$).

$$u_A=\gamma_{ua}u_{rms}(S_k-A_s) \tag{A.14}$$

Bed level change Bed level changes are a result of gradients in sediment transport as formulated in the following equation:

$$\frac{\partial z_b}{\partial t}=-\frac{f_{mor}}{(1-\rho)}\left(\frac{\partial S_x}{\partial x}+\frac{\partial S_y}{\partial y}\right) \tag{A.15}$$

In this equation ρ stands for porosity, f_{mor} is the morphological acceleration factor (morfac) for bed level changes and S_x and S_y are the computed sediment transport rates in x- and y-direction. Sediment transport rates are calculated as follows:

$$\begin{aligned} S_x &= hC(u^E + u_A \sin\theta) + \frac{\partial}{\partial x}\left(D_s h \frac{\partial C}{\partial x}\right) \\ S_y &= hC(v^E + u_A \cos\theta) + \frac{\partial}{\partial y}\left(D_s h \frac{\partial C}{\partial y}\right) \end{aligned} \tag{A.16}$$

In order to simulate dune slumping during storms and to let sediment move from a dry regime to a wet, avalanching is introduced in XBeach in order to update the bed evolution with an additional term. This works by introducing a critical bed slope m_{cr}, both for dry and wet slopes. Bed level change is then calculated by:

$$\begin{aligned} \Delta z_b &= \left(\left[\frac{\partial z_b}{\partial x}\right] - m_{cr}\right)\Delta x \text{ for } \frac{\partial z_b}{\partial x} > 0 \\ \Delta z_b &= -\left(\left[\frac{\partial z_b}{\partial x}\right] - m_{cr}\right)\Delta x \text{ for } \frac{\partial z_b}{\partial x} < 0 \end{aligned} \tag{A.17}$$

A.4 Comparison with Delft3D

Delft3D (Lesser et al., 2004; Deltares, 2011a) is a multi-dimensional (2DH or 3D) hydrodynamic and morphological model which has been developed to describe a large number of phenomena. Delft3D includes a FLOW-module and a WAVE-module (SWAN, stationary) which communicates every communication time step. The main advantage of XBeach over Delft3D is related to the following two aspects:

1. Long wave propagation: in Delft3D the bound long wave is only calculated at the boundary, it is not possible to compute the generation of the bound long wave as a result of wave group motions. In XBeach this is possible due to the formulation of Van Dongeren (2003).
2. The momentum-conserving staggered scheme of Stelling and Duinmeijer (2003) is used to describe to propagation of *shock* waves on the beach. This makes it possible to describe dry-wet interactions. In addition, the avalanching algorithm makes it possible for material from higher ground to avalanche downwards. These features are of importance for dune erosion and overwash, but cannot accurately be described by Delft3D.

Downside of XBeach related to Delft3D are:

1. Depth-averaging (2DH): complex motions such as spiral flow are not taken into account. However, De Vet (2014) concluded that depth-averaging is not a limitation when describing overwash and breaching. A 3D approach has advantages for wind driven flow, vertical turbulence mixing and vertical acceleration.

A.5 Model settings

A.5.1 Introduction

The XBeach simulations are carried with a Linux build XBeach version of February 2014, version 1.21.3657, code name 'Groundhog Day'. The model has a lot a freedom for the input parameters in XBeach. In general the 'default' settings are used. Some settings are explained below. This includes various settings related to interaction with hard elements, wave asymmetry and skewness, bottom friction, the avalanching algorithm and the depth scale.

A.5.2 Interaction by hard structures

XBeach underestimates the scour hole in front of hard structures. In order to reproduce this morphological response in a better way the $jetfac$ option can be activated in order to mimic the turbulence production near revetments (Deltares, 2013). The limited amount of turbulence created, is related to processes like wave reflection and wave run-down which are explicitly described in the source code (Van Thiel de Vries, 2009a). The $jetfac$ is parametric relation in which a value of 0.1 can be seen as recommended. The meaning of this keyword is that part of the short wave energy is used for the production of turbulence.

On top of that, short wave run-up is assumed to be an important parameter in order to describe the longshore effect of hard elements, as stated by Van Geer et al. (2012). By default XBeach only calculates the long wave run-up. In XBeach, the short wave run-up can be included with the keyword $swrunup$. Besides applying this parametric relation (=1) also a calibration factor for short wave run-up, $facrun$, needs to be applied. The recommanded value is 0.8. The general reasoning is that the long wave run-up is extended with a certain part short wave run-up based on the equation below:

$$R = \gamma_{runup} H_{rms} \cos(\theta) \min(\zeta, 2.3) \tag{A.18}$$

A.5.3 Wave asymmetry

When waves propagate to the nearshore, their shapes gradually change due to the combination of wave shoaling, breaking and nonlinear interactions. As incident waves shoal they become positively skewed with a peak, narrow crest and a flat wide trough. The strongest velocities are therefore directed onshore. Maximum values of flow velocity skewness have been reported in the breaker zone, which is linked to sediment supply (Roelvink and Stive, 1989).

Wave skewness means waves will get long and flat troughs, but narrow and peaked crests (asymmetry in the vertical). Wave asymmetry are pitched forward shaped waves, which eventually will break (asymmetry in the horizontal). However, in XBeach individual waves are not described as a result of phase-averaging of high frequency waves. Therefore, the asymmetric velocities as a result of skewness and wave asymmetry cannot be calculated directly.

As can be seen in Equation A.13, the parameter $facua$ is used to describe the importance of the onshore directed asymmetric flow. Besides this parametric term also the u_{rms}, S_k and A_s contribute to the asymmetric velocity. By default the value for $facua$ is 0.1, but in literature also higher values of for example 0.3 have been found (Van Rooijen, 2011). The reason that higher values can be

applied, is that XBeach is designed for erosive processes and the processes related to accretion are only limited represented in the source code. By increasing the $facua$ the erosive processes will be (partly) counteracted with an asymmetric onshore sediment transport. One hypothesis is that on steep beaches wave asymmetry becomes more important. For example for intermediate-to-reflective beaches Vousdoukas et al. (2012) needed calibration of the $facua$ in order to achieve positive skill scores.

The model is calibrated by varying the $facua$ between 0.0 and 0.4. Analysis in Section 4.4.4 have shown that a $facua$ of 0.25 result in an accurate morphological result for the case study of Hurricane Sandy on the beaches of New Jersey.

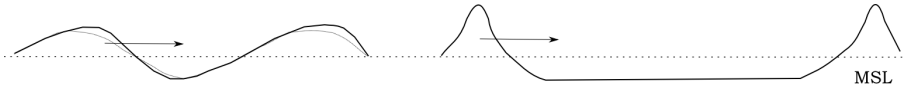

Figure A.4 *Definition sketch of wave asymmetry (left) and skewness (right).*

A.5.4 Bottom friction / roughness

Implementation in XBeach In XBeach it is possible to calculate the bed friction with the dimensionless friction coefficient (c_f) or by the Chezy coefficient (C). By default the c_f coefficient has a value of 0.003, which represents a Chezy value of 57 $m^{0.5}.s^{-1}$. In coastal application friction factors are used for the bed stability and the sediment transport via the formulation of the bed shear stress (τ_b), as can be seen in Equation A.8.

$$\tau_{bx} = c_f \cdot \rho \cdot u^E \sqrt{2 \cdot [1.16 u_{rms} + u^L]} \tag{A.19}$$

Different empirical formulations The version of XBeach used in this thesis, Groundhog Day, has the implementation of the Chezy and the dimensionless friction coefficient. In other process-based models also other formulations are used. For example in Anglo-Saxon countries there is more experience with the Manning coefficient. An implementation of Manning is in XBeach, as demonstrated by De Vet (2014). However, in the Netherlands there is more experience with the application of Chezy (Van Velzen et al., 2003). The Manning equation has, on the other hand, a more sound theoretical derivation and there is more experience in applications with Manning than Chezy (Huthoff and Augustijn, 2004).

For hydraulic rough flow its known (Van Rijn, 1990):

$$\begin{aligned} C &= 18 \log\left(\frac{12R}{k_s}\right) \\ k_s &\approx 3 \cdot D_{90} \end{aligned} \tag{A.20}$$

For the estimation of the Manning coefficient (n) in terms of k_s and D_{50} the following formulas can be used according to Marriott and Jayaratne (2010):

$$\begin{aligned} C &= \frac{R^{\frac{1}{6}}}{n} \\ n &\approx 0.04 \cdot D^{\frac{1}{6}} \end{aligned} \tag{A.21}$$

In these equations the R represents the hydraulic radius which is equivalent to the water depth for coastal applications. The k_s value is the Nikuradase sand roughness.

Application in for XBeach For the default settings a Chezy value of 55 $m^{0.5}.s^{-1}$ is applied. This is based on a depth (h_{min}) of 0.1 m and a k_s of 0.001 m. The Nikuradase sand roughness can be calculated with the help of Equation A.20

For a situation with hydraulic rough flow on top of a barrier island the k_s needs to be higher than the default value. This higher sand roughness represents friction due to the presence of structure and/or vegegation. In fact the friction can be used as a sump for all kind of different contributions that will have an impact on the flow. The Chezy value on floodplains vary between Chezy values of 10-40 $m^{0.5}.s^{-1}$ (Van Velzen et al., 2003). This can be converted to a Manning value of 0.02 up to 0.1 [-] (Jarrett, 1985). A Nikuradase sand roughness of 0.5 m in a water depth of 1 m results in a Chezy value of 25 $m^{0.5}.s^{-1}$ or a value for Manning of 0.04.

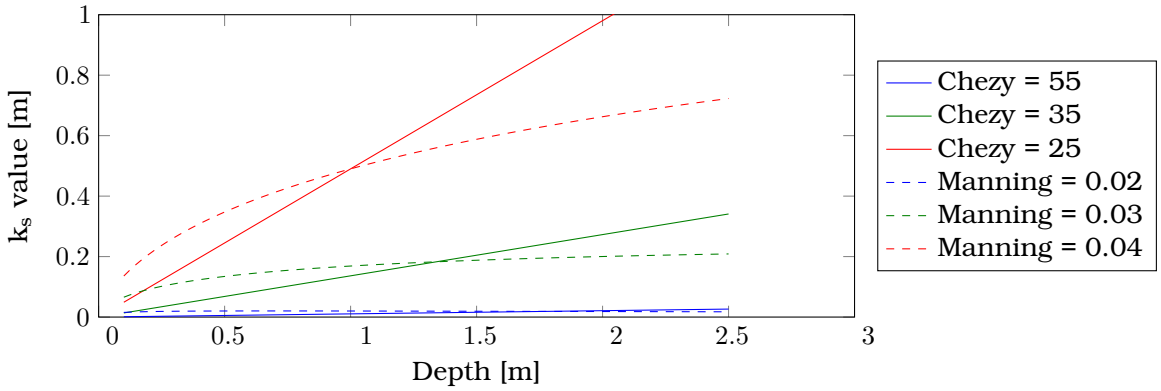

Figure A.5 *Meaning of various Chezy and Manning values in terms of k_s*

A.5.5 Avalanching algorithm

The avalanching algorithm is a relative simple tool in dune erosion models to describe the process of dune face erosion during storm conditions. The general idea is that a sandy slope will avalanche when a certain critical bed slope is exceeded. The algorithm contains a critical wet slope ($m_{cr,wet}$) and a dry slope ($m_{cr,dry}$)

$$\left|\frac{\partial z_b}{\partial x}\right| > m_{cr} \text{ or } \left|\frac{\partial z_b}{\partial y}\right| > m_{cr} \tag{A.22}$$

By default the critical dry and wet slopes are set to 1 and 0.3. Once the algorithm is triggered, sediment is exchanged between the adjacent cells to bring the slope back to the critical slope. The transition of the critical wet slope to the critical dry area takes place at the specified water depth (h_{min}). Also a maximum dune face erosion rate is specified (dz_{max}) to overcome instabilities.

Van Thiel de Vries (2009b) conducted Delta Flume experiments in order to propose specific user-defined values in the avalanching algorithm (like h_{min}). For reasons unknown some of the values in the avalanching algorithm are currently not the default setting values in XBeach. In Table A.1 the value of both Van Thiel de Vries and XBeach default are compared:

Table A.1 *XBeach settings related to the avalanching algorithm.*

	XBeach: default	Van Thiel de Vries	Value
$m_{cr,wet}$	0.3	0.1	>
$m_{cr,dry}$	1.0	1.0	=
dz_{max}	0.05	0.003	>
h_{switch}	0.1	0.1	=

There is a discrepancy between the maximum wet slope and for the maximum dune face erosion rate per time step. The higher default value for the wet slope will result in less erosion, but has a more clear physical background. The difference for the value of dz_{max} is most likely related to scaling. One hypothesis is that during the past years one forgot the scaling relation of dz_{max} and one had the idea to work with default values(Delta Flume scale), but instead they were working with prototype scale (6 times as large), since $0.003 \cdot 6^{1.5} \approx 0.05$.

A.5.6 Depth scale

XBeach aims to be applicable in a wide range of applications from laboratory scale up to super storm scale. With the introduction of the depth scale parameter (Brandenburg, 2010) the user can steer on its application. The general idea is that several parameters are not universal but need to be scaled with the scale of the experiment. XBeach is mainly validated on Delta Flume experiments were a scale of 1/6 is used. On this scale the dunes have a height of 6 m above MSL. When calculating a Dutch prototype scale the user should apply a depth scale of 1/6.

1. The eps parameter determines if a cell is wet or dry. The default value is 0.005 m. When applying a depth scale of 1/6 the value will be 0.03 m. In the case study the eps will be set on 0.05 m to overcome instabilities in XBeach. The exact reasoning for these instabilities are not known, but the instabilities are related to the combination of hard elements and water levels. For collision cases the default value is used.
2. The other depth scale related parameters are applied default. This means for h_{min} a value of 0.2, $m_{cr,wet}$ of 0.3 (which is not scaled with the depth scale in newer versions of XBeach) and a h_{switch} of 0.1. The parameters h_{min} and h_{switch} change linear with the depth scale and an increase in scale means a decrease in parameter value.
3. The maximum erosion rate as a result of avalanching (dz_{max}) has an incorrect default value according to Van Thiel de Vries (2009b) and Brandenburg (2010) . The default value of dz_{max} in XBeach is 0.05 $m^3 \cdot ms^{-1}$, but should be 0.003 (which can scaled to 0.0441 for Dutch prototype scale). More information about this parameter and the avalanching algorithm can be found in Appendix G.4.

A.5.7 Additional explanations

The most important parameters are explained above. In general the 'default' settings are used. Some additional settings are explained below.

1. A schematic time-varying JONSWAP spectrum is used in order to simulate the incoming waves in a realistic way. Therefore, the instat=41 is used. A JONSWAP spectrum is used in order to reproduce the most realistic spectrum.

2. In the conceptual model a fully normal-incident wave attack is used. Therefore, the following setting is used: s = 10.000. This option is used to exclude the effect of directional spreading of waves. In addition the randomiser of the wave boundary is set on 0 during the conceptual study. For the case study randomness of the waves are included and a spectrum will used in which the directional spreading is taken into account.
3. A maximum Courant number (CFL-condition) of 0.7 is used. This is equivalent as the default setting in XBeach and can be seen as a good trade-off between limitation of numerical dissipation and relative fast computational time. An increase in CFL condition means an increase in numerical dissipation (McCall, 2008).
4. A morfac of 1 is used in the conceptual study in order to accurate and physically correct reproduce the morphological response of the system. This is equivalent as the default setting in XBeach. For the case study a morfac of 10 is used.

Appendix B

Evaluation method

Introduction In order to evaluate the outcome of hydrodynamic and morphodynamic models an objective evaluation method is needed. According to Sutherland et al. (2004) a performance can be assessed by calculating the bias, accuracy and skill. In the following paragraphs all the different equations used in this thesis are presented.

Bias and Relative bias The bias is the difference in central tendencies of the computed values (X) and the observations (Y) . Both the bias and the relative bias are used and can be computed with equation below. Bias and relative bias are used for both hydrodynamic and morphological models in order to analyze the systematic error. A positive bias means that the water or bed level is higher in the computed data set than the measurements. The bias can be concluded with:

$$Bias = \frac{1}{N}\sum_{i=1}^{N}(Y_i - X_i) \tag{B.1}$$

Accuracy: Root-mean-square-error (RMSE) Accuracy can be seen as the average size of the difference between a set of computed values (X) and the observations (Y). A common used measure for accuracy is the RMSE which can be calculated with the equation below. Accuracy is mainly used for water levels. The RMSE can be concluded with:

$$RMSE = \sqrt{\frac{1}{N}\sum_{i=1}^{N}(Y_i - X_i)^2} \tag{B.2}$$

Skill: Brier Skill Score The Brier Skill Score (BSS) is used to qualify the accuracy of morphological models. A skill score provides an objective method for assessing the performance of morphological models. The classification used, is from Van Rijn (2003) in which a score of 0.8-1.0 is excellent, 0.6-0.8 is good, 0.3 - 0.6 is reasonable, 0-0.3 is poor and below 0 is bad. The BSS can be concluded with:

$$BSS = 1 - \frac{\left\langle (z_{b,c} - z_{b,m})^2 \right\rangle}{\left\langle (z_{b,o} - z_{b,m})^2 \right\rangle} \tag{B.3}$$

Appendix C

Supportive material for conceptual study simulations

C.1 Overview: simulations carried out

The conceptual study has proven to be a successful tool in order to have a sound understanding of all the processes involved before modeling the case study of Hurricane Sandy. The conceptual study contained 2 set-ups: for the collision regime (based on (Deltares and Arcadis, 2013)) and the overwash regime (based on the case study of this thesis). For the conceptual study the following simulations have been carried out.

Table C.1 *Description of all the simulations carried out for the conceptual study for both the collision and the overwash regime in this thesis.*

Regime	Type	Approach	# simulations	Description
Collision	Baseline	1D	2	Focus: cross-shore effect
	Scour analysis	1D	2	Impact of variation in SSL
	Baseline	2DH	5	Focus: longshore effect
	Wave obliquity	2DH	16	Analysis: cause and impact
	Boundary conditions	2DH	56	Sensitivity - 1
	Object size	2DH	42	Sensitivity - 2
	Settings	2DH	8	Sensitivity - 3
Overwash	Baseline	1D	4	Collision versus overwash
	Scour analysis	1D	4	Impact of variation in SSL
	Baseline	2DH	4	Focus: longshore effect

C.2 Collision situation

C.2.1 Calculation of the retreat line, increased set-back and influence length

Retreat line There are multiple methods in order to calculate the retreat line (R) or the retreat distance (ΔR). The approach applied in this thesis contains 3 steps.

1. Find the highest point in a cross-section.

2. Find the first point from seaward direction of this level minus 0.25 m. (This step is needed for robustness of the algorithm.)
3. Place the x and y coordinates of this point in the memory of Matlab. All the x-coordinate together are the retreat line. The retreat distance is a method to exclude the influence of a reference frame.

Increased set-back / additional erosion adjacent locations In this thesis the terms increased set-back (d_2) or additional erosion in adjacent locations (A_2) are applied to quantify the longshore effect of hard structures. The method applied is based on the difference in retreat line between the hard and the soft profiles. An algorithm finds the maximum difference between the two profiles in the expected area (often an influence length of 200 m). For the additional erosion a similar approach has been applied.

Influence length The influence length (l_2) is determined by subtracting the total impact (erosion and accretion) of both the reference simulation without a structure (A configuration) as well as the simulation with a structure (B or C). When the total impact is larger than 5 $m^3 \cdot m^{-1}$, the cross-section is noticed as *effected*. The total effected area is the influence length.

C.2.2 Baseline 1D: causes of the impact

General In this subsection the causes for the impact in the conceptual study for the collision regime in 1D are analyzed. This will be done by identifying the patterns in waves, flow, sediment concentration and sediment transport.

Waves In Figure 3.5 the development of the time-averaged root-mean-square wave height (H_{rms}) of short and long waves is displayed for both the soft as well as the hard barrier. The difference in short and long waves is made, since long waves dominate the water motions in very shallow water (Van Thiel de Vries, 2009b), but short waves are important in describing the undertow and stirring up of sediment.

During the storm the breaker point moves in seaward direction and short waves start to break further offshore. This is related to the sediment which is deposited in the nearshore. Throughout the storm the height of short waves that do reach the dunes decreases with a $H_{RMS,HF}$ of 0.32 m (-13%). The height of long waves increases due to shoaling. As the storm continues the importance of long waves increases. On top of that, as a result of dune retreat, higher wave conditions can be found closer to the hinterland.

Two important aspects can be distinguished when comparing the differences between the soft and the hard response. First of all short waves remain high near the hard structure throughout the storm, since there is less deposition of sediment in the nearshore. This results in higher energetic conditions in front of the hard structure (H_{RMS}:+0.26 m). Higher turbulence intensities will result in the development of a scour hole. Second, the relative importance of the long wave will stay constant.

Flow In Figure C.1 the time-averaged Eulerian velocity for every hour is displayed for both the soft and for the hard barrier. The development of the Eulerian velocity is important since the undertow-driven transport is responsible for most of the offshore sediment transport.

The simulated time-averaged Eulerian velocity decreases as the storm continues with -31% (-0.27 $m.s^{-1}$). The major reason for this effect is the decrease in mass flux which is related to the increase in dissipation due to sediment deposition. Velocities as a result of wave asymmetry and long waves hardly vary as the storm progresses.

The decrease in Eulerian velocity is larger for the hard barrier than for soft barrier. The major reason for this effect is the decrease in the return current driven by larger water depths. The maximum Eulerian velocity at the hard barrier is 12% lower than for the soft barrier.

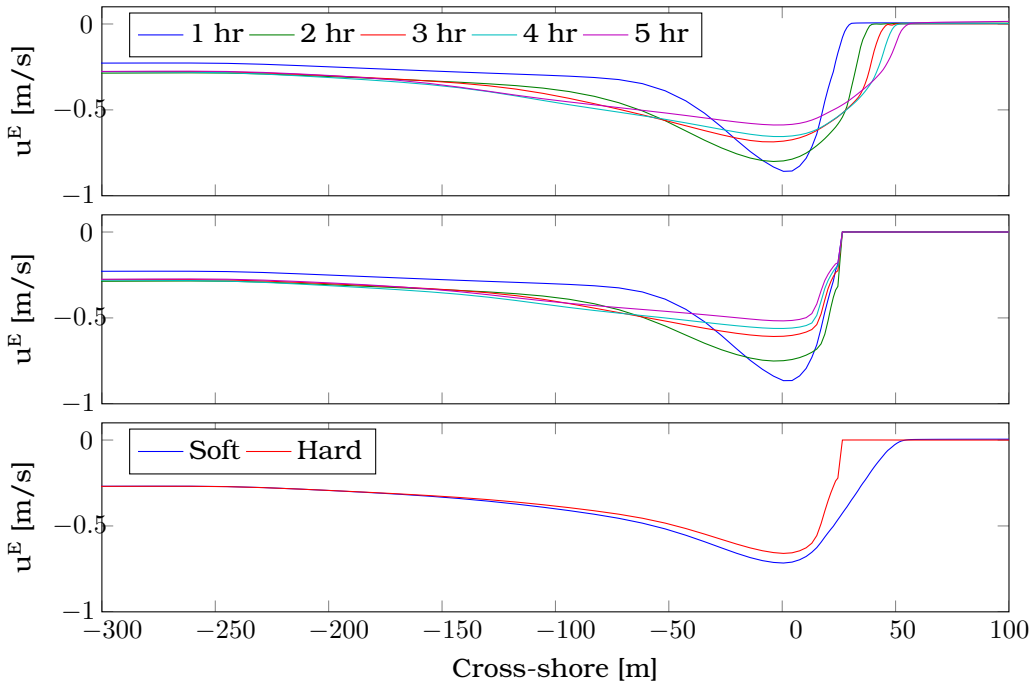

Figure C.1 *Development of the Eulerian velocities for both the soft barrier (upper panel) and the hard barrier (middle panel) plus a comparison between storm-averaged velocities (lower panel).*

Sediment concentration In Figure C.2 the storm-averaged sediment concentrations and turbulence intensities due to wave breaking are displayed for both the soft as well as the hard barrier. This can be argued with the relation between turbulence-induced stirring up of sediment and sediment concentration.

During the storm more wave energy is dissipated in the nearshore. The reason behind this dissipation is sediment deposition caused by a sediment rich coastline. This result in a decrease in depth and in more dissipation of short waves. The dissipation of wave energy occurs in a broader area nearshore and therefore the sediment concentrations decrease with 28% (-0.035 $m^3.m^{-3}$).

The hard element cuts off the supply of sediment and thus part of the sediment deposition in the nearshore cannot take place. This results in higher energetic conditions in front of the structure which will result in higher turbulence intensities. In reality the turbulence intensities increase even more as a result of the combination of wave reflection and wave run-down. In XBeach these processes are taken into account via the parametric term $jetfac$. This means that a fraction of the short wave energy will be used for mimicking this extra turbulence near the toe of the structure. More background information of this parametric relation can be found in Appendix A.5. The result of activating the $jetfac$ can be seen in the peak in Figure C.2 (peak in red). Still the maximum sediment

concentration for hard cross-sections is 31% lower than that of soft barriers. The turbulence intensities are, however, 20 times higher.

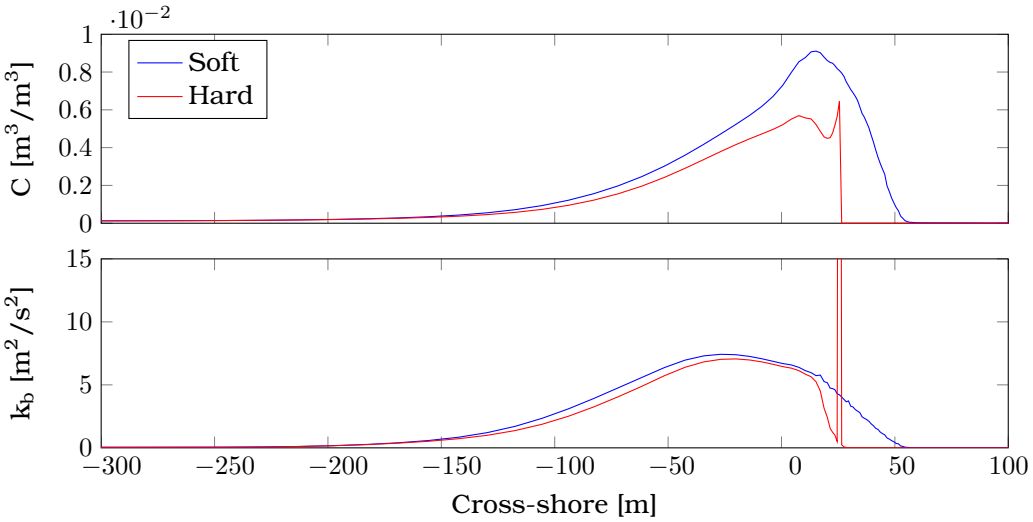

Figure C.2 *Development of the sediment concentrations (upper panel) and turbulence intensities (lower panel) for the complete soft barrier (blue) and hard (red).*

Sediment transport Sediment transport can be separated in transport associated with short wave and roller-driven undertow (S_R), long waves (S_L) and with velocities generated by nonlinear waves (S_W). The reproduction of these three components follows the approach of Roelvink and Stive (1989). In XBeach also change in the sediment diffusion coefficient can result in sediment transport, as can be seen in Appendix A, however this part is not taken into account in this analysis.

$$\begin{aligned} S_W &= \overline{u_A C h} \\ S_L &= \overline{u^L C h} \\ S_R &= \overline{(u^E - u^L) C h} \end{aligned} \tag{C.1}$$

In these equations u_A is used for the velocity as a result of wave asymmetry and skewness, u^L stands for the Lagrangian velocity, and u^E is used for Eulerian velocity. C is used for concentration and h for the water depth. In Figure C.3 the storm-averaged sediment transport components for both the soft barrier and hard can be found.

During the storm the maximum sediment transport decreases and the sediment transport reaches further offshore. The direction of the transport is negative, which means it is offshore directed. The total offshore directed flow is mainly driven by the undertow, but also some transport is associated with bound long waves. The wave asymmetry and the released long wave compensates some of this offshore direct sediment transport.

For soft situations the undertow driven return current has the most important contribution to the amount and the shape of the total sediment transport. The long wave has hardly a net effect and the wave asymmetric flow has a net transport in the order of 0.004 $m^2.s^{-1}$ and compensates thus part of the undertow.

For the situation with a hard element the other transport components are getting, percentage-wise, more important. The total of storm-averaged sediment transport is less and also distributions in the

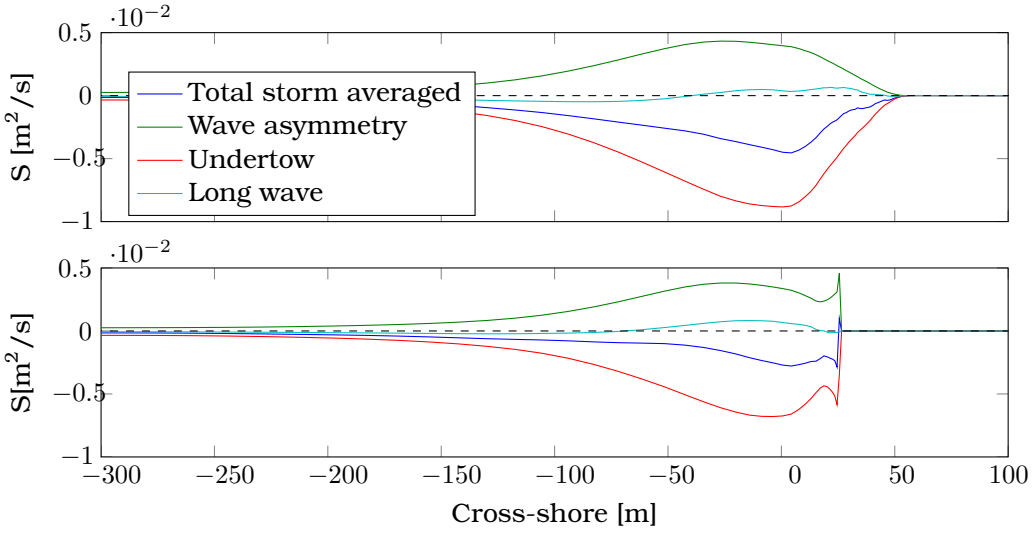

Figure C.3 *Development of the complete storm averaged simulated sediment transport separated into 3 main hydrodynamic components for both the complete soft barrier (upper panel) and the hard barrier (lower panel).*

cross-shore are different.

The total transport has a peaked distribution when looking in cross-shore direction. This is the result of a peak in all the velocities components in the scour hole. In total a net onshore transport in the scour hole can be distinguished. After the scour an increase in undertow is responsible for the peak in total offshore sediment transport. This is the result of both higher concentrations due to wave breaking and the $jetfac$. The maximum total transport is however 36% lower compared to soft barriers.

C.2.3 Baseline 2DH: causes of the impact

General In this subsection the causes for the impact in the conceptual study for the collision regime in 2DH are analyzed. This will be done by identifying the patterns in waves, flow, sediment concentration and sediment transport.

Waves In front of the hard element the nearshore rises less than in front of the soft cross-section since the cut off of sediment supply as a result of the presence of the structure. This means that in front of the hard element waves are dissipated less, which will result in higher short wave heights at the toe of the structure. Therefore, in the last hour the mean simulated short waves increases with +0.38 m (+30%).

This will have the following three effects:

1. An scour hole is formed in front of the hard structure due to the higher energetic conditions at the toe. The depth of the scour hole is with the use of the default settings in XBeach underestimated. (Van Thiel de Vries, 2009a), but with the use of several parameters the higher turbulence near the toe can be mimicked. A scour hole is a typical cross-shore effect of hard elements. In this study a scour of 4.65 m developed. This is somewhat deeper than the 1D simulation generated by the spiral movement (as will be described in the following paragraph).

2. Due to bed level differences between the hard and the soft cross-section, waves will break later in front of the structure. The result is lower water levels in front of the hard structure compared to the soft cross-section. This water level gradient is in the order of 0.1-0.2 m.
3. At soft side of the transition locally higher waves arrive. This can be decomposed in mainly higher short waves (+0.22 m, +19%) and higher long waves (+0.17 m, +6%) and has the following two reasons:
   (a) Sediment is taken from the soft cross-section and placed in front of the hard structure. This results that waves in the soft cross-section will be dissipated less.
   (b) Part of the higher waves in the hard cross-section will diffract around the element and hit the soft side of transition.

Flow The water motions of interest can be divided into: Eulerian, nonlinear (due to asymmetry and skewness) and orbital velocities. First the Eulerian velocities will be discussed.

In the normal soft situation the Eulerian velocity has only an offshore component and a maximum mean of about 0.57 $m.s^{-1}$ averaged over the last simulation hour. In the situation with a structure the velocities increases, at some points even doubling. Two interesting effects can be distinguished. First of all, the general increase of velocities at the soft side of the transition. Second, an increase in longshore velocity just at the hard side of the transition.

There are three reasons for these increasing velocities:

1. Increase of the velocities with +0.48 $m.s^{-1}$ (+95%) at the soft side of the transition. This occurs mainly just at the side of the structure:
   (a) The difference in wave breaking causes a set-up difference, creating a water level gradient from the dune towards the structure. The mean difference is in the order of 0.10 - 0.20 m and drives an alongshore increase in velocity. The increase is 0.03 $m.s^{-1}$ and is active in a broad area (large area cross-shore). The morphological effect is less accretion at the soft side.
   (b) The return current increases since the mass flux above wave trough level increase. This is related to the increase in wave height. The result is an increase of the cross-shore component of the Eulerian velocity. The increase is 0.44 $m.s^{-1}$ (+87%). The morphological effect is more erosion at the soft transition. This increase is mainly active at the side of the structure.
2. Increase of the velocities at the hard side of the transition. This is related to waves hitting the element which results in relatively high water levels compared to the soft cross-section. The effect is a velocity from the hard structure towards the dune. The signal is peaked and has large maximum values, therefore a mean signal direct away from the structure can be measured. The increase is 0.64 $m.s^{-1}$ and is active in a small area. The morphological effect is more erosion in the scour hole. This can be noticed in the bed level pattern of Figure 3.8.

The mean flow due to asymmetry and skewness is both used in the advection-diffusion equation as well as in the sediment transport formulation. The orbital velocities are used to calculate the equilibrium sediment concentration. Both velocities differ little when comparing the normal sandy response (A-configuration) with configurations like B1 or C1. At the soft sides of the transition a small increase of both is visible, which is a result of the increase in wave energy.

Sediment concentrations Sediment concentrations are closely related to sediment supply and turbulence by depth-induced breaking. Just in front of the hard element a peak in turbulence is measured. This is partly the result of the parametric relation $jetfac$, which mimics the turbulence generated by effects like wave reflection and waves run-down. In addition, sediment supply is lacking due to the presence of the structure. In a 2DH XBeach model the sediment concentrations varied in the alongshore. An increase in concentration at the soft side of the transition is distinguished. This is the combined effect of turbulence generated at the hard structure and due to the presence of locally higher short waves. This increase is 0.0018 $m^3.m^{-3}$ (+25%).

Sediment transport Sediment transport is the result of the combination of sediment concentration and velocity. In a complete sandy situation there is only cross-shore sediment transport and no longshore component is present. When comparing this response with the situation with a hard element in the barrier the transport rates are in the first 2 hours more or less similar. After this period the decrease of sediment transport per period of time more or less stops. When looking in more detail, one can distinguish two important areas where an increase in sediment transport occurs.

1. When comparing the simulation with and without a structure, the maximum cross-shore sediment transport, averaged for the last simulation hour, increases with 0.0051 $m^2.s^{-1}$ (offshore directed). This increase occurs since locally short wave heights and thus undertow velocity increase.
2. A longshore sediment transport component is developed. The longshore sediment transport has circular moment and two main components can be distinguished:
   (a) Component towards the hard structure. This mean sediment transport, 0.00084 $m^2.s^{-1}$, is related to the difference in wave breaking and thus set-up. This transport component is active in the area 50 - 250 m from the hard structure .
   (b) Component from the hard structure. This maximum peak sediment transport, 0.02640 $m^2.s^{-1}$, is related to the high water levels that occur when the higher energetic conditions hit the structure. This transport component is active in the area 0 - 50 m from the hard element.
   (c) Component both towards as well as from structure. This mean sediment transport, 0.00157 $m^2.s^{-1}$, is related to wave diffraction and is active at the sides of the structure.

Overall at the tip of the structure there is a mean cross-shore component of 0.0119 $m^2.s^{-1}$ and a mean longshore component of 0.0061 $m^2.s^{-1}$. It is therefore fair to say that that 2/3 of the transport is cross-shore-related and 1/3 is longshore-related. Presenting this ratio and coupling it direct with sedimentation and erosion patterns is an oversimplification. The full complexity is presented in Figure C.5.

Gradients in sediment transport are responsible for bed level change. An negative gradient in sediment transport will result in deposition and a positive gradient in erosion. For the complete sandy situation there is only a cross-shore gradient in sediment transport. For the situation with a hard element, sediment transport increases both due to an alongshore sediment transport (driven by a water level gradient) as well as an increase in cross-shore transport (driven by higher waves). Material is transported from the barrier and both deposited in the nearshore of the soft cross-section and at the tip of the transition at the side of the hard structure.

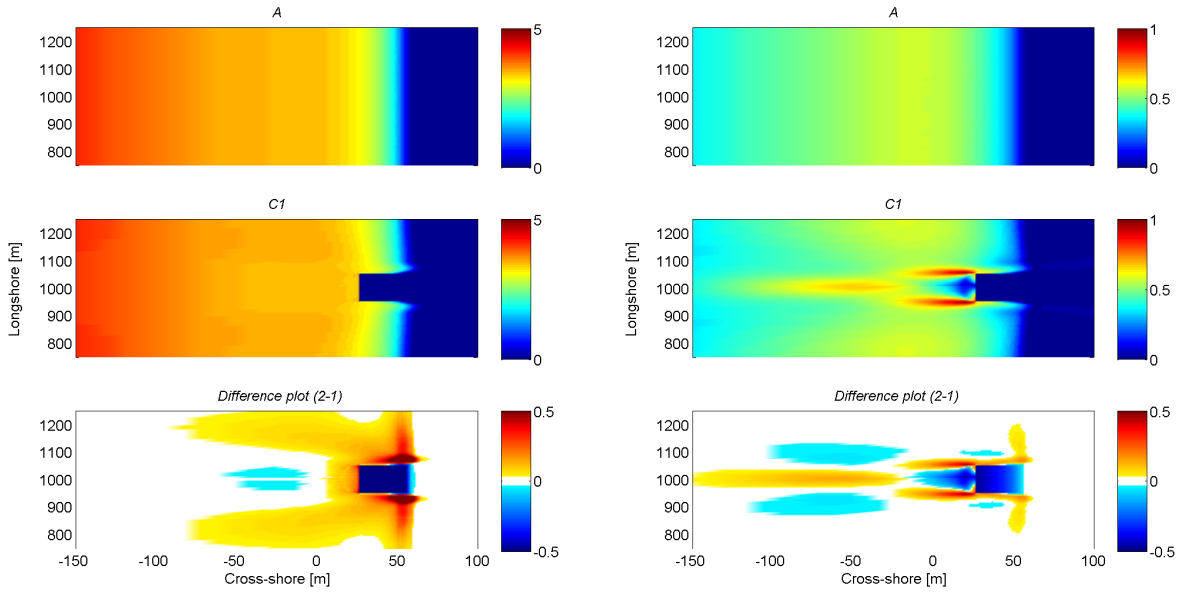

(a) *Short + long wave height* **(b)** *Eulerian velocity*

Figure C.4 *Short + long root-mean-square wave heights in meters and Eulerian velocity in* $m.s^{-1}$ *time-averaged for the last simulation hour.*

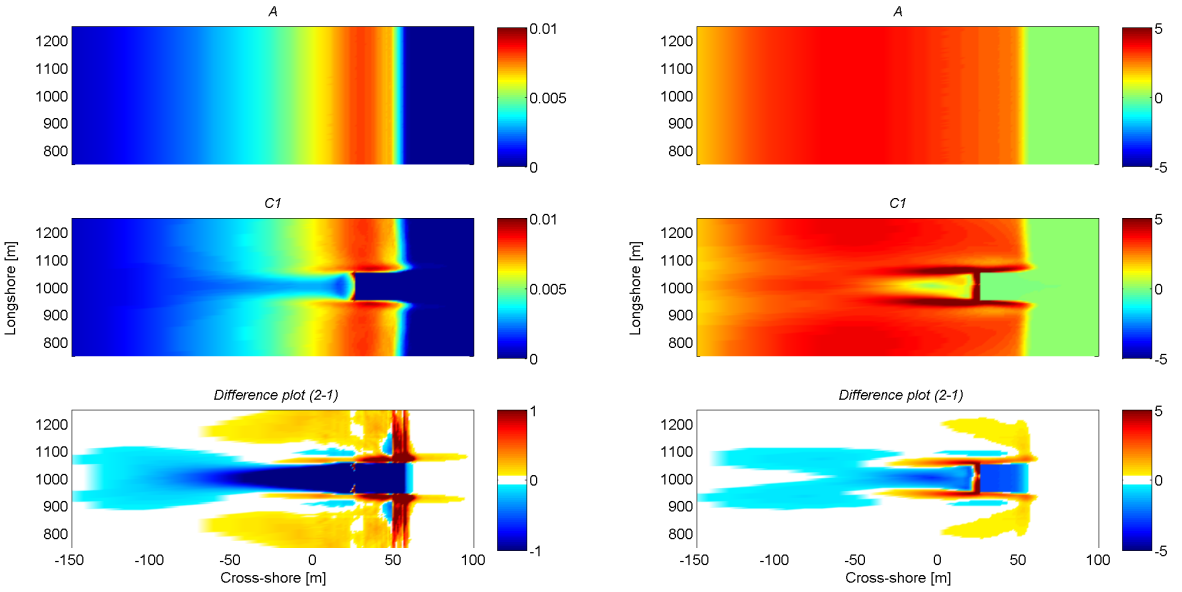

(a) *Concentration* **(b)** *Transport*

Figure C.5 *Sediment concentration in* $m.s^{-1}$ *and transport rates in* $m^2.s^{-1}$ *time-averaged for the last simulation hour.*

C.2.4 Wave obliquity: detailed analysis

General The majority of dune erosion experiments plus models only include cross-shore dimensions. However, in a conceptual XBeach model the effects of wave obliquity on dune erosion has been demonstrated (Den Heijer, 2013). The suggestion of Den Heijer is to work with a relative increase according to Equation C.2, in which θ stands for the wave angle related to the shore normal. The reason for this increase in erosion volume is that besides cross-shore sediment transport also a longshore component is present. For the longshore effect of hard structures also some differences in impact are expected (WL | Delft Hydraulics, 1993). In XBeach simulations wave obliquity resulted both in an increase as well as decrease in impact (depending on the location of the transition and the wave angle) (De Vries, 2011). In this analysis several XBeach simulations have been carried, in which the main wave angle have been varied between normal incident waves and wave angles of 30 degrees with respect to shore normal. The results are presented in Table C.2.

$$\Delta A = \cos^2\theta \sin\theta \tag{C.2}$$

Mean erosion volume: reproduction Den Heijer (2013) One can first of all notice that the mean erosion volume will increase when the obliquity increases. For example for a wave angle of 15 degrees the erosion volume increases with 9.4%. This is somewhat less than the suggestion of Den Heijer (2013) which would calculate an increase of 25%. For a wave angle of 30 degrees with respect to shore normal the erosion volume increases even further to a relative increase of 20.9%. The reason for these increasing values is that in a wider cross-shore area higher sediment concentrations can be found. This facilitates an increase in offshore sediment transport. On the other hand undertow velocities will decrease (Den Heijer, 2013). A similar pattern, as found for the erosion volume, is found for the retreat distance.

Direction spreading: s = 10.000 versus 20 When comparing the baseline configuration (presented in Section 3.4.1) and the simulations in this subsection, the following differences can be remarked. In the collision cases a directional spreading of s = 10.000 was applied. When a value of s = 20 (practical default value) is applied the ratio between the increased set-back and influence length decreases. For simulations with a s = 10.000 the ratio between the DnA calculation rules and XBeach was 47-78%. For lower values of s the ratio decreases down to 27%. However, the ratio for the increased set-back does not vary. This mean that lower influence lengths are expected when a lower s is applied.

Causes: importance of individual effects Overall one can conclude that during wave obliquity the causes for the impact of dune erosion will change. Sediment concentrations increases and the cross-shore undertow decreases when wave angles increases. For the effect of hard structures two of the three causes become of less importance. Both the exchange of sediment in alongshore direction driven by a water level gradient in alongshore direction (less accretion in soft cross-sections and more accretion in hard cross-sections) as well as the decrease of dissipation in the soft influenced cross-section (partly) will not occur. The only effect left is the increase in short wave height due to diffraction around the structure. These higher short wave heights will, generated by obliqueness, be distributed in a broader area downstream. The longshore transport also becomes important, due to oblique wave attack. Longshore velocities will develop. In simulations the values were in the order of 0, 1.2 up to 2.0 $m.s^{-1}$ for 0, 15 and 30 degrees with respect to shore normal. In comparison, cross-shore velocities are in the order of 0.6 $m.s^{-1}$.

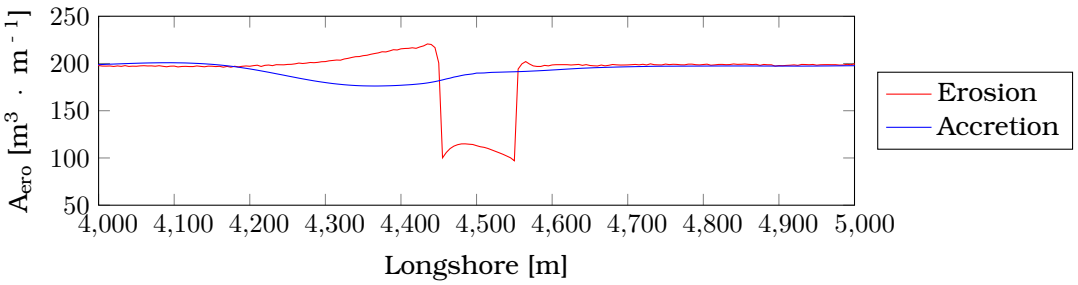

Figure C.6 *Morphological response of the barrier in erosion and accretion for configuration C*

Detailed comparison: fixed dimensions versus half infinite structures both for normal-incident waves and oblique wave attack There are three causes specified in this thesis for the longshore effect of hard structures. In the previous paragraph it was already concluded that only the locally higher short waves will be of importance. On top of that the path of the individual waves will be somewhat different, which results in an unilateral increased set-back over broader area. In a previous analysis in this thesis it was concluded that after a width of 100 m a structure can be seen as semi-infinite. However, this analysis has been carried out for shore normal wave attack and is thus not valid for oblique attack.

Regardless of the structure width there will be the phenomenon called updrift and downdrift. This is related to gradients in longshore transport and develops when the longshore transport is (partly) intersected with a structure. In this situation a NWO is responsible for this gradient. The impact will increase for larger wave angles (since the longshore velocity and thus transport will increase) and for NWO's which are placed in a more seaward direction (since it blocks larger part of the surfzone).

For the situation with a semi infinite structure high longshore velocities (7 $m.s^{-1}$) at the toe of the structure develop. The result is a locally very high longshore transport. At the transition hard-soft therefore a combination of both this strong longshore transport as well as downdrift is active. The strong longshore velocity will have a significant draining effect on the hard-soft transition, since the longshore transport is unsaturated. In addition, downdrift is active. Eventually the water column is oversaturated, which results in deposition of sediment downstream. These effects mentioned, do not develop for structures with a limited width (order of 100 m), because the longshore velocity will normally not develop in such high magnitude.

In the further analysis the focus will be on NWO's with fixed dimensions. The maximum increased set-back (d_2) does not become larger in downstream locations for this configuration. This is in contrast to the suggestion of De Vries (2011). The reason for this difference is related to the used configuration, since De Vries used a structure that was semi-infinite.

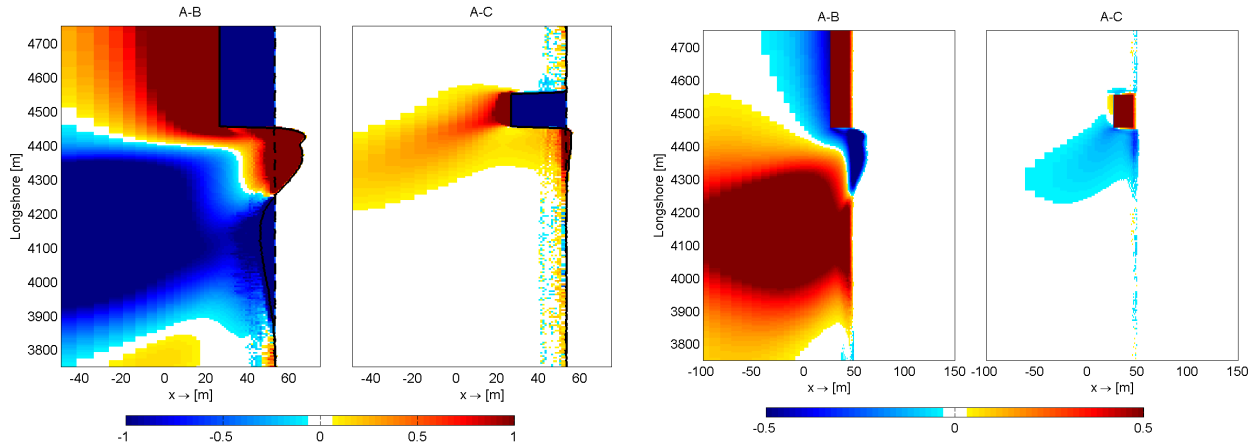

(a) *Bed level* (m) **(b)** *Short wave height* (m)

Figure C.7 *Comparison between configuration A and B plus C for two output parameters. Retreat is given in the black line in left panel (dashed: without structure, solid: with structure).*

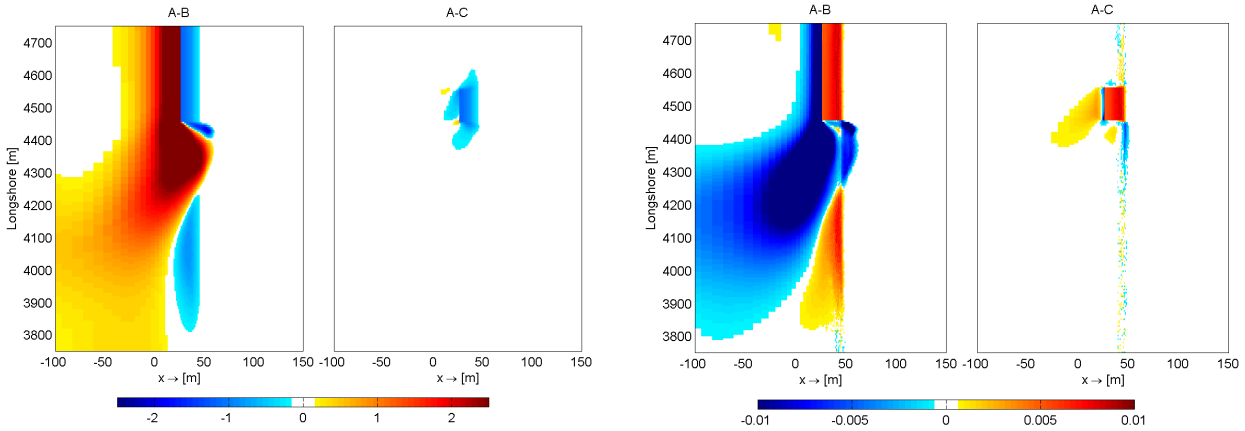

(a) *Longshore velocity* $(m.s^{-1})$ **(b)** *Sediment concentration* $(m^3.m^{-3})$

Figure C.8 *Comparison between configuration A and B plus C for two output parameters. In the left panel to redness of the color represents velocity magnitude towards to bottom (lower* y*). In the right panel the blueness of the color represents higher sediment concentrations for B or C.*

Effect: impact in terms of increased set-back, influence length and (sum of) additional erosion
In upstream direction sediment will pile up against the structure resulting in a decrease in retreat. The effect for wave angles larger than 20 degrees is already enough for the accretion to counteract the erosive processes. This means a decrease in retreat distance can be found in upstream locations.

In downstream direction extra sediment will be eroded, but this is not resulting in an increase in retreat. However, there is a relation between increasing values for wave obliquity and increasing values for the influence length. This relation is both valid in absolute values as well as factor for the increased set-back. For shore normal wave attack the ratio set-back and influence length was 8.2. This ratio increases up to 90.9 (+1009%) for wave attack with an angle of 30 degrees. The suggestion of the DnA calculation rules is a ratio of 30. In absolute numbers the influence length increases with

a factor 5. The reason for this increase is bi-pirate. First of all, higher short waves are distributed in a broader area downstream. Second, there is an effect called downdrift. The ratio between the normal set-back and the increased set-back decreases from 0.21 tot 0.08 for wave angles of 30 degrees, which is a direct result of the distribution of locally higher short waves over a large influence length downstream.

The total alongshore additional erosion ($\sum A_2$) first decreases with 28% for wave angles of +10 degrees with respect to shore normal and eventually increases 16% for wave angles of +25 degrees. The reason for this distribution is that the upstream additional erosion is linear decreasing for increasing wave angles. With every increase of 5 degrees the total upstream erosion volume decreases with 250 $m^3 \cdot m^{-1}$. The downstream additional erosion has a sigmoid shape (S-curve: first hardly increasing, from 15 degrees quickly increasing). Every increase with 5 degrees the total downstream erosion volume increases with 83-665 $m^3 \cdot m^{-1}$.

Table C.2 *Morphological results in 2DH for wave obliquity simulations both as calculated with DnA + XBeach without a structure (DnA) as well as simulated with XBeach with a structure (XB.). Erosion volumes are given in $m^3 \cdot m^{-1}$. XBeach simulated values are presented on the left (L.) and right (R.) side of the structure. Simulations noted with '-s' are modeled with a directional spreading of 10.000.*

Type	General $R*$ [m]	$\overline{A_{ero}}$	d_2 [m] DnA	XB. -R.	XB. -L.	l_2 [m] DnA	XB. -R.	XB. -L.
270	50.3	181	7.2	4.8 (67%)	4.9 (68%)	146	40 (27%)	40 (27%)
275	51.2	186	7.4	3.2 (44%)	5.2 (70%)	156	35 (22%)	50 (32%)
280	52.4	192	7.8	2.0 (26%)	4.9 (63%)	146	25 (17%)	65 (45%)
285	53.2	198	8.0	1.1 (13%)	4.2 (53%)	127	20 (16%)	95 (75%)
290	54.5	208	8.4	0.4 (5%)	3.7 (44%)	110	0 (0%)	140 (127%)
295	55.2	213	8.6	0.0 (0%)	2.1 (24%)	63	0 (0%)	190 (304%)
300	56.2	219	8.9	0.0 (0%)	2.2 (24%)	65	0 (0%)	235 (360%)
300-s	65.3	252	11.6	0.0 (0%)	2.1 (18%)	63	0 (0%)	365 (577%)

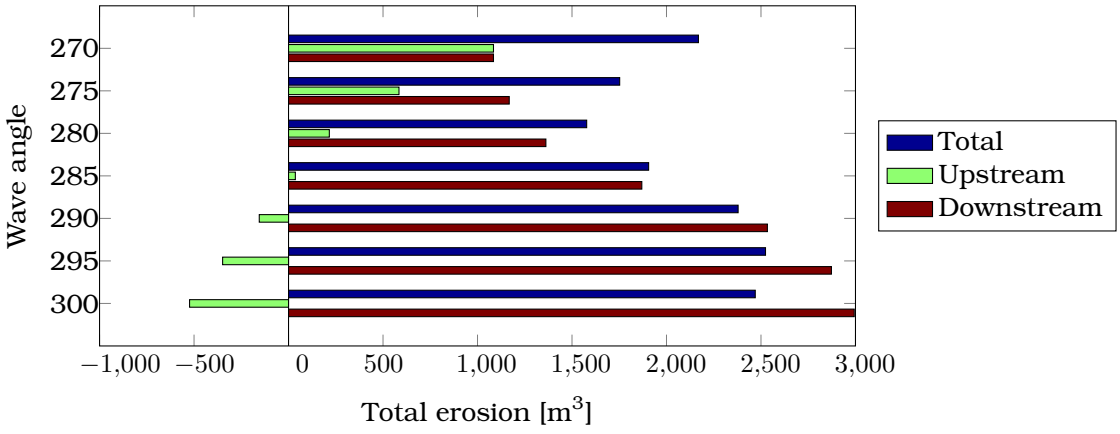

Figure C.9 *The total alongshore eroded sediment for different wave angles. The upstream additional erosion is linear decreasing and downstream part has a S-shape. The total additional varies in a band of -28% down to +16%.*

C.2.5 Sensitivity analysis: storm-induced and coastal parameters

General The morphological response of the coastal system depends on the parameters of the storm, the coastal system and the object itself. In this subsection the sensitivity of the morphological response for the storm-induced parameters and coastal system is analyzed. The parameters that have been varied are: root-mean square height wave (H_{rms}), spectral-mean wave period ($T_{m-1.0}$), sediment diameter (D_{50}) and relative dune height (D_{SSL}). Relative dune height is the height difference between the dune top and the SSL in m.

Supporting figures are given on the next page. The line through the points calculated by XBeach is found with the Matlab function $polyfit$. This function finds the coefficients of a polynomial $p(x)$ of the first degree that fits the data best in a least-squares sense. The values presented in Table C.3 are the p_2 of the formula: $f(x) = p_1 + p_2 \cdot x$. Also the $R2$ of the fit is given.

Mean increase of retreat line ΔR and point ΔP In the baseline computation for A the increase in the retreat line and the retreat point had a value of 42.2 m and 23.3 m.

1. Overall the retreat point is a less sensitive parameter for change in storm-induced and coastal parameters compared to the retreat line.
2. H_{rms} has a small positive relation for ΔR, but does not change for ΔP. This was expected on forehand, since the erosion patterns become more supply-driven which underlines the increasing importance of avalanching triggered by the long wave (Van Thiel de Vries, 2009b).
3. An increase in $T_{m-1.0}$ resulted in a less steep dune profile. Therefore, the retreat line has a stronger feedback than the retreat point on varying wave periods (Van Gent et al., 2008).
4. Decrease in relative dune height has the strongest relation for both the retreat line and the retreat point. The factorial response, both for ΔR and ΔP, is three times the change in factorial value.

Erosion volumes In the baseline computation for A the erosion above SSL was 194 $m^3 \cdot m^{-1}$ and the total erosion was 213 $m^3 \cdot m^{-1}$.

1. The difference between the total erosion volume and the volume measured above SSL varies between 4 - 18 %. For the H_{rms}, $T_{m-1.0}$ and D_{50} the ratio varies between 9 and 10 %. For the D_{SSL} this value increases for a factorial decrease in relative dune height.
2. Change in relative dune height and spectral mean wave period have the largest effects (+1.39 and -1.39) on the erosion volume in XBeach. When comparing these values with Delta Flume experiments the effect of the wave period is possibly overestimated. In those experiments a relation of +1.15 was found (Van Gent et al., 2008).
3. The effect of change in D_{50} is possibly underestimated in XBeach. In XBeach a relation of -0.19 is found. In a similar study with DUROSTA a relation of -1.5 was found (Hoonhout, 2009).

Response in DnA output variables In the baseline computation for C1 the increased set-back d_2 was 7.5 m with an influence length l_2 of 155 m.

1. The response of change in coastal-related and storm-induced parameters is somewhat comparable with the response in terms of retreat line and increased set-back.

2. For both the H_{rms} and $T_{m-1.0}$ a proper fit is found of +1.24 and +2.30, which is for both larger than that for the retreat line.
3. The increased set-back is remarkable sensitive for change in relative dune height. A small percentage change in relative dune height will already have an enormous impact on the increased set-back. The factorial response is an order larger than the factorial change in input parameter.
4. It is not possible to find a proper linear fit for the relation between the different factorial values and the factorial influence length. (values not presented in the table)

Table C.3 *Sensitivity values in terms of relation p and regression $R2$ of ΔR, ΔP, erosion volume, d_2 and l_2 for H_{rms}, T_p, D_{rel} and D_{50}.*

Term	Response	H_{rms}	T_p	D_{SSL}	D_{50}
ΔR	p	0.78	2.01	-2.85	-0.12
	$R2$	1.00	0.97	0.88	0.99
ΔP	p	0.02	0.70	-3.30	-0.40
	$R2$	0	0.95	0.99	0.98
Erosion	p	0.49	1.38	-1.39	-0.19
	$R2$	1.00	1.00	0.99	1.00
d_2	p	1.24	2.30	-10.41	-0.09
	$R2$	0.95	0.95	0.18	0

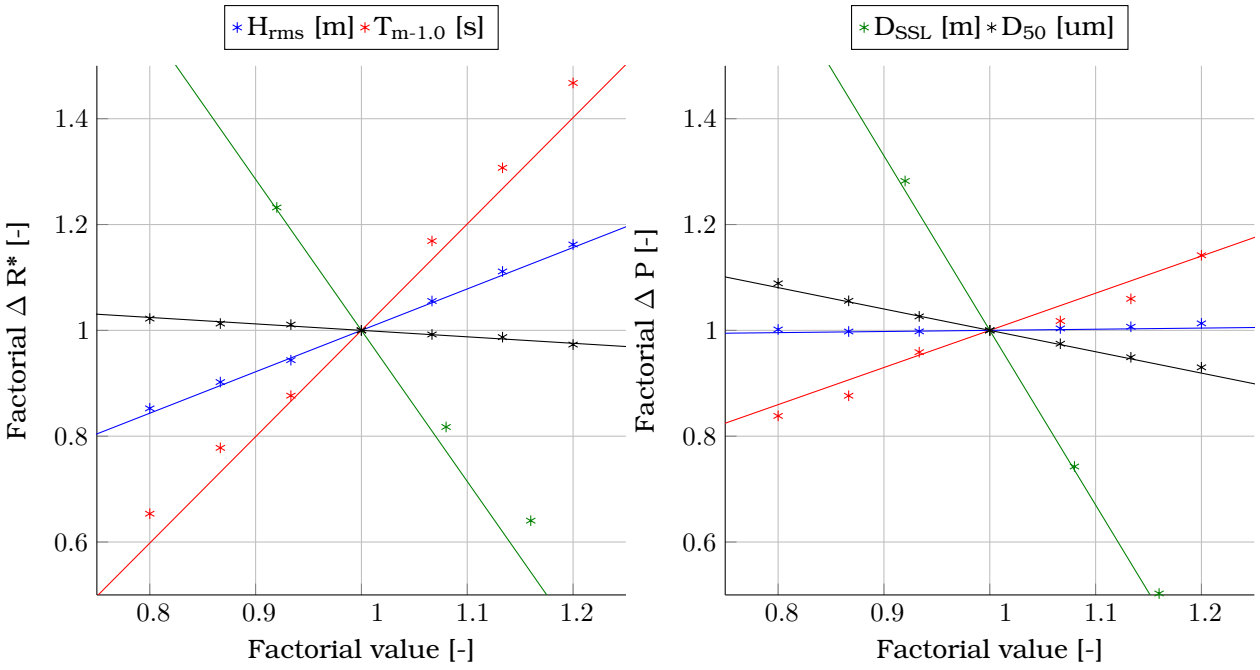

Figure C.10 *Factorial deviation model for mean retreat line ΔR and retreat point ΔP for configuration A*

C.2.6 Sensitivity analysis: object size

General The effect of a structure on the coastal system is closely related to the object size. In the DnA calculation rules the front position of the structure is already implicitly taken into account with the use of the interaction parameter (d_1). However, the effect of the width of the object and the back position is not taken into account. In this subsection the sensitivity of morphological response related to the position, width and length of the structure is analyzed.

On the next page the results are presented in which the blue values are calculated values by XBeach and the black values are the DnA calculation rules. The line through the blue XBeach measurement points in indicative and made by applying an exponential fit of the form $f = s_1 + s_2 \cdot e^{\frac{-t}{s_3}}$ through the points.

Front position The front position of the structure has been varied in multiple XBeach simulations between a position 50 meters seaward (like a pier) down to 20 meters landward (like a NWO, for example an underground parking).

The relation of the increase in retreat line ΔR alongshore per configuration, presented in Figure 3.20, shows that the location of the maximum increased set-back d_2 varies. The larger the front position of the structure the further away from the structure the maximum set-back occurs. This is related to diffraction of short waves.

In Figure C.14 the relation between the increased set-back and the front position of the structure is presented. For simulations with a position of 10 meters seaward the increased set-back follows the relation described by the DnA calculation rule. Objects which are placed even more in seaward direction do not result in more increased set-back due to the creating of a shadow zone, which will reduce the wave impact and thus erosion. The difference between the calculated and modeled influence length increases from front positions of 0 or more m seaward.

Width In multiple XBeach simulations the width of the object has been varied between values of 5 m (like a groin) up to 250 m (like a hotel).

In Figure C.15 the relation between the increased set-back and the width of the structure is presented. For structures with a width smaller than 50 meters the increased set-back decreases considerably. The reason for this decrease is that the nearshore in front of the element is more or less similar as the 'normal' nearshore. This underlines the fact the difference in cross-sectional surface is one of the drivers of increased set-back. The increase in increased set-back d_2 and influence length l_2 stops for structures with a width larger than 100 meters. This is equivalent to the deep water wave length. It is questionable if this is coincidence or a fixed relation based on physics.

Back position The study towards the relation between length of the structure and the morphological response is a bit academic, because in practice structures would have a length of at least +/- 10 meter. However it is for the bigger picture interesting also to analyze this relation. In these simulations the length of the structure varies between 1 (like a salient) up to 90 meters (like a hotel).

In Figure C.16 the relation between the increased set-back and the length of the structure is presented. For lengths smaller than 20 meters the effect of the structure on the erosion pattern decreases. This is related to the effect of disconnecting the structure with the rest of the barrier. Behind the structure a reduction of wave energy will result in some accretion. This accretion will

partly counteract the erosion due to higher wave heights. This is more or less similar as the effects observed in the field at salients and tombolos.

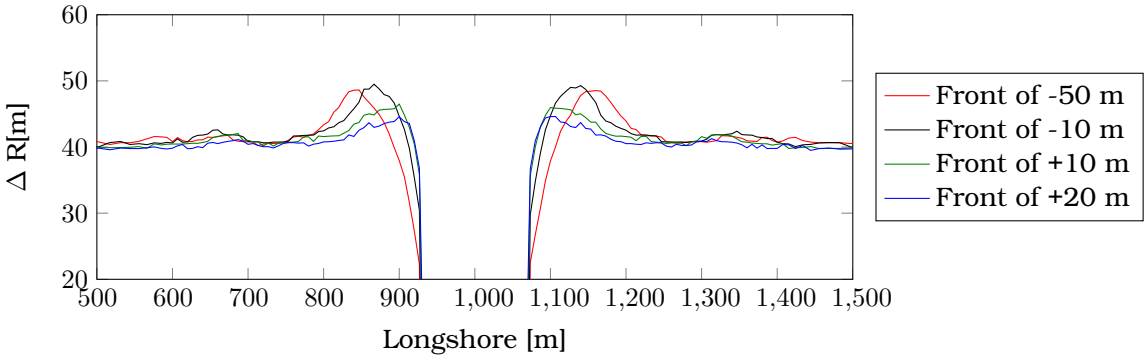

Figure C.11 *Increase in retreat line alongshore for multiple values of front position of the hard element.*

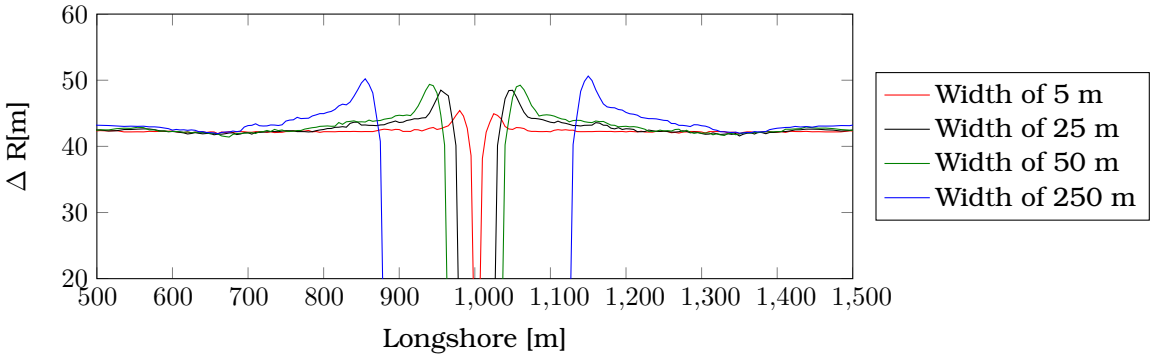

Figure C.12 *Increase in retreat line alongshore for multiple values of width of the hard element.*

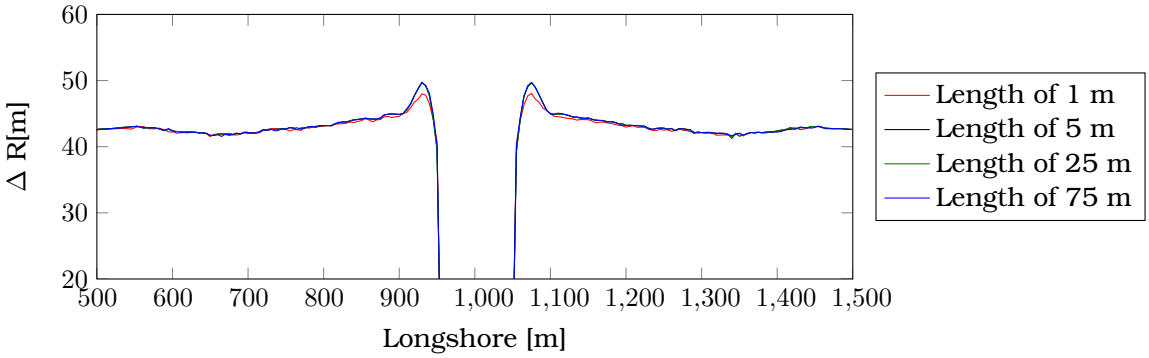

Figure C.13 *Increase in retreat line alongshore for multiple values of length of the hard element.*

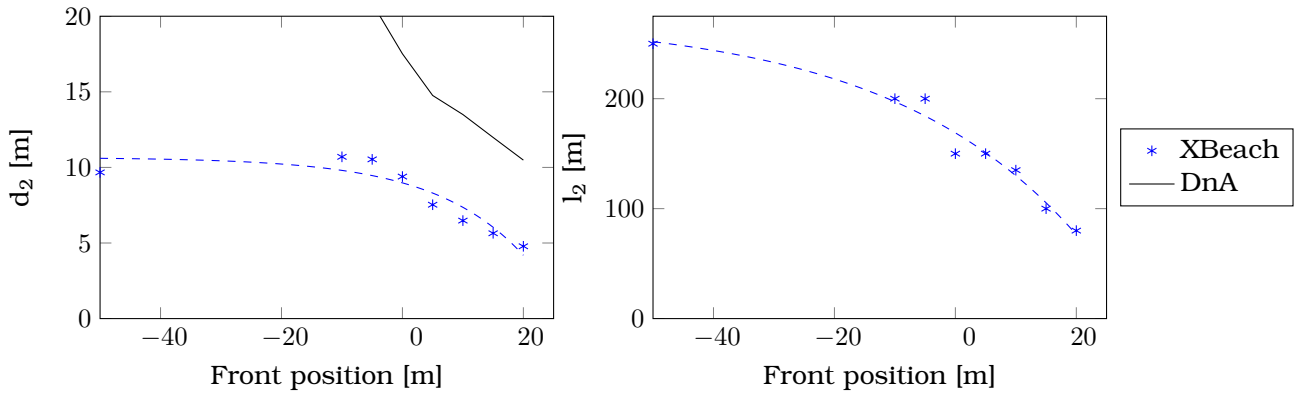

Figure C.14 *Morphological response of the barrier in d_2 and l_2 for multiple values for the structural front position.*

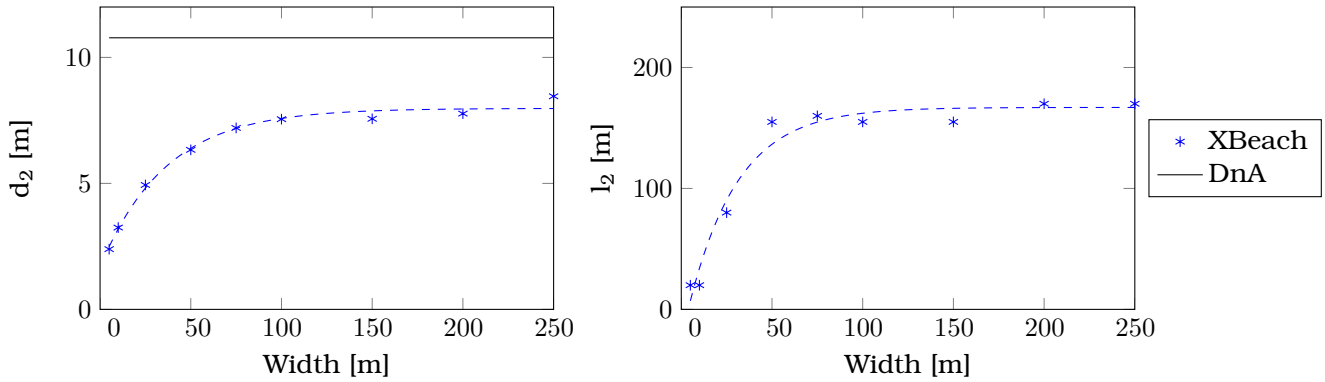

Figure C.15 *Morphological response of the barrier in d_2 and l_2 for varying measures of width of the hard element.*

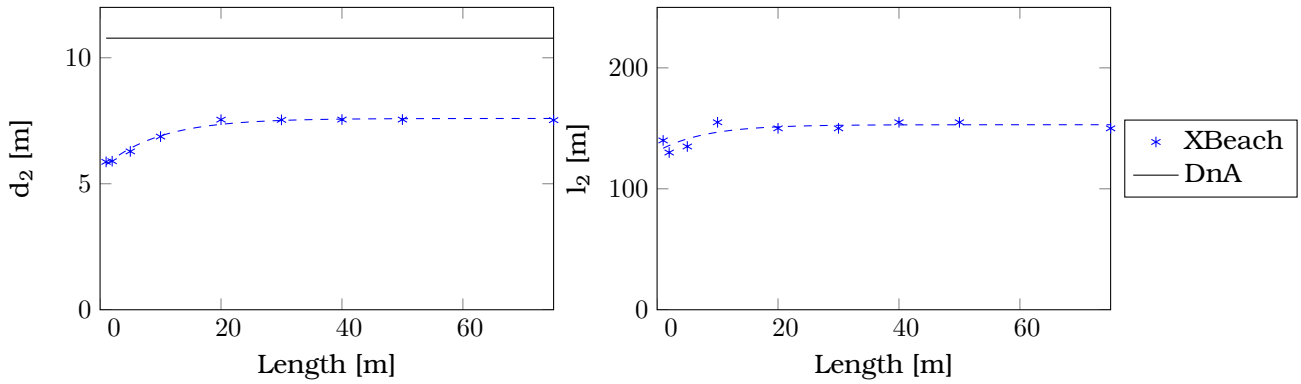

Figure C.16 *Morphological response of the barrier in d_2 and l_2 for varying measures of length of the hard element.*

C.2.7 Sensitivity analysis: XBeach settings

General In this subsection the impact of several XBeach settings is investigated. This is done in order to obtain a feeling of the sensitivity of several physical / model parameters and in order to put the results of the conceptual model in some perspective. The parameters varied are the parametric relations short wave run-up (via $swrunup$) and scour hole development (via $jetfac$), directional spreading (s) and the influence of long waves. On top of that variation in simulation time is applied. Besides the physical related parameters also an analysis for effect of non-physical parameters like version, CFL, morfac and MPI is applied.

Short wave run-up The short wave run-up (keyword $swrunup$) is included as parametric relation since XBeach version 1.20.3606, code name 'Sinterklaas', released on December 5th 2013. According to Van Thiel de Vries (2009a) the short wave run-up only slightly effects the simulated profile evolution without a revetment since near dune hydrodynamics are dominated by long waves, but the short wave run-up is mainly needed for triggering the sediment on top of a structure to avalanche down.

The introduction of short wave run-up in XBeach will result in more erosion of barrier. The effect is noticeable when comparing simulation with and without $swrunup$. The retreat line increases with +1.97 m (+3.3%) and the erosion volume increases with +1.9 $m^3.m^{-1}$ (+0.9 %). The reason for these differences are that material from higher grounds will avalanches down and the beach steepness will thus be less. It is however not necessary to include short wave run-up in order to describe the increased set-back (d_2). The same retreat line pattern can be derived with or without introducing the $swrunup$. This is in contrast to the suggestion of Van Geer et al. (2012).

Scour hole development XBeach underestimates the scour hole in front of a hard element. In order to reproduce the morphological response in a more accurate way the $jetfac$ option can be activated in order to mimic the turbulence production near the toe of structures. This relation is also included since XBeach version 'Sinterklaas'.

The introduction of the $jetfac$ will, logically, result in more turbulence and thus more erosion in front of the structure. The increase of turbulence is in the order of 120 $m^2.s^{-1}$. This will result in a 2.5 meter deeper scour hole. It is however for calculating the increased set-back in XBeach not necessary to activate the option of the $jetfac$. Simulations with and without $jetfac$ result in more or less a similar retreat line. From Figure C.17 one can conclude that activating the $jetfac$ the exchanged sediment between the A and B profile is larger. This is the result of the larger cross-sectional difference between these profiles. However, in XBeach these differences are not the effect responsible for driving the impact in terms of increased setback. One hypothesis is that in XBeach the increased set-back is insensitive for scour hole development, but is sensitive for less sediment supply in the hard cross-section.

Directional spreading In all the simulations in this conceptual study of collision the directional spreading (s) applied had a value of 10.000 [-]. This means that all the wave energy will come from one fixed direction. This is done in order to be able to compare 1D simulations with 2DH, as stated by Deltares and Arcadis (2013). For practical applications this will *not* be the case and then the default value for s of 20 should be applied. When a simulation is performed with this value the system will first of all erode less. The reason for this difference is the fact that energy is distributed in a broader range and the energy is thus less centralized. The difference in retreat line is 8.4 m (-14.0%) and the erosion volume decreases with 19.7 $m^3.m^{-1}$ (-9.5 %).

When this simulation is corrected for these initial differences the results around the hard element are more or less similar. The major difference is related to the influence length. For $s = 20$ the influence length is about half the default value with a $s = 10.000$. This is most likely related to the larger distribution of energy that will result in a stronger alongshore sediment exchange. Lower values for directional spreading have a smoothing effect on the barrier (Van Thiel de Vries et al., 2008).

Long wave importance According to the theory described in Chapter 2 water motions near the coastline are dominated by long waves. In XBeach it is possible to deactivate the generation of these infragravity waves. In these simulations the barrier suffers from less erosion. The reason for this difference is that the avalanching algorithm is triggered less. This decrease in sediment supply will result in a decrease in retreat line of 18.8 m (-31.5%) and a decrease in erosion volume with 50.4 $m^3.m^{-1}$ (-24.4%). In a previous study XBeach simulations without long waves resulted in 30% less erosion (Van Thiel de Vries, 2009b).

This simulation can also be corrected for this fundamental difference. The result in terms of retreat is comparable with the default set-up. Also similar patterns for the influence length are found. However, less accretion in front of the structure is observed. This gives rise to the idea that the alongshore distribution of sediment is (partly) long wave driven. XBeach simulations suggests that 28% of the sediment exchanged in longshore direction is long wave driven.

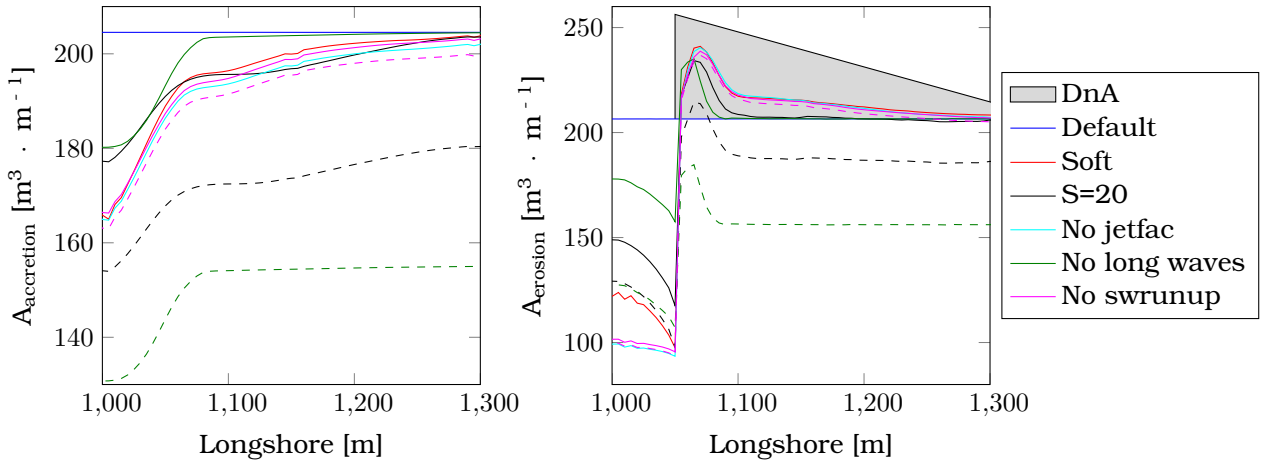

Figure C.17 *Morphological response of the barrier in erosion and accretion alongshore for several parameters. In the grey area the extended DnA calculation rules are presented. Dashed lines are non-corrected.*

Time In the previous calculations, only storm of 5 hours were simulated, is based on the approach of Vellinga (1986) in which a 5 hour storm on SSL has the same effect as a 30 hour storm with tidal effect. For the sack of illustration the duration of the simulated storm is extended in this paragraph. The simulation time used is 15 hours.

In 3.4.1 the parabolic increase in retreat line is reproduced. When extending the simulation time with a factor 5 the exponential development continues. The increased set-back and influence length have the same parabolic shape. The difference between the normal soft response and the increased retreat line increases. After 5 hours the increased set-back has a value of 6.2 m. This increases

up to 20.0 m after 15 hours. This was expected based on the linear relation between d_1 and d_2, as suggested by the Deltares and Arcadis (2013).

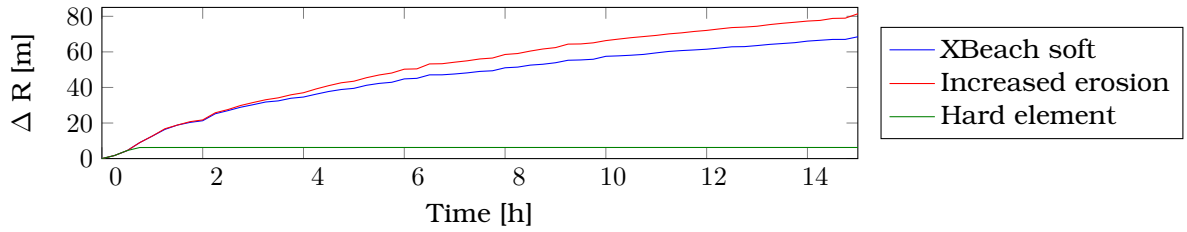

Figure C.18 *Development of the increase in retreat line for three cross-sections.*

Non physical parameters A comparison is made between the XBeach version 1.21.3657, code name 'Groundhog Day', released on February 7th 2014 and version 1.20.3606, code name 'Sinterklaas', released on December 5th 2013. The reason for this comparison is to check the differences between versions. The differences in terms of retreat line is in the order of 1 up to 2 m.

The computational time step can not be chosen explicitly in XBeach, only the CFL-number is a variable which the user can change. Theoretical the model should remain stable if the CFL-coefficient is chosen equal to or less than one. The default value for this condition is 0.7, which is a trade-off between numerical accuracy and time efficiency, since the CFL condition and numerical dissipation are closely related to each other. An increase of the CFL coefficient means an increase in numerical dissipation (McCall, 2008). The retreat line and retreat point have the suggested relation with the CFL-condition. An increase in CFL condition means a decrease of the retreat line and retreat point of 0.1 up to 0.2 meter and the other way around. This mechanism is a result of the numerical dissipation which has impact on the wave energy that reaches the shore.

The morfac is a well-known numerical method in reducing the computational time. The general idea is that each morphological step is applied several times. This is not physically correct, but applying a morfac of 2 already means a reduction of about roughly 2, in terms of computational time, and therefore it is a powerful trick. In this paragraph the effect of the morfac is analyzed. When applying a morfac the morphological response and thus erosion of the system is overestimated. The overestimation increases when higher values for the morfac value are applied. The overestimation for morfac 2, 5 and 10 is respectively 0.7 m (1.4%), 1.1 m (2.4%) and 3.5 m (7.5%). The response in bed level, sediment transport and velocities is more or less similar when comparing different options for a morfac value.

MPI is a standard which makes it possible to apply parallel computation in XBeach. This is of great value, since parallel computation reduces the computational time with a factor 2 up to 8 without the downsides of a morfac. The general concept is that the whole domain is split in multiple domains. Each domain is calculated separate and information at the boundaries is shared through the MPI. Simulations in XBeach have showed that the effect of MPI on the end result are limited. The only effect noticeable is the result of the absence of communicating of the avalanching algorithm.

C.3 Overwash situation

C.3.1 Causes of the impact for 1D

General In this subsection the causes for the impact in conceptual study for overwash in 1D are analyzed. This will be done by identifying the patterns in waves, flow, sediment concentration and sediment transport.

Waves Storm-averaged patterns in short and long waves are for Profile 1 more or less comparable with the patterns retrieved in the conceptual study for the collision regime. For Profile 2, where overwash occurs , set-up decreases. This is related to long waves that will flow over the barrier instead of contributing to the set-up. The water motions on top of the barrier are mainly long wave driven.

Flow The main difference between the collision and overwash regime is that in overwash conditions the run-up exceeds the dune top level. The effect is that a positive onshore Eulerian velocity can be found on top of the barrier. When averaging these velocities a signal in the order of +0.03 $m.s^{-1}$ (onshore) can be found. For the morphological response of the system the peak velocity is also of interest. The peak velocity measured during overwash is in the order of +0.50 $m.s^{-1}$. Mainly during these peaks sediment is transported from the dune towards the back barrier. For Profile 1 (collision) a mean velocity of -1.24 $m.s^{-1}$ (offshore) and a maximum of -2.40 $m.s^{-1}$ is modeled by XBeach.

Sediment concentration For the simulations in the collision regime there is a relation between depth-induced breaking, turbulence and sediment concentration. For the overwash regime this pattern does not hold. The reason is the fundamental difference in water motion. Overwash conditions result in a local increase of sediment concentrations in the order of 0.0003 $m^3.m^{-3}$ and has a maximum value of ten times the mean. When a profile suffers from larger overwash velocities, higher sediment concentrations can be found on top of the barrier. For Profile 1 (collision) a mean concentration of 0.0004 $m^3.m^{-3}$ and a maximum value of ten times the mean is calculated by XBeach. The concentration patterns and values are thus more or less similar on top of the barrier and in the nearshore.

Sediment transport The combination of velocity and sediment concentration will result in sediment transport. The sediment transport patterns for Profile 1 are comparable with the patterns retrieved in the conceptual study for the collision regime. Profile 2 has a storm-averaged onshore sediment transport of +0.0004 $m^2.s^{-1}$ and maximum of two times the mean. Sediment transport on top of the barrier is more concentration-driven than sediment transport in the nearshore. In addition, sediment transport on top of the barrier is long wave driven. The decomposition one can find in Figure C.19.

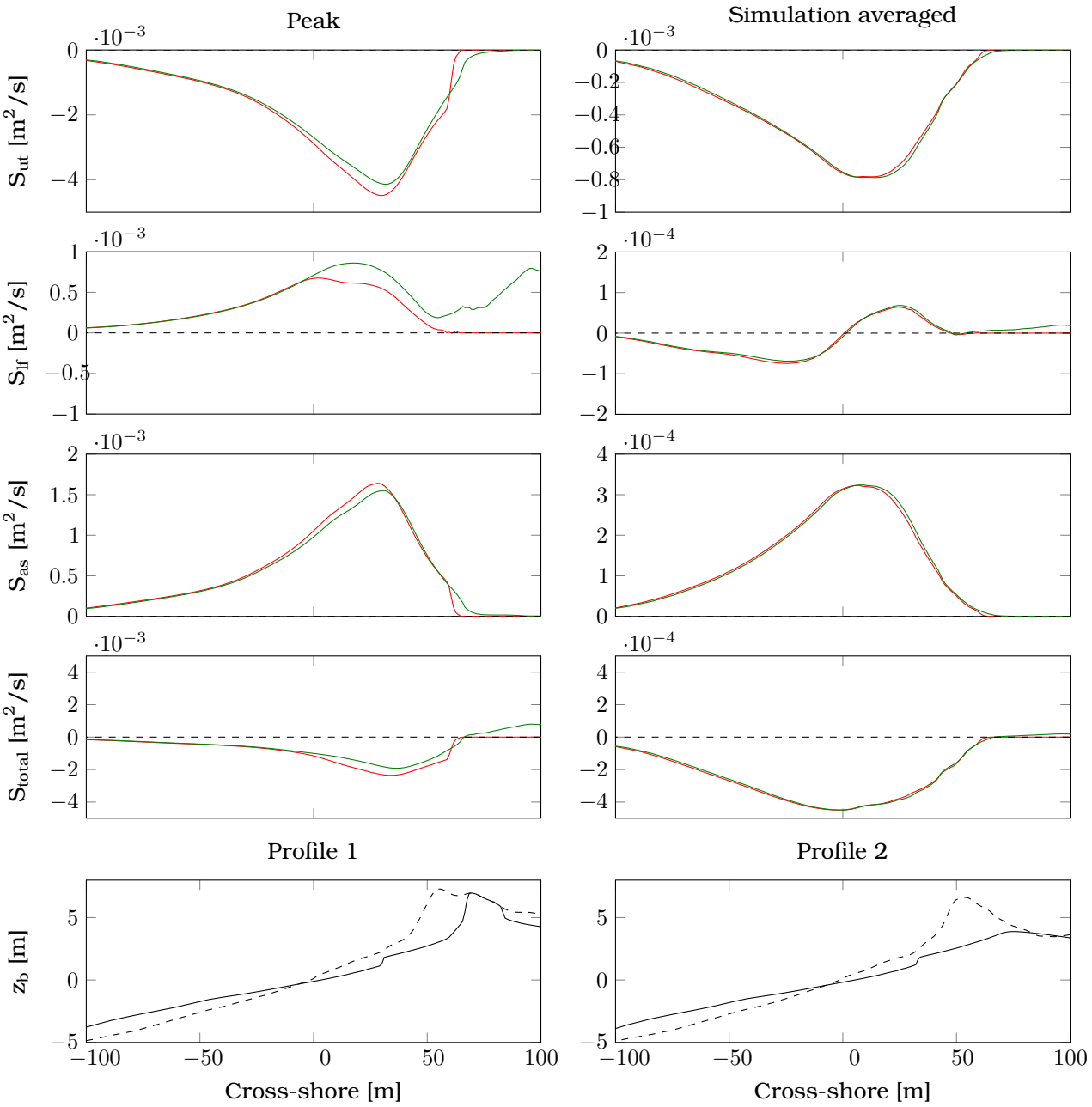

Figure C.19 *Peak-averaged (left panels) and storm-averaged (right panels) sediment transport components for Profile 1 (red) and Profile 2 (green). Transport is separated in undertow-driven (upper panels), long wave driven (2nd panels), asymmetric-driven (3rd panels) and total transport (4th panels), related to the bathymetry of both profiles (lower panels).*

C.3.2 Scour depth analysis for variation in SSL

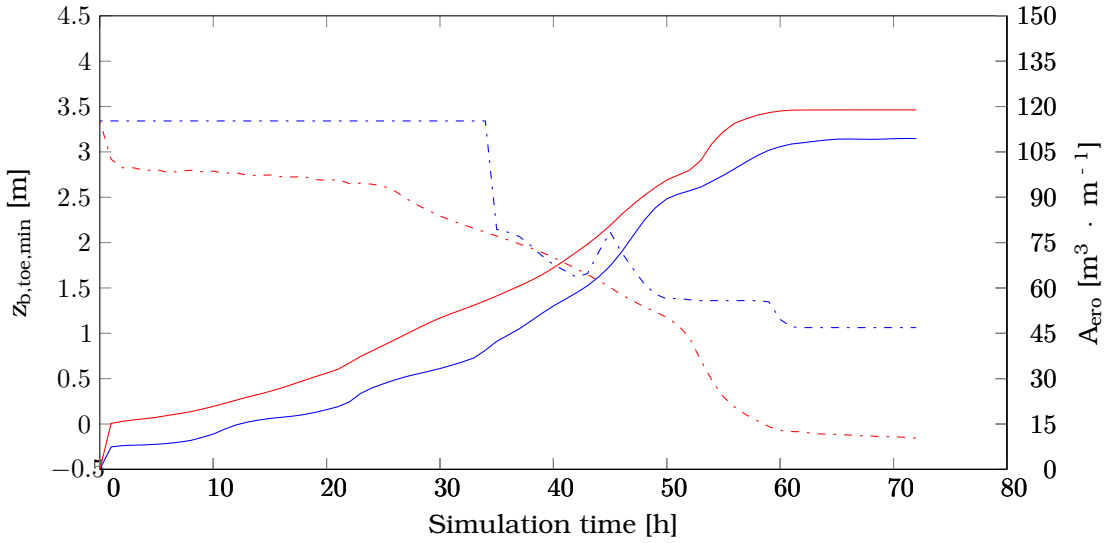

Figure C.20 *Scour depth (dashed) and erosion volumes (solid) plotted for simulation with (red) and without (blue) constant SSL.*

C.3.3 Causes and impact for 2DH

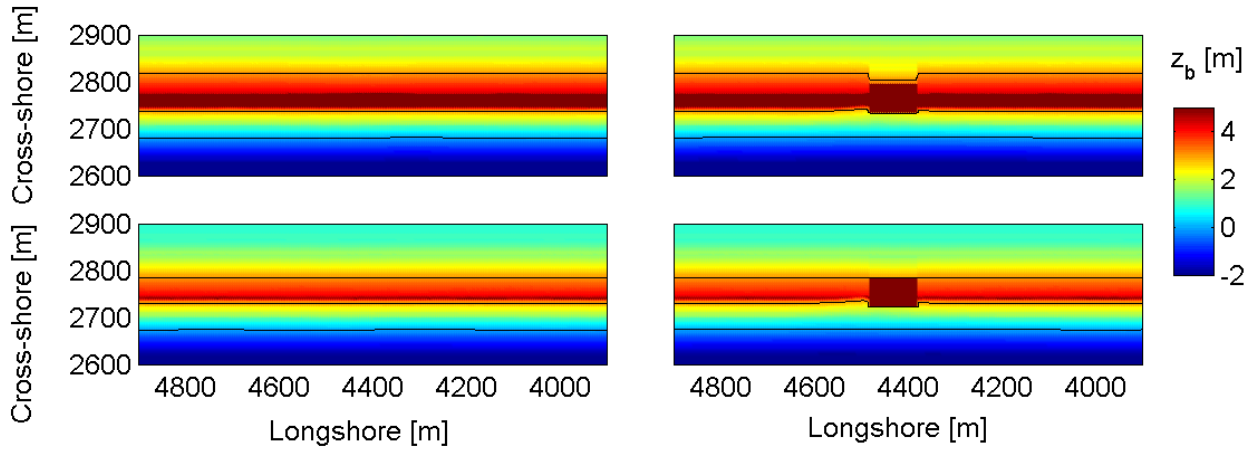

Figure C.21 *Spatial bed level plot for different configuration after the complete simulation in which the bed level is in m. Top panels are for Profile 1. Lower panel for Profile 2. Left panel are for the A configuration. Right panels for the C configuration.*

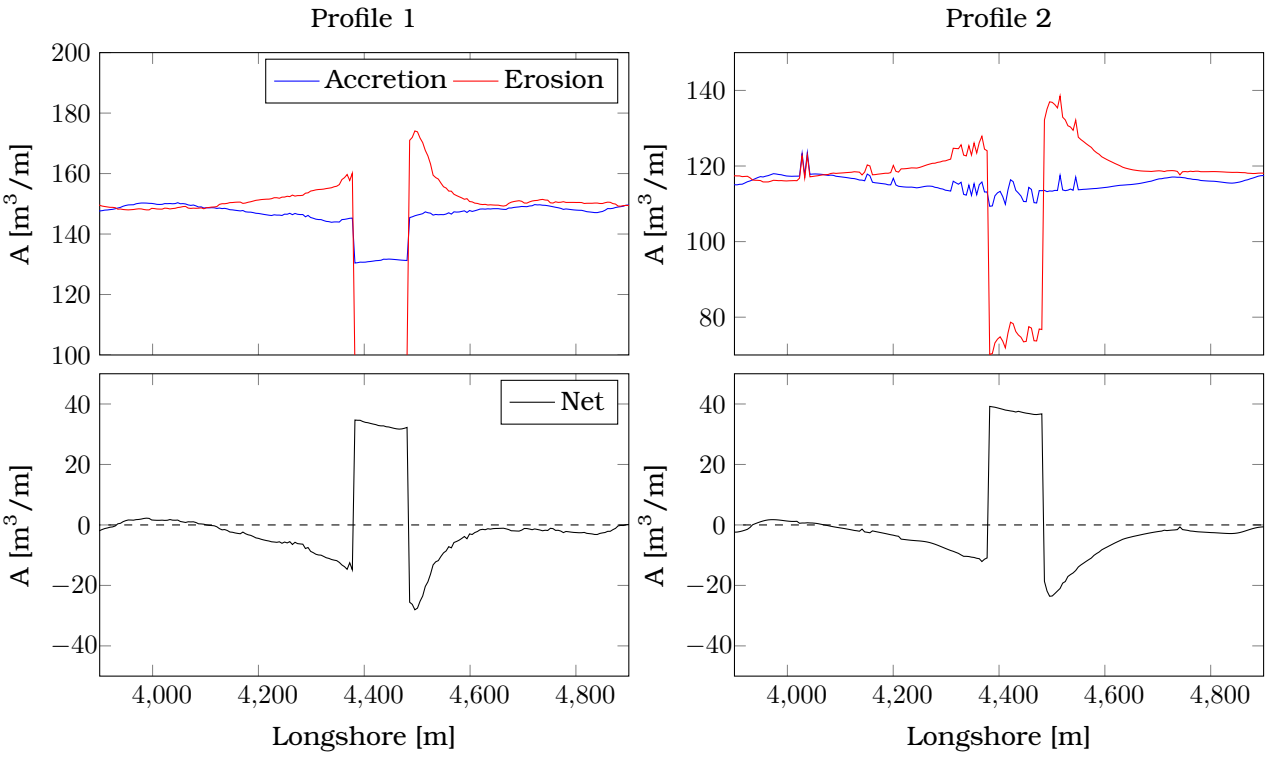

Figure C.22 *Erosion plots both for the individual parts (top): accretion (blue, top) plus erosion (red, top) and net (bottom). Plots are presented for Profile 1 (left) and Profile 2 (right).*

Appendix D

Aerial and satellite photographs of the impact of Sandy

In this Appendix oblique and satellite images of the devastating effect of Hurricane Sandy are presented. This is done for the two sites modeled in the case study. The images of Bay Head, NJ, can be found in D.2 and Camp Osborne, Brick, NJ, in D.3. Also two general images of the impact of Sandy are added in D.1.

D.1 General impact Sandy

The devastating effect of Hurricane Sandy can be seen clearly on oblique photographic material. Direct after Sandy the backside of the barrier is still flooded due to the higher water levels in the bay. On top of that, the deposits still are visible in the streets. The images attached below show the devastating impact of the storm conditions that occurred during Hurricane Sandy.

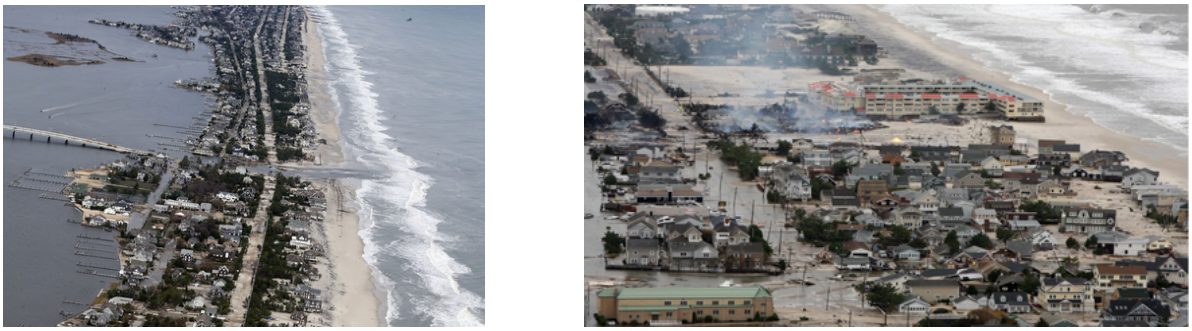

(a) *Breach near Mantoloking* **(b)** *Camp Osborne, Brick*

Figure D.1 *Photo material is taken from Harnden (2012). Pictures were taken on 30 (b) and 31 (a) of October 2012. Both pictures are facing North.*

D.2 Bay Head

After Hurricane Sandy a relic seawall became visible, this to the surprise of may residents. The seawall was pre-Sandy covered with 0.5 up to 1 meter of sand. These images can be found below:

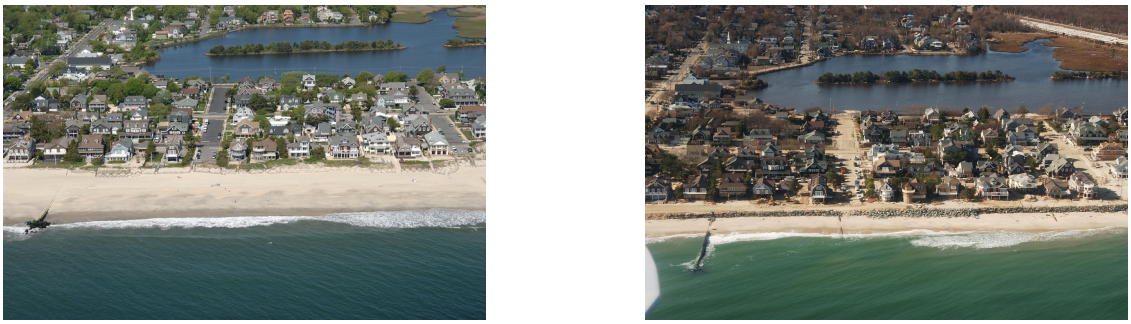

(a) *Pre-Sandy* **(b)** *Post-Sandy*

Figure D.2 *Oblique photo material from USGS at Bay Head. Pictures are taken on 21/05/2009 and 05/11/2012. Taken from the U.S. Geological Survey (USGS) website*

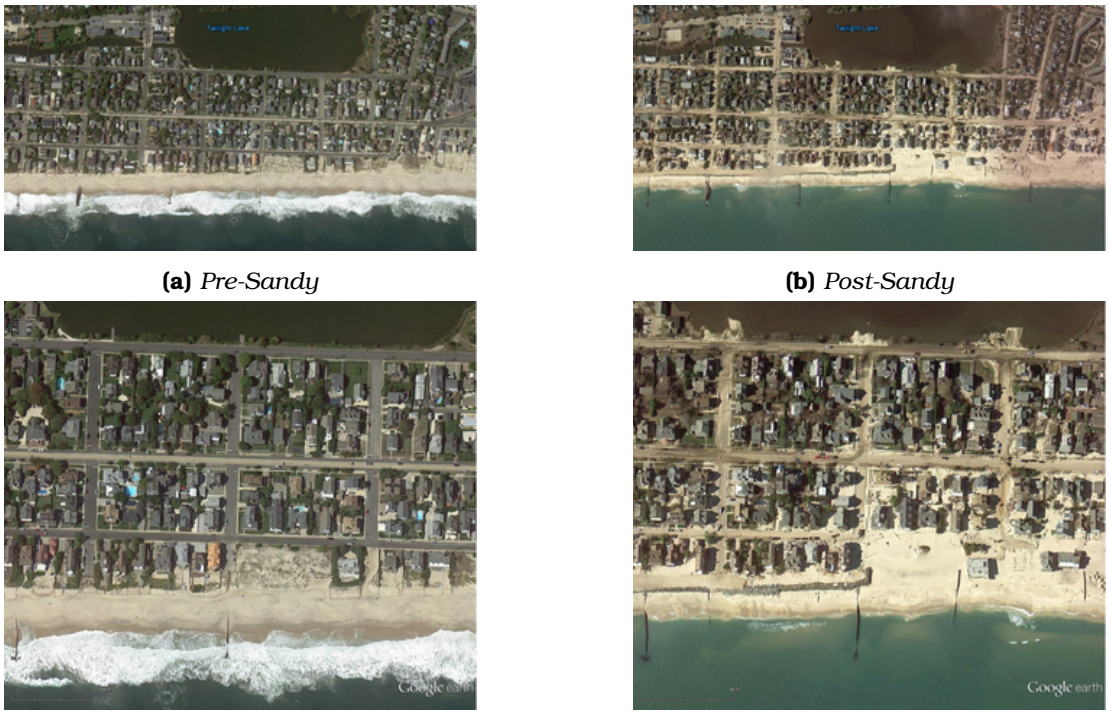

(a) *Pre-Sandy* **(b)** *Post-Sandy*

(c) *Pre-Sandy* **(d)** *Post-Sandy*

Figure D.3 *Overview and detail images of Bay Head from Google Earth. Pre- information is from 21/09/2012 and post-Sandy image is from 04/11/2012.*

D.3 Camp Osborne

The impact of Hurricane Sandy on Camp Osborne can be seen clearly on a Google Earth image. The first observation is that more erosion occurred at the left side of the condo. These images can be found below:

(a) *Pre-Sandy*

(b) *Post-Sandy*

Figure D.4 *Oblique photo material from USGS at Camp Osborne. Pictures are taken on 21/05/2009 and 05/11/2012. Taken from the U.S. Geological Survey (USGS) website*

(a) *Pre-Sandy*

(b) *Post-Sandy*

(c) *Pre-Sandy*

(d) *Post-Sandy*

Figure D.5 *Overview and detail images of Camp Osborne from Google Earth. Pre- information is from 21/09/2012 and post-Sandy image is from 04/11/2012.*

Appendix E

Bathymetric data sets used

In this Appendix the three different bathymetric data sets are presented. Also the basic approach for setting-up the model in XBeach is explained. There are three different data sources used, knowing: LiDAR (USACE, 2010, 2012; USGS, 2012a) the DUCKS-data from Stevens Institute of Technology (Lopez-Feliciano, 2014) and the Coastal Relief Model CRM (NGDC, 2014). The vertical orientation used is the NAVD88 in which depths are negative. In the different data sources multiple spatial orientations are used, both the New Jersey Plane Coordinates System and UTM are applied. Distances are in m. For the actual XBeach model set-up the universal UTM system is used in combination with a horizontal orientation in NAD83.

Table E.1 *Overview of the available bathymetry data sources.*

	Dataset	Date	Accuracy	Type	Return	Source
Pre	LiDAR	28-08-2010	0.75-0.20 m	Last and filtered	$z_b > 0$	USACE
Pre	DUCKS	22-09-2011	0.1 m	-	$5 > z_b > -10$	Stevens
Pre	CRM	05-08-2012	1.0 m	-	Full	NOAA
Post	LiDAR	16-11-2012	0.75-0.20 m	Last and filtered	$z_b > 0$	USACE
Post	LiDAR	16-11-2012	0.75-0.20 m	First and unfiltered	$z_b > 0$	USGS

E.1 LiDAR provided by the USACE and USGS

LiDAR (Light Detection and Ranging) is an optical remote-sensing technique that uses laser light to sample the surface of the earth. The result is highly accurate x,y,z measurement data. LiDAR is primarily used in airborne laser mapping applications. The USACE and USGS apply LiDAR to study changes along the entire US coast. The latest information prior Sandy was collected on Augustus, 28, 2010 (USACE, 2010). The latest data set after Sandy was collected on November 16, 2012 (USACE, 2012; USGS, 2012a). It is important to note that the difference between the impact of Sandy and the measurement data is 15 days. This will result that already some human impact of the sedimentation and accretion have happened. Photographic images have shown that the first human impact on the deposited sand on the barrier was a day after Sandy made landfall (Lopez-Feliciano, 2014).

The LiDAR data used is pre-processed by the USACE which removed any noise in the data and filtered out structures. The LiDAR used has an horizontal accuracy of 75 cm and a vertical accuracy of 20 cm. If possible the last return of the LiDAR data is used. The last return will result in the highest chance of getting the actual ground elevation instead of getting the elevation of nearby houses or trees. For the area around Bay Head this filtered data of the USACE is available. For the area around Camp Osborne not. In this area the unfiltered first response data is used.

With the use of LiDAR it is possible to accurate distinguish the impact of Sandy. For example in

Figure E.1 the area near Bay Head is presented. At this part of the barrier storm surge and waves overwashed the dunes. The result were devastating. Buildings were destructed, dunes were flatted and overwash deposits remained in streets. This effect, erosion of the barrier in combination with deposits on the barrier island, can be seen consistently throughout the different cities.

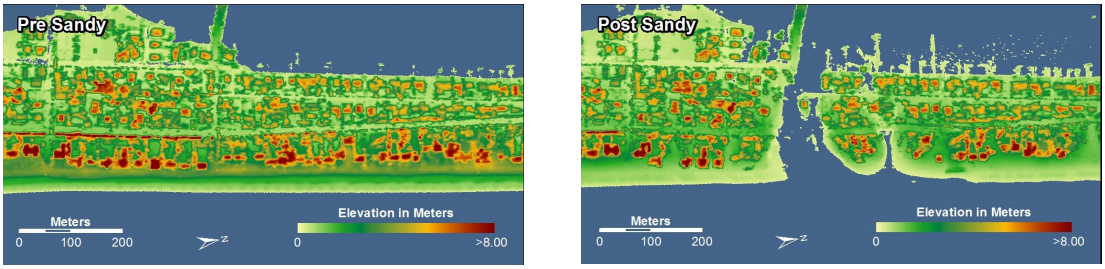

(a) *Pre-Sandy* **(b)** *Post-Sandy*

Figure E.1 *LIDAR-data of the Mantoloking from USGS. Pre- image is from Augustus 2010 and post-Sandy data is from November 2012.*

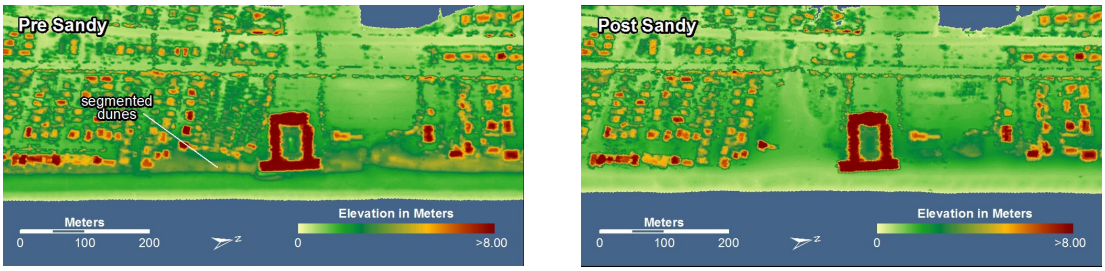

(a) *Pre-Sandy* **(b)** *Post-Sandy*

Figure E.2 *LIDAR-data of the hotel at Camp Osborne from USGS. Pre- image is from Augustus 2010 and post-Sandy data is from November 2012.*

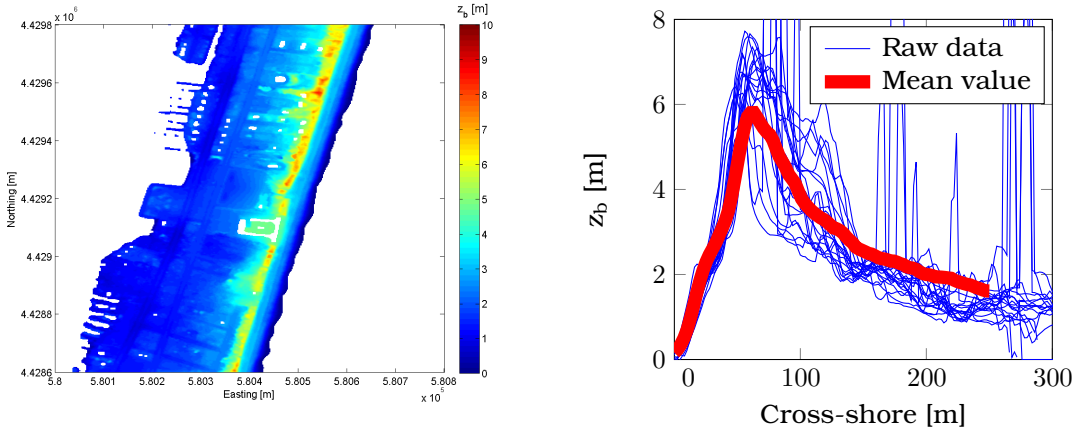

(a) *Raw LiDAR data from USGS from the barrier island at Camp Osborne (USACE, 2012)*

(b) *Mean barrier profile*

Figure E.3 *Profiles of the barrier island near Camp Osborne, New Jersey.*

E.2 DUCKS-system from Stevens

In order to set-up an XBeach model also information in the bay and bathymetry of the nearshore are needed. Stevens Institute of Technology made use of a Dynamic Underwater and Coastal Kinematic Surveying (DUCKS) system (Miller et al., 2009) to gather elevation profiles of a nearby groin field on September 22, 2011 at the city of Bay Head. For the case study an *averaged* nearshore profile is used. It is assumed that this profile is representative for all locations modeled in this case study. The maximum distance between the location of the measurements and the location were the information is used is 20 km. The information of nearshore of Stevens is used down to NAVD88 -10 m after this point the more coarse CRM will be used.

There is also data gathered of the beach and seawall, both pre- and post-Sandy, near a (buried) seawall in Bay Head (Lopez-Feliciano, 2014). This information will be used in the analysis of the 1D cross-shore effect of a hard element which is described in Section 4.4.

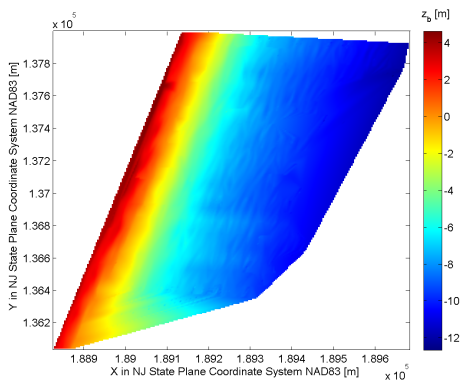

(a) *Raw data from Stevens of the nearshore Lopez-Feliciano (2014)*

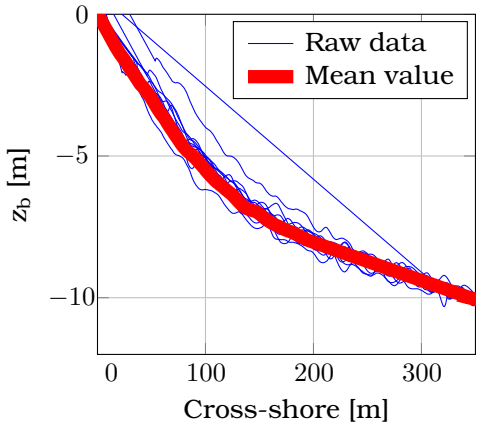

(b) *Mean nearshore profile*

Figure E.4 *Nearshore profiles of the barrier island at Camp Osborne, NJ.*

E.3 Coastal Relief Model (CRM)

For the remaining undescribed parts of the bathymetry the Coastal Relief Model (CRM) (NGDC, 2014) will be used. This model provides digital elevation data, but is coarse. For the bay side the CRM will be used directly, for the sea-side the data is used in combination with DUCKS. The date of the used information is not known and can therefore not be used in the post-storm analysis. The data is coarse, but gives a responsible indication.

E.4 Model set-up

E.4.1 Combine the different data sources

When the three data sources are combined, the bathymetry covers the entire domain. At a depth of more than NAVD88 -10 m the CRM model will be used. A smooth interpolation between the CRM and DUCKS model will be applied. On the barrier the LIDAR can directly be used. The uniform profile generated, by combining DUCKS and CRM, will be used down to a depth of NAVD88 -25 m. This uniform profile will be applied in all the field studies of Hurricane Sandy near the cities Bay Head, Mantoloking and Brick (all New Jersey).

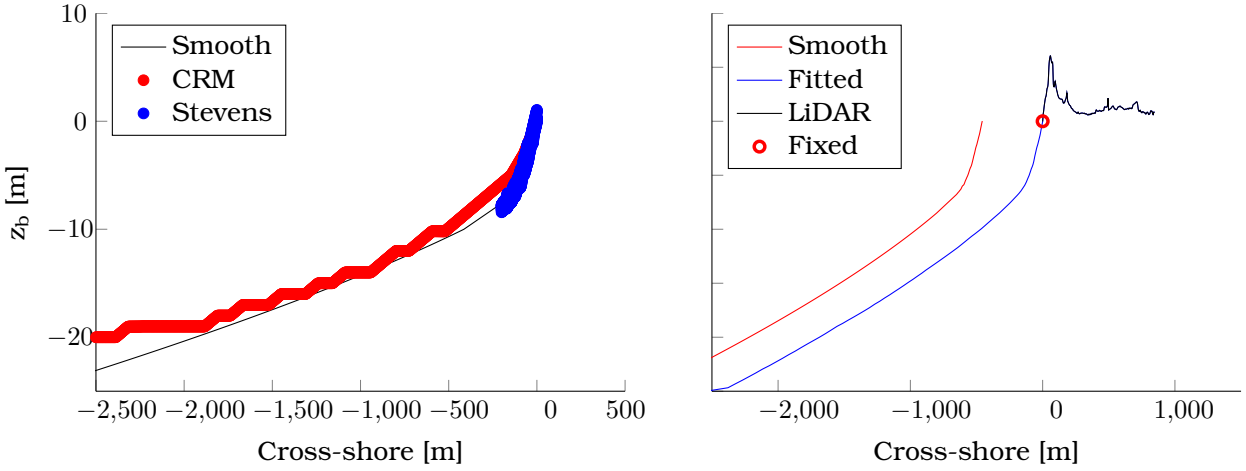

Figure E.5 *Visual description of the method used to combine different bathymetric sources.*

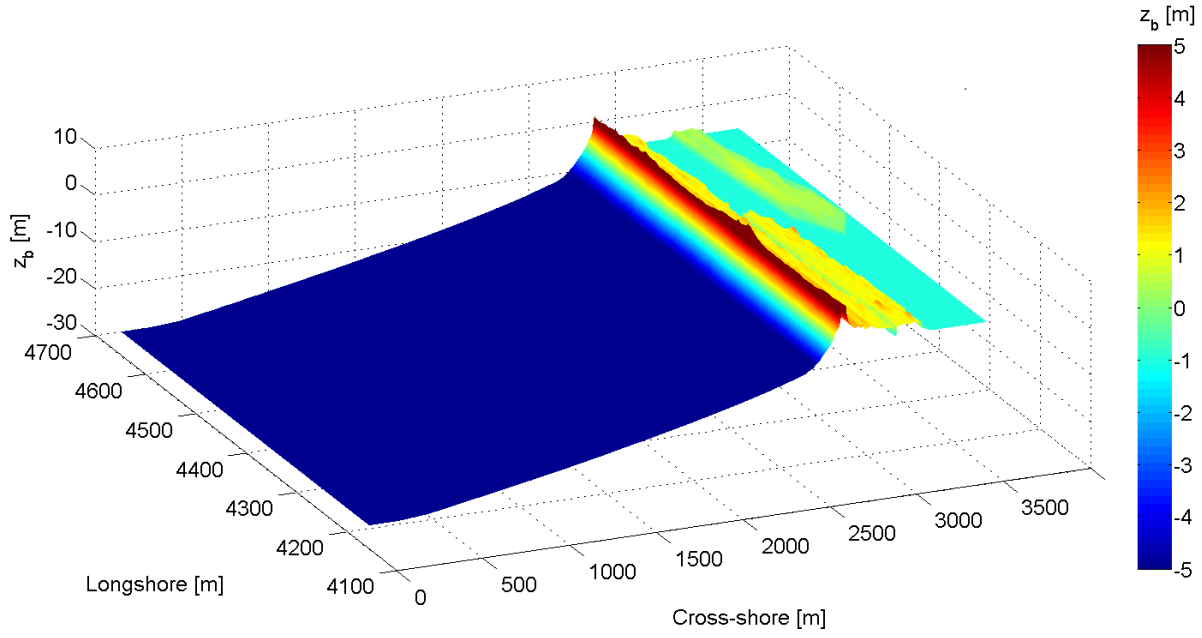

Figure E.6 *Pre-Sandy model bathymetry for Bay Head.*

E.4.2 Making the computational grid

The grid has a minimal dimension of 2 by 5 m (in x and y-direction). For deep water larger grid cells can be applied. Based on a minimum number of points per wave length the optimized grid was determined with the help of the Open Earth Toolbox.

Besides variation in x direction also a variation in y-direction can be applied. The 2DH model of Sandy needs to have large shadow zones since waves do not travel perpendicular towards the shore. The computational time is reduced by applying a maximum grid size in y-direction of 50 meter. The same toolbox is used for this variation.

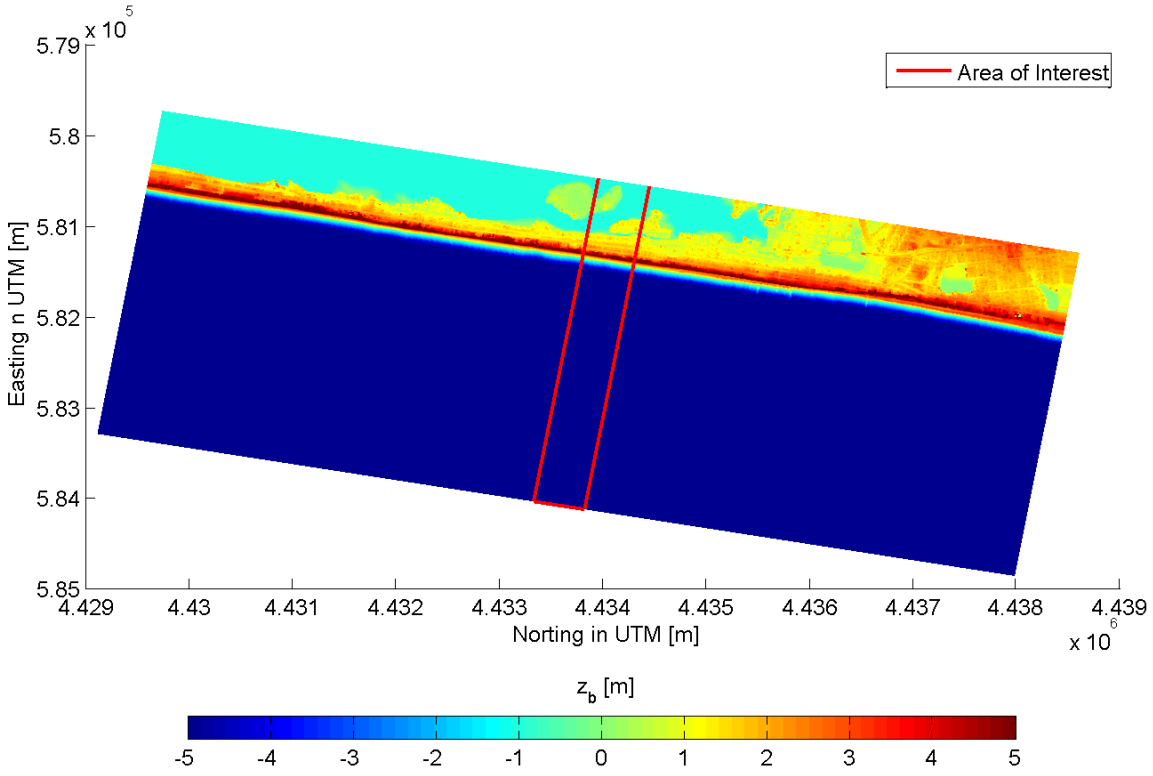

Figure E.7 *Model grid coverage for Bay Head.*

Appendix F

Hydrodynamic conditions used

F.1 Data sources available

In this Appendix three different data sources are used in order to validate the nesting of XBeach. The data sources used are:

Table F.1 *Overview of the available hydrodynamic data sources.*

Type	Number	Source	Location	Special
Tidal	8534720	NOAA	Atlantic City	Hard to hindcast
Tidal	8531680	NOAA	Sandy Hook	Stopped recording
Tidal	8518750	NOAA	Battery	-
Tidal	01408050	USGS	Manasquan	In a river
Wave	44065	NOAA	30 km offshore Sandy Hook	Used for NYC
Wave	44025	NOAA	60 km offshore Atlantic City	-

F.2 Description: impact of Hurricane Sandy

Hurricane Sandy traveled from the Caribbean to the eastern seaboard of the United States between October 22th and October 28th. Eventually on October 29th Sandy moved more to the north north-west and made landfall near Atlantic City, NJ. Landfall occurred right before midnight and resulted in a combination of winds of 130 $km.h^{-1}$, water levels up to 3.5 m and offshore significant wave heights of 9 m. In the following figures the patterns of the wind speeds and the high water levels and the wave height are plotted.

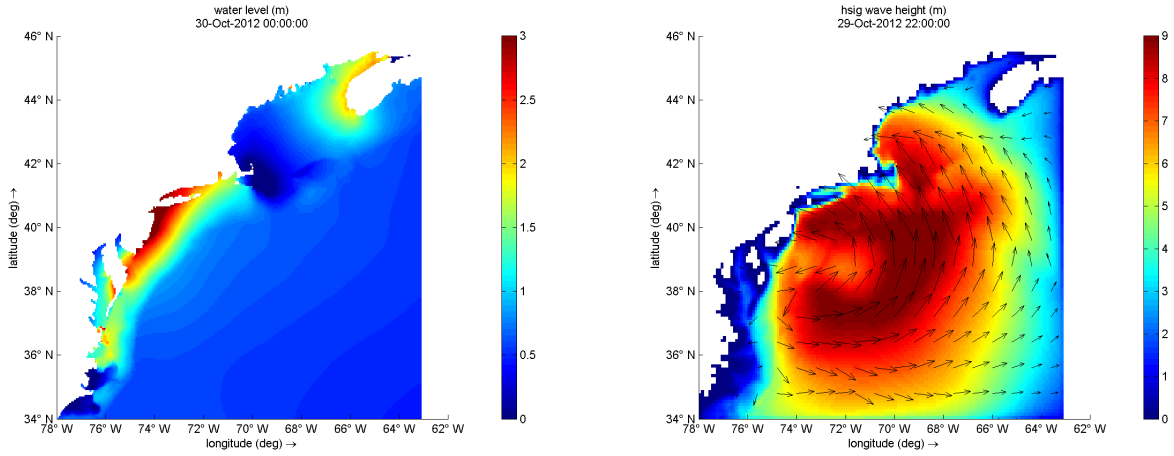

(a) *Water levels [m]* **(b)** *Wave height [m]*

Figure F.1 *Values as calculated by Delft3D during the peak of the storm, right before landfall in Atlantic City, NJ. Highest wave recorded during landfall. The highest waves 2 hours earlier.*

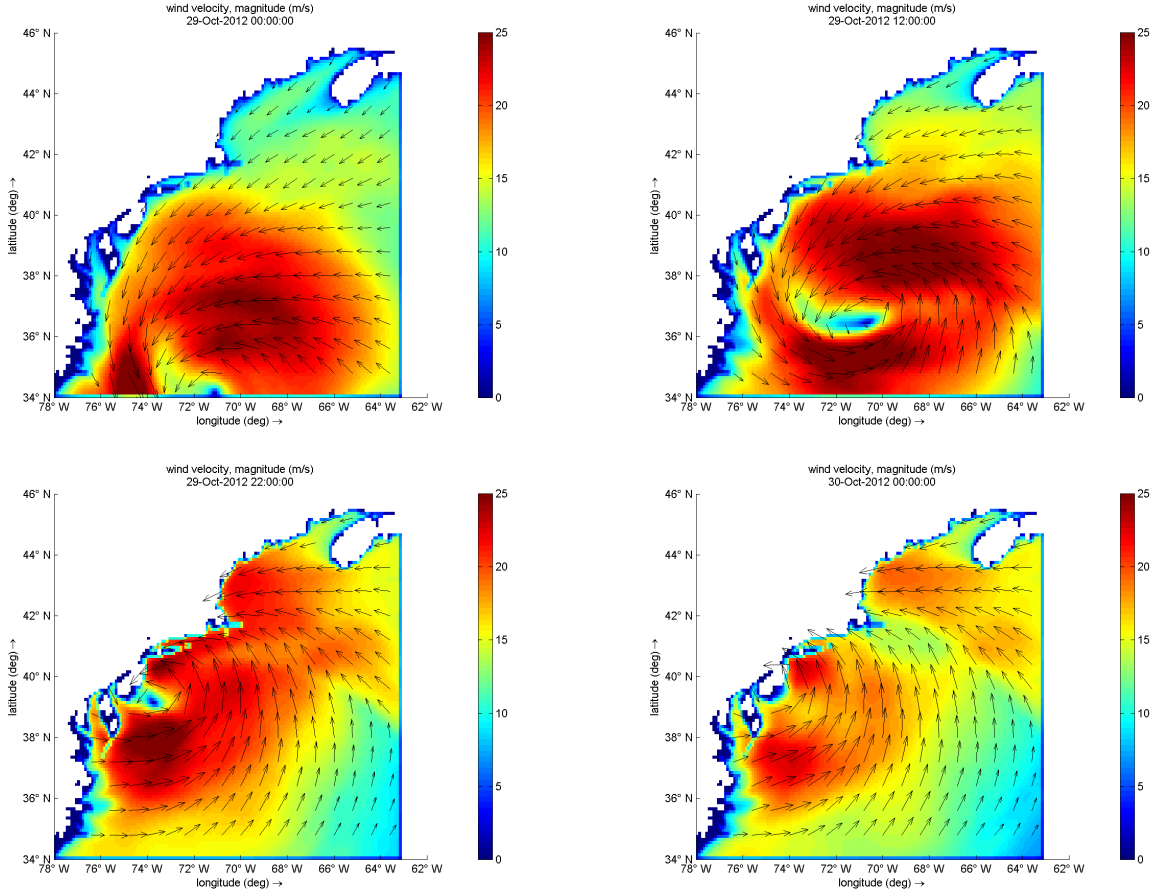

Figure F.2 *Development of the depression around Sandy: wind speed are plotted to visualize the path of Hurricane Sandy.*

F.3 Validation of existing model

F.3.1 Water levels on sea

The NOAA has three tidal gauge stations in the area of interest: Sandy Hook, Atlantic City and Battery on top of that the USGS has a gauge at Manasquan. All these measurement stations will be used for the validation of two models: Delft3D and sECOM.

Near Sandy Hook Delft3D underestimates the tidal movement with 0.2 meter, but is accurate during the peak of Sandy. The model has an almost complete fit during the first peak. The second peak is overestimated by the model. This overestimation could also be the result of model uncertainty right before the station stopped recording. However, the overestimation of the water level is most likely the result of an overestimation of wind speeds. The RMSE is 0.31 m.

The tidal signal near Atlantic City is also underestimated by Delft3D. During the peak of the storm the model however overestimates the surge with almost 0.8 m. The probable reason for this large overestimation is the exact location of the wind field in relation with the measurement station. The RMSE is 0.53 m.

For the other stations a more or less similar picture can be distinguished. Overall Delft3D predicts the water levels reasonable for the area of interest. The tidal movement is somewhat underestimated with 0.1 up to 0.2 m and the set-up during Sandy is overestimated with 0.5 up to 1.0 m. sECOM is overall more accurate. The RMSE tends to be half of that of the Delft3D model. For example Manasquan, NJ, the RMSE of Delft3D is 0.42 m and for sECOM 0.22 m.

Table F.2 *Difference in bias and RMSE between the Delft3D and the eSCOM model.*

	Bias [m]			RMSE [m]		
Location	eSCOM	Delft3D	Difference	eSCOM	Delft3D	Difference
Atlantic City, NJ	0.16	0.40	-0.24	0.20	0.53	-0.33
Battery, NY	-0.04	0.05	-0.09	0.14	0.39	-0.25
Manasquan, NJ	0.18	0.19	-0.01	0.27	0.42	-0.15
Sandy Hook, NJ	-0.00	0.03	-0.03	0.12	0.31	-0.19
Mean	0.07	0.17	-0.09	0.18	0.41	-0.23

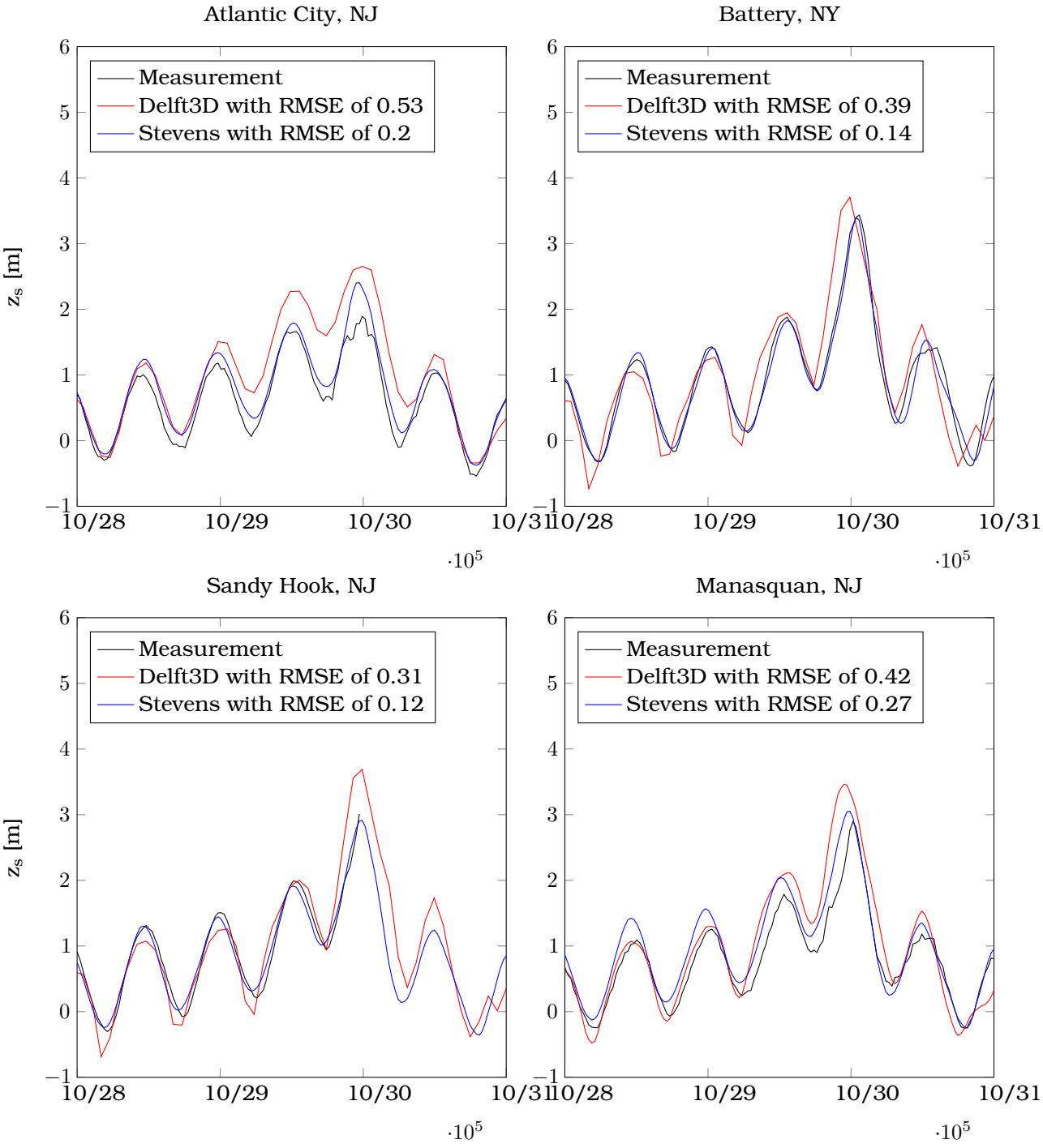

Figure F.3 *Water levels plotted for four measurement stations compared to model results as computed by Delft3D-FLOW and eSCOM.*

F.3.2 Wave height, period and direction

There are two wave buoys in the area of interest. One buoy is located near Sandy Hook and used for the New York City harbor. In addition there was also a buoy further offshore available during Hurricane Sandy. In this subsection the eSCOM model is not validated, since the error for the wave heights is an order of magnitude higher than Delft3D. The reason for this error is that the model is based on the Great Lakes model.

Delft3D-WAVE shows a good comparison with the measurements near Sandy Hook. The maximum observed significant wave height is reproduced and the rest of the storm is also reasonable modeled. There is a RMSE of 0.83 m. Modeling of wave periods is harder and the mean period is underestimated with 2 s.

The buoy further on sea is somewhat less predicted by Delft3D. The significant wave height is the entire storm, from 10/28 until 10/31 underestimated with 1.5 m. This results in a RMSE of 1.5 m, which is twice the error of the buoy near Sandy Hook. The error in wave period is similar as for the other buoy.

Overall Delft3D-WAVE shows a reasonable comparison for the wave height, but underestimates the wave periods with 2 s for all measurement. The differences between observed wave direction and modeled direction is large. The reason for this difference is not known. On top of that, the spatial distribution of wave heights is not represented in the model. However, there is no better nesting option available and therefore the spectra calculated is directly incorporated into XBeach.

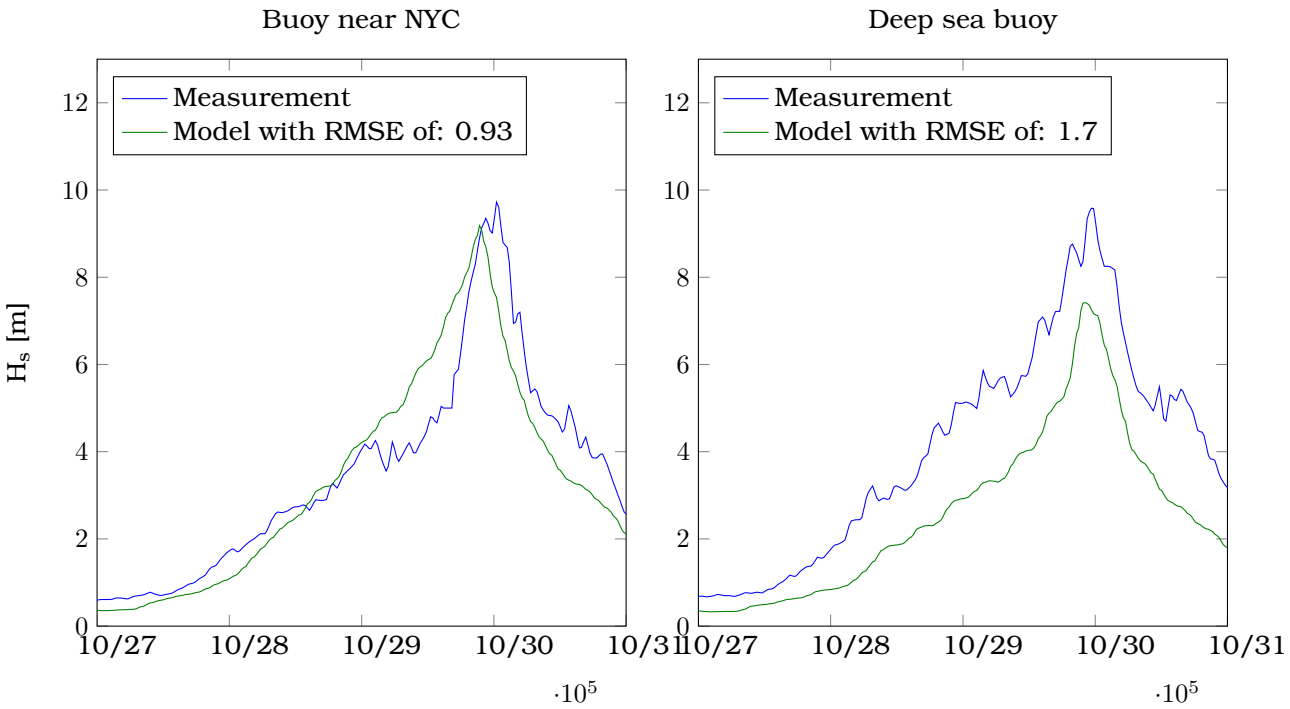

Figure F.4 *Wave heights plotted for two measurement stations compared to model results as computed by Delft3D-WAVE.*

F.3.3 Water levels in the bay

There is no model available which describes the water levels in the bay. Therefore, all the different measurement stations in the Barnegat Bay are compared. The difference in maximum water levels is limited and the maximum difference of 0.25 m develops over a distance of 3 km. The moment of the peak is for all stations similar. It can therefore be concluded that the water levels recorded at Mantoloking, NJ, can be directly imposed in the XBeach model.

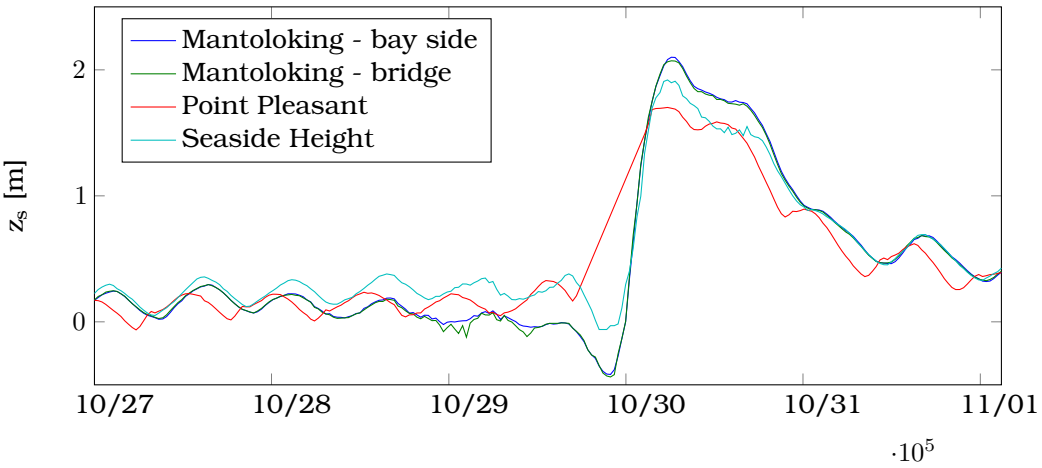

Figure F.5 *Multiple measurement points in the bay*

Appendix G

Supportive material for the case study simulations

G.1 Calibration of the $facua$

G.1.1 Hard cross-section: validation

XBeach has by default a $facua$ value of 0.1 and the model is calibrated by varying this value between 0.00 and 0.4, as can be seen in Table G.1. The highest skill score is achieved with a $facua$ value of 0.25.

Table G.1 *Results of a single hard cross-section for various values of $facua$.*

$facua$ value	A_{ero} $[m^3 \cdot m^{-1}]$	$z_{b,toe,min}[m]$	BSS [-]	Bias $[m]$
0.00	155.20	-5.1	0.09	-1.04
0.05	142.78	-4.8	0.33	-0.88
0.10	129.13	-4.3	0.56	-0.71
0.15	114.23	-3.6	0.74	-0.51
0.20	97.45	-3.0	0.89	-0.27
0.25	79.99	-2.5	0.97	-0.02
0.30	62.22	-2.3	0.95	0.24
0.35	46.30	-2.0	0.79	0.60
0.40	31.92	-1.6	0.57	0.87

G.1.2 Soft cross-section: evaluation

The first calibration step is carried out for an 1D hard cross-section within groins. In order to evaluate the calibration step of a higher $facua$ three soft cross-section are selected. This is carried out since the parameter has a large impact on the morphological behavior.

For lower values of $facua$ the system will erode too much. For example for a value of 0.10 the system will eventually breach. Interesting to see that a beach will (partly) result in sediment transport from the barrier in offshore direction. Between -100 and 0 m cross-shore the barrier will adapt to the new breach with deposition. This process is driven by the water level gradient which is during a period of time negative which means that water flows from the bay to sea. An ebb-tidal delta is created.

The evaluation shows that a higher $facua$ is defensible. The highest BSS is achieved with a value of 0.25 for the asymmetric sediment transport parameter. When comparing the variation of the bias

one could conclude that maybe even a higher value is desirable. Overall it seems that the erosion volumes are calculated accurate and thus it is assumed that a $facua$ setting of 0.25 is a proper value for this case study.

Table G.2 *Results of several soft cross-sections for various values of* $facua$

	BSS [-]				Bias [m]
$facua$	Profile 1	Profile 2	Profile 3	Mean	Mean
0.10	-2.07	0.64	0.46	-0.32	-1.030
0.15	0.04	0.75	0.67	0.48	-0.624
0.20	0.49	0.81	0.80	0.70	-0.437
0.25	0.90	0.82	0.85	0.86	-0.144
0.30	0.91	0.78	0.81	0.83	-0.008

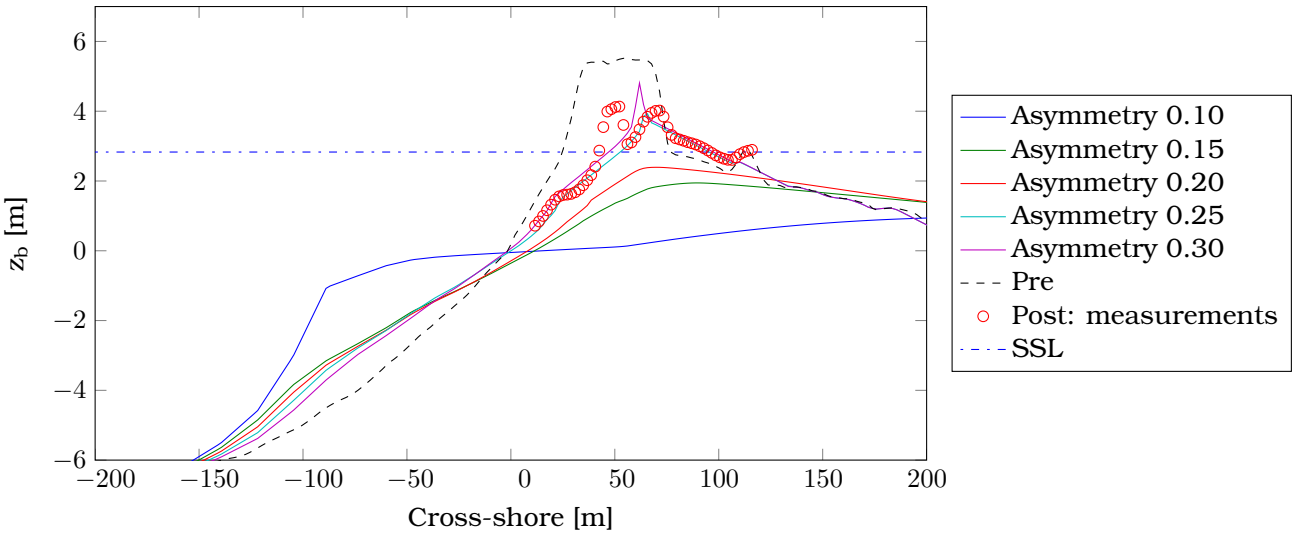

Figure G.1 *Post bed levels for a single soft cross-section for various values of* $facua$

G.2 Sensitivity analysis: (buried) seawall

G.2.1 Uncertainty in boundary conditions

Variation in water levels have been created by adjusting the amplitude of the tidal record. This is done both by changing the entire record for the positive bias of the used model and for the difference between sECOM and Delft3D. The changes variation applied are +0.1 and -0.1 m for all the water level on sea. On top of that the peak has been enhanced and reduced since the uncertainty described in Appendix F.3. The variation applied is +0.5 and -0.5 m for the peak water levels on sea.

Variation of these four simulation shows that the shape of the post simulation bed level is not noticeable different than the default run. Also the BSS and bias stays remarkably unchanged. Most change occurs in the development of the minimum bed level at the toe of the revetment. A 0.5 m higher peak results in a deeper scour hole than the simulation with an increase of +25% in spectrum energy. For all the simulations this scour hole is filled up again after the peak of Sandy.

Besides variation in water level also a variation in the spectrum energy is applied. There is a discrepancy between measurement data and Delft3D-WAVE. It is not clear how large the uncertainty is. Therefore, just a simple variation of +25 and -25% of the spectrum energy is applied. The results are a variation in erosion volume. The variation confirms a linear relation between the wave impact force and the erosion rate, according to Fisher et al. (1986). The impact on the bed level at the toe is limited, especially when comparing the large change in erosion volume and increase in spectrum energy. The bias values start to variate between -0.22 and +0.28 m, but the BSS stays remarkably high.

Table G.3 *Results for variations in boundary conditions compared to the default settings for erosion volume, scour depth, BSS and bias scores.*

Profile	A_{ero} $[m^3 \cdot m^{-1}]$	$z_{b,toe,min}[m]$	BSS [-]	Bias $[m]$
Default	79.99	0.7	0.97	-0.02
Wave energy +25%	98.13	-0.5	0.92	-0.22
Wave energy -25%	60.95	3.7	0.97	0.28
Base +0.1 m	81.79	0.1	0.96	-0.04
Base -0.1 m	78.30	0.8	0.97	0.01
Peak +0.5 m	83.53	-0.7	0.96	-0.04
Peak -0.5 m	77.85	1.7	0.97	-0.00

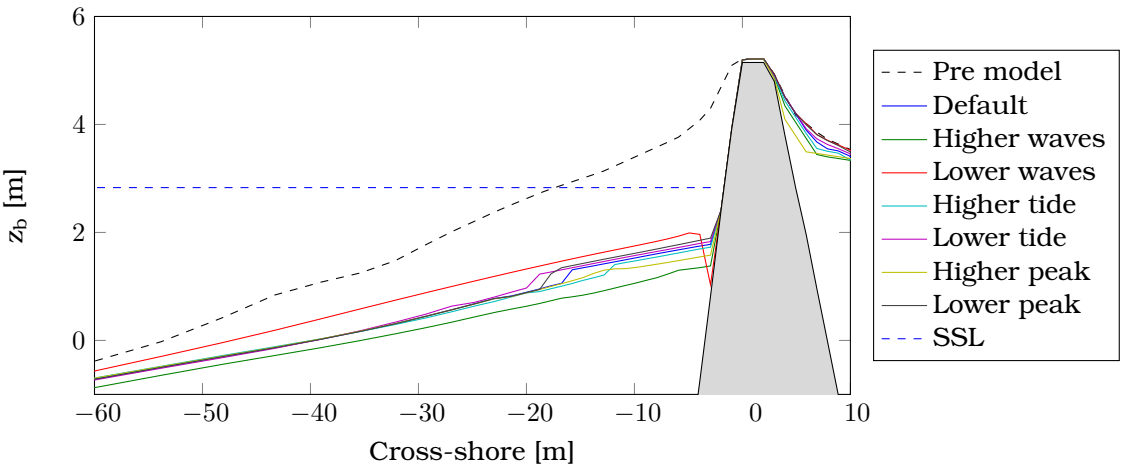

Figure G.2 *Post storm bed level for variations in boundary conditions.*

G.2.2 Scour hole development

The shape of the post Sandy bathymetry at the buried seawall was remarkable, since no clear scour holes were present. From theory one would have expected that the clear scour holes were noticeable in front of the seawall. From XBeach simulations it was concluded that infilling of scour occurred after the peak of Sandy. The suggestion was that this effect is closely related to the tidal water movement on sea. In this paragraph a reference simulation is carried out in which a constant SSL.

The result of this reference simulation in XBeach with a constant SSL is first of all 20% more erosion and second the development of clear scour hole in front of the structure. This confirms the

suggestion made in this thesis that scour is closely related to the water levels on sea. The reference simulation can be found in Figure G.3.

When the development of scour and erosion over time is plotted, it is noticed that at the moment SSL is decreasing the scour is filled up. The simulation without SSL variation has also some infilling. This infilling is not the result of material which avalanches from the top of the seawall, but is the result of a (temporary) decrease of offshore sediment transport component (decrease spectrum energy, result in decrease in undertow), but a more or less constant onshore component (generated by waves and driven by asymmetric terms).

Overall one can conclude that the variation in hydrodynamic forcing is of major importance in accurately reproducing the morphological response of the system, especially for the development of scour. Variation in SSL is the most important driven for describing the development of scour over time.

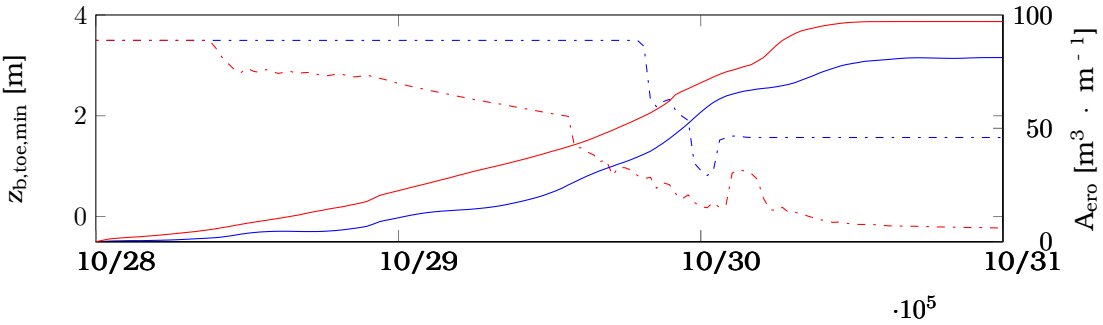

Figure G.3 *Scour depth (dashed) and erosion volumes (solid) plotted for simulation with (red) and without (blue) constant SSL.*

G.2.3 Importance and sensitivity of several XBeach parameters

In XBeach several physical descriptions are represented in source code in order to reproduce the morphological behavior in the most accurate way. These contributions can be deactivated in order to analyze the impact of each factor. In this paragraph the contribution of short waves, long waves, $swnrunup$ and the $jetfac$ are analyzed. Last two relations are implemented since the version of 'Sinterklaas' based on the recommendations described by Van Geer et al. (2012). Related to this analysis Table G.4 and Figure G.4 are presented.

First of all it is remarkable that the impact of the $jetfac$ is hardly represented by the model. Simulations with and without this contribution will result in comparable end results, comparable minimal bed levels and almost the same erosion volumes. This can mean two things. First it is possible that in this particular situation the turbulence generated at the toe is not relevant. More likely seems the possibility two which means that the $jetfac$ is not triggered.

The erosion volume without $swnrunp$ is 1.5% smaller than the base simulation. Also the depth of the scour hole is similar. In this simulation the $swnrunp$ is most likely of no importance since the storm conditions during Sandy were severe. The small difference in erosion volume is related to the erosion at the back of the seawall. This erosion occurs since short waves which are able reach run-up since the formulation of $swnrunp$.

When comparing the impact of both short as well as long waves it is first of all clear that without the undertow of the short waves hardly any sediment will be transported. This results in a post-storm

bathymetry which is almost similar as the pre-storm bathymetry. Only 2.4 $m^3 \cdot m^{-1}$ is transported. When the long waves are deactivated about 68% of the erosion still occurs. This is similar as Van Thiel de Vries (2009b), which stated that without long waves 70 % of the erosion occurs. Also the beach slope is somewhat less steep. Avalanching is in this situation of minor importance in order to calculate the erosion volumes. For the post bed level avalanching is of importance, since without avalanching the seawall would have been still buried.

Table G.4 *Results for variations in XBeach settings with the default settings for erosion volume, scour depth, BSS and bias scores as computed by XBeach*

Profile	A_{ero} $[m^3 \cdot m^{-1}]$	$z_{b,toe,min}[m]$	BSS [-]	Bias $[m]$
Default	79.99	0.7	0.97	-0.02
No $jetfac$	79.98	0.7	0.97	-0.02
No $swrunup$	78.78	0.7	0.97	-0.01
No long waves	54.19	1.7	0.97	0.41
No short waves	2.38	3.7	0.02	1.32
No avalanching	75.86	1.7	0.88	0.12

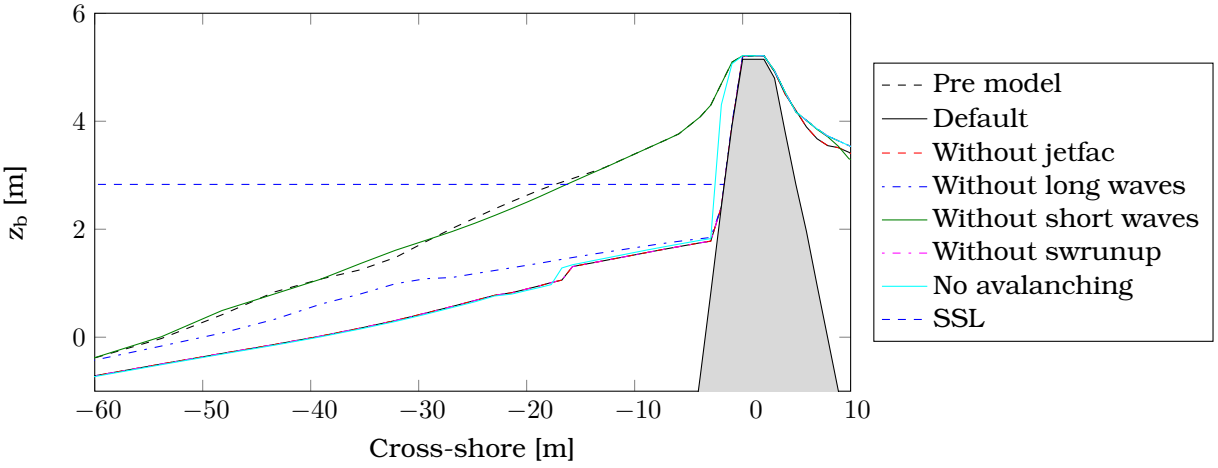

Figure G.4 *Post bathymetry for a several sensitivity runs of different processes*

G.3 Calibration of the Chezy coefficient

G.3.1 Morphodynamics: general

When applying a Chezy value of 55 $m^{0.5}.s^{-1}$ in the simulation the barrier will breach at 8 individual spots. This is related to the fact that sediment can be transported easily during overwash conditions. At every overwash spot large amounts of sediment are taken away. When a lower Chezy value is applied, transport will be reduced. A lower Chezy value can be seen as the friction generated by the presence of vegetation and/or structures. A Chezy coefficient of 30 $m^{0.5}.s^{-1}$ will result in the highest BSS, lowest bias and more or less similar amount of erosion. When the Chezy value is lowered even more, the model will introduce too much friction and will thus hinder to formation of breaches completely.

One can conclude that applying a higher roughness on the barrier is needed to model overwash in XBeach. Overall a Chezy value of 30 $m^{0.5}.s^{-1}$ will result in the best fit, but local features like a breach at y = 4700 m, are not reproduced with this uniform approach. The erosion volume is slightly underestimated with 3% and the mean dune top in the area is 0.50 m overestimated.

Table G.5 *Model performance indicators for several values of barrier roughness in Chezy for the area of interest at Bay Head*

Chezy value	BSS [-] All	Erosive	Bias [m] All	Erosive	Other A_{ero} [$m^3 \cdot m^{-1}$]	Breaches	$\overline{D_{\max}}$ [m]
55	-2.814	-0.285	-1.282	-2.320	882.6	7	1.87
45	-1.852	0.044	-0.940	-1.745	715.7	7	2.52
40	-1.136	0.271	-0.675	-1.252	578.7	6	3.06
35	0.331	0.725	-0.152	-0.250	307.1	3	3.91
30	0.844	0.909	0.104	0.464	177.6	1	4.45
25	0.835	0.898	0.118	0.565	168.9	0	4.61
20	0.829	0.887	0.124	0.632	161.6	0	4.70
15	0.825	0.881	0.129	0.676	156.8	0	4.73

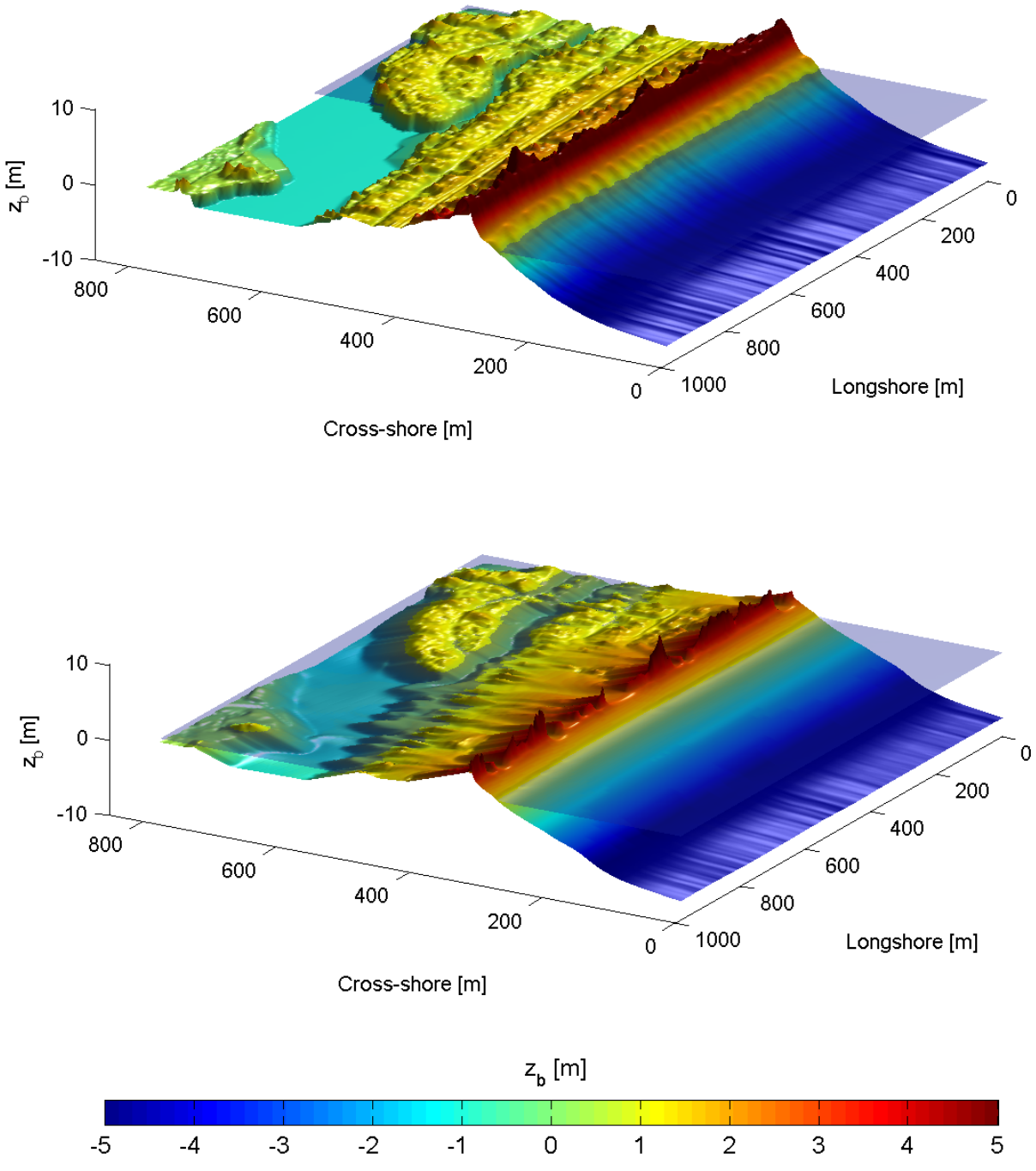

Figure G.5 *Pre- (top panel) and post-Sandy (lower panel) in a three dimensional plot with both bed and water levels of the site of Bay Head.*

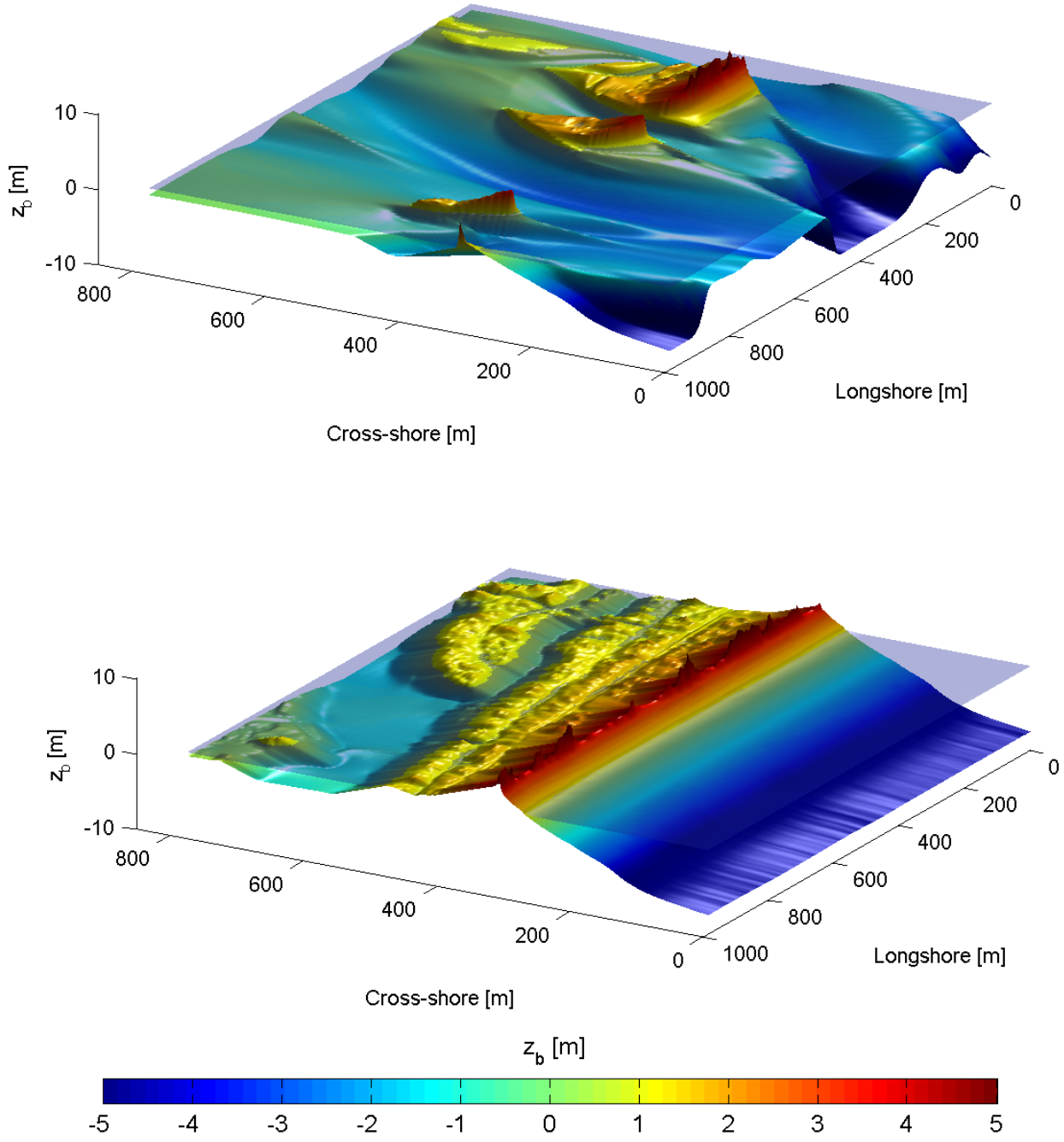

Figure G.6 *Post with a Chezy value of 55 (top panel) and post with a Chezy value of 15 (lower panel) in a three dimensional plot with both bed and water levels of the site of Bay Head*

G.3.2 Uncertainty in the sediment diameter

Table G.6 *Various morphological results for different values for sediment diameter (D_{50}).*

D_{50} [μm]	BSS [-] All	Erosion	Bias [m] All	Erosion	Other A_{ero} [$m^3 \cdot m^{-1}$]	Breaches	$\overline{D_{max}}$ [m]
150	-1.288	0.210	-0.747	-1.624	660.5	4	2.11
225	0.792	0.913	0.015	0.033	231.1	1	3.73
300	0.844	0.909	0.104	0.464	177.9	0	4.45
450	0.784	0.842	0.145	0.762	149.5	0	5.13
600	0.733	0.789	0.166	0.920	135.6	0	5.49

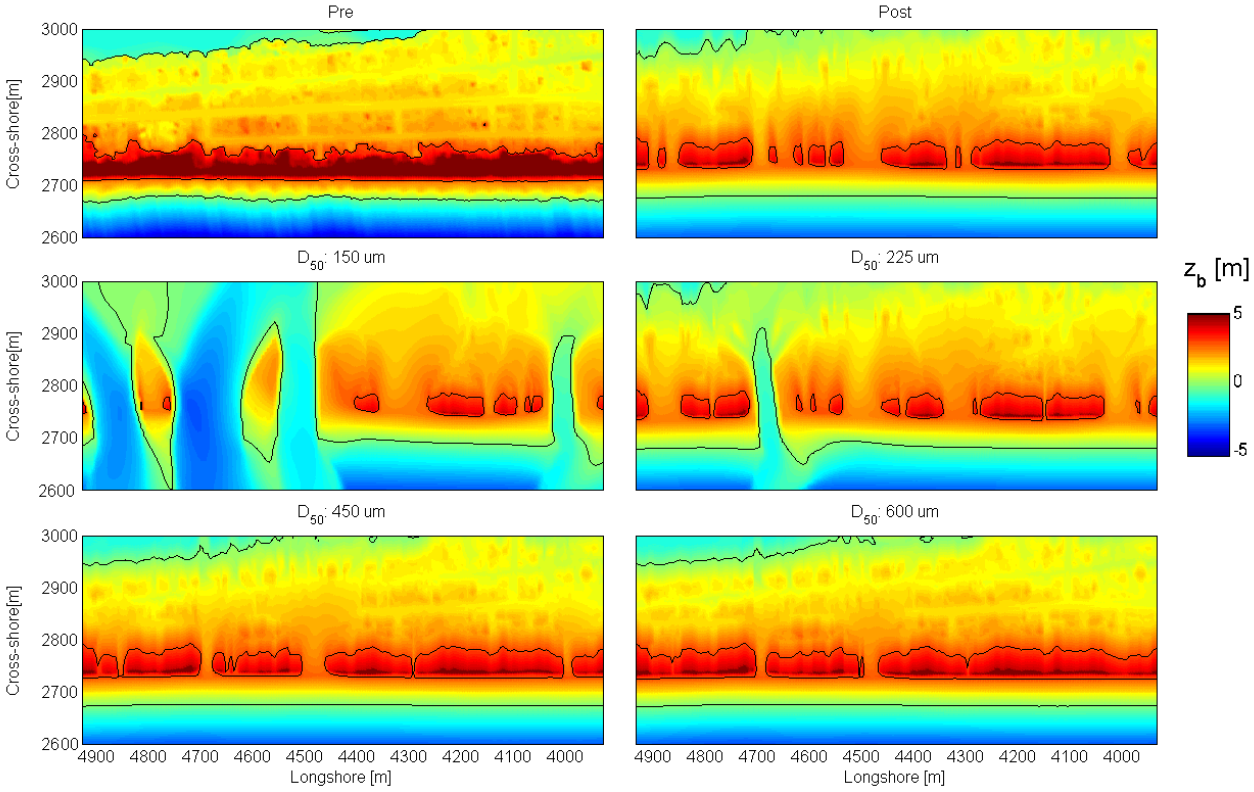

Figure G.7 *Spatial post bed levels plots after the storm event presented for the area of interest at Bay Head for three D_{50} applied. The black depth contours are provided at an elevation of 0 and 3 m relative to NADV88.*

G.3.3 Hydrodynamics: evaluation

Comparison of water marks with simulation

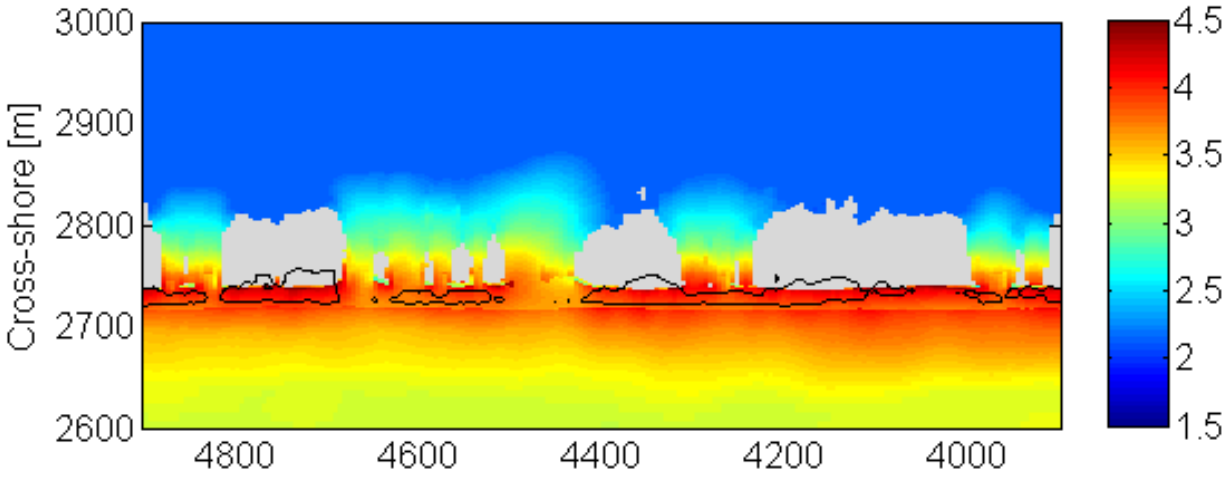

Figure G.8 *Alongshore variability for the maximum modeled water marks in XBeach. At locations were the barrier is overwash water marks are higher than at parts which are only affected by the second flood event. Grey areas were dry in the entire simulation.*

Spotting the trend of hydrodynamics

Table G.7 *Various hydrodynamic results for different roughness values, in which* u_e *is given in* $m.s^{-1}$ $H_{rms,LF}$ *and* $H_{rms,HF}$ *is used for the wave height in* m *.*

	u_e		$H_{rms,LF}$		$H_{rms,HF}$	
Chezy value	Max	Mean	Max	Mean	Max	Mean
15	0.02	0.00	0.31	0.03	0.16	0.03
20	0.03	0.00	0.41	0.05	0.22	0.04
25	0.05	0.00	0.57	0.07	0.26	0.05
30	0.10	0.01	0.77	0.11	0.30	0.06
35	3.27	0.27	2.13	0.21	0.44	0.09
40	3.93	0.78	2.73	0.51	0.56	0.15
45	4.03	1.39	3.48	0.77	0.70	0.27
55	4.06	1.92	3.51	0.96	0.93	0.44

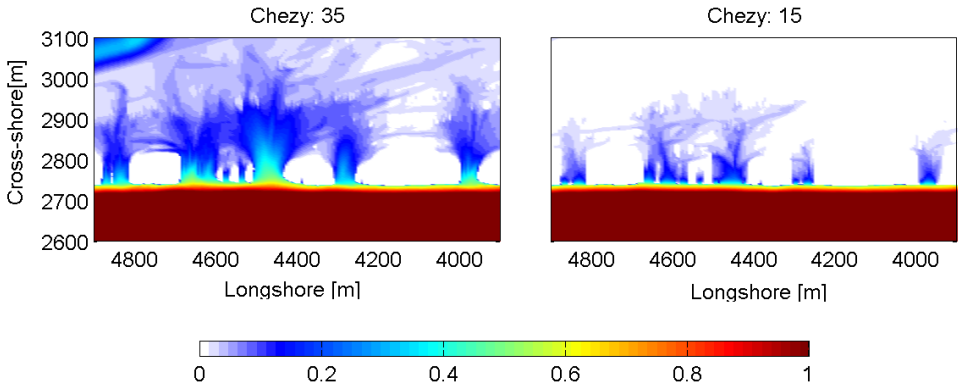

Figure G.9 *Spatial plot of the storm-maximum root-mean square short wave height [m] for both a Chezy value of 35 as well as 15 $m^{0.5}.s^{-1}$. Smoother barrier islands will have a higher mean short wave height on the barrier.*

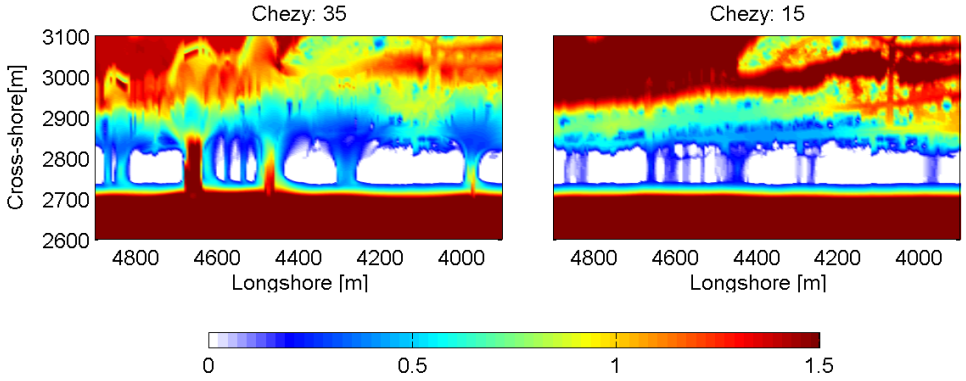

Figure G.10 *Spatial plot of the storm-maximum root-mean square long wave height [m] for both a Chezy value of 35 as well as 15 $m^{0.5}.s^{-1}$. Smoother barrier islands will have a higher mean long wave height on the barrier.*

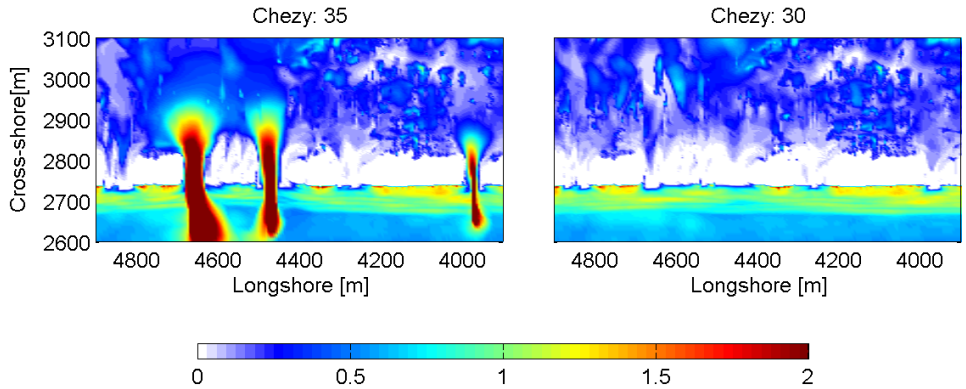

Figure G.11 *Spatial plot of the storm-averaged maximum Eulerian velocity [$m.s^{-1}$] for both a Chezy value of 35 as well as 30 $m^{0.5}.s^{-1}$. Remarkable is the decrease in velocity on the barrier for slightly rougher barrier.*

G.4 Sensitivity: avalanching algorithm for Bay Head

In Table G.8 the results of multiple simulations, in which a number of parameters, are varied presented. Variation in critical dry slope, h_switch and dz_{max} have only limited impact. A decrease in $m_{cr,dry}$ means an increase erosion volume and a somewhat higher BSS, but the effect is limited (in the order of 0.21 % per 0.1 change in critical slope in terms of erosion volume). A decrease in water depth interface of 0.025 m will result in a 0.34% increase in erosion volume. A higher maximum dune face erosion rate increases the erosion somewhat (+0.9 %). As described in Appendix G.4 the default value in XBeach for the maximum dune face erosion rate is somewhat too high, but the impact in terms of morphological behavior is limited.

The model is sensitive for change in critical wet slope. A decrease of 0.1 in slope results in an increase of 16% in terms of erosion volume. In addition this value also controls the amount of overwash that occurs during the simulation. Higher critical slopes will mean less erosion than low critical slopes. In practice a critical slope is a soil property and not a calibration parameter. However, a data analysis has showed that in the (filtered, last-response) LiDAR the maximum wet slope is 0.22. Therefore, in the model set-up, a critical wet slope of 0.2 instead of the default 0.3 is applied. In this analysis however the highest BSS is achieved with a value of 0.10 instead of 0.3 (default) or 0.20 (the found level).

Besides erosion volumes and BSS also the mean dune top is an output parameters of interest. Only variation in critical wet slope has an impact of more than 0.1 m. A decrease in critical wet slope with 0.1 will result in a decrease of the mean dune top of 0.8 up to 1.2 m.

Without the avalanching algorithm XBeach is not capable in reproducing the morphological behavior with a BSS of higher than 0.28. The erosion volumes are underestimated with 56% and the mean dune top is similar as the initial bathymetry.

Table G.8 *Model performance indicators for several values for the avalanching algorithm for the area of interest at Bay Head.*

Runs	BSS [-] All	Erosive	Bias [m] All	Erosive	Other A_{ero} [$m^3 \cdot m^{-1}$]	$\overline{D_{\max}}$ [m]
$m_{cr,wet}$: 0.3	0.801	0.857	0.125	0.654	161.2	5.3
$m_{cr,wet}$: 0.2	0.844	0.909	0.104	0.464	177.6	4.5
$m_{cr,wet}$: 0.1	0.867	0.952	0.063	0.190	206.2	3.3
$m_{cr,dry}$: 0.9	0.802	0.858	0.125	0.661	160.2	5.3
$m_{cr,dry}$: 0.8	0.806	0.861	0.124	0.656	160.7	5.2
m_{cr}: 0.2-0.9	0.846	0.912	0.102	0.454	178.8	4.4
m_{cr}: 0.1-0.8	0.867	0.952	0.062	0.184	206.7	3.3
h_{switch}: 0.075 m	0.807	0.864	0.125	0.637	162.5	5.2
h_{switch}: 0.050 m	0.811	0.868	0.123	0.627	163.6	5.2
dz_{max}: 1 $m^3.ms^{-1}$	0.846	0.912	0.101	0.448	179.2	4.4
dz_{max}: 0.003 $m^3.ms^{-1}$	0.764	0.813	0.126	0.725	155.7	5.5
No avalanching	0.077	0.080	0.282	1.741	78.3	6.5

G.5 Sensitivity analysis: Camp Osborne

G.5.1 Sensitivity of the calibration steps applied

In this subsection the complete analysis of the sensitivity of calibration steps applied is analyzed. In Table G.9 the results of this analysis are presented. Below the analysis can be found:

The same pattern in importance for the simulations of Bay Head as for Camp Osborne are found. By default XBeach predicts a mean erosion of 1193 $m^3 \cdot m^{-1}$. This is 7 times the modeled erosion when a higher $facua$ and some barrier roughness is applied.

XBeach simulations of the area of interest are mainly sensitive for variation of barrier roughness. Varying roughness on the barrier makes it possible to determine the amount of erosion during overwash. A variation of 5 $m^{0.5}.s^{-1}$ will increase / reduce the mean erosion with 52 down to 12 %. One alongshore uniform roughness is however an oversimplification. The mean distribution of sediment can be reproduced, but for example the erosion peak next to the condo would have behaved morphological more correct with a Chezy value of 25 $m^{0.5}.s^{-1}$. It is therefore assumed that the calibration of roughness results in a too smooth barrier for Camp Osborne. At least too smooth for the spot next to the condo.

The model is also sensitive for a variation in $facua$. A variation of 0.05 results in 25-30 % more/less mean erosion and also the dune top will be 0.4 m higher/lower. Interesting to see that the erosion at the side of the condo will reduce with 60% when a $facua$ of 0.30 instead of 0.25 is applied. This gives rise to the idea that the erosion spot next to the condo is eroded (forced) sufficient in the base simulation and a small decrease of forcing (or increase of the onshore transport via $facua$) can keep this point in a position were it is not vulnerable for the second flood event via the bay.

Also a reference simulation with s_{max} is applied. The mean erosion volume calculated is however 25% lower and also the mean dune top level is not reproduced correctly. The option of both a higher asymmetric sediment transport component and higher friction on the barrier will result in better skill scores, better reproduction of the mean erosion volume and a mean dune top level more comparable with the measurement data.

Running an XBeach model without a higher value for the $facua$ and no increased roughness on the barrier will result in too much erosion, both in the earlier collision regime as well as during the peak of the storm when the barrier is overwashed. The combination of the two makes it possible to describe the field case in a morphological accurate matter with a BSS of 0.89. When only the $facua$ is applied the collision regime (dune erosion) is modeled accurately (with less offshore sediment transport when compared the default XBeach run). However, when at a spot overwash occurs, too much sediment is transported. Roughness is needed to reduce erosion during overwash conditions. The simulation with only an increased barrier roughness will reduce the sediment transportation during overwash, but both the time period and the areas where overwash occurs, are overestimated. This is related to more dune erosion and therefore the dune top will avalanche faster. Also a reference simulation with s_{max} is applied. The results are *good* (BSS of 0.61). Applying a artificial limiter, like s_{max}, makes it possible to reasonable predict hurricane events on barrier islands without the need to calibrate.

Table G.9 *The sensitivity for calibration steps in terms of skill and erosion patterns. Erosion volumes are given in* $m^3 \cdot m^{-1}$.

	BSS [-]		Bias [m]		A_{ero}		D_{max} [m]	
Runs	All	Erosive	All	Erosive	Max	Mean	Min	Mean
Blank	-1.900	-2.508	-3.143	-2.847	2125.6	1193.3	-0.7	2.2
Only $facua$	-1.315	-1.437	-2.650	-1.907	2043.6	908.7	-1.0	3.4
Only Chezy	0.027	0.412	-1.487	-1.027	1108.8	328.6	0.2	3.6
Both	0.216	0.893	-1.225	-0.245	512.1	169.7	1.1	4.6
Chezy - 25	0.223	0.937	-1.211	-0.119	213.5	149.9	2.4	4.8
Chezy - 30	0.216	0.893	-1.225	-0.245	512.1	169.7	1.1	4.6
Chezy - 35	0.090	0.627	-1.380	-0.546	1050.3	258.1	0.3	4.3
$facua$ - 0.20	0.167	0.741	-1.312	-0.581	823.9	226.6	0.3	4.2
$facua$ - 0.25	0.216	0.893	-1.225	-0.245	512.1	169.7	1.1	4.6
$facua$ - 0.30	0.219	0.924	-1.183	0.091	202.5	133.7	2.4	5.0
s_{max}	0.191	0.607	-1.161	0.421	140.0	100.8	3.8	6.2

G.5.2 Impact of variation in bay water and bed levels

In this subsection the complete analysis of the impact of the bay bed and water levels is analyzed. The analysis is presented below:

When the water level gradient is reduced to almost zero by applying the same water level at sea as in the bay the mean amount of erosion is more or less similar. The effect is similar since negative and positive processes cancel each other out. First, the impact of increasing water levels in the bay is avalanching at the bay side of the back barrier (more erosion). Second, reduction of the water level gradient results erosion in the overwash regime (less erosion). Antoher effect is that the alongshore variation in erosion decreases. For example: the peak in erosion next to the condo does not occur. A constant bay level at NAVD88 will also result in more smooth alongshore erosion patterns, but will not result in more erosion as seen in other simulations (McCall, 2008). These patterns give rise to the idea that an alongshore variation of erosion is related to a bay influence. Remarkable is that the morphological accuracy of both runs increases. The lack of erosion peak is responsible for this increase.

Measurements have shown that there was a phase lag between the surge on sea and in the bay. In fact the area of interest was hit by two separate flood events. The system is sensitive when this phase lag is reduced or increased. On average a lag of 4 hours means an increase in erosion volume of 10%. Overall a phase lag between the sea and the bay will result in higher mean erosion volume and a more discontinuous distribution alongshore due to that initial small breaches erode even more driven by more backwash.

The depth in the bay is not completely known and based on the CRM. On average a bay bed level of NAVD - 1 m is applied. Simulations suggest that for the overall morphological response of the system the bed level in the bay is of minor importance. When this bed level bay is reduced to NAVD -0.5 m the mean erosion decreases somewhat, but the erosion peak next to the condo increases with 8%. A decrease in erosion volume of 2.5% can be found for a bay level which is more deep. These patterns are related to the formation of the ebb tidal delta.

Table G.10 *The influence on skill and erosion patterns for several changes related to both the water and the bottom level in the bay. Erosion volumes are given in* $m^3 \cdot m^{-1}$.

	BSS [-]		Bias [m]		A_{ero}		D_{max} [m]	
Runs	All	Erosive	All	Erosive	Max	Mean	Min	Mean
Default	0.216	0.893	-1.225	-0.245	512.1	169.7	1.1	4.6
$z_{s,sea}$ = $z_{s,bay}$	0.229	0.936	-1.208	-0.121	190.0	142.7	2.6	4.8
Constant $z_{s,bay}$	0.214	0.926	-1.234	-0.208	266.3	168.8	2.0	4.6
No lag $z_{s,bay}$	0.227	0.929	-1.208	-0.173	203.7	149.0	2.2	4.7
More lag $z_{s,bay}$	0.207	0.888	-1.245	-0.254	576.8	184.5	0.8	4.6
z_b = -0.5 m	0.224	0.883	-1.207	-0.252	553.6	175.6	4.6	0.9
z_b = -1.5 m	0.192	0.897	-1.267	-0.250	500.4	176.6	4.6	1.2

G.5.3 Uncertainty in boundary conditions

In this subsection the complete analysis of the impact of uncertainty in the boundary conditions is analyzed. The analysis is presented below:

In Section 4.4.4 the linear relation of Fisher et al. (1986) was reproduced for a hard cross-section. Variation in wave spectrum relates for soft 2DH models as expected, but has a weaker relation for decreasing spectrum energy than suggested. Spectrum energy is dominant in steering the amount of erosion, but is for the mean dune top level of less importance. In terms of morphological accuracy a reduction in wave energy will result in a better BSS and a lower bias. The range of the BSS varies between 0.81-0.92 which is for all simulations *excellent*. When the spectrum energy has 25% more energy the overwash fans next to the condo would have completely breached. The reason for the better scores for lower conditions are related to the overestimation of the erosion in the overwash fan next to the condo. The ratio between the maximum and mean erosion volume stays remarkably large (2.5x, 3x and 3.5 times the mean erosion)

Small variations in water level have already a high morphological impact. A water level which is increased with +0.1 m will already result in 17% more erosion. This increase in erosion will also be reflected by the extreme erosion peak next to the condo. Remarkable is the increase in predictive skill for a base simulation with lower water levels.

The peak in the water level is the most dominant variation. A peak which is 0.5 m higher will mean that the entire system will suffer from two times as much erosion. The mean bed level will be 0.9 m lower and just like the simulation with the increase in wave energy the weak spot near the condo would have breached. A decrease of the peak level with 0.5 m, on the other hand, results in no clear overwash fan, a decrease of 40% in terms of erosion and an 1.2 m higher mean dune level. On top of that, the ratio maximum and mean erosion decreases considerably to 130%.

Overall the field case of Camp Osborne is mainly sensitive for a variation in water level. For decreasing values of the hydrodynamic forcing simulations will have a somewhat higher BSS and a less negative bias. This gives rise to the idea that the conditions occurred in reality are somewhat lower than modeled in XBeach.

Table G.11 *The sensitivity in skill and erosion patterns for variations in the boundary conditions. Erosion volumes are given in* $m^3 \cdot m^{-1}$.

Runs	BSS [-] All	Erosive	Bias [m] All	Erosive	A_{ero} Max	Mean	D_{max} [m] Min	Mean
Default	0.216	0.893	-1.225	-0.245	512.1	169.7	1.1	4.6
Waves +25%	0.190	0.808	-1.282	-0.468	703.1	204.7	0.5	4.4
Waves -25%	0.224	0.914	-1.204	-0.153	425.2	155.7	1.4	4.8
Base +0.1 m	0.196	0.828	-1.256	-0.391	690.0	199.8	0.6	4.3
Base -0.1 m	0.218	0.923	-1.214	-0.109	266.4	150.1	1.9	4.9
Peak +0.5 m	-0.026	0.409	-1.505	-0.867	1157.1	346.8	0.3	3.5
Peak -0.5 m	0.209	0.823	-1.214	0.118	158.1	121.1	3.5	5.8

G.5.4 Importance and sensitivity of several XBeach parameters

In XBeach several physical descriptions are represented in the source code in order to reproduce the morphological behavior in the most accurate way. These contributions can be deactivated in order to analyze the impact of each factor. In this paragraph the contribution of $swnrunup$, $jetfac$, short waves, long waves and avalanching are analyzed. The results are presented in Table G.12.

When comparing the simulation with and without the $jetfac$ activated, the impact is negligible. It is not known if the $jetfac$ relation is not activated or is compensated by a specific process (counter force). This lack of effect was also found for the buried seawall.

The profile without the parametric relation short wave run-up ($swrunup$) seems to represent the post profile in a *more* accurate way. This is most likely related to a bug in the XBeach source code. It looks that the critical wet slope is applied on the entire barrier island when the keyword is activated. Therefore, the profiles on the bay are not modeled correctly and is it possible to achieve a higher BSS, lower bias and less erosion (both mean and max) when *not* applying short wave run-up.

Without the contribution of long waves only 60 % of the erosion would have occurred. This is related to the function of the long waves to trigger the avalanching algorithm. This percentage is somewhat lower than the 75% in the conceptual collision study (Chapter 3.4). The reason for this increase is the fact the avalanching algorithm is of more important for overwash, since long waves are needed to trigger the avalanching algorithm. Without the short-wave driven undertow only 15% of the erosion will occur and about half of the erosion is direct avalanching-related.

Table G.12 *The sensitivity for several parameters in XBeach in terms of skill and erosion patterns. Erosion volumes are given in* $m^3 \cdot m^{-1}$.

Runs	BSS [-] All	Erosive	Bias [m] All	Erosive	A_{ero} Max	Mean	D_{max} [m] Min	Mean
Default	0.216	0.893	-1.225	-0.245	512.1	169.7	1.1	4.6
No $jetfac$	0.216	0.892	-1.225	-0.245	516.7	169.8	1.1	4.6
No $swnrunp$	0.227	0.901	-1.215	-0.137	438.0	145.7	1.4	4.8
No long waves	0.213	0.710	-1.163	0.309	135.1	103.1	4.1	6.2
No short waves	0.086	0.022	-1.093	1.478	56.4	23.9	4.3	6.5
No avalanching	0.148	0.118	-1.194	0.533	102.7	81.5	4.3	6.5

G.6 Validity of the morfac

General The morphological accretion factor (morfac) reduces the computational time by applying the morphological changes for a certain factor. This means that the hydrodynamic results are used for a number of times, as can be seen in Equation A.15. In this thesis, field cases are applied with a morfac of 10. With this factor the simulation time is 36 hours when using 8 computational cores. Without this factor the time needed will be a factor 10 higher. The effects of a acceleration factor are on forehand not completely known, but in previous studies for the morphological effects of hurricane impact with XBeach similar acceleration factor has been used (McCall, 2008; De Vet, 2014). In this section the impact of the morfac will be analyzed for both Bay Head (Section 4.5) as Camp Osborne (Section 4.6).

G.6.1 Bay Head

The information of the comparison is presented in Table G.13 and the figures below. In general, the following conclusions can be drawn:

1. The patterns in post-Sandy bathymetry are comparable. Locations were with morfac = 10 an overwash fan develops are similar as with morfac =1.
2. A morphological acceleration factor will result in more dune erosion than simulations without this acceleration. This is related to the feed-back loop in the process-based model. For example, dune erosion will result sedimentation in the nearshore. This results in more dissipation of waves and thus less erosion will occur the next time step. The difference in erosion volume is 7.5%.
3. The effect of this decrease in erosion volume is that the mean dune top will be 0.4 m higher. This is visible at y = 4700 - 4800 m.
4. The effect of a higher morfac on the development of overwash fans is that the width of these fans will decrease with several meters. This effect is visible at y = 3950 m.
5. The model is currently calibrated for a morfac = 10. This can be seen clearly when comparing the BSS and bias. Higher BSS scores and lower bias values are achieved for morfac=10.
6. Based on these observations it is clear that differences exist between a simulation with morfac = 10 and morfac = 1. For the collision regime these differences can be compensated with calibration of the $facua$. For the overwash regime these difference are accepted compared to the advantages of a shorter simulation time.

Table G.13 *Model performance indicators: BSS, bias, mean erosion volume and mean dune top height for different morphological accretion factors.*

Runs	BSS [-] All	Erosive	Bias [m] All	Erosive	Other A_{ero} [$m^3 \cdot m^{-1}$]	$\overline{D_{max}}$ [m]
morfac: 10	0.844	0.909	0.104	0.465	177.0	4.5
morfac: 1	0.812	0.873	0.117	0.590	163.6	4.9

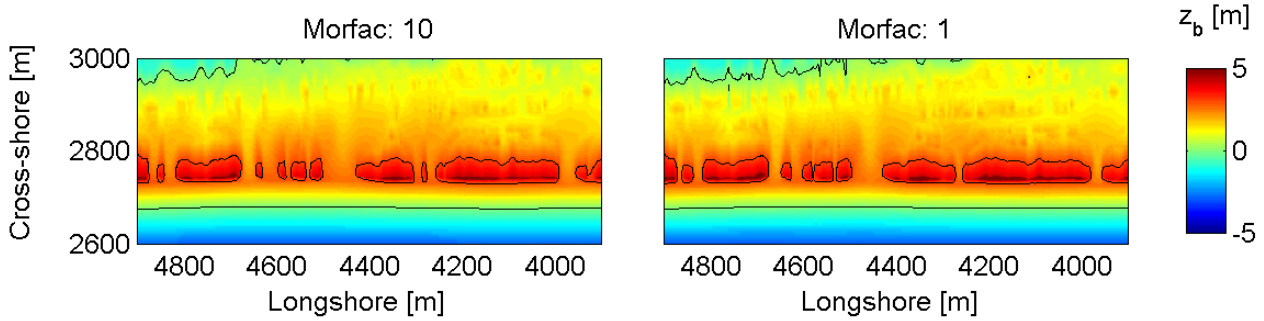

Figure G.12 *Spatial post bed level plots for the area of interest at Bay Head for morfac = 10 and 1. Spots without data are marked white. The black depth contours are provided at an elevation of 0 and 3 m relative to NADV88.*

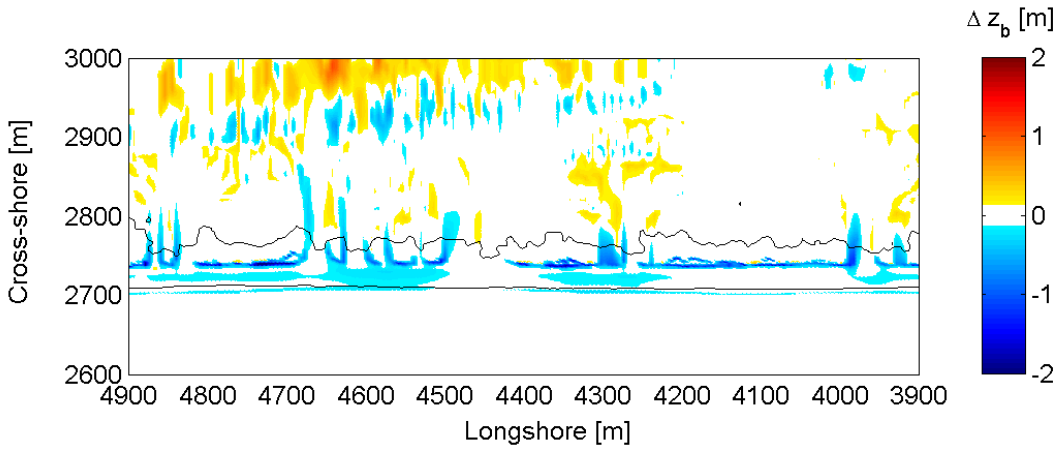

Figure G.13 *Spatial post bed level comparison for the area of interest at Bay Head between morfac = 10 and 1 (10 -1). Spots without data are marked white. The black depth contours are provided at an elevation of 3 m relative to NADV88 of the pre-Sandy bathymetry.*

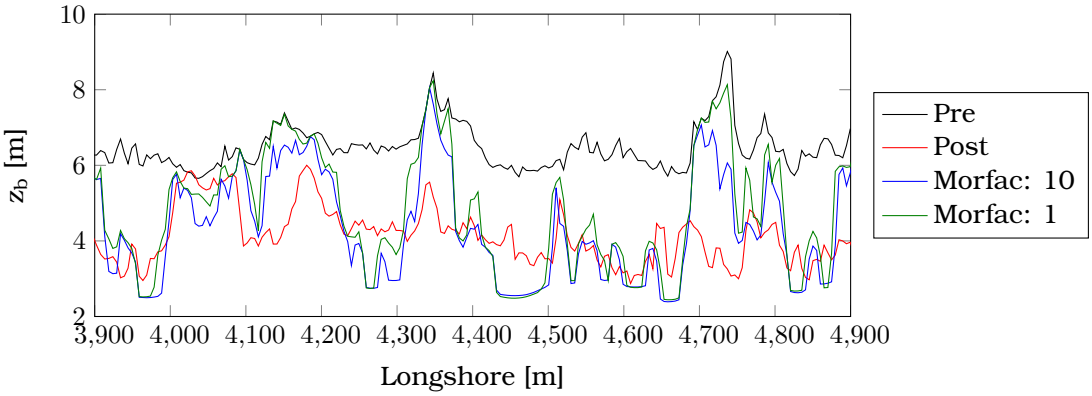

Figure G.14 *Maximum crest height in longshore direction pre-Sandy, post-Sandy and as calculated by XBeach for morfac = 10 and = 1 for Bay Head*

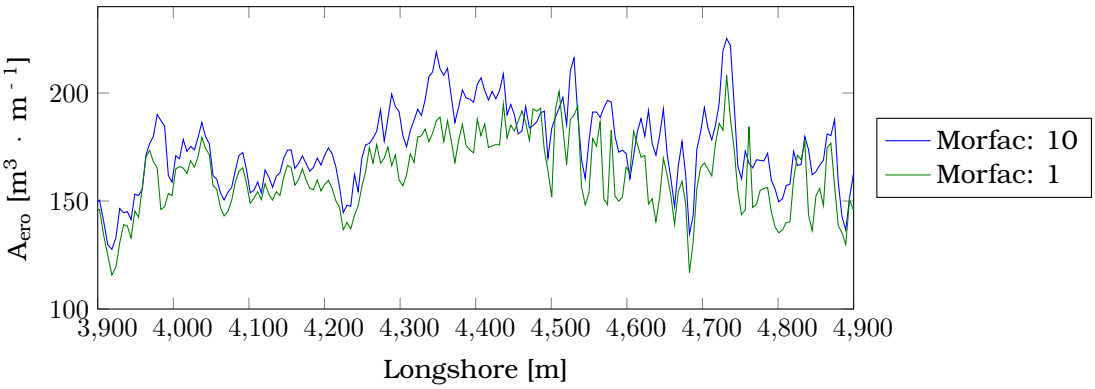

Figure G.15 *Differences of the alongshore erosion volume in $m^3 \cdot m^{-1}$ for the area of interest between morfac = 10 and =1 at Bay Head.*

G.6.2 Camp Osborne

The information of the comparison is presented in Table G.14 and the figures below. In general, the following conclusions can be drawn:

1. The overall patterns in post-Sandy bathymetry are more or less comparable. Locations were with morfac = 10 an overwash fan develops are similar as with morfac =1. Some differences are present next to the condo.
2. A morphological acceleration factor will result in more dune erosion than simulations without this acceleration. However, in this specific comparison the mean erosion volume decreases only with 1.3%. This is related to the fact that for backwash a morfac will enhance the erosion volume, this is in contrast to dune erosion.
3. The main difference occurs at the weak spot next of the condo. At y = 4500 m the combination of a weak spot, hotel and backwash creates a small breach. In the reference simulation with a morfac = 1 the breach is located somewhat more close to the condo and the scour is somewhat deeper.
4. Based on these observations it is clear that differences exist between a simulation with morfac = 10 and morfac = 1. For the collision regime these differences can be compensated with calibration of the $facua$. For the overwash and backwash these difference are accepted compared to the advantages of a shorter simulation time.

Table G.14 *Model performance indicators: BSS, bias, mean erosion volume and mean dune top height for different morphological accretion factors.*

Runs	BSS [-] All	BSS [-] Erosive	Bias [m] All	Bias [m] Erosive	Other A_{ero} [$m^3 \cdot m^{-1}$]	Other $\overline{D_{max}}$ [m]
morfac: 10	0.200	0.905	-0.975	0.035	167.7	4.6
morfac: 1	0.194	0.886	-0.972	0.094	165.6	4.8

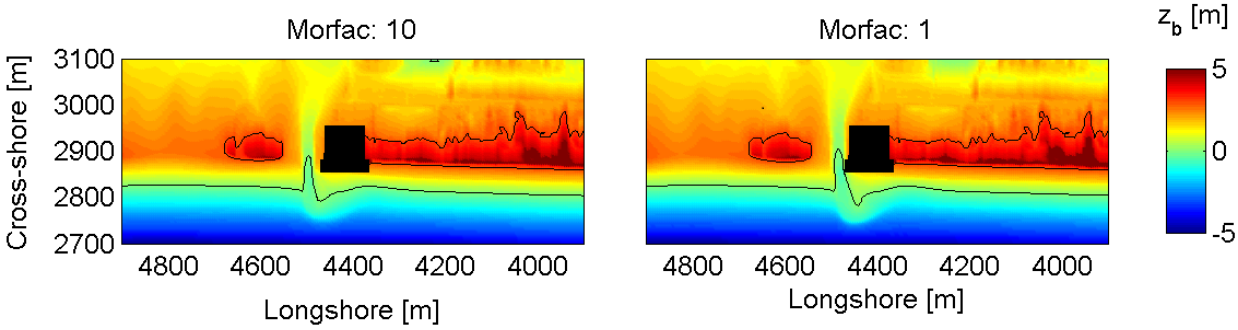

Figure G.16 *Spatial post bed level plots for the area of interest at Camp Osborne for morfac = 10 and 1. Spots without data are marked white. The black depth contours are provided at an elevation of 0 and 3 m relative to NADV88.*

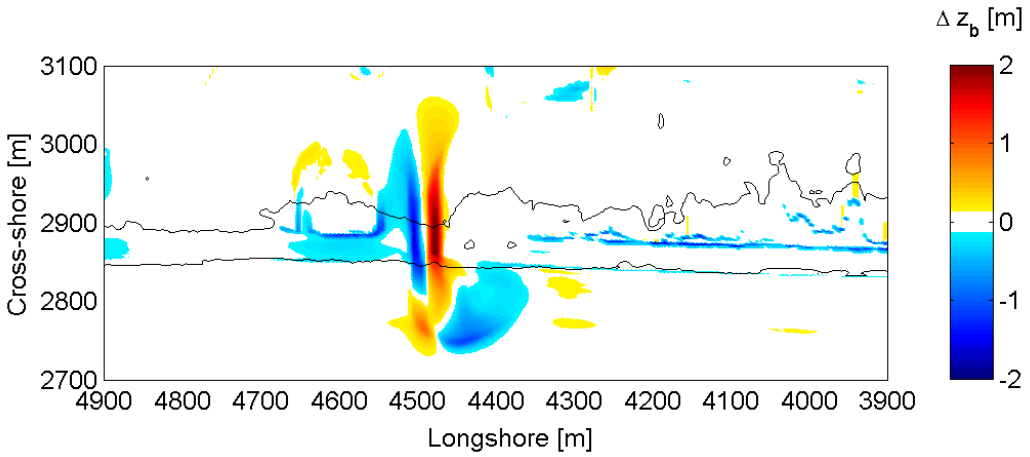

Figure G.17 *Spatial post bed level comparison for the area of interest at Camp Osborne between morfac = 10 and 1 (10 -1). Spots without data are marked white. The black depth contours are provided at an elevation of 3 m relative to NADV88 of the pre-Sandy bathymetry.*

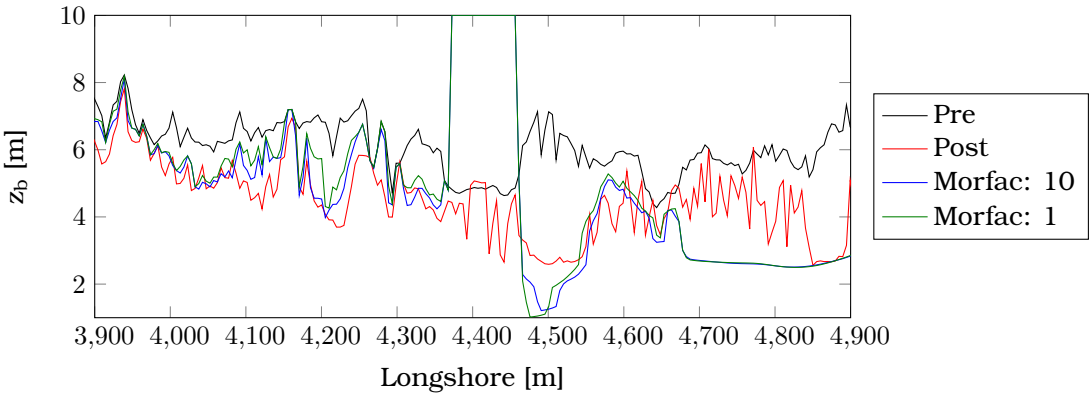

Figure G.18 *Maximum crest height in longshore direction pre-Sandy, post-Sandy as well as calculated by XBeach for morfac = 10 and = 1 for Camp Osborne*

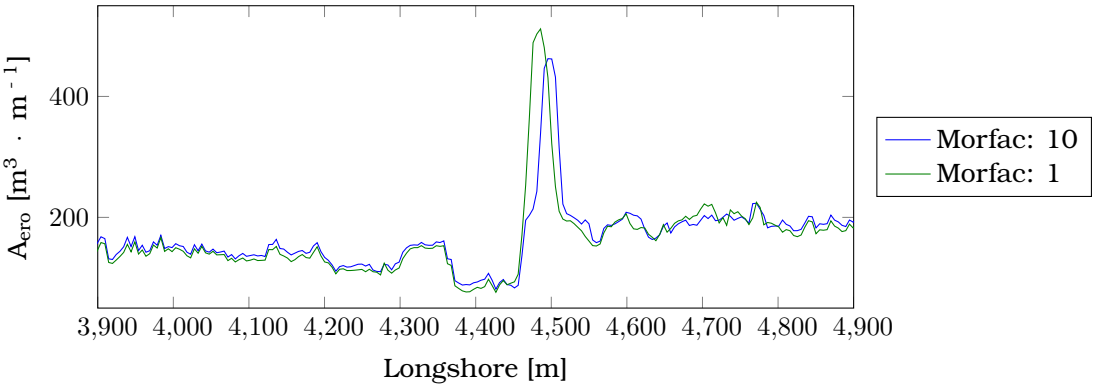

Figure G.19 *Differences of the alongshore erosion volume in $m^3 \cdot m^{-1}$ for the area of interest between morfac = 10 and =1 at Bay Head.*